

NASA CR-141701
ERIM 190100-46-F

Final Report

INVESTIGATIONS RELATED TO MULTISPECTRAL IMAGING SYSTEMS

RICHARD F. NALEPKA AND JON D. ERICKSON
Infrared and Optics Division

DECEMBER 1974

PRICES SUBJECT TO CHANGE

REPRODUCED BY
NATIONAL TECHNICAL
INFORMATION SERVICE
U.S. DEPARTMENT OF COMMERCE
SPRINGFIELD, VA. 22161

Prepared for
NATIONAL AERONAUTICS AND SPACE ADMINISTRATION

Earth Observations Division
Lyndon B. Johnson Space Center, Houston, TX
NAS9-9784
Technical Monitor: Dr. A. E. Potter/TF3

**ENVIRONMENTAL
RESEARCH INSTITUTE OF MICHIGAN**
FORMERLY WILLOW RUN LABORATORIES, THE UNIVERSITY OF MICHIGAN
BOX 618 • ANN ARBOR • MICHIGAN 48107

NOTICES

Sponsorship. The work reported herein was conducted by the Environment Research Institute of Michigan for the National Aeronautics and Space Administration, Earth Observations Division, Lyndon B. Johnson Space Center, Houston, under contract NAS9-9784. Dr. Andrew E. Potter/TF3 is Technical Monitor for NASA. Contracts and grants to the Institute for the support of sponsored research are administered through the Office of Contracts Administration.

Disclaimers. This report was prepared as an account of Government-sponsored work. Neither the United States, nor the National Aeronautics and Space Administration (NASA), nor any person acting on behalf of NASA:

- (A) Makes any warranty or representation, expressed or implied with respect to the accuracy, completeness, or usefulness of the information contained in this report, or that the use of any information, apparatus, method, or process disclosed in this report may not infringe privately owned rights; or
- (B) Assumes any liabilities with respect to the use of, or for damages resulting from the use of any information, apparatus, method, or process disclosed in this report.

As used above, "person acting on behalf of NASA" includes any employee or contractor of NASA, or employee of such contractor, to the extent that such employee or contractor of NASA or employee of such contractor prepares, disseminates, or provides access to any information pursuant to his employment or contract with NASA, or his employment with such contractor.

Availability Notice. Requests for copies of this report should be referred to:

National Aeronautics and Space Administration
Scientific and Technical Information Facility
P.O. Box 33
College Park, Maryland 20740

Final Disposition. After this document has served its purpose, it may be destroyed. Please do not return it to the Environmental Research Institute of Michigan.

TECHNICAL REPORT STANDARD TITLE PAGE

1. Report No. NASA CR- ERIM 190100-46-F		2. Government Accession No.		3. Recipient's Catalog No.	
4. Title and Subtitle INVESTIGATION RELATED TO MULTISPECTRAL IMAGING SYSTEMS (Final Report)				5. Report Date December 1974	
				6. Performing Organization Code	
7. Author(s) Richard F. Nalepka and Jon D. Erickson				8. Performing Organization Report No. 190100-46-F	
9. Performing Organization Name and Address Infrared and Optics Division Environmental Research Institute of Michigan P.O. Box 618, Ann Arbor, MI				10. Work Unit No.	
				11. Contract or Grant No. NAS9-9784	
12. Sponsoring Agency Name and Address National Aeronautics and Space Administration Earth Observations Division Lyndon B. Johnson Space Center Houston, TX 77058				13. Type of Report and Period Covered Final Report; 26 July 1969 through 15 May 1974	
				14. Sponsoring Agency Code	
15. Supplementary Notes Dr. Andrew E. Potter/TF3 is currently Technical Monitor for NASA; earlier technical monitors on this contract were W. E. Hensley and L. B. York.					
16. Abstract <p>This report contains a summary of technical progress made during a five-year research program directed toward the development of operational information systems based on multispectral sensing and the use of these systems in earth-resource survey applications. Efforts were undertaken during this program to: (1) improve the basic understanding of the many facets of multispectral remote sensing, (2) develop methods for improving the accuracy of information generated by remote sensing systems, (3) improve the efficiency of data processing and information extraction techniques to enhance the cost-effectiveness of remote sensing systems, (4) investigate additional problems having potential remote sensing solutions, and (5) apply the existing and developing technology for specific users and document and transfer that technology to the remote sensing community.</p>					
17. Key Words Remote sensing Earth resources Pattern recognition			18. Distribution Statement Approval for public release; distribution unlimited.		
19. Security Classif. (of this report) UNCLASSIFIED		20. Security Classif. (of this page) UNCLASSIFIED		21. No. of Pages 188	
				22. Price	

PREFACE

This final report summarizes a comprehensive program of research in multi-spectral remote sensing of the environment from aircraft and satellites. The research was carried out for NASA's Lyndon B. Johnson Space Center, Houston, Texas, by the Environmental Research Institute of Michigan (ERIM).^{*} The basic objective of this program was to develop remote sensing as a practical tool for obtaining extensive environmental information quickly and economically.

Timely information from remote sensing will be important to such people as the farmer, the city planner, the conservationist, and others who are concerned with a variety of problems such as crop yield and disease, urban land studies and development, water pollution, and forest management. The scope of our program included: extending understanding of basic processes; developing new applications, advanced remote sensing systems, and automatic data processing techniques to extract information in a useful form; and assisting in data collection, processing, and analysis including material spectra and ground-truth verification.

The research covered in this report was performed under Contract NAS9-9784 and covers the period from 26 July 1969 through 14 May 1974. During this period, W. E. Hensley, L. B. York, and Dr. Andrew Potter have been Technical Monitors for NASA. The program was directed by R. R. Legault, Vice-President of the Environmental Research Institute of Michigan (ERIM); J. D. Erickson, Principal Investigator and Head of the ERIM Information Systems and Analysis Department; and R. F. Nalepka, Head of the ERIM Multispectral Analysis Section. The ERIM number for this report is 190100-46-F.

The authors wish to acknowledge the assistance and direction provided by Mr. R. R. Legault. As one might expect in a program of this duration, many professional staff members contributed to the technical effort. A hopefully complete alphabetical listing of contributing staff members is included in Appendix I. Where sections of this report are largely taken from contract technical reports, those reports are referenced and the authors are acknowledged in the appropriate sections.

^{*}Prior to January 1973, ERIM was associated with The University of Michigan and was known as The Willow Run Laboratories. Nevertheless, for the sake of simplicity, the title ERIM is used when reference is made to the contract organization anywhere in this document.

CONTENTS

PREFACE	3
FIGURES	6
TABLES	7
1. SUMMARY, CONCLUSIONS, AND RECOMMENDATIONS	9
2. INTRODUCTION	11
2.1 Introduction	11
2.2 Background	14
3. IMPROVING BASIC UNDERSTANDING	21
3.1 Signature Library	21
3.2 Sources and Effects of Variation	24
3.2.1 Theoretical	27
3.2.2 Empirical Determination of Effects of Variation	54
3.3 Data Collection System	59
3.3.1 Detector Utilization	59
3.3.2 Performance Evaluation	60
4. IMPROVING ACCURACY OF EXTRACTED INFORMATION	63
4.1 Data Preparation	64
4.2 Geometric Correction, Area Determination, and Location Accuracy	69
4.2.1 Estimating Proportions	72
4.2.2 Geometric Correction	78
4.3 Spatial-Spectral Information	81
4.4 Geological and Natural Resource Signatures and Applications	84
5. IMPROVING EFFICIENCY OF EXTRACTING INFORMATION	91
5.1 Feature Selection	91
5.2 Linear Decision Rule	100
5.3 Signature Extension	104
5.4 Efficient Processing Systems	122
6. ADDITIONAL APPLICATIONS FOR AND MODIFICATIONS TO SCANNER SYSTEMS	129
6.1 Radiation Balance Mapping	129
6.2 Water Depth Determination	131
6.3 Multi-Aspect Data Collection	137
6.4 Active Scanner	142
6.5 Multispectral Parameter Mapping	146
7. TECHNOLOGY: APPLICATION AND TRANSFER	148
7.1 Scanner Design, Development, and Evaluation	148
7.2 User Data Processing	153
7.3 Multi-Agency Programs	157
7.3.1 Corn Blight Watch Experiment	157
7.3.2 CITARS	161
REFERENCES	165
Appendix I: ERIM PROFESSIONAL STAFF CONTRIBUTORS TO NAS9-9784	179
Appendix II: CONTRACT NAS9-9784 REPORTS, JOURNAL ARTICLES, AND PAPERS	180
DISTRIBUTION LIST	187

FIGURES

1. Schematic of Multispectral Scanner and Image Processor	18
2. Composite Plot of Corn Leaf Reflectance	23
3. Dependence of Transmittance on Wavelength and Scan Angle	26
4. Dependence of Path Radiance on Time and Scan Angle	26
5. Progressive Stages Leading to Sinkhole Collapse	33
6. Surface Expression of a Collapsed Sinkhole	34
7. Sinkhole-Induced Moisture Stress	37
8. Thermal Properties of Tampa Soil as a Function of Gravimetric Moisture Content	37
9. Typical Diurnal Variation of Meteorological Parameters for Tampa in March	39
10. Diurnal Surface Temperature Fluctuations of Tampa Soil for Two Weather Conditions	42
11. Temperature Contrast of Sinkhole to Its Background for Two Weather Conditions	42
12. Idealized Layer Structure of a Canopy	48
13. Optical Cross-Sections by Projections	48
14. Effects of Atmospheric Backscatter as Functions of Wavelength Region and Altitude	50
15. ERIM's Radiative Transfer Model for Hazy Atmospheres	53
16. Dependence of Sky Radiance on Zenith Angle in Solar Plane for Clear Sky Conditions	53
17. Mean Spectral Radiance from (a) Bare Soil, (b) Corn, and (c) Soybeans at 1000 and 5000 ft	56
18. Dark-Level Variations in Unclamped Data (Analog) for Segment 203, Mission 43.	67
19. Average Angular Variation of Signal for Mission 43	68
20. Histograms of Signals from Soybeans and Trees as a Function of Location in Scene	70
21. Range of Signal Means for Corn	71
22. Reflectance Spectra	73
23. Reflectance Spectra of Mixtures	73
24. Well-Conditioned Signature Simplex	76
25. Ill-Conditioned Signature Simplex	76
26. Schematic for Data Averaging	76
27. Emissivity Spectra of Silicate Rocks (from Lyon Data)	86
28. Analog-Processed IR Images of Sand Quarry from 25 July 1970 Flight over Mill Creek, Oklahoma	87

29. Comparison of Linear Combinations with Subsets of Channels for Test Fields	101
30. Linear Versus Quadratic Decision Rules for Single Training Fields	105
31. Linear Versus Quadratic Decision Rules for Combined Training Fields No. 1	105
32. Linear Versus Quadratic Decision Rules for Combined Training Fields No. 2	106
33. Comparison of Classification Accuracy for Four Signature Extension Techniques for Segment 204, Mission 43, 1971	115
34. Comparison of Classification Accuracy for Three Signature Extension Techniques for Segment 203, Mission 43M, 1971	116
35. Comparison of Classification Accuracy for Three Signature Extension Techniques for Segment 212, Mission 43M, 1971	117
36. Overall MIDAS System Block Diagram	125
37. Sea State of a Moderately Well Defined Swell and Its Fourier Transform, Puerto Rico	134
38. Change During Shoaling in Wave-Length Ratio Versus Relative Depth	135
39. Normal and Tilted Geometries	139
40. Typical Leaf Reflectance Spectra	147
41. Illustration of Multispectral Parameter Computation	147

TABLES

1. Spectral Bands of ERIM's M7 Multispectral Scanner After March 14, 1974	18
2. Soil-Profile Descriptions	40
3. Meteorological Sequences	40
4. Comparison of Channel Selection Methods for Nine Signatures	95
5. Performance of Linear Channel Selection for Seven Pairs of Signatures	95
6. Results of Cluster Analysis Using Three Centroids for Corn, Soybeans, and Trees at 0° , $\pm 25^\circ$, $\pm 40^\circ$	110
7. Results of Cluster Analysis Using Eight Centroids for Corn, Soybeans, and Trees for Segment 204 at Scan Angles 0° , $\pm 25^\circ$, $\pm 40^\circ$	111

INVESTIGATION RELATED TO MULTISPECTRAL IMAGING SYSTEMS
(Final Report)

1

SUMMARY, CONCLUSIONS, AND RECOMMENDATIONS

Several major contributions to the body of remote sensing techniques and applications originated or bore fruit in this contract. Some are further along than others, naturally. We have grouped them in this report into (1) understanding and insight, (2) accuracy of information, (3) efficiency in time and cost, (4) applications development, (5) user demonstrations and (6) education.

Use of pattern recognition with careful feature extraction to obtain uniqueness and invariance of features was an important contribution to large-area surveys. Contributing to an understanding of how to achieve uniqueness and invariance were major developments in modeling radiative interaction with the atmosphere, vegetation canopies, rock and mineral surfaces, and other object-of-interest/background combinations. Active MSS sensors were examined which may yield more unique and invariant data than that available from passive MSS sensors.

Other accuracy developments of significance are the proceduralization of signature extension and information extraction techniques in agricultural crop identification applications, and the development of both adaptive classifier techniques and geometric correction and rectification schemes. A better understanding of classifier training is still needed. Multi-stage area sampling and bias correction techniques can improve accuracy in some resource-limited situations.

For satellite data, the development of proportions estimation techniques has major importance for area determination.

Second only to accuracy is efficiency. The need is very great for modern processors to be fast and cheap without loss of accuracy. Of course, they also need to be convenient and easy to use as well. The earliest breakthroughs to operational applications may come from developments such as MIDAS, a special purpose MSS processor, augmented by registration capability. Significant developments in linear combinations, fast channel selection, and linear decision rules have helped the general purpose computer approach to be more efficient. Geological techniques have been developed which are now being used operationally for resource exploration. These include sequential classifier and techniques employing laboratory spectra in decision rules.

Although not developed in many respects on this contract, a substantial software system embodying accurate and efficient procedures and techniques for information extraction exists and has been communicated, with documentation, to the user community as well as NASA.

It is a single system of flexible, user-tested algorithms as well as research techniques still under development. A computer-based data management system for fast data location and retrieval also is employed routinely.

ERIM's facilities in areas such as field measurement equipment, laboratory measurement equipment, general and special purpose computers, and others have been effectively employed to aid in the developments on this contract.

As a result of this contract, important relationships have been established between ERIM and NASA as well as other leaders in the community of remote sensing. These relationships have led and contributed to the interchange of ideas and transfer of technology and to the cooperative multi-agency programs which are so necessary for the development of operational remote sensing systems.

We believe that as a result of this and other contracts under the ERTS and SKYLAB programs and also through contracts with various state and federal user agencies (these other efforts are not reported in this document), very significant contributions have been made toward the advancement of remote sensing technology by the full-time, professional research staff at ERIM. An important factor in ERIM's contribution has been our involvement in all aspects of remote sensing—from the design, construction, and operation of remote sensing data collection systems through the extraction of resource information and its transmittal to the resource manager in the terms and forms he desires. Partly as a result of this diversified experience, we have been able to anticipate and address many remote sensing problem areas (e.g., signature extension, proportion estimation, and efficient processors) before their importance was recognized by the remote sensing community as a whole.

As for the future, we believe that substantial technological improvements are yet to be made and we look forward eagerly to participating with NASA in the further developments for the benefit of the users of these information systems. The potential of multitemporal coverage may lead to accuracy improvements (particularly for agricultural surveys) and possibly efficiency improvements as well if the ground observation requirements are reduced more than the registration requirement imposes. With the availability of satellite coverage providing the needed repetitive data in quantity, the development of multitemporal techniques, already begun, can proceed. Spectral-spatial features also show potential for improving classification accuracy.

Greater spectral coverage in more bands than ERTS-1 at some finer spectral resolution (narrower bands) and radiometric sensitivity (higher signal-to-noise) for automatic processing of future MSS satellite data may also yield benefits. S-192 was a step in this direction, but finer spatial resolution may also be needed by those users interested in certain terrain applications as opposed to ones in oceanography.

2

INTRODUCTION

2.1 INTRODUCTION

This final report presents a summary of technical progress made during this five-year research program directed at adding to our understanding of multispectral scanner imaging systems and improving the capability for multispectral remote sensing in operational earth-resource survey applications. After presenting some definitions and background, we will briefly discuss the various research tasks undertaken in this program. Technical reports which describe the results of the research in greater detail than attempted in this report are referenced in the appropriate sections.

With the launching of the Earth Resources Technology Satellite in 1972 and the manned Skylab orbiting workshop with its Earth Resources Experiment Package in 1973, the NASA Earth Resources Survey Program began employing large-scale space technology to add to the previous programs of remote sensing from aircraft. The transition was a smooth one, partly because of techniques developed and tested in this contract. Today, although remote sensing is still characterized by feasibility demonstrations in a wide variety of applications, significant progress is being made toward the operational use of the information obtained by remote sensing for decisions affecting the management of resources through various applications systems' verification test programs [1].

Remote-sensing information systems to aid in the inventory, allocation, and management of Earth's resources make use of a combination of disciplines. These systems employ a priori knowledge of common practice and ecological relationships, modern sensors and data processing equipment, information theory and processing methodology, communications theory and devices, space and airborne vehicles, and large-systems theory and practice. There are, of course, many different remote sensing techniques—e.g., gravity and seismic sensors; acoustic sensors; static magnetic- and electric-field sensors; gamma- and x-ray sensors; sensors of electromagnetic radiation in the ultraviolet, visible, infrared, microwave, and radiofrequency regions of the spectrum. The remote sensing techniques which can be used from aircraft or spacecraft are, however, limited to sensing electromagnetic radiation from the ultraviolet through radio frequencies. The basic foundation of remote sensing is the use of these transducer and sensor outputs to identify automatically materials on the Earth's surface and to determine their conditions. This is referred to as the discrimination capability of remote sensing.

1. Office of Applications Earth Resources Program Plan, NASA JSC, Houston, December 1973.

As used here, discrimination means the successive classification of larger classes of materials into smaller, more finely divided subclasses, as in discrimination of conditions within a type or species after the type or species of the identified object is established. The main concern is the extent to which these successively finer classifications can be made automatically, if they can be made at all. The division into classes is based upon information sensed from a distance as opposed to in situ contact measurements. The economy and convenience of the information system will vary directly with the degree to which these classifications can be made automatically from remotely sensed data.

The rationale for automatic processing of multispectral scanner data is summarized as follows:

1. Automatic processing can be done in quasi-real time, that is, before the information content of the data can significantly decay in value.
2. Automatic processing of large volumes of data can be accomplished more cost-effectively (not necessarily more cheaply) than manual processing and interpretation but requires non-general-purpose computers for operational systems.
3. Although information of the desired kind may be scanty, the data volume is exceedingly high. Automating the reduction of this data volume to information frees people for other creative tasks.
4. Automatic processing offers a potential for a greater consistency of results with objective classification standards. Here, some would also mention its higher accuracy as compared to manual processing.
5. Derived information from automatic interpretation is in a form for quick and easy integration with other data bases in automatic information systems such as for automatic mapping and compilation of statistical records or summaries.
6. Multispectral scanner data are generated and recorded in electronic form intended for automatic processing, in contrast to photography in which film is the recording medium (which has poor radiometric fidelity compared to that needed in automatic processing).

Basic to this process of classification or discrimination, is the concept of a signature. In general, a signature is any collection of observable features of a material or its condition that can be used for precise classification. The features that make up a signature may all be observed simultaneously or in a sequence of observations spread over a considerable time period. The research reported here was directed primarily at signatures characterized by instantaneous observations of all features; but there is a strong need to use time-distributed or multitemporal signatures in some applications.

Variations in four characteristics of electromagnetic radiation can be used to effect discrimination between signatures. They are: (1) spectral variations (i.e., variations in radiant power as a function of wavelength); (2) spatial variations; (3) polarization variations; and (4) time variations, which can be of two types. The first type of time variation consists of changes rapid enough to cause a Doppler shift in reflected radiation. The second type consists of slower changes such as diurnal and seasonal changes. Each of these four variations in radiant power may be employed separately in discrimination, even though they interact with each other. However, in the research and processing results reported here, the emphasis is on spectral discrimination, because some powerful techniques have been developed which exploit the spectral variations (although the research is not yet complete).

A basic element of spectral discrimination theory is the realization that spectral signatures cannot be completely deterministic. That is, spectral reflectivity and emissivity measurements of natural objects exhibit some dispersion around a mean value (i.e., spectral signatures are statistical in character). This should be expected, since it is well known that taxonomy based on any characteristic shows dispersion. Thus, as we will use the term, a spectral signature is a probability density function (or set of such functions) which characterize the statistical attributes of a finite set of observations of a material and can be used to classify the material or its condition to some degree of fineness.

In this report, we are specifically concerned with nonphotographic imaging sensors which operate in the ultraviolet, visible, and infrared regions of the spectrum, i.e., multispectral scanners. An elementary description of a multispectral scanner is given in Section 2.2.

Even before developing the first multispectral scanner, ERIM emphasized research and development of information systems which used nonphotographic imaging sensors, because of the advantages they offer and because of their (at that time) less developed state for use in remote sensing. Information systems employing a combination of sensors, in fact, may yield the most information to the resource specialists. Those systems that provide the desired information most quickly and cheaply will be used.

The basic ERIM Earth Resources Survey Program automatic processing R&D objective is simply stated as follows:

To make large area and small area MSS-based Earth Resources Survey (and land use and pollution monitoring) information systems practical by:

- a. increasing accuracy of information extraction (mensuration, location, and correct classification)
- b. decreasing cost (through powerful processing techniques which can use fewer ground observations and fast processing on low-cost equipment)

- c. developing means to disseminate information in user applications terms (e.g., volume of production, not simply area planted to a crop)
- d. decreasing time for information extraction to preserve information value from decay
- e. demonstrating utility in user applications of simple techniques to meet desired performance and documenting performance achieved with various techniques to allow design of operational systems
- f. employing multistage area sampling and bias correction wherever accuracy requirements can be met through this cost-saving approach
- g. relaxing costly constraints on data acquisition imposed solely by weak processing techniques

After we first present below a brief background of optical remote sensing technology, the remainder of this report will deal with research and development tasks undertaken in this program. Section 3 describes our efforts to improve the basic understanding of the many facets of multispectral remote sensing. This understanding is improved by investigating the characteristics and effects of the resources themselves, the environment in which they are observed, and the system observing and recording the information. Section 4 discusses methods we have developed to improve the accuracy of earth resource information which can be extracted from multispectral scanner data. Section 5 addresses the problem of efficiency and cost-effectiveness of data collection, data processing, and information extraction and presents approaches to improve the efficiency of these operations. Methods to extend the utility of scanner data to additional resource problem areas are discussed in Section 6. In Section 7 we briefly describe our efforts under this contract for a number of users representing many disciplines for whom we processed and analyzed scanner data. We also describe our involvement in joint efforts between NASA, ERIM, and other contractors to address specific user problems. We then discuss the documentation and transfer to NASA of knowledge gained during this program. In Section 8 we present conclusions and recommendations resulting from this program.

2.2 BACKGROUND

The past 25 years have witnessed impressive advancements in optical remote sensing technology, as each succeeding step has been forced by the momentum of success in previous work. The beginning of this sequence can be traced to a rather lengthy period of component development and to the study of science for its own sake. As a result, it became possible to design and build lenses to fulfill a much wider but more stringent set of specifications; photographic films acquired improved sensitivity and resolution; a wide variety of quantum detectors became available, the performance of which is limited by radiation noise; optical materials and filters became available for operating readily at wavelengths up to 25 μm ; and miniature, solid-state electronics were

developed that can be used with all sensors that have electronic outputs. The list is really much longer, but this provides the essence of the early technical accomplishments. During this era, camera and film were the primary tools of remote sensing. The photointerpreter was the data processor, and his profession an art rather than a science.

The information contained in radiation from a scene is found in the spatial distribution, the spectral distribution, temporal variations, the state of polarization of the radiation, and the variation of these parameters with angle of observation. By their very nature, cameras (and all image-forming sensors) produce graphic presentations of the spatial distribution of radiation from the scene. Interpretation of such imagery relies heavily on shape recognition of key elements within the scene. To be sure, some cameras take advantage of the spectral distribution of the target and background radiation and increase the contrast between objects and backgrounds through the selection of optimum film-filter combinations (spectrozoal photography). The relative tone of objects within the scene of spectrozoal photography has proven to be useful for: differentiation of types of forest plantations; soil classification; land-use classification; early detection of some crop diseases; and agricultural crop identification. In these instances, a rather limited specific wavelength region is used where major spectral differences occur between objects or effects being sought and their backgrounds. While quantitative evaluation of tonal variations in single-band imagery has many limitations, it offers a limited means for automatic interpretation of some types of imagery. For example, in agriculture, the conditions of fields undergo dramatic changes as a function of time, because of seasonal planting and growth.

Advances in component development provided the engineer with detectors and optical elements which operated outside the spectral range of photographic or photoemissive detectors. The major development which resulted is the optical mechanical scanner, which can generate imagery in many regions of the electromagnetic spectrum. In most instances, these scanners use the sensitive area of a detector element as the scanning aperture. When mounted in an aircraft or spacecraft, the scanning mirror sweeps the scanning aperture in lines perpendicular to the flight path, and the forward motion of the vehicle provides scan-line advance. With suitable processing and printing, the resulting image is a strip map of the scene below, not unlike a television picture with an endless frame. The optical-mechanical scanners have several useful features. For example: (1) the object plane is usually scanned and, therefore, the collector optics are used on-axis; (2) on-axis optics are generally reflective and can operate in almost any wavelength region of the spectrum; and (3) the detector response is usually linear, and its output is an electrical video signal that is amenable to electronic processing.

By using sensors sensitive to the infrared spectrum, the scanner could record imagery from an object's thermal radiation (emission) rather than from its reflection of sunlight, and the infrared scanner was highly developed as a nighttime sensor. Use of the widest possible spectral

bandwidth (as determined by the sensor) was considered advantageous because of the low emission levels of terrain features at ambient temperatures. The resulting imagery is a gray-scale representation of the relative temperature of everything in the field of view of the infrared scanner, with warm spots appearing brighter than cool spots. Although many objects could be identified by the shape of their thermal image, the gray-scale presentations of relative temperatures were often surprising and sometimes baffling. Interpretation of this imagery required not only a keen eye and a knowledge of the physics of thermal emission, but also an understanding of natural science phenomena which would indicate, for example, when to expect a body of water to be warmer or cooler than the surrounding terrain.

The acquisition of infrared imagery opened a whole new field for application of remote sensing to earth-science studies. The detection and mapping of thermal pollution in rivers and lakes is perhaps the most obvious application; more subtle is the detection of disease in plants as manifested by small differences in the temperature of the foliage (relative to healthy plants). Such applications are possible because the sensors are extremely sensitive to small temperature changes, and a gradient resolution less than 0.5°C is readily obtainable. Calibration of the scanner so that absolute temperature values can be obtained from the imagery has proven to be a formidable task which is only now being solved satisfactorily. Thermal maps can now be made to $\pm 3^{\circ}\text{C}$ or better accuracy, provided that the attenuation of the intervening atmosphere is taken into account. Even better relative accuracy is attainable.

As exploratory work continued with new detectors, film-filter combinations, and laboratory studies of the optical properties of materials, an appreciation developed for the information being lost because of the broadband nature of the instruments. Assume that an object's tone can be determined to within one of ten gray levels in any given spectral interval. A measurement made in 20 different wavelength bands would be capable of distinguishing 10^{20} different states. Admittedly, this number of states does not exist in practice. Large spectral variations in reflectance and emittance do not occur over narrow spectral intervals in a random manner; variances can occur in a given class of objects; most materials exist as mixtures; and the spectral distribution of the scene illumination varies. Nonetheless, it is obvious that the operation in multiwavelength channels permits one to distinguish between considerably more objects than does single-band operation.

The first multispectral scanner (MSS) was developed at ERIM in 1964 [2] with the M-5 single line of sight scanner developed in 1966 when ERIM was still known as the Willow Run

2. D. S. Lowe, et al., Multispectral Data Collection Program, Third Symposium on Remote Sensing of Environment, Willow Run Laboratories of the Institute of Science and Technology, The University of Michigan, Ann Arbor, October 1964.

Laboratories. It is essentially a combination of an optical-mechanical scanner [3] and a multi-channel spectrometer as illustrated in Figure 1. In this system, each detector of the spectrometer simultaneously observes the same resolution element of the scene, but in a different wavelength region. The 1974 spectral bands of the ERIM M7 MSS are given in Table 1 [4]. The output signal from each detector element is a video electrical signal corresponding to the apparent scene radiance in the wavelength region of operation defined by the position of the detector in the spectrometer. This video signal can be used to generate an image of the scene in that wavelength region. The rationale for using MSS in earth resources surveys [5 and 6] includes:

- a. Measurement of spectral radiance outside the photographic wavelength region
- b. The output signals are in electrical form for accuracy and ease of subsequent use including automatic processing (film has poor radiometric fidelity compared to that needed in automatic processing).
- c. Simultaneous collection of data from one ground resolution element in many wavelength bands
- d. Greater information content due to wider dynamic range of transducers as compared to photographic film
- e. One can obtain quantitative radiometric measurements.

With the ability to gather large amounts of data as a result of the sensor development, automatic data-processing equipment and techniques were required to efficiently extract the necessary resource information [7]. This, too, has been partially accomplished, though it is far from complete; the analog and digital techniques now at our disposal are discussed in some detail in subsequent sections. In 1965, the first digital general purpose computer recognition processing scheme [8], and by 1968, the first near real-time special purpose parallel computer

-
3. M. Holter and W. Wolfe, Optical-Mechanical Scanning Techniques, Proceedings of the IRE, September 1959.
 4. P. G. Hasell, et al., Michigan Experimental Multispectral Mapping System: A Description of the M7 Airborne Sensor and Its Performance, ERIM Report 190900-10-T, January 1974.
 5. M. Holter and R. Legault, Motivation for Multispectral Sensing, Third Symposium on Remote Sensing of Environment, The University of Michigan (WRL), Ann Arbor, October 1964.
 6. D. S. Lowe, Line Scan Devices and Why Use Them, Fifth Symposium on Remote Sensing of Environment, The University of Michigan (WRL), Ann Arbor, April 1968.
 7. R. Legault and F. Polcyn, Investigations of Multispectral Image Interpretation, Third Symposium on Remote Sensing of Environment, The University of Michigan (WRL), Ann Arbor, October 1964.
 8. D. S. Lowe, An Investigative Study of A Spectrum-Matching Imaging System, The University of Michigan (WRL), Ann Arbor, Report 8201-1-F, October 1966.

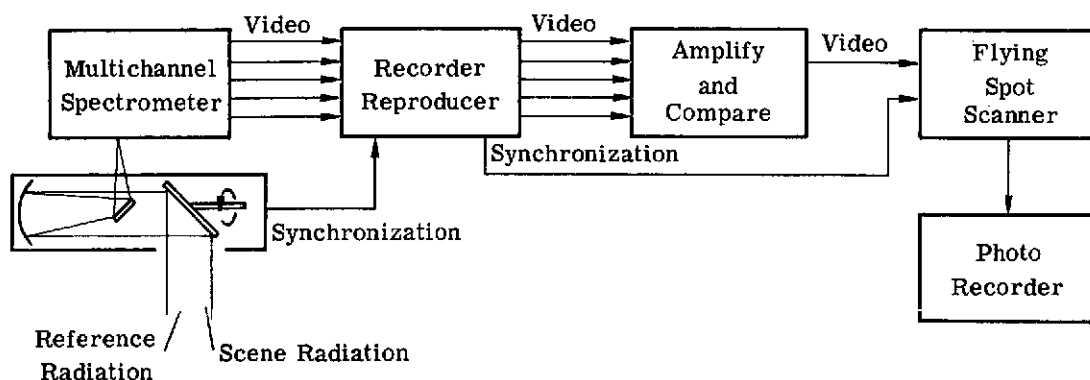


FIGURE 1. SCHEMATIC OF MULTISPECTRAL SCANNER AND IMAGE PROCESSOR

TABLE 1. SPECTRAL BANDS OF ERIM'S M7
MULTISPECTRAL SCANNER AFTER
MARCH 14, 1974

50% Response Points (μm)	Peak Response Points (μm)
0.33 - 0.38	0.36
0.41 - 0.44	0.425
0.44 - 0.46	0.445
0.46 - 0.48	0.47
0.48 - 0.52	0.505
0.52 - 0.56	0.54
0.56 - 0.61	0.58
0.61 - 0.69	0.655
0.69 - 0.77	0.725
0.86 - 1.04	0.93
1.0 - 1.4	1.2
1.5 - 1.8	1.65
2.0 - 2.6	2.3
8.0 - 14.0	(This region can be split into bands by choice of filters)

Note: Of the 19 bands which are optional,
only 12 can be recorded at any one time.

(SPARC) for low cost recognition processing of multispectral scanner data [9 and 10] were designed and developed at ERIM. Presently, under NASA Advanced Applications Flight Experiment Contract NAS1-13128, ERIM is developing, constructing, and testing an all-digital, near real time, special purpose computer having a user-oriented, color interactive capability for recognition processing of MSS data at low cost [11]. This multivariate interactive digital analysis system (MIDAS) has a feature extractor and a Bayesian or multivariate normal maximum likelihood classifier which can accept up to 16-band data and can classify into 16 classes at 200,000 data vectors per second (peak rate). This system is intended as a prototype for systems which make large-area surveys practical and operational. Remote access for users through terminals can be achieved by interfacing this now stand-alone system to a host computer supporting the terminals. ERIM has consistently maintained that large general purpose computers did not offer sufficient promise for large-area surveys, even given a sampling approach. They cannot keep up with the data volume that needs to be processed.

The development of automatic classification techniques and information systems based on remotely sensed spectral information has been pursued by ERIM with U.S. Army and U.S. Air Force support for the past fifteen years. In 1964 (NASA Grant 715), ERIM began investigating the applicability of these techniques and systems to agricultural problems [12]. Since that time, other applications of these techniques and information systems have been developed for related NASA programs in geology and mineralogy, geography, cartography, urban land use, hydrology, water pollution, oceanography, and lunar exploration [13]. Support has also come from the Department of the Interior, the U.S. Navy, the Department of Transportation, the Environmental Protection Agency, and others.

The development of remote sensing techniques is resulting in operational applications, as remote sensing becomes a tool for the earth sciences and for resource managers. In this form, remote sensing represents a return for the development and research investment made.

9. F. Kriegler and M. Spencer, A Statistical Spectral Analysis and Target Recognition Computer (SPARC), The University of Michigan (WRL), Ann Arbor, Report 8640-17-F, September 1968.

10. F. Kriegler and M. Spencer, SPARC, A Special Computer for Target Recognition in Real Time by Statistical Spectral Analysis of Multichannel Scanner Data, Proc. IRIS, Vol. 14, No. 2, August 1970, p. 413; paper given at 16th National IRIS, May, 1968.

11. F. Kriegler, et al., MIDAS: Prototype Multivariate Interactive Digital Analysis System—Phase I, ERIM Report 195800-25-F (in 3 vols.), August 1974.

12. R. Nalepka, et al., Investigation of Multispectral Discrimination Techniques, The University of Michigan, (WRL) Report 2264-12-F, January 1970.

13. J. Erickson and F. Thomson, Investigations Related to Multispectral Imaging Systems for Earth Resource Surveys, The University of Michigan (WRL), Ann Arbor, Interim Report 31650-17-P, September 1971.

Presently, emphasis is on the development of optical remote sensing technology. An imposing array of available remote sensors can provide a great quantity of spatial and spectral data in the ultraviolet, visible, and infrared regions. We have aircraft and spacecraft that can assure repeated coverage by these sensors of almost any desired terrain feature, and we know how to process the data automatically to reduce its quantity to manageable levels. A recent review of the status of MSS information systems is described in [14].

14. J. Erickson, Automatic Extraction of Information from Multispectral Scanner Data, International Archives of Photogrammetry, Vol. 17, August 1972, (ISP Invited paper).

IMPROVING BASIC UNDERSTANDING

At the inception of this contract in July 1969, ERIM's M-5 airborne multispectral scanner had been operating for some three years. By this time, certain capabilities had been established; however, a great deal still needed to be learned before earth resources survey information systems could be operationally deployed. In this section, we discuss some of the efforts undertaken in this program to improve the basic understanding of various aspects of remote sensing in order to provide the information necessary to make multispectral remote sensing a practical tool.

3.1 SIGNATURE LIBRARY

One necessary step for improving the basic understanding of remote sensing is to better define and understand the reflectance and emittance characteristics of the targets to be viewed from the remote platforms. As a part of this contract, we undertook to gather, review, analyze, catalog, and computerize available laboratory and field reflectance and emittance data for natural targets of interest to the remote sensing community.

The system of spectral data and computer programs for updating the signature library, for retrieving data from the library, and for analyzing the data is known as the Earth Resources Spectral Information System (ERSIS) [15-19]. The ERSIS which was generated for use by the remote sensing community is available both at ERIM and at NASA's Johnson Space Center (JSC) in Texas.

Sources for the ERSIS data provided by ERIM under this contract were reports published by laboratories making such measurements and, in some cases, unpublished data acquired directly from an experimenter. In the gathering process, each report was examined for data to be added to the system. Selected curves were then manually digitized. Great care was exercised to preserve all significant details of the original curve except those details attributable to instrument noise. Data points were taken in such a way that the new curve formed by connecting the

15. V. Leeman, D. Earing, R. K. Vincent, S. Ladd, The NASA Earth Resources Spectral Information System: A Data Compilation, The University of Michigan (WRL), Ann Arbor, Report 31650-24-T, May 1971.

16. D. L. Earing and V. W. Leeman, NASA/MSU Earth Resources Spectral Information System Procedures Manual, The University of Michigan (WRL), Ann Arbor, Report 31650-32-T, 1971.

17. V. Leeman, R. Vincent, and S. Ladd, The NASA Earth Resources Spectral Information System: A Data Compilation First Supplement, The University of Michigan (WRL), Ann Arbor, Report 31650-69-T, 1972.

18. V. Leeman, NASA/MSU Earth Resources Spectral Information System Procedures Manual, Supplement, The University of Michigan (WRL), Ann Arbor, Report 31650-72-T, September 1971.

19. R. Vincent, The NASA Earth Resources Spectral Information System: A Data Compilation, Second Supplement, ERIM, Ann Arbor, Report 31650-156-T, January 1973.

data points with straight lines would duplicate the original curve. The curves were then given an identification number, and coded with subject descriptors denoting the material and/or object measured and the complete conditions of the experiment. These descriptors provide the basis for retrieval. Among the spectral reflectance, transmittance, and emittance curves (or data sets) in the current NASA/JSC Earth Resources Spectral Information System, there are approximately 700 for rocks and minerals, 3005 for vegetation, 1100 for soil, and 60 for water.

Three kinds of measurements are represented: (1) laboratory measurements of materials, such as leaves, rocks, and soil; (2) ground-based field measurements of objects, such as plants and soil plots; and (3) a few uncorrected airborne measurements of scenes in a special category. In the optical portion of the spectrum, laboratory-measurement programs are far more numerous than either ground-based field measurement or airborne measurement programs.

Separate, master magnetic tapes are kept for soil and water, vegetation, and rock and mineral spectra. The present retrieval system allows for the selection of any of a group of coded descriptors, specified experimental conditions, or individual curve identification numbers. Interpolation of the digitized data points to find the reflectance (transmittance, emittance) at a particular wavelength is also performed. In addition, mean values, standard deviations, and maximum-minimum envelopes of the digitized curves may be routinely computed for a retrieved subset of data. A single composite plot of corn leaf reflectance spectra is shown in Figure 2. The "Earth Resources Spectral Information Procedures Manual" [18] describes the organization of the data on the master tape, input specifications for retrieval-analysis programs, and actual operating instructions for the Univac 1108 computer located at the Johnson Space Center in Houston, Texas.

Although ERSIS contains approximately 5000 spectra of natural materials collected from the open literature and contractor-report sources, the need still exists for new data, especially in some categories in which the paucity of data is quite pronounced. An effort was undertaken as a part of this contract to identify those data categories where the data shortage was greatest relative to our estimate of the required data, so that the general scientific community could be made aware of where contributions were most needed. When insufficient data of a given type exist, we refer to this condition as a data gap.

The following is a summary of the major data gaps (see Ref. [20] for more details): Vegetation data are required (1) at wavelengths greater than 3 μm , (2) on plants native to southern and western U.S. and to foreign countries (especially tropical plants), (3) on spectra related to vigor, and (4) on spectra related to plant maturity. Rocks and mineral data are required (1) in all wavelength regions, but particularly for those less than 8 μm , (2) on the spectral effects

20. R. K. Vincent, Data Gaps in the NASA Earth Resources Spectral Information System, The University of Michigan (WRL), Ann Arbor, Report 31650-25-T, March 1971.

CORN
Live and Healthy

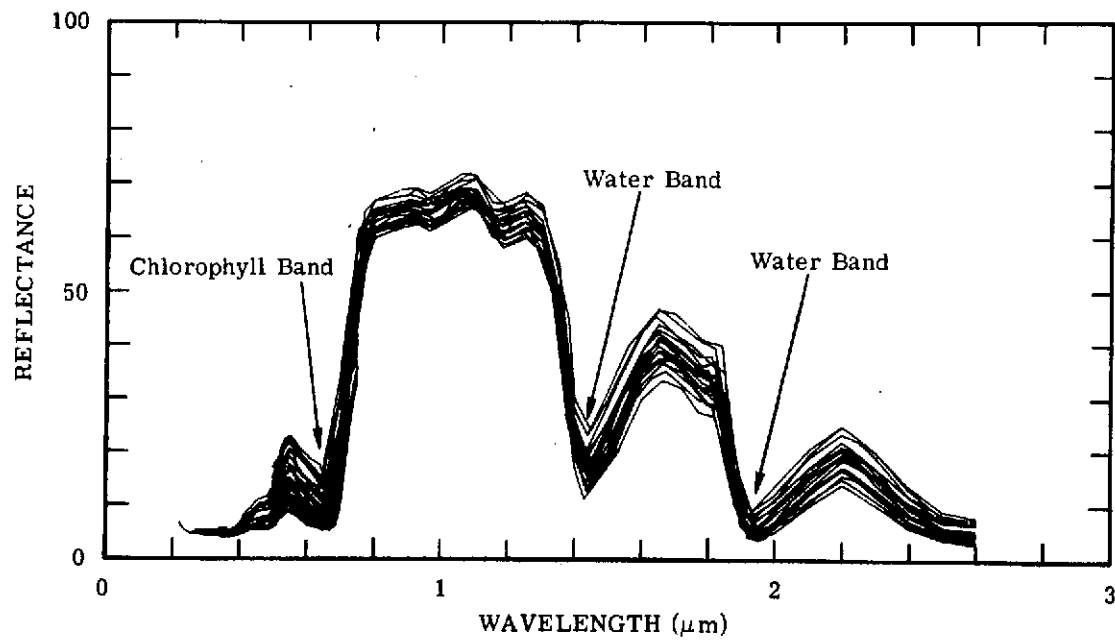


FIGURE 2. COMPOSITE PLOT OF CORN LEAF REFLECTANCE

of surface-roughness variations, and (3) on the spectral indices of refraction for minerals, particularly in the infrared region. Soils and water data are required (1) for wavelengths greater than $3 \mu\text{m}$, (2) on water, ice, and snow, and (3) on the spectral refractive indices of ice. Although the information contained in ERSIS is incomplete, it has been very useful to date (see Section 3.4) and efforts should be pursued to eliminate the data gaps and keep the library current.

3.2 SOURCES AND EFFECTS OF VARIATION

One of the difficulties which was not too obvious during the multispectral scanner remote sensing feasibility studies carried out during the first few years of the existence of scanners was the effect of the variability of many factors on limiting the operational utility of multispectral scanner data. In this section, we briefly discuss sources of variation in the signals generated by a multispectral scanner. We then describe our efforts to better understand the effects of variations, from both theoretical and empirical points of view.

Simply speaking, the radiation sensed by a multispectral scanner in each spectral band is given by

$$L_o = \rho ET + L_p$$

where the target, exhibiting a reflectance ρ for the existing scanner-target-sun geometry, has an irradiance E incident upon it. The radiance reflected in the direction of the scanner (ρE) is then attenuated by a factor T as it traverses the atmospheric path between the ground and the scanner. There is also a contribution by radiation which is scattered into the scanner field of view. This quantity, the path radiance (L_p), is added to the radiation reflected from the target. Thus, the radiance observed at the scanner (L_o) consists of radiation reflected by the target as modified by both additive and multiplicative factors.

Multispectral remote sensing is based on the premise that a unique vector of reflectances (ρ) is associated with most object classes. The first problem in recognition processing arises because the scanner senses not ρ , but L_o . Moreover, and this is a second problem, the values of E , T , and L_p are generally not constant over the whole data set. They will vary. Let us next examine why these three quantities vary and to what extent.

Many factors can cause variation in scanner signals. Some of these are listed below, where we have broken them down into three categories: instrumental sources, environmental sources, and scene-related sources of variation.

SOURCES OF VARIATION IN MULTISPECTRAL SCANNER SIGNALS

- A. Instrument
 - Scanner electronics and recorder instabilities
 - Gain changes
 - Nonuniform angular responsivity
- B. Environment
 - Changes in irradiance
 - Changes in atmospheric transmittance
 - Changes in atmospheric path radiance
- C. Scene
 - Geometric effects
 - Reflectance effects

Instrumental sources are associated with the mechanics, optics, and electronics of the multispectral scanner. Included in this category are gain changes, nonuniform angular responsivity, and other recorder and electronic instabilities. Since many of these effects are deterministic, they can be eliminated from the data during an initial data preparation stage (see Section 4.1).

Environmental sources of variation include changes in the magnitude and spectral make-up of the irradiance at ground-level, changes in atmospheric transmittance, and changes in path radiance. Changes in irradiance result from changes in the atmospheric state (i.e., the type, number, and location of clouds and the existence of other absorbing and scattering aerosols and gases) as well as from solar positional changes that occur during or between the times area survey data sets are collected.

Atmospheric transmittance and path radiance will also change as the atmospheric state changes. These quantities are also functions of scan angle since they vary depending on the path length from the ground to the scanner. An example of the effect of angular variation on atmospheric transmittance is shown in Figure 3. It can be seen that the effect is largely parabolic and symmetric around the nadir. The information shown here was computed using a radiative transfer model developed at ERIM which is described in Section 3.2.1.

Model calculations are seen in Figure 4 for variation in path radiance as a function of scan angle and time of day for an East-West flight direction. Path radiance increases rapidly near the extreme scan angles. When the angle of view of the scanner is opposite the sun, the path radiance reaches a local maximum. This is seen in Figure 4 as occurring near noon.

The quantities T and L_p will vary with scan angle over a single scan line and the quantities E , T , and L_p may vary during the time a data set is collected. Therefore, the signal generated when viewing a single object class may exhibit a wide range of multivariate values. Under such conditions, different object classes viewed at various locations in the data set may result in identical scanner signals. Thus, for example, the same scanner signal may be generated for

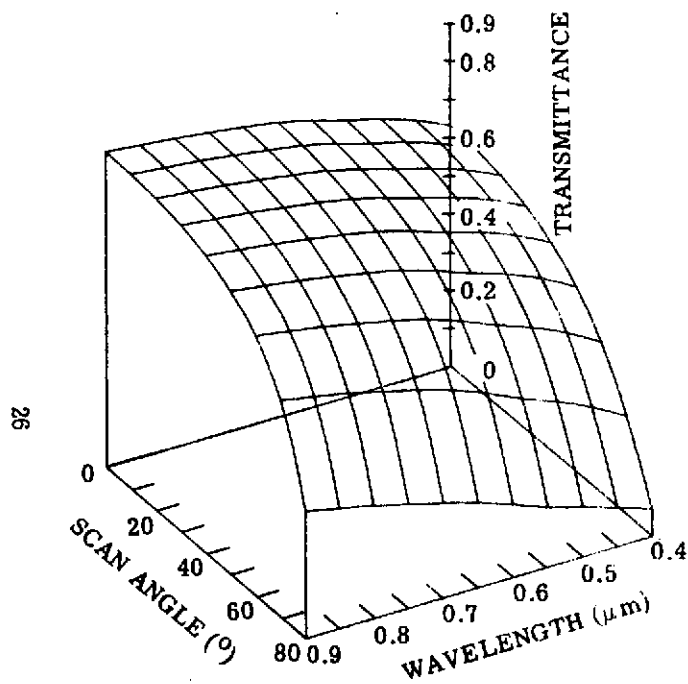


FIGURE 3. DEPENDENCE OF TRANSMITTANCE ON WAVELENGTH AND SCAN ANGLE. Visual range = 8 km; altitude = 1 km.

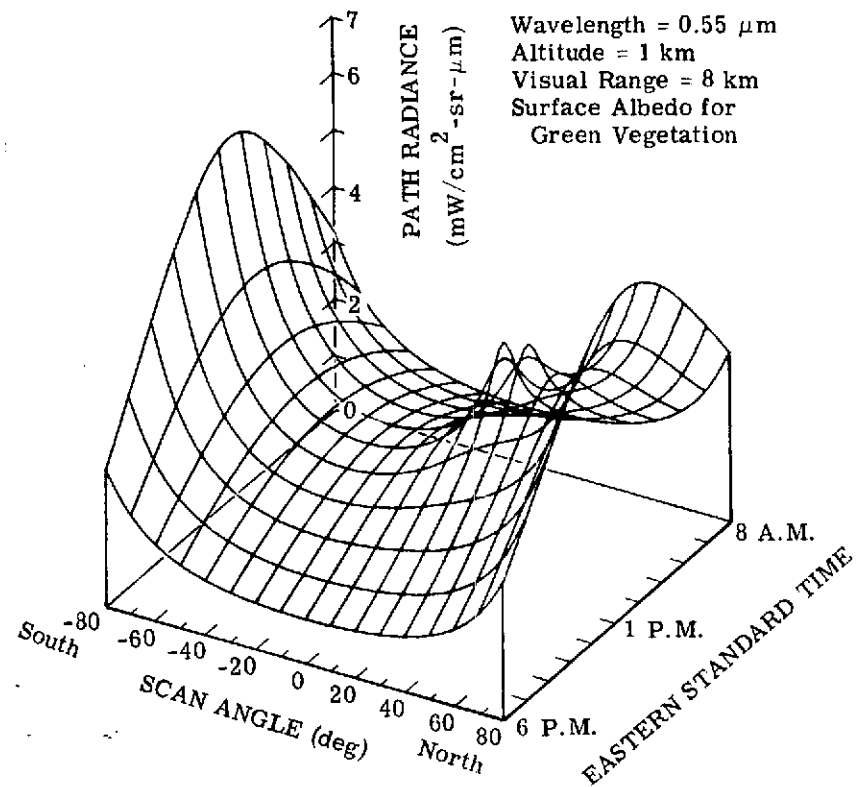


FIGURE 4. DEPENDENCE OF PATH RADIANCE ON TIME AND SCAN ANGLE. Southeastern Michigan, 1 September 1971.

object class 1 at one location, object class 2 at a second location, object class 3 at a third . . . , etc. Obviously, under such conditions obtaining accurate recognition results may not be possible. The situation becomes even more acute when one considers the variations in E , T and L_p that may occur between data sets.

Even if the variations associated with the atmosphere were eliminated, there still would be other potential sources of variation or change in the radiance observed when viewing any one object class on the ground. First of all, most objects of interest are geometrically complex (e.g., corn plants). Because of this complexity, the illumination of elements of such objects by direct sunlight (the primary source of radiation) depends on the location of the sun in the sky. Some elements may be illuminated at certain times of the day or year and not at others. Similarly, depending on the location of such objects under the scanner, certain elements may or may not be visible to the scanner. Clearly, such effects will cause variations in the radiance observed.

Another scene-related source of variation is associated with the reflectance characteristics of the object being viewed. Since most object materials are not Lambertian reflectors, the distribution of radiation reflected from them will be nonuniform; this will be independent of the geometric effects. Therefore, the radiance observed when viewing a geometrically simple object or material (e.g., a field of bare soil, a paved road, or a calm body of water) will be a function of the view angle as well as the angular distribution of radiation incident upon the object. Of course, this is also true for geometrically complex objects.

Except for the deterministic instrumental variations, the other variations are interrelated to a great extent. For instance, a change in atmospheric state will cause changes in both the magnitude and the spatial distribution of the incident irradiance at any particular wavelength. Because of the change in the spatial distribution of incident radiation, the radiation reflected in the direction of the sensor will be modified additionally through purely geometric effects as well as by the non-Lambertian character of the object being viewed. This reflected radiation will then be attenuated to a lesser or greater extent before reaching the sensor, while at the same time more or less path radiance will be incident at the sensor altitude. So, theoretically, a relatively small change in atmospheric state could result in a potentially significant change in the radiation detected by the sensor. In the remainder of this section, theoretical and empirical approaches developed and employed under this contract are discussed.

3.2.1 THEORETICAL DETERMINATION OF EFFECTS OF VARIATION

We shall now describe a number of theoretical efforts undertaken to better understand the effects on scanner signals of varying some of the above factors.

Thermal Model

The use of thermal-infrared line scanners aboard aircraft platforms has, for many years, been an established remote-sensing technique. Though initial developments in the field were undertaken to meet military needs, the utility of these data for numerous civilian applications has been repeatedly demonstrated, particularly in those fields dealing with geophysical processes and natural resources.

Through the years, many interpretive techniques have evolved through which one can attempt to understand the implications of the data recorded in the thermal-infrared region. A general body of knowledge, consisting primarily of basic "rules of thumb," has empirically developed and has proven useful in the initial phases of each application. Increasingly apparent, however, is the fact that a qualitative understanding of the processes leading to a particular thermal signature provides, at best, only a marginal capability to interpret and understand the wealth of information contained in infrared data.

Certainly, instrumentation advances, particularly in terms of calibrated thermal mappers and computerized pattern-recognition analysis techniques, have put a strain on this established, qualitative, interpretation methodology. To a greater extent, however, it is the application of thermal sensing to problems in geophysics and natural resources that has shown most pointedly the limitations of the now classical approaches to thermal-image interpretation. Simplistic, qualitative concepts, such as hot-spot detection, have only limited utility in defining natural processes, since much of the significant information lies in thermal relationships which are usually subtle and often extremely tenuous. Full utilization of the potential of thermal-infrared remote sensing in the natural and earth sciences requires, ultimately, both qualitative and quantitative understanding of each element of interaction between an object and its environment. Such understanding can be achieved through the application of realistic theoretical modeling techniques in which each significant form of thermal interaction is described and in which the parametric effects of each factor can be investigated.

Many objects of interest can be thought of as planar in form (e.g., roads, agricultural fields). The thermal interaction of these objects can be considered as having only one significant spatial dimension, both in terms of geometric description and in terms of the direction of the heat fluxes involved. The general one-dimensional case yields a mathematically tractable solution of realistically described thermal interactions. Such a one-dimensional thermal model does exist and is capable of realistically modeling an object into a natural environment [21]. As part

21. D. Bornemeier, R. Bennett, and R. Horvath, Target Temperature Modeling, RADC-TR-69-404, Rome Air Development Center, Air Force Systems Command, Griffiss Air Force Base, NY, under A.F. Contract F30602-68-C-0099, December 1969.

of the NASA Program and in direct support of the data acquisition and analysis portions of that program, the effort described below [22] was undertaken to demonstrate and apply the existing thermal modeling capabilities to specific problems associated with data-acquisition mission planning and data analysis.

The model is based on the assumption that for a large class of objects the most significant heat fluxes are vertical, and transverse heat flow is negligible. This is surely the case for objects which are uniformly illuminated, have an essentially horizontal observable surface, and whose horizontal spatial extent is significantly greater than the depth of penetration of the diurnal temperature cycle. Furthermore, the object's properties are considered homogeneous in its transverse dimensions. Under these assumptions, the spatially and temporally varying temperature $T(z, t)$ is given by solution of the one-dimensional heat diffusion equation

$$\frac{\partial T}{\partial t} = \frac{k}{\rho c} \frac{\partial^2 T}{\partial z^2}$$

subject to the boundary conditions

$$\sum_{i=1}^n q_i = 0 \text{ at } z = 0$$

and either

$$\sum_{i=1}^m q_i = 0 \text{ at } z = d$$

or

$$T(z, t) = f(t) \text{ at } z = d$$

The observable (upper) surface is at $z = 0$, the lower surface is at $z = d$, and ρ , c , and k (all functions of z) are the density, specific heat capacity, and thermal conductivity, respectively. The ratio $k/\rho c$ is the thermal diffusivity. The q_i represent heat fluxes at the surface of the slab target.

The realistic accuracy of this model depends to some extent on the degree to which the thermal characteristics can be approximated by piece-wise constant values (i.e., constant within a layer), and the physical configuration can be approximated by a stack of infinite planar

22. R. Vincent, R. Horvath, F. Thomson, and E. A. Work, Remote Sensing Data Analysis Projects Associated with the NASA Earth Resources Spectral Information System, The University of Michigan (WRL), Ann Arbor, Report 31650-26-T, April 1971.

slabs. More importantly, however, it depends upon the quantitative accuracy of the approximations q_i , which represent the actual time-dependent, heat-transfer processes which take place at the surface exposed to the natural meteorological driving functions.

For nonvegetated surfaces, six essential heat-transfer processes must be taken into account: (1) body conduction, (2) solar absorption, (3) net thermal radiative transfer, (4) convection, (5) rain, and (6) evaporation. An additional transpiration term must be considered if the surface sustains living vegetation. The detailed derivation of fluxes has been given elsewhere [23]; here, we will describe only briefly their individual dependencies on the measurable meteorological parameters (such as ambient air temperature, horizontal wind velocity, relative humidity, cloud cover, and cloud type) which are, in general, time-dependent input data for the model.

(1) **Body Conduction.** This term accounts for the conduction of heat away from the upper surface into the interior of the target (or vice versa); it depends simply on the thermal conductivity of the surface material and the temperature gradient in the material evaluated at the surface.

(2) **Solar Absorption.** In order to allow for the many different illumination conditions possible in a diurnal cycle, this term is in an arbitrarily specifiable, tabular form—viz., the total direct and diffuse solar irradiance multiplied by the total solar absorptivity of the surface.

(3) **Net Thermal Radiative Transfer.** Net thermal radiation is specified by the difference between the instantaneous total graybody radiation emitted by the surface and that absorbed by the surface from a radiating atmosphere, the mean total emittance of which is an analytical function of the time-varying relative humidity, cloud cover, and cloud type.

(4) **Convection.** The relative contribution of the convective process can vary over several orders of magnitude, from a very small rate (molecular conduction) for stable, no-wind conditions to a very large rate (forced convection) for unstable atmospheric conditions and high windspeeds. The convective flux is described by a semi-empirical, analytical expression involving air temperature, windspeed, the height above the surface at which these parameters are measured, and an aerodynamic roughness height for the modeled surface. Basically, this convection term is capable of describing quantitatively the heat transfer which can take place under the various conditions of stable, neutral, and unstable temperature- and wind-profile combinations which encompass the conditions from laminar flow to turbulent mixing.

23. R. Horvath and D. D. Bornemeier, *Infrared and Photo Record Analysis, Vol. I: A Mathematical Predictive Model for Target Temperature as a Function of Environment*, Report RADC-TR-66-117, Rome Air Development Center, Griffiss Air Force Base, NY, April 1967.

(5) Rain. The intensity (depth/time) and temperature of rain falling on the surface are specifiable as arbitrary (tabular form) functions of time. The immediate thermal effect is accounted for by a temperature equilibrating heat exchange between the water and the surface.

(6) Evaporation. A certain portion of the rainfall (that remaining after runoff) is susceptible to evaporation. In computing the rate of heat transfer resulting from evaporation, an analytical formulation is used which accounts for the effects of wind-turbulent mixing and diffusion in the immediate atmosphere. This term depends on the windspeed, the relative humidity and temperature of the air, and the surface (water) temperature.

The model allows the object to be geometrically described by stacked horizontal layers (maximum of 6), each of arbitrary thermal properties and arbitrary thickness. Hence, to define the object thermally, the density, specific heat capacity, and conductivity of each layer must be specified. In addition, the total solar absorptivity, thermal emissivity, and surface roughness of the top layer must be specified.

The boundary conditions to be imposed on the lower side of the layered object will depend mainly upon the object being modeled, whereas essentially the same form of boundary conditions at the upper surface apply to almost all objects. For example, if one is modeling a roadway, the convenient condition would be to assign a realistic temperature at some depth into the ground below the level of significant temperature fluctuation, say, 6 ft below the surface. Conversely, the bottom-boundary condition may also be specified in terms of meteorologically dependent heat fluxes. If, for example, a bridge spanning a river is being modeled, the underside of the bridge would be subjected to convection by a time-dependent air temperature and wind velocity and also to a radiative exchange with the water in the river; some solar wavelength energy would also impinge on this lower side.

The solution of the partial differential equation requires that the spatial-temperature distribution be specified at some time, $t = t_0$. This distribution is the cumulative result of the effect of the thermal environments which prevailed prior to t_0 . The response of the target to the environments occurring after t_0 will be influenced by the spatial temperature distribution at t_0 . However, this dependence decreases as time increases and finally becomes negligible after an interval comparable to the "time constant" of the system. The model (computer program) uses as input data the time-dependent solar insolation, horizontal windspeed, ambient air temperature, relative humidity, percent cloud cover, and cloud type for many diurnal cycles. Several of these diurnal cycles are normally used to obtain the initial temperature distribution for the start of the subsequent cycles of interest. Thus, initial conditions are fabricated merely by applying realistic meteorological driving forces for sufficient time prior to the days of interest. Experience with the model has shown that 3 to 4 cycles are sufficient to establish the thermal history effects for most modeled objects.

In order to demonstrate the potential utility of such a model, we present the following example of its use. In cooperation with the U.S. Geological Survey and as part of the NASA program, the ERIM-instrumented C-47 aircraft accomplished a data-acquisition mission in the Tampa, Florida area during March 1970. One purpose of this mission was to gather, with thermal-infrared remote-sensing techniques, more detailed information regarding the detectability of incipient sinkhole activity. Previous experience [24] had indicated the feasibility and desirability of such an approach. Thermal modeling of the sinkhole phenomenon was undertaken prior to the mission in order to assist not only in the analysis of the airborne data, but, more significantly, to assist in the mission planning. Specifically, it was desired to predict the optimum mission profile in terms of optimum time of day and weather conditions and expected thermal contrast of the incipient sinkhole in relation to its background.

Sinkhole features, known also to geologists as karst topography, are common in certain areas of Florida. The physical character and development of a sinkhole can be seen schematically in Figure 5. The first element necessary to the process is the presence of limestone bedrock. Florida, of course, is essentially entirely underlain by limestone because of its oceanic sedimentary origins. As a result of the relatively high solubility of limestone as compared to other bedrock, large voids can be formed in the bedrock, usually along fault lines (Fig. 5b). So long as the water remains above the top of the void, mechanical integrity is maintained since the incompressible water counters the downward forces upon the thin limestone arch. However, lowering of the water table, either by natural processes or by man's actions, to a point below the limestone cap leads to an unstable mechanical structure (Fig. 5c) in which the thin limestone arch eventually fails (often catastrophically) under the weight of the unconsolidated overburden (Fig. 5d). This final result is rendered at the surface as a sinkhole with dimensions commonly tens of feet in depth and significantly more in breadth. Unexpected occurrence of such an event can obviously lead to innumerable undesirable consequences, such as shown in Figure 6.

Once a sinkhole has initiated collapse at the surface, any number of remote-sensing approaches can be postulated to detect its presence. However, if the presence of a sinkhole at that point were economically significant in any way, the people or industries involved would no longer need remote-sensor data to apprise them of its presence. Thus, the significant problem is one of predicting such collapse in advance.

24. A. E. Coker, R. Marshall, and N. S. Thomson, Application of Computer Processed Data to the Discrimination of Land Collapse (Sinkhole) Prone Areas in Florida, Proc. 6th Symposium on Remote Sensing of Environment, Vol. I, Ann Arbor, pp. 65-77, October 1969.

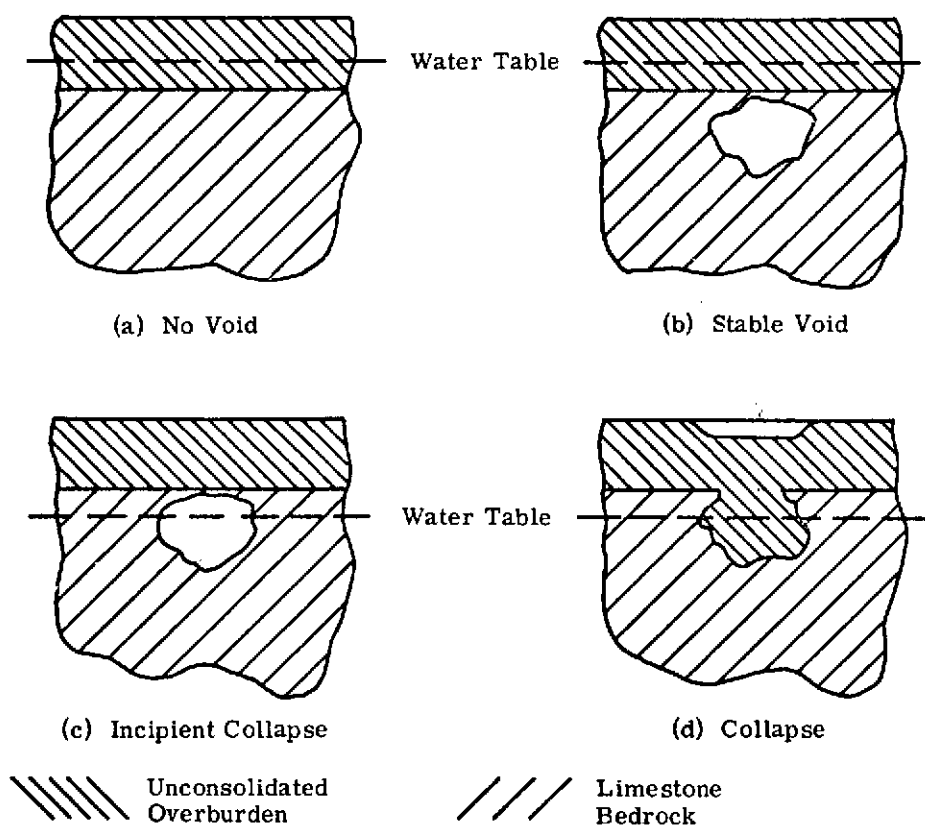


FIGURE 5. PROGRESSIVE STAGES LEADING TO SINKHOLE COLLAPSE

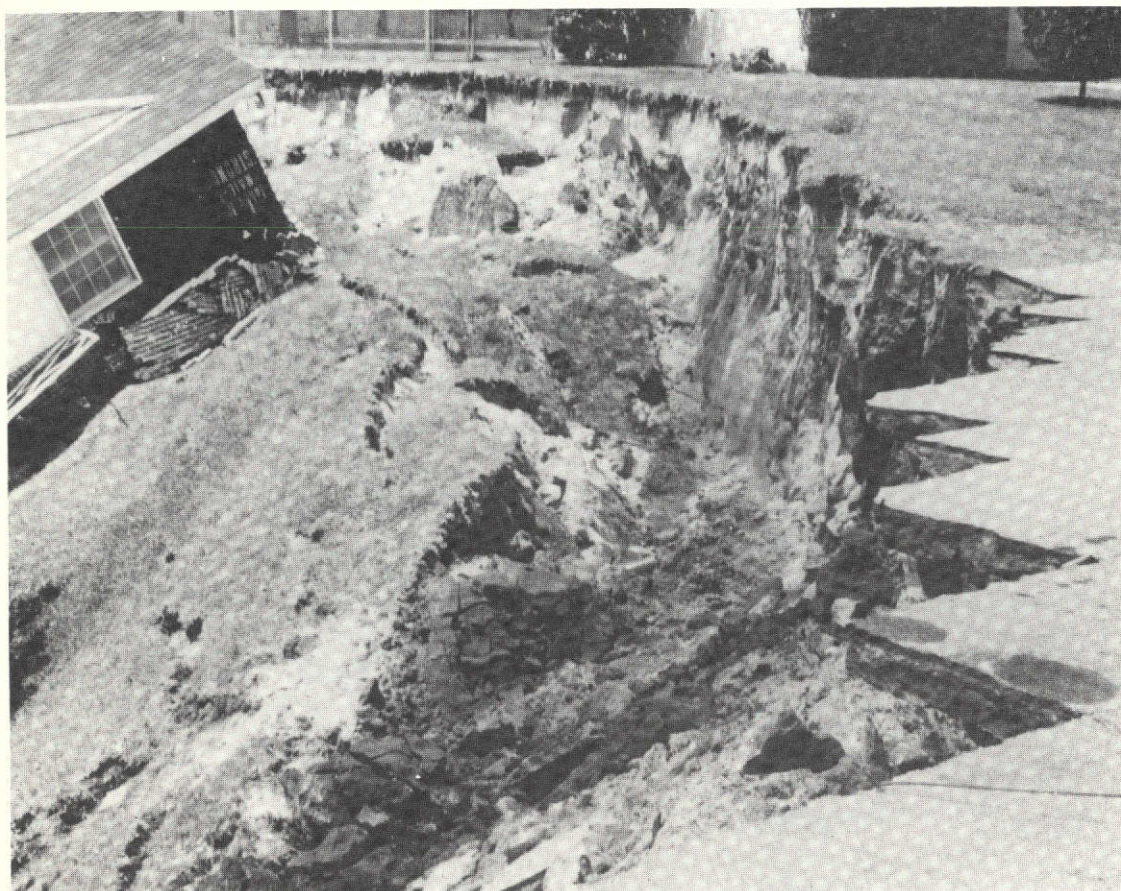


FIGURE 6. SURFACE EXPRESSION OF A COLLAPSED SINKHOLE

One phenomenon which is both characteristic of an incipient sinkhole and significant from an optical remote-sensing standpoint is the effect the opening void in the bedrock has upon the distribution of soil moisture in the overburden. As the water table recedes into the void, a moisture sink is established, which deforms the otherwise straight isomoisture contours and tends to produce a drier zone immediately over the void area. This process is shown schematically in Figure 7. In Florida, where much of the soil is quite sandy, this effect is enhanced by the permeability of the sand. The result, then, is not only a vertical moisture gradient, but also a horizontal moisture gradient of somewhat symmetric circular shape.

It was postulated that the resultant symmetric, horizontal, moisture gradient would produce a symmetric horizontal gradient in surface temperature resulting from the significant variation of thermal properties as a function of soil moisture content. Such generally symmetric temperature effects have been observed previously and correlated to incipient sinkhole activity [24]. While the magnitude of the surface-temperature differentials in question cannot be expected to be extreme, the associated symmetric geometry should facilitate detection within a randomly cluttered scene. The approach thus constituted modeling the parametric effects of moisture content upon the time-varying surface temperature for a soil characteristic of the Tampa area and for a variety of environmental conditions expected in the region during the time of the mission. The results of this modeling would then be analyzed to: (1) determine optimum time and weather conditions for observing such thermal phenomena associated with incipient sinkholes and (2) provide expected temperature differentials available for producing the symmetric thermal anomalies on thermal-infrared imagery.

Soil samples were collected for analysis from a known sinkhole area near Tampa. The collection and analysis were performed under the direction of A. E. Coker, U.S.G.S. (Tampa). The resulting data indicated a sand-organic soil composed in general of 78% (by volume) pure quartz sand and 22% organic matter. Particle sizing indicated that about 85% of the particles were within the diameter range 0.12 to 0.24 mm, with about 5% above this range and 10% below.

Density or compaction measurements were not made for the soil. However, assuming reasonable values of 110 lb/ft³ (dry density) for pure quartz sand and 20 lb/ft³ for pure organic (peat) soil would imply a density of

$$\gamma = (0.78)(110) + (0.22)(20) \approx 90 \text{ lb/ft}^3$$

This value is considered reasonable for a sand-organic soil of this type.

Measurements of soil moisture at the Tampa site indicated a moisture content, W , of about 0.10 to 0.12 (mass of water per unit dry masses of soil) near the surface, and values near 0.06 to 0.08 at and below the 1-ft depth. This moisture inversion was the result of rainfall several days prior to sampling. Soil-moisture measurements were also performed upon samples

taken from an established sinkhole. The values obtained were anomalously large because the depressed surface acted as a catch basin, particularly since an impervious, hardpan stratum was also present under the surface. Neither of these conditions is typical of an incipient sinkhole, and the high values of soil moisture obtained were not considered relevant to the problem under investigation.

The field measurements of moisture content resulted in the definition of two general vertical profiles representative of expected terrain conditions. For each of these profiles, two degrees of anomalous drying caused by incipient sinkhole activity were postulated, thus leading to four possible target (incipient sinkhole) to background (general terrain) comparisons. The soil-moisture profiles defined as shown in Table 2.

Experimentally determined values of the thermal properties of a sand-organic soil of the Tampa type are not available in the literature. However, rather detailed data is available for the individual constituents, including the parametric effects of moisture content and compaction [25]. These data were used as inputs to standard theoretical techniques [26] to determine the thermal properties of the mixture defined earlier. The results are shown graphically in Figure 8. The only assumption necessary in deriving the thermal properties of this soil concerned the way in which soil water would be associated with each constituent. It was assumed that the moisture was distributed such as to produce equal degrees of saturation in each constituent. This assumption resulted in approximately 60% of the water being associated with the sand and 40% with the organic material.

Computation of the meteorologically dependent heat fluxes at the upper surface requires specification of the surface's solar absorptance, thermal emittance, and surface roughness. No measurements of these quantities were made. However, literature data indicate that the expected range of variability for the soil type in question is not great [26, 27]. The following values were chosen as representative of the soil in question within the range of near-surface moisture content applicable:

25. M. S. Kersten, *Laboratory Research for the Determination of the Thermal Properties of Soils*, Engineering Experiment Station, University of Minnesota, Minneapolis, 1949.

26. W. R. VanWijk, *Physics of Plant Environment*, North Holland Publishing Co., Amsterdam, 1963.

27. R. Geiger, *The Climate Near the Ground*, Harvard University Press, Cambridge, 1965.

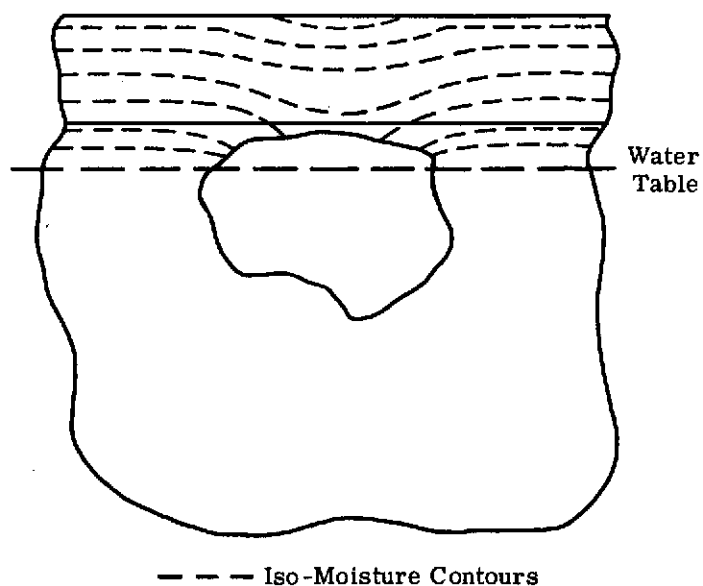


FIGURE 7. SINKHOLE-INDUCED MOISTURE STRESS

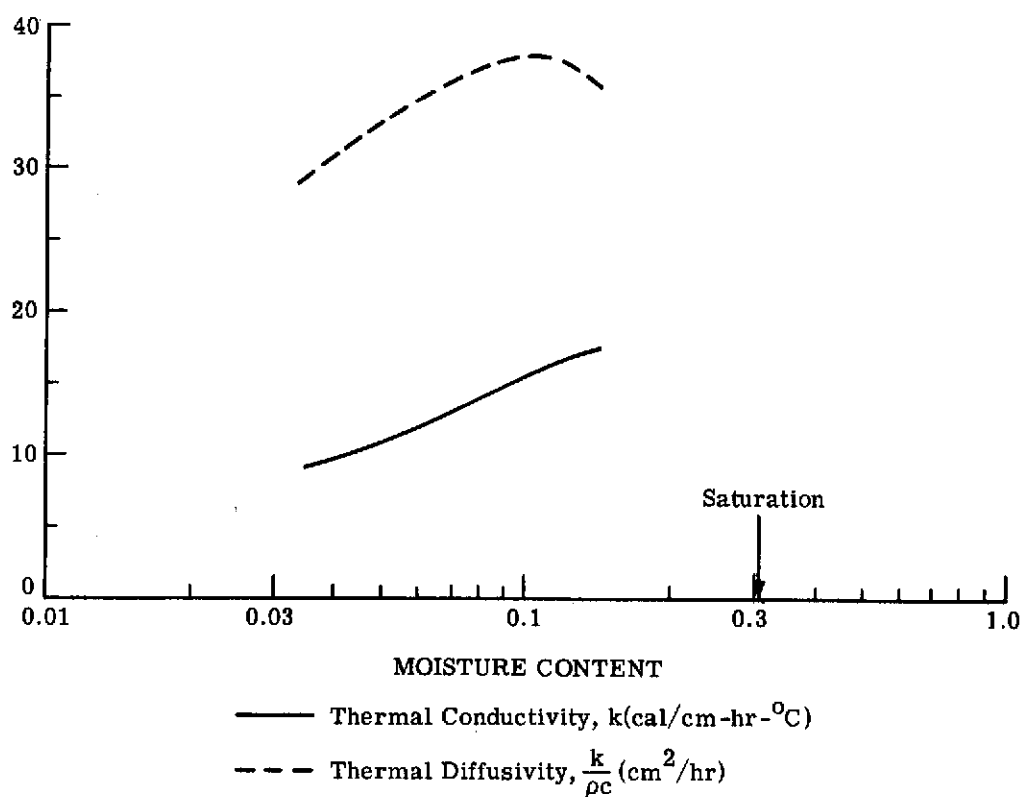


FIGURE 8. THERMAL PROPERTIES OF TAMPA SOIL AS A FUNCTION OF GRAVIMETRIC MOISTURE CONTENT

Solar Absorptance = 0.70

Thermal Emittance = 0.95

Aerodynamic Surface Roughness = 1.0 cm

The boundary heat fluxes determining the total heat flux at the upper soil surface require specification of the following time-varying meteorological parameters: solar irradiance, air temperature, relative humidity, windspeed, and cloud cover. Climatological records for the Tampa area were obtained in order to determine the range of values expected during the month of March when the remote-sensing mission would be flown. Analysis of these data, combined with some subjective judgments as to what factors were significant to the problem, led to the specification of three typical diurnal meteorological cycles. The basic difference between these three cycles is the degree of cloud cover. Three values, 0.0, 0.5, and 0.9, were chosen. The heat-flux components thus affected directly were the solar irradiance and the thermal-infrared irradiance from the sky hemisphere onto the surface. The meteorological description of these three diurnal cycles is shown in Figure 9. By means of various permutations of these three diurnal cycles, eight typical 9-day meteorological sequences were defined. These are shown in Table 3.

The bottom-boundary condition was chosen as a constant temperature of 59.7°F at a depth of 100 cm, independent of moisture content. The assumption of a constant temperature at the 100 cm depth is valid for soils over a 9-day period. The assumption that this temperature will be independent of moisture content is not strictly true. However, it is difficult to predict a priori exactly how the moisture content will affect the temperature. In any case, the effect upon the calculated surface temperature of a slightly erroneous temperature specification at the 100 cm depth would not be great, and the effect upon the calculated surface temperature difference between similar soils of slightly different moisture content would be even less significant.

Identical initial soil-temperature conditions were specified for all data runs. The error introduced into the calculations by forcing all soil profiles to start with the same temperature distribution is essentially negligible after several diurnal cycles of computation, during which temperature profiles appropriate to the specific thermal properties of a given soil profile will have developed. One consequence is that the surface-temperature data from the first few days in each meteorological sequence cannot be considered realistic and, thus, cannot be used in subsequent analyses.

Each of the six soil profiles (Table 2) were assigned appropriate thermal properties (Fig. 8) and modeled into each of the eight 9-day weather sequences (Fig. 9 and Table 3) to produce forty-eight 9-day sequences of calculated surface temperatures. By comparing calculated surface temperatures for each of the four sinkhole-background sets for the 23 unique, diurnal cycles shown in Table 3, a total of 92 unique, diurnal cycles of surface-temperature contrast

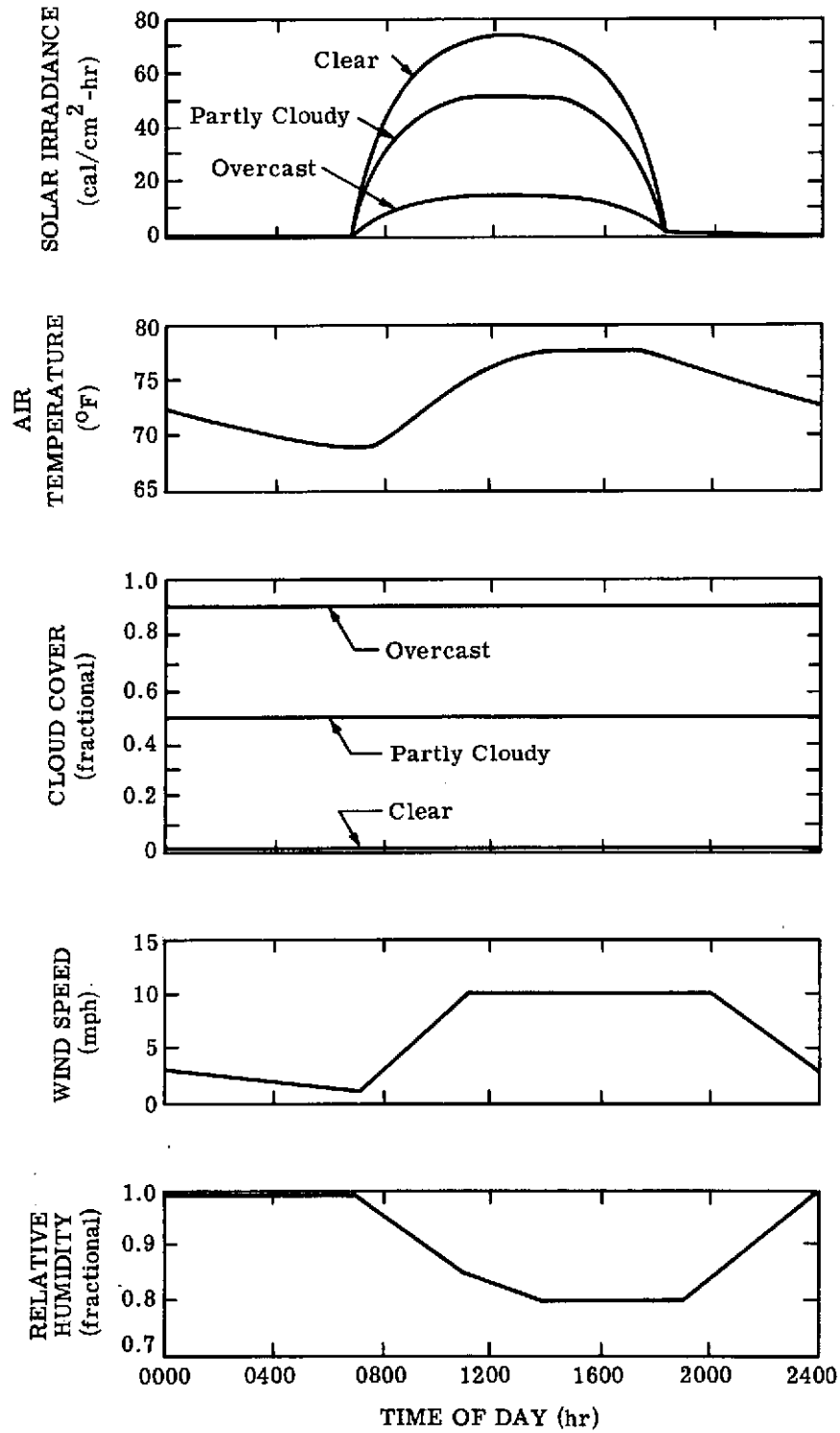


FIGURE 9. TYPICAL DIURNAL VARIATION OF METEOROLOGICAL PARAMETERS FOR TAMPA IN MARCH

TABLE 2. SOIL-PROFILE DESCRIPTIONS

Profile	Description	Moisture Content, W		
		(0 - 10 cm)	(10 - 20 cm)	(20 - 100 cm)
Ia	General background	0.12	0.10	0.06
Ib	Slight drying	0.10	0.08	0.04
Ic	Moderate drying	0.08	0.06	0.03
IIa	General background	0.10	0.085	0.06
IIb	Slight drying	0.08	0.06	0.04
IIc	Moderate drying	0.06	0.05	0.03

TABLE 3. METEOROLOGICAL SEQUENCES. C = clear.
PC = partly cloudy. OC = overcast.*

Sequence	1	2	3	4	5	6	7	8	9
I	C	C	C	C	C	C	C	C	C
II	C	C	C	C	C	OC	C	C	C
III	C	C	C	C	C	OC	OC	C	C
IV	C	C	C	C	C	OC	OC	OC	C
V	C	C	C	C	C	PC	OC	OC	C
VI	C	C	C	C	C	PC	PC	OC	PC
VII	C	C	C	C	C	PC	PC	PC	OC
VIII	C	C	C	C	C	PC	PC	PC	C

*The 23 days to the right of the dashed line represent those diurnal cycles which are unique in terms of the sequence of meteorology prior to and during them. The days to the left of the dashed line are either redundant or represent the days used to establish realistic initial temperature conditions.

(difference) between an incipient sinkhole and its surrounding terrain were produced. These 92 diurnal cycles of temperature contrast provided the data necessary to determine the parametric effect of (1) general terrain moisture, (2) degree of drying over sinkhole, (3) instantaneous meteorology, and (4) past meteorology upon the thermal contrast of an incipient sinkhole to its background.

Figure 10 depicts the extremes in absolute surface temperature predicted for the several soil profiles. The surface temperature of the soil on a clear day (preceded by clear days) varied from a minimum of about 60°F at dawn to a maximum of about 120°F during mid-day. However, as might be expected, the variation on an overcast day (preceded by overcast days) varies only from 68°F to 83°F. All soil states exhibited similar diurnal temperature variations within about $\pm 5^\circ\text{F}$ during the day and $\pm 3^\circ\text{F}$ at night.

The temperature difference between two objects of only slightly different thermal properties is normally greatest when the thermal driving forces are at a maximum. Thus, it would be expected that maximum thermal contrast between an incipient sinkhole and its background would be largest for the clear-sky conditions. This fact is demonstrated in Figure 11 which shows the thermal contrast (surface temperature difference) between an incipient sinkhole and its background for the same conditions as in Figure 10. Near sunrise and under clear skies, the sinkhole surface is about 2°F cooler than the background terrain; in the midafternoon, it is about 5°F warmer. For overcast conditions, however, the thermal contrast is much smaller and less variable diurnally, being always positive and never more than 1.3°F.

Each of the 92 unique, diurnal cycles of temperature contrast exhibited variations roughly within the extremes shown in Figure 10. The following general conclusions for mission planning were indicated. (All times stated are Eastern Standard Time and are based upon a 0625 hours sunrise and an 1835 hours sunset at the position 28°N, 82°W on 16 March.)

- (1) Under optimum conditions (clear skies and at least a moderate degree of drying over the sinkhole), thermal contrasts would be equal to or greater than $+5^\circ\text{F}$ during the afternoon and -3°F at night.
- (2) Thermal detection of incipient sinkholes would be highly unlikely whenever the cloud cover exceeded 60%.
- (3) Thermal detection of incipient sinkholes would be highly unlikely whenever the degree of drying over the sinkhole was less than moderate.
- (4) Optimum thermal contrasts would occur between 1200 and 1700 hours (positive contrast) and between 0400 and 0630 hours (negative contrast).
- (5) Detectable thermal contrasts would occur at the optimum times if a heavily clouded condition changes to an essentially clear condition at least 5 hours prior to that time.

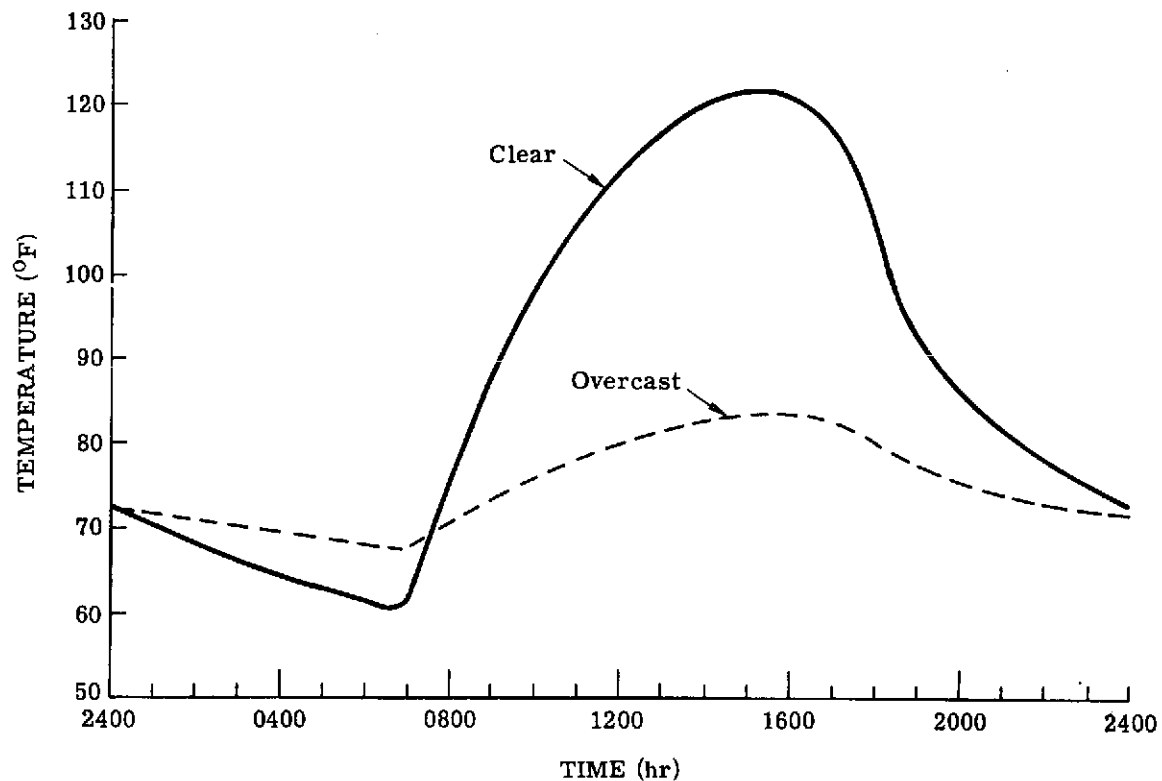


FIGURE 10. DIURNAL SURFACE TEMPERATURE FLUCTUATIONS OF TAMPA SOIL FOR TWO WEATHER CONDITIONS

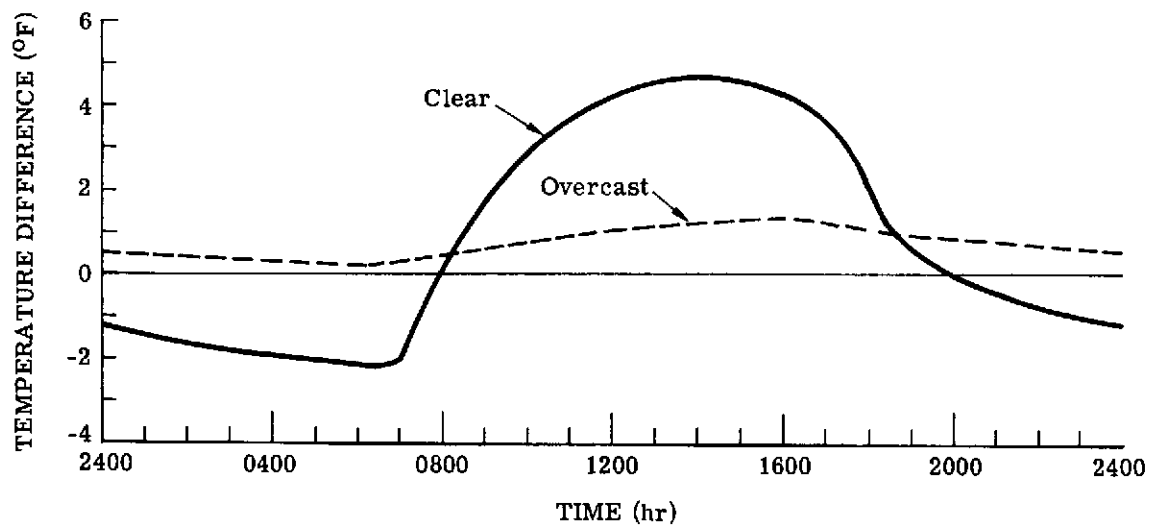


FIGURE 11. TEMPERATURE CONTRAST OF SINKHOLE TO ITS BACKGROUND FOR TWO WEATHER CONDITIONS

- (6) The most inopportune flight times for any weather condition would occur between 0700 and 0830 hours and between 1800 and 0100 hours.

These criteria were used to establish an optimum mission profile for the March 1970 field exercise at Tampa. Unfortunately, the weather degraded to the point where the entire mission had to be cancelled. Data collection was subsequently rescheduled to September 1970 and was accomplished. The mission profile was again established based upon the thermal modeling conclusions. The only changes required were in terms of specification of optimum flight time. These times were altered slightly in view of the difference in sunrise-sunset times between September and March. All other conclusions were considered applicable to either time of year. The general meteorological differences would have little effect upon the temperature contrast of an incipient sinkhole to its background even though the absolute temperatures of either would undoubtedly be affected.

Geological Models

The problems encountered in geological remote sensing differ in several aspects from remote sensing problems with vegetative targets. First, temporal changes for geological targets are much slower than for vegetative ones. Second, for rock-type identification, variations in spectral emittance or reflectance are much more important than geometrical variations (in shape, shadowing, observation angle, etc.) across the scene, whereas both are relatively important for the identification of vegetative targets. Third, the thermal-IR spectral region contains more information than the visible-reflective IR wavelength regions concerning the chemical composition of rocks, whereas the converse is true for vegetative targets.

In the thermal-IR region rocks and minerals present a special problem not normally encountered in the shorter wavelength regions. Thermal IR wavelengths ($\approx 10 \mu\text{m}$) dimensionally approach the particle diameters of some of the grains in fine-textured rock surfaces, and this produces some complex optical phenomena related to surface roughness. For instance, Lyon [28] and other investigators have noted that the spectral emittance within the major reststrahlen bands (interatomic vibration modes in this case) of silicate rocks and minerals tends to increase with decreasing particle size. Later work [29] has shown that in spectral regions of moderate to small complex refractive index outside the reststrahlen bands (which are associated with a large complex refractive index), the emittance can either increase or decrease with decreasing particle size.

28. R. J. P. Lyon, Evaluation of IR Spectrophotometry for Compositional Analysis of Lunar & Planetary Soils: Rough and Powdered Surface, Final Report, Part II, NASA Contract NASr-49(04), Stanford Research Institute, Menlo Park, 1964.

29. R. K. Vincent and G. R. Hunt, Infrared Reflectance from Mat Surfaces, Applied Optics, Vol. 7, p. 53, 1968.

The dependence of spectral emittance on particle size is an important factor in geological remote sensing, because textural variations from rock to rock may mask differences in chemical composition, and vice versa. It is therefore necessary to separate, insofar as possible, the textural and chemical effects on the spectral emittance. To gain insight into this problem, a model of rough rock and mineral surfaces is sought which can at least qualitatively explain the effect of textural variations on the IR spectrum of those surfaces.

Two models were selected to describe qualitatively the effects of surface roughness on the infrared spectral emittance of rock and minerals. Both models require the calculation of single-particle scattering parameters and emittance of a homogeneous, semi-infinite, optically thick "cloud" of particles with a radiative transfer model devised by Conel [30]. The contribution under this contract was to extend Conel's theory to account for birefringence effects which, in the infrared wavelength region, are important for most natural geologic materials.

Rather than further describe the two models here, we refer the interested reader to ERIM Report No. 190100-30-T, Ref. [31], and present below some of the conclusions resulting from the development of the two models.

Two methods were developed for modeling the spectral emittance of irregular rock surfaces. One method can be used only for simple monomineralic rocks consisting of uniaxial crystals, while the other can be applied to any kind of rock. More laboratory data are required to evaluate the accuracy of both methods, though the second method is preferred for its slightly better correlation with laboratory spectra and also for its simpler procedure.

As a part of this effort, the spectral emittances of two minerals (quartz and calcite) and four rocks (limestone, chert, dunite, and andesite) were calculated. The results indicate that for silicate rock surfaces, texture* does not control spectral emittance as much as chemical composition, as long as the diameters of particles comprising the surface are on the order of 30 μm or greater—which is the case for most rocks not covered with products of weathering. The relevance of these results to geological remote sensing is that variations of texture indigenous to silicate rock genesis most likely will not mask the effect of rock composition on spectral emittance in the 8-14 μm wavelength region. Still other effects could seriously impair

30. J. E. Conel, Infrared Emissivities of Silicates: Experimental Results & a Cloudy Atmosphere Model of Spectral Emission from Condensed Particulate Mediums, *J. Geophys. Res.*, Vol. 74, p. 1614, 1969.

31. R. K. Vincent, New Theoretical Methods in Ratio Imaging Techniques Associated with the NASA Earth Resources Spectral Information Systems, ERIM, Ann Arbor, Report 190100-30-T, 1973.

*Texture here refers to size of crystals or other particles composing the rock.

compositional remote sensing of silicate rocks in the thermal-infrared wavelength region; these might arise, for example, from layers or coatings of weathering products, which in some cases can be an optically thick covering composed of very fine particles. The effects of such coverings on the spectral emittance of naturally-exposed rock surfaces have not been adequately investigated; the second model would no doubt be useful in such a study. For carbonate rocks, textural effects on spectral emittance can be appreciably large, though not of such a nature as to cause misidentification of carbonates as noncarbonates. These effects may eventually be helpful for determining the effective particle sizes of remote carbonate target surfaces, which in some cases may exhibit meaningful spatial patterns. For instance, coral beach sands are composed primarily of CaCO_3 , and are sometimes graded into well-ordered particle size distributions by wave action. The production of infrared ratio images for one spectral channel in the 11.1-11.6 μm region and another in the 10.6-11.1 μm region may not only be useful for identifying the presence of carbonates, but possibly for also mapping gradations in particle sizes. Laser scanners of the future most likely will be additionally useful for discriminating among carbonate rocks on the basis of the spectral position of the sharp feature near 11.4 μm .

Before either of the models in this report can be made quantitatively useful, a laboratory program is needed whereby samples are polished, measured for spectral reflectivity, ground up to various particle sizes, and again carefully measured. This would allow calculated emittances to be compared with lab spectra of the same rock samples. Should this comparison produce positive results, the models would then need to be expanded to permit calculation of spectral emittances and transmittances of aerosol clouds or irregular rock surfaces with a range of particle diameters, instead of using one effective particle diameter to describe the cloud or rock surface. Following these two steps, attempts could then be made to make the models quantitatively accurate.

Vegetative Canopy Reflectance Model

The need for the identification of vegetative canopies and the detection of stresses in vegetative canopies by remote sensing techniques has continued to grow in economic importance. The management of natural resources, such as forests and wetlands, and the prediction of yields and assessment of pest damage of agricultural crops require survey techniques that are both timely and economical in order to supply the basic information for the formulation and execution of effective management strategies.

The major weakness of present remote sensing techniques is the difficulty in relating subtle reflectance differences to the elemental causative factors which could be recognized and classified by botanists on the ground. Unless some insight is achieved in connecting causative factors with detected effects, there is no foundation for claiming that a specific cause is uniquely coupled with a detected effect. Certain detected effects could have spurious causes which may be

transient and fundamentally unconnected with the condition of interest to the remote sensor user, even though the occurrence of the detected effect appears to be associated with this condition at any one time and location.

Under this contract, partial support was provided for the development of a vegetative canopy model. This canopy model, developed by Dr. Gwynn Suits of ERIM [32-37], is an extension of the Allen, Gayle, Richardson (AGR) model [38]. This extension overcomes the principal difficulty with many of the previously available plant canopy models in that they do not account for directional reflectance changes as a function of view angle, nor do they permit changes in reflectance of the canopy to be traceable to the specific causative factors of geometric and spectral changes in a particular class of components within the canopy.

In the Suits model the canopy is divided into a number of infinitely extended horizontal canopy layers. Within each layer, the components of the canopy are considered to be randomly distributed and homogeneously mixed. Figure 12 illustrates the geometry of the model.

Many vegetative canopies have a distinct layer structure. Wheat, for example, produces the grain at the top layer of the canopy, while the stalk and leaves occupy a second layer. In a mature corn field, corn tassels occupy the top layer while leaves and ears occupy a second layer. A leaf slough-off layer may occur as a lower third layer. Forests frequently exhibit a layered structure with the components of different species occupying different layers. The order and content of these layers will affect the canopy directional reflectance. The lowest layer is always bounded by the soil.

32. G. H. Suits, R. K. Vincent, H. M. Horwitz, and J. D. Erickson, Optical Modeling of Agricultural Fields & Rough-Textured Rock & Mineral Surfaces, ERIM Report 31650-78-T, 1973.

33. G. H. Suits, Prediction of Directional Reflectance of a Corn Field Under Stress, Presented at 4th Annual Earth Resources Program Review, NASA/MSC, Houston, ERIM Report 31650-95-S, 1972.

34. G. H. Suits, The Calculation of the Directional Reflectance of a Vegetative Canopy, Remote Sensing of Environment, 2, pp. 117-25, 1972.

35. G. H. Suits and G. R. Safir, Verification of a Reflectance Model for Mature Corn with Applications to Corn Blight Detection Remote Sensing of Environment, 2, pp. 183-92, 1972.

36. G. H. Suits, The Cause of Azimuthal Variations in Directional Reflectance of Vegetative Canopies, Remote Sensing of Environment, 2, pp. 175-82, 1972.

37. G. R. Safir, G. H. Suits, and M. V. Wiese, Application of a Directional Reflectance Model to Wheat Canopies Under Stress, International Conference on Remote Sensing in Arid Lands, November 9, 1972, Tucson, Arizona.

38. W. A. Allen, T. V. Gayle, and A. J. Richardson, Plant-Canopy Irradiance Specified by the Duntley Equations, J. of the Optical Soc. of Amer., 60, 372, 1970.

Each component of the canopy, such as a leaf or stalk, is idealized as a combination of vertically and horizontally oriented, flat, diffusely reflecting and transmitting panels. The size and spectral properties of the panels are obtained from physical measurements of canopy components. In general, the objective is to determine the size of panels which would intercept the same amount of radiant flux as would the component. The projections of a component on horizontal and vertical planes define panel areas which are fairly close to meeting this criterion while retaining geometric simplicity for the model. Component projections are used to calculate optical cross sections in this model as illustrated in Figure 13. The laboratory hemispherical spectral transmittance and reflectance of the component are taken to be those of the radiatively equivalent panels of the model.

Thus, every physical part of a plant yields two kinds of model components—vertical and horizontal—the sizes and number of which can be found from physical measurements of representative plants. If a plant canopy is stressed by some pathogen, or environmental condition, the changes in plant component geometry induced by the stress led in a cogent fashion to a corresponding change in the sizes of model panels. For instance, moisture stress causes leaves, which are normally horizontal, to droop. The vertical components of the model then increase in area at the expense of horizontal components of the model to correspond to the geometric change in orientation of leaves. If all other factors governing canopy reflectance are considered fixed, the calculated change in canopy reflectance can be attributed to the drooping of the leaves alone.

This improved model differs from previous models in three respects. First, it allows for more than one canopy layer, whereas past models have been monolayered. This is an important feature because it offers a means to account for greatly different plant components at various heights above the ground. For instance, corn tassels differ in shape and color from corn leaves and stalks; in this model, a top layer would primarily consist of corn tassels (just before harvest) and lower layers would be composed of leaves and stalks. Secondly, this model actually relates laboratory spectra of plant components (leaves, stalks, etc.) and approximate plant geometry (planting density and average horizontal and vertical component cross-sections) to the reflectance of the crop field. Heretofore, empirical constants were used to calculate field reflectance. Thirdly, unlike the Lambertian field reflectance assumptions of previous models, this model allows for the calculation of bidirectional reflectance of a field crop. The model has been verified for two corn fields, with worst-case errors of approximately 15% [35, 36]. Other verification is underway for certain grass canopies—e.g., wheat [37].

Radiative Transfer Model

Many problems associated with target recognition and image interpretation in remote sensing are caused by the presence of Earth's atmosphere. One problem is clearly evident in

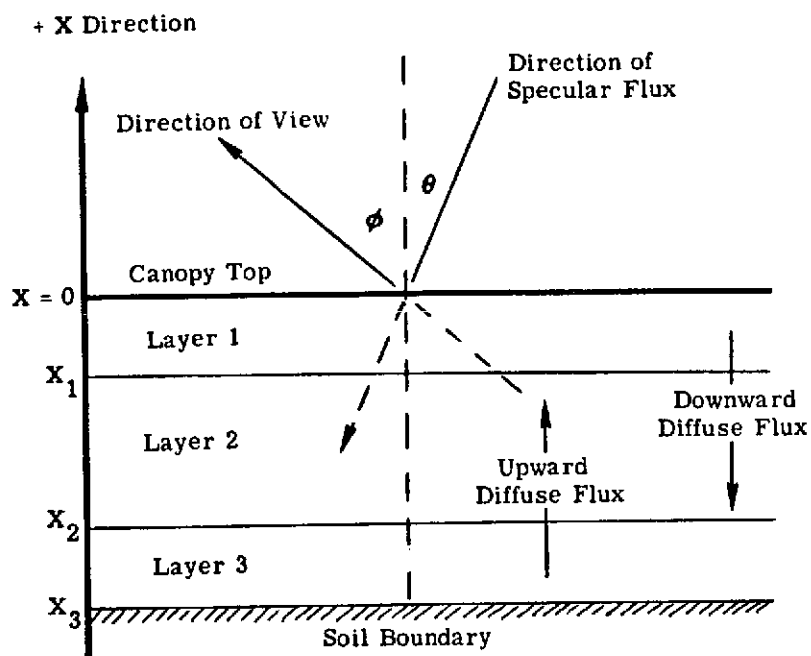


FIGURE 12. IDEALIZED LAYER STRUCTURE OF A CANOPY

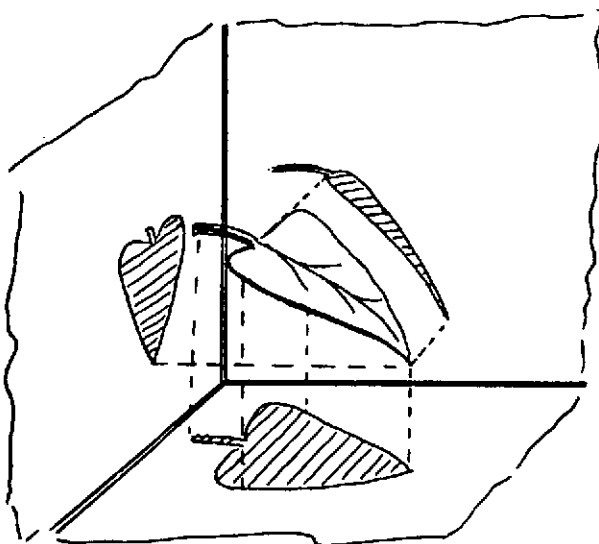


FIGURE 13. OPTICAL CROSS-SECTIONS BY PROJECTIONS

photographs of the Earth's surface taken from orbiting spacecraft. The general bluish tint in many of these photographs arises from radiation that has been scattered one or more times by the molecules and particulate material which compose the atmosphere. This scattered radiation adds to the received signals spectral variations which are not truly representative of surface features.

Since most remote sensing operations involve observation paths within or through Earth's atmosphere, each investigator must consider the effects of the atmosphere on the radiation signals produced by the sensors as well as the consequent effects on his use and interpretation of the data. If the atmospheric effects on the signals are serious enough, he should then consider ways and means of reducing or overcoming these effects.

Atmospheric haze has several deleterious effects on remote sensor data, no matter whether such data be in the form of imagery or of electrical signals processed on computers. First, haze reduces the visual contrast between adjacent surface features and makes imagery interpretation more difficult. In Figure 14 one can see that contrasts are reduced on images obtained in two spectral bands at 5000-ft altitude as compared to similar images obtained at the 2000-ft altitude.

Second, as a result of scattering in the atmosphere, the spectral distribution of radiation received by a detector is different from that which originates at the ground surface, i.e., the atmospheric effects are more pronounced at some wavelengths than at others. For example, in Figure 14, the effect of the haze is much greater for the wavelength band, 0.55-0.58 μm , than for the band at longer wavelengths, 0.80-1.0 μm . It is this spectral dependence of scattering which accounts for the blueness in color photography and color-composite imagery taken from high-altitude aircraft and spacecraft.

Finally, atmospheric effects can reduce the amount and quality of information that can be extracted from the data by computer processing. That is, the first two effects discussed with regard to imagery and its interpretation are also important in the recognition processing of multispectral remote sensor data. The effects of atmospheric haze can reduce the recognition computer's ability to discriminate between surface materials that resemble each other, and can limit the extent of the area over which satisfactory recognition results can be easily obtained.

For immediate application to problems of discrimination in remote sensing, a user needs a simplified, workable model which can be applied to a wide range of atmospheric and surface conditions with a minimum of computational effort. Under this contract we have developed such a model. Our model is especially equipped to deal with plane-parallel, homogeneous,* hazy atmospheres, under a variety of situations.

*By homogeneous, we mean that the proportions of constituents are constant throughout all altitudes, even though the actual density varies drastically with altitude.

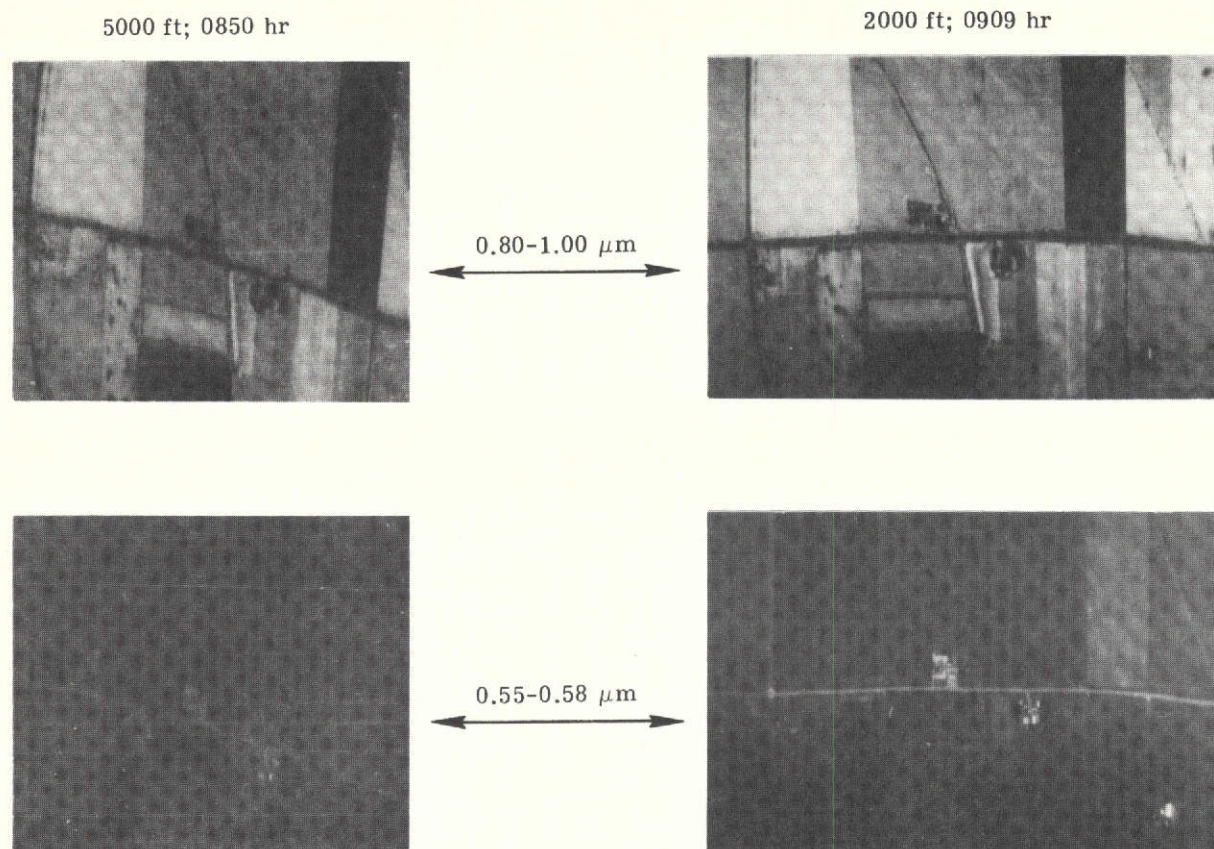


FIGURE 14. EFFECTS OF ATMOSPHERIC BACKSCATTER AS FUNCTIONS OF WAVELENGTH REGION AND ALTITUDE. Agricultural areas near Ann Arbor, Michigan; 3 September 1969.

Realizing that aerosol scattering occurs predominantly in the forward direction, we can approximate the phase function by a sum of delta functions, i.e.,

$$p(\mu, \phi, \mu', \phi') = F\delta(\mu - \mu')\delta(\phi - \phi') + B\delta(\mu + \mu')\delta(\pi + \phi - \phi') \quad (1)$$

where $F = 4\pi\eta$ and $B = 4\pi(1 - \eta)$, p being the fraction of the radiation which is scattered into the forward hemisphere. Inserting Eq. (1) into the following radiative transfer equation:

$$\mu \frac{dL}{d\tau} = L(\tau, \mu, \phi) - \frac{1}{4\pi} \int_0^{2\pi} \int_{-1}^1 p(\mu, \phi, \mu', \phi') L(\tau, \mu', \phi') d\mu' d\phi' - \frac{E_s(\tau)}{4\pi} p(\mu, \phi, -\mu_0, \phi_0) \quad (2)$$

allows us to separate the equation into two simple differential equations. $E_s(\tau)$ is the attenuated solar spectral irradiance, and $\mu_0 (= \cos \theta_0)$, ϕ_0 are the coordinates of the sun. Assuming a surface reflectance of zero, we solve the equations for the spectral irradiances in the upward and downward hemispheres at any optical depth τ . Then, assuming a perfectly diffuse surface reflectance, we find the radiation field resulting from surface reflection and combine these irradiances to determine a "source" radiance, i.e.,

$$L(\tau, \mu, \phi) = \frac{1}{\mu_0} \left[E'_+(\tau) \delta(\mu - \mu_0) \delta(\pi + \phi_0 - \phi) + E'_-(\tau) \delta(\mu + \mu_0) \delta(\phi - \phi_0) \right] + \frac{E''_+(\tau) + E''_-(\tau)}{2\pi} \quad (3)$$

where $L(\tau, \mu, \phi)$ represents the source radiance and is to be inserted into the integral of Eq. (2). Equation (2) can then be solved to determine the spectral sky radiance and the spectral path radiance at any point in the atmosphere. The boundary conditions for the spectral radiance are:

$$L(0, -\mu, \phi) = 0 \quad (4)$$

$$L(\tau_0, \mu, \phi) = \int_0^{2\pi} \int_0^1 \mu' \rho(\mu, \phi, -\mu', \phi') \tilde{L}(\tau_0, -\mu', \phi') d\mu' d\phi' \quad (5)$$

where $\rho(\mu, \phi, -\mu', \phi')$ is the bidirectional reflectance of the surface and $\tilde{L}(\tau_0, -\mu', \phi')$ is the total (direct plus diffuse) spectral radiance at the surface. It should be noted that for the case of a perfectly diffuse (Lambertian) surface, Eq. (5) reduces to

$$L(\tau_0, \mu, \phi) = \frac{\rho}{\pi} \tilde{E}_-(\tau_0) \quad (6)$$

where ρ is the hemispherical reflectance, and $\tilde{E}_-(\tau_0)$ is the total downward irradiance at the surface.

Finding the radiance in terms of optical depth τ instead of altitude h allows one to modify the state of the atmosphere without affecting the radiative transfer calculations. In the model

currently being used at ERIM, we utilize the optical depth-altitude-wavelength relationship as determined by Elterman [39] for visual ranges from 2 to 23 km. The actual scattering phase functions for a haze, taken from Deirmendjian [40], are then used in the solution of the radiative transfer equation. Assuming some surface reflectance, we can then determine the spectral radiances in the atmosphere for a variety of conditions. An outline of the general capabilities of our current radiative transfer program is illustrated in Figure 15.

The ultimate test for the validity of any theoretical model lies in its agreement with experiment. In Figure 16, a comparison is made between calculations made with our model and experimental data obtained by Ivanov [41].

Since its initial development, numerous improvements have been made to the model. Among these is an ability to handle anisotropic scattering phase functions, inhomogeneous atmospheres, and aerosol absorption. To date, the effects on target radiation of transmittance, path radiance wavelength, sensor altitude, surface albedo, sensor scan angle, solar altitude, and atmospheric state have been investigated. (See Figs. 3 and 4 for sample output plots.) In addition to the better understanding of radiative transfer processes which has been achieved, the model is beginning to be used to establish corrections for application to satellite multispectral scanner data. (For more details see Refs. [42-54].)

39. L. Elterman, Vertical-Attenuation Model with Eight Surface Meteorological Ranges 2 to 13 Kilometers, AFCRL-70-0200, Air Force Cambridge Research Laboratories, Bedford, Mass., 1970.

40. D. Deirmendjian, Electromagnetic Scattering on Spherical Polydispersions, American Elsevier Publishing Co., Inc., New York, NY, 1969.

41. A. I. Ivanov, Spectral Brightness of the Sky, Atmospheric Optics, N. B. Divari, ed. Consultants Bureau, New York, NY, 1970.

42. R. Horvath, M. Spencer, and R. Turner, Atmospheric Correction and Simulation of Space-Acquired Remote Sensor Data: 0.4 to 1.0 μm Spectral Range, The University of Michigan (WRL), Ann Arbor, Report 10657-5-F.

43. D. Anding, R. Kauth, and R. Turner, Atmospheric Effects on Infrared Multispectral Sensing of Sea-Surface Temperature from Space, The University of Michigan (WRL), Ann Arbor, Report 2676-6-F.

44. R. Turner, Simulation Analysis of Systematic Effects of Multispectral Scanner Data, Presented at a Review Meeting for Atmospheric Studies in the NASA SR&T Work, Houston, January 21, 1972, The University of Michigan (WRL), Ann Arbor, Report 31650-108-S.

45. W. A. Malila, R. B. Crane, C. A. Omarzu, and R. E. Turner, Studies of Spectral Discrimination, The University of Michigan (WRL), Ann Arbor, Report 31650-22-T, May 1971.

46. R. Turner, W. Malila, R. Nalepka, Importance of Atmospheric Scattering in Remote Sensing, or Everything You've Always Wanted to Know About Atmospheric Scattering But Been Afraid to Ask, Seventh International Symposium on Remote Sensing of Environment, Ann Arbor, June 1971.

47. W. Malila, R. Crane, R. Turner, Information Extraction Techniques, The University of Michigan (WRL), Ann Arbor, Report 31650-74-T, June 1972.

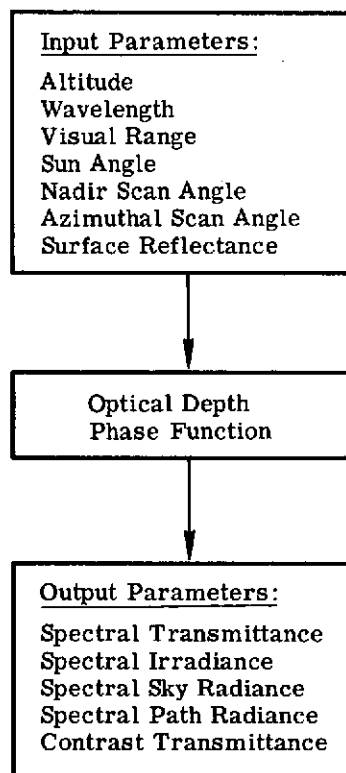


FIGURE 15. ERIM'S RADIATIVE
TRANSFER MODEL FOR HAZY
ATMOSPHERES

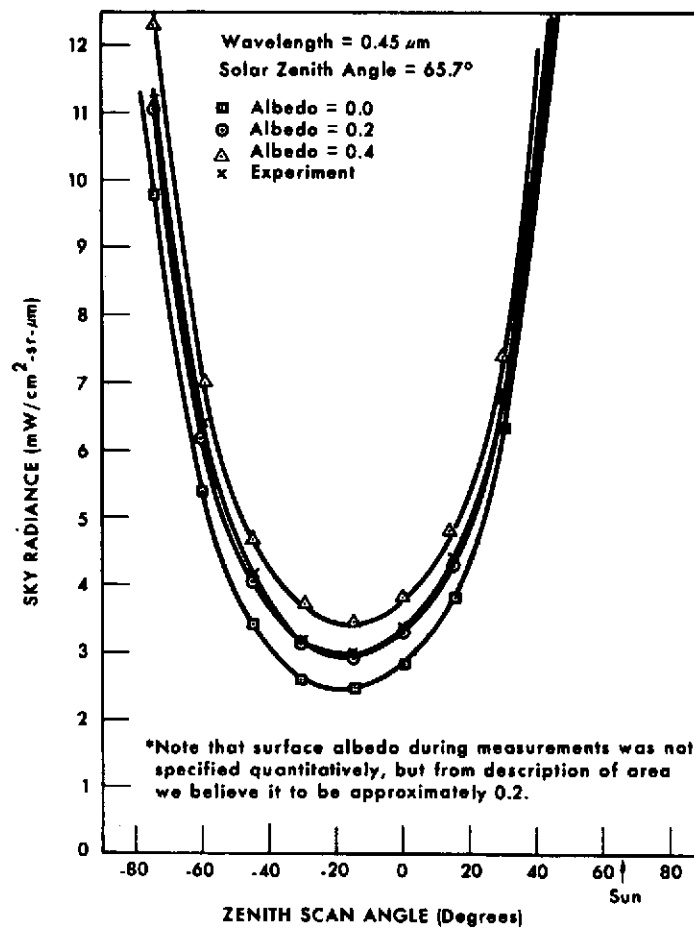


FIGURE 16. DEPENDENCE OF SKY RADIANCE ON
ZENITH ANGLE IN SOLAR PLANE FOR CLEAR SKY
CONDITIONS

3.2.2 EMPIRICAL DETERMINATION OF EFFECTS OF VARIATION

During the contract there were numerous empirical studies to determine the effects of variation in the data. These studies examined the variation of data as a function of haze, altitude, and time of day. Brief discussions follow on each of these studies as well as one other which addressed the appropriateness of the Gaussian or multivariate normal signal distribution assumption.

Haze and Altitude Effects

For this study [55], aircraft multispectral scanner data were gathered over an agricultural scene at altitudes of 500, 1000, 5000, and 10,000 feet.

Path radiance was found to seriously distort the target radiance spectra sensed at the receiver. In fact, under certain circumstances, the received radiance assumed the spectral characteristics of surrounding objects, that is, objects not in the receiver's instantaneous field of view (IFOV). Here it was found that the primary component of nontarget radiation was being reflected by objects outside the receiver's instantaneous field of view and was being scattered into the receiver by the intervening atmosphere. As the aircraft's flight altitude increased, this component of path radiance became less significant as direct scattering of solar radiance in the atmospheric path between the sensor and the ground increased rapidly.

48. W. A. Malila, R. B. Crane, W. Richardson, and R. E. Turner, Information Extraction Techniques for Multispectral Scanner Data, presented at 4th Annual Earth Resources Program Review, NASA/MSC, Houston, January 17, 1972, and published in Proceedings.

49. R. Turner, Remote Sensing in Hazy Atmosphere, presented to the ACSM/ASP Convention in Washington, March 1972, published in the Journal of Photogrammetric Engineering and in ACSM/ASP Proceedings.

50. R. E. Turner, Atmospheric Effects in Remote Sensing, presented at Second Conference on Earth Resources Observation and Information Analysis System, U. of Tennessee Space Institute, Tullahoma, March 1972 and published in Proceedings.

51. Robert E. Turner and Margaret M. Spencer, Atmospheric Model for Correction of Spacecraft Data, Eighth International Symposium on Remote Sensing of Environment, October 1972, The University of Michigan, Ann Arbor, and published in Proceedings.

52. R. Sharma, Enhancement of Earth Resources Technology Satellite (ERTS) & Aircraft Imagery Using Atmospheric Corrections, Eighth International Symposium of Remote Sensing of Environment, October 1972.

53. R. Turner, Radiative Transfer in Real Atmospheres, July 1974, ERIM, Ann Arbor, Report 190100-24-T.

54. R. E. Turner, Contaminated Atmospheres and Remote Sensing, Third Annual Remote Sensing of Earth Resources Conference, University of Tennessee Space Institute, Tullahoma, March 1974.

55. R. Nalepka, H. M. Horwitz, and N. S. Thomson, Investigations of Multispectral Sensing of Crops, The University of Michigan (WRL), Ann Arbor, Report 31650-30-T, May 1971.

Of course, with an increase in atmospheric path length, the transmission of radiation reflected by ground objects was reduced. The combination of rapidly increasing path radiance along with a reduction in received target radiance resulted in received radiance spectra which were less and less characteristic of the objects being viewed. This effect was demonstrated quantitatively by calculating the contrast transmittance as a function of flight altitude. These calculations showed that at $0.46 \mu\text{m}$, the contrast at 10,000 ft was reduced by a factor of 25 from that at 500 ft. Even in the $0.805 \mu\text{m}$ band, where the atmospheric scattering was less serious, contrast was reduced by almost an order of magnitude.

As a part of this study the radiance statistics for each of three training fields (one each for bare soil, corn, and soybeans) were computed for the data gathered at 1000 and 5000 ft. The mean-radiance spectra are plotted in Figure 17; one fact is immediately obvious on examining this figure. The entire 1000-ft radiance spectrum for bare soil lies below the 5000-ft spectrum. For corn and soybeans at $0.805 \mu\text{m}$, however, the spectral radiance received at 1000 ft exceeds that received at 5000 ft.

At first glance, this result seems to indicate an error in the calculations. However, further examination of the equation which describes the total radiance input to the scanner provides an argument for the plausibility of the results. The difference in total radiance received when viewing an object from two altitudes, H_1 and H_2 , is given by:

$$L(H_2) - L(H_1) = \Delta L(H_{2,1}) = E\rho[\tau_A(H_2) - \tau_A(H_1)] + [L_P(H_2) - L_P(H_1)]$$

where each of the quantities is defined as before. For H_2 greater than H_1 , the difference in transmittance is a negative value, while the difference in the path radiance is positive. The sign of $\Delta L(H_{2,1})$ then depends on the relative magnitudes of the terms in the equation. For certain atmospheric conditions, the value of the object reflectance would be enough to cause the sign of $\Delta L(H_{2,1})$ to swing from positive to negative. This seems to have been the case in the $0.805 \mu\text{m}$ spectral channel where the reflectance of bare soil is much less than the reflectance for either corn or soybeans. One can see that the variation in the received radiance spectrum is a complex function of conditions existing at the time of the flight, and that intuitive feelings for the effects of certain parameters can often be in error.

Time of Day Effects

This in-depth study was unique in the extent of its direct comparisons, on matching graphs, between empirical data and theoretical predictions of variations; these comparisons were made in more detail for more times, fields, and ground covers and wavebands than in any other treatment of the subject we have seen. The extent of the analysis was made possible by the unique data set used: it was obtained in 14 successive passes over the same ground-truthed strip at different times on the same day. Previous time-of-day studies have compared only data taken

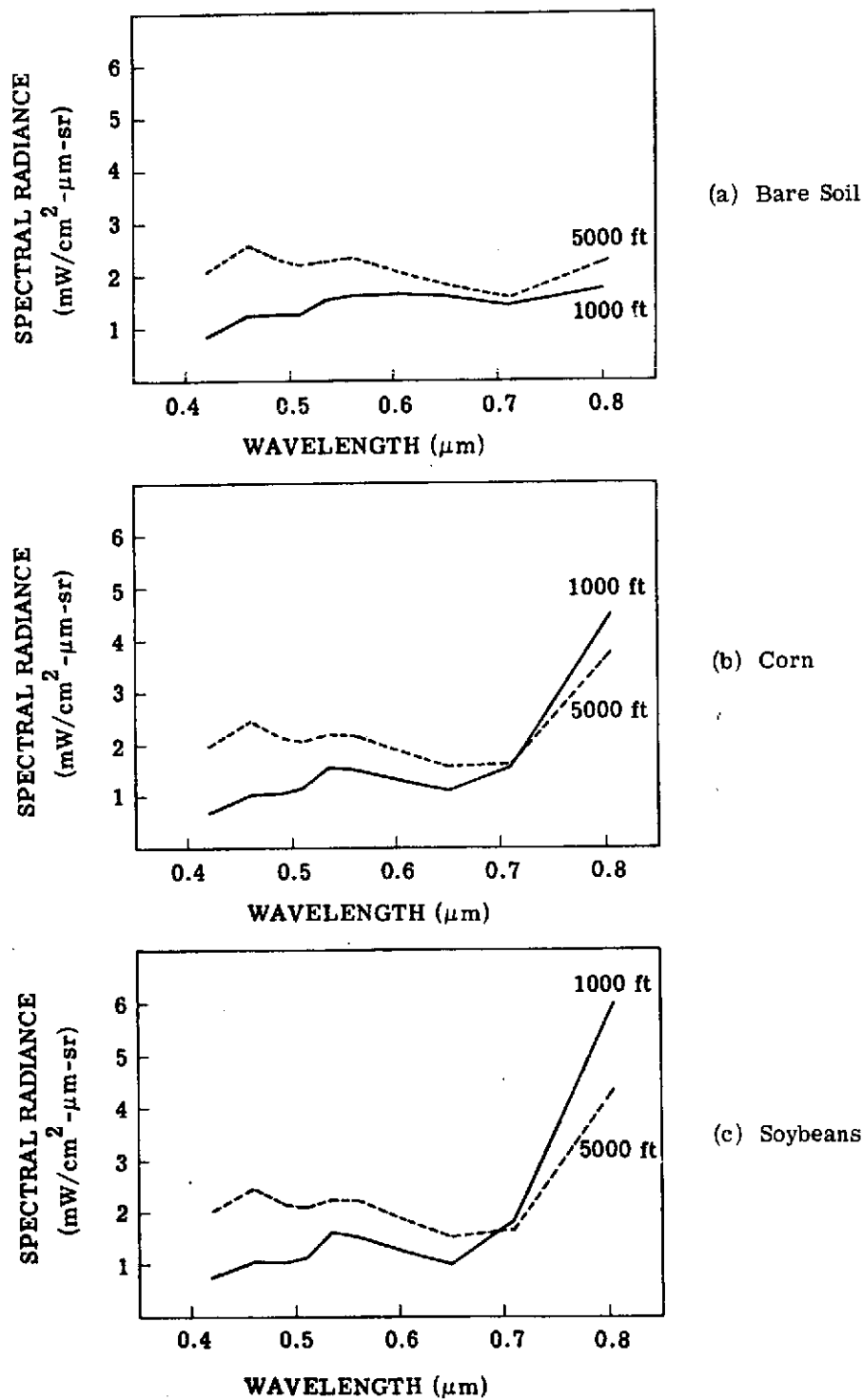


FIGURE 17. MEAN SPECTRAL RADIANCE FROM BARE SOIL, CORN, AND SOYBEANS AT 1000 AND 5000 ft

over the same area during a few passes on one day, over different areas on the same day, or over different areas on different days. In contrast to these compromises, the availability of repeated data for identical fields, at the same scan angles and on the same day, eliminates many extraneous sources of data variation.

Rather than recite the details of this study, we instead refer the interested reader to ERIM Report No. 190100-27-T [56] and include here some conclusions drawn as a result of the study.

- (1) There are sizable variations in signature means as a function of both time of day and scan angle.
- (2) The radiative transfer model (described earlier) was successful in predicting the trends in the data at the shortest wavelengths, but it did not include all variations at the longer wavelengths. Two forms of deviation we found may be attributable to causes explicitly excluded from this model:
 - (a) Brighter than predicted signals in the afternoon at all wavelengths may be caused by higher overall illumination from high thin cirrus clouds (known to be present) which reflect additional light to the ground—the present model assumes no cloud cover.
 - (b) Additional anti-solar peaking, especially at longer wavelengths, is apparently caused by bidirectional-reflectance properties of the surfaces which are not included in this model—the model assumes Lambertian (perfectly diffuse) surface reflectors.
- (3) Comparison of empirical data at longer wavelengths with predictions of Suits' canopy reflectance model shows similar curve shapes, though the model predicts less variation than is observed in the data. However, model calculations were made for somewhat different conditions and, for a truer comparison, should have been more closely matched to the observed conditions.
- (4) Time-of-day effects cannot be ignored. This is shown by the serious degradation when signatures from the first run were used in classification tests on later runs: recognition decreased from an average 84% correct on the first run at 9:33 AM to essentially 0% correct by 11:33 AM.
- (5) Recognition was 0% correct in the afternoon when we had expected the accuracy to rise again to approach that for morning runs having corresponding solar angles. The reasons for this are not fully understood; however, we suspect uncorrected run-to-run

56. W. A. Malila, R. Hieber, and J. Sarno, Analysis of Multispectral Signatures Investigation of Multi-Aspect Remote Sensing Techniques, ERIM Report 190100-27-T, July 1974.

calibration changes for one or more channels, because χ^2 calculations indicated that use of fewer channels (in particular, four calibrated in this study) would give better results with the current data.

- (6) Some means of signature extension is needed to compensate for temporal variations during large-area surveys with airborne scanner data.
- (7) The behavior in the far-infrared (direct-thermal) radiance channel was analyzed separately since different physical processes are involved. The temperatures rose during the morning, then, as anticipated, stayed roughly constant throughout the afternoon, rather than declining as does reflected radiance at shorter wavelengths. There was a clear-cut difference between the temperatures of the various ground covers, with trees staying cooler than corn and corn cooler than pasture—this is physically reasonable and expected. Finally, the temperatures of surfaces within any one crop were not uniform, the sunlit side being slightly, but definitely, warmer.

Test of Gaussian Assumption

Multivariate normal (Gaussian) probability density functions are usually used in classification decision (i.e., recognition) processes on multispectral scanner data. The mean and covariance matrix of the normal density function is usually estimated from a training data set. In this study, a comparison was made to determine whether or not improved classification results could be obtained by use of a different form—namely, an empirical multivariate probability density histogram of decorrelated variables—to represent the probability density functions. First, tests were made of the normality of the individual subsets of data, and all were found to be non-normal at the 1% level of significance using a standard chi-square goodness-of-fit test. Operating characteristic curves then were generated to represent decisions made with each form between each given class and a uniformly distributed alternative class; a uniform distribution was chosen because the results are then least dependent on the choice of the alternative data set. We found that the probabilities of misclassification using the two forms were approximately identical for almost every data set even though a large number of individual data points were classified differently. It was concluded that a decision rule based on the assumption of multivariate normal distributions of scanner signals performs sufficiently well, in comparison with a more accurate but more complicated rule, to warrant its continued use in recognition processing. (See Refs. [45], [47], and [57] for details.)

57. R. B. Crane, W. A. Malila, and W. Richardson, Suitability of the Normal Density Assumption for Processing Multispectral Scanner Data, IEEE Transactions on Geoscience Electronics, Vol. GE-10, No. 4, pp. 158-65, October 1972.

3.3 DATA COLLECTION SYSTEM

In addition to achieving a better understanding of the target and the environment in which it is viewed, this contract supported efforts to better understand the data collection system. Two of these efforts are briefly discussed below.

3.3.1 DETECTOR UTILIZATION IN LINE SCANNERS

The goal of this study [58] was to determine the noise limitations of detector-preamplifier combinations for optical-mechanical line scanners. The procedure was: to model several types of detectors and appropriate operational amplifier preamplifiers; to measure the noise performance of certain critical preamplifier components; and to predict the limitations of two typical multispectral line-scanning systems. Types of detectors considered were: silicon, indium-arsenide, indium-antimonide, mercury-cadmium-telluride, and mercury-doped-germanium. The results of this study indicate characteristic parameters of key importance in designing preamplifiers for several types of detectors.

The general conclusion of this study is that, in most cases, the design of the preamplifier is critical to good performance from the line scanner. Many factors can limit the preamplifier performance, but the Johnson noise from the feedback resistor usually dominates in the low-frequency portion of the bandpass, while the input-voltage noise from the operational amplifier dominates in the high-frequency portion. The high-frequency portion tends to dominate when integrated over the total bandwidth.

The Johnson noise current divided by the square root of bandwidth is proportional to the square root of the resistor temperature and inversely proportional to the square root of the resistance. For improvement the solution is to cool the resistor and/or to raise its resistance. Raising the resistance, however, usually means compensating for the stray capacitance across the feedback resistor. Inaccurate compensation may limit the overall accuracy. The noise current resulting from the amplifier-noise voltage is proportional to the noise voltage, the operating frequency, and the capacitance from the amplifier input to all other points; improvement can be achieved by reducing any or all of these parameter values. Cooling the input stage of the preamplifier, along with its feedback resistor, also usually improves noise performance. This process both reduces the feedback-resistor Johnson noise and, by eliminating connector and cable capacitance, reduces the capacitance from the preamplifier input.

58. L. Larsen, Detector Utilization in Line Scanners, The University of Michigan (WRL) Report 31650-29-T, August 1971.

We reached two general conclusions related to the ease of building detector-noise-limited preamplifiers:

(1) Generally, it is easy to build preamplifiers for GeHg or HgCdTe thermal detectors, since the thermal background radiation results in high detector noise. This is true even if a detector is small and cold-filtered to narrow the spectral bands. Nor is it difficult to build preamplifiers for an unfiltered InSb detector, which also receives substantial thermal background radiation from the long-wavelength portion of its spectral response. If, however, the long-wave response is attenuated by a cold filter, the thermal background is reduced and the noise-limiting job becomes more formidable.

(2) It is difficult to construct detector-limited preamplifiers for Si and InAs photovoltaic detectors and InSb photovoltaic detectors which have been cold-filtered to minimize the thermal background. To reach this conclusion, we assume that the leakage current of the detectors is negligible. The preamplifiers are harder to construct if there is a reduction in either the detector quantum efficiency or the incident rate of arrival of photons on the detector.

3.3.2 SCANNER PERFORMANCE EVALUATION

Many users of remote sensing data gathered by the ERIM M7 scanner system are interested in extending spectral classification and mapping capabilities from one flightline to another, even when such lines are flown days apart. Such a capability obviously offers tremendous savings in manpower (including ground truthing teams) as well as in data processing time. In most cases, however, attempts to recognize objects in one flightline using signatures and decision rules generated from another line (even with flightlines only several minutes apart) have been characterized by significant decreases in the percentages of objects correctly classified.

From the viewpoint of the data analyst, it would be very helpful to know the magnitude of the scanner-associated signal variations one might expect during the course of a three- or four-hour mission. Information on longer-term signal variations covering three or four months would also be helpful. By knowing all the sources of signal variations and their characteristics to be encountered over long periods of time—including scanner, atmospheric, and seasonal changes—the analyst has a better chance of extending object classification capabilities from one flightline to another.

Toward answering the question of short- and long-term scanner signal variations, one of the approaches we used [59] was to analyze the so-called "standardization" tests conducted

59. S. Stewart, D. Christenson, and L. Larsen, Systematic Monitoring of M-7 Scanner Performance and Data Quality, ERIM Report 190100-23-T, July 1974.

periodically in the course of normal data collection over the past year and one-half. These tests were devised originally to indicate changes in system response. Forty tests, covering the periods 5 May 1972 to 25 January 1973 and 22 June to 12 August 1973, were analyzed with a program called CALIB., which was written expressly for the purpose of calculating a set of statistics concerning the solar reflective reference source of the M7 scanner. Some of these statistics, plotted by the computer as graphs of mean signal voltage versus test date, showed that under normal circumstances standard deviations of the mean lamp signal amounting to not more than 10% could be expected over several months and that in most cases the deviation figure was less than 5%. A few instances of much larger changes were noted but these were under unusual circumstances.

Since these standardization tests are planned to serve as continuing indicators of scanner performance, we designed a system for rapid, computerized data reduction. Once implemented, this system will enable one-day retrieval of desired data on the performance characteristics as monitored in the standardization tests.

Also completed during this study were three other programs designed to help determine the impact of scanner signal variation and calibration on data processing. One of these programs, THERML., provides a set of statistics on thermal reference sources as a function of time—much as the program CALIB. does in obtaining the solar reflective statistics. NEΔTs* for the hot, cold, and ambient reference plates were calculated and compared as a function of time to qualitatively assess thermal data performance. In addition, a new technique for evaluating the accuracy of temperature calibration was perfected which made use of THERML. output. Also, we made a quantitative analysis of the frequency content of the thermal channel by using the output of another program called DGNSTC. The results of this study indicated that a line-by-line dynamic temperature calibration was necessary to minimize errors resulting from noise. DGNSTC. was also used to determine the darkest region in the scanner's field-of-view and thus permit uniform baseline corrections for all processors of M7 data.

The last program, called LAMRAD., was written to automatically calculate M7 scanner radiance calibration constants for each spectral channel. New methods employed in this subroutine greatly improve the signal-to-noise ratio of the scanner signals as compared to old techniques. NEΔLs** (radiance differences) were also calculated by LAMRAD.

*Noise Equivalent Temperature Difference

**Noise Equivalent Radiance Difference

As a result of this study it was demonstrated that valuable information about scanner performance can be gained from the calibration data recording during "standardization" runs on data acquisition missions. In the solar reflective region, noise information (as a function of frequency) obtained digitally from such standardization runs can indicate possible amplifier, detector, or recorder problems. To permit up-to-date monitoring of these noise figures, it is recommended that standardization data be acquired at least once every flight. Rapid processing of this information is essential to its optimal use.

A region of darkness viewed by the rotating scan mirror in one 360° swing was obtained for baseline correction. It is recommended that all data processors of M7 multispectral data use this region, which is located beyond the lamp reference but before the sky reference.

We also examined a new technique for obtaining values for the reference lamp pulse. This technique, which uses integration instead of peak pulse value, is advantageous in that more points are available for averaging—hence, lower noise figure results. In addition, the integration is relatively insensitive to jitter in lamp pulse position. For optimal use of the reference lamp pulse information, this technique should be applied to all software associated with the extraction of radiance information.

Analyses of all past laboratory radiance calibrations on the M7 scanner have revealed large differences between "adjacent" measurements (currently scheduled approximately every two months). Such differences (as large as 50%) appear even in the absence of a physical alteration in the system—such as a new reference lamp, for example. If smaller changes between radiance calibration measurements are desired, these measurements will have to be made more frequently, most likely every two to three weeks.

Finally, methods were tested for evaluating both thermal reference plate performance and overall detector, amplifier, and tape recorder performance in the thermal region. Plate failure often begins to occur long before it is observed by the scanner operator. But it is possible, by using an ambient plate as a third reference, to determine whether thermal reference plates are failing. Thus, inclusion of an ambient reference in the standardization measurements made every flight would be desirable in order to permit reference plate evaluation as often as possible. An overall thermal region performance indicator has been demonstrated by the use of NEAT calculations which permit a theoretical tape recorder noise limit to be compared to actual measured values. Since the system is in most cases tape-recorder-noise-limited, any NEATs larger than the theoretical limit can indicate some type of excessive noise in the system.

In summary, it has been shown that systematic recording and digital analysis of M7 scanner calibration signals can be valuable in evaluating both scanner performance and data quality.

IMPROVING ACCURACY OF EXTRACTED INFORMATION

Through a better understanding of both the capabilities and limitations of existing multi-spectral scanner data processing and information extraction systems and techniques, new approaches were developed and investigated to improve the accuracy of the information which could be extracted from scanner data [60]. The remainder of this section discusses these efforts as well as what is meant by "accuracy."

By "accuracy" we mean freedom from error or degree of conformity of a measure to a standard. In a statistical sense we mean by accuracy freedom from bias (as a measure of difference from a standard) where precision is a measure of repeatability with minimum variance. Mensuration or area determination accuracy, then, is the estimate of area in various classes made from a set of measurements with an MSS compared to the area ascertained by ground surveys or other, perhaps less accurate, means adopted as a standard. With MSS data, the usual procedure is to sum the elemental areas associated with each picture element or pixel. These elemental areas can be a function of scan angle with the area smallest at nadir.

At the foundation of discrimination theory is the necessity to realize that optimum discrimination techniques require not only that the procedures be tailored to recognize the item or material of interest, but also simultaneously, that they be tailored to reject other items or materials lying in the vicinity of the desired materials but not of interest, i.e., the backgrounds in which the items of interest are embedded. Two types of error are possible: (1) failure to classify all of the desired class actually present as that class, and (2) misclassification of other classes as that class. Photointerpreters commonly call them errors of omission and commission, respectively. Errors of the first kind can be reduced by matching the decision process as well as possible to the desired class. This is not very useful, however, because the errors of class two will be very large; i.e., many things will be misclassified as the desired class, and whatever information is to be extracted will be grossly in error. It can be shown that in all but trivial cases class two errors are always large when the discrimination technique is matched only to the item of interest. To do any better requires simultaneous tailoring of the process to discriminate for the item of interest and to reject those items not of interest. It is this need that gives rise to the central importance of signatures of both items of interest and the backgrounds in which they may be embedded.

60. J. D. Erickson, A Summary of Michigan Program for Earth Resources Information Systems, presented at the 4th Annual Earth Resources Program Review, NASA/MSC, Houston, January 17, 1972, and published in Proceedings.

A performance matrix allows full presentation of the two classes of error. Labels on the rows are ground observations while the columns are classifier results. Thus the diagonal elements give the correct classification percentage for each class while the off-diagonal elements represent the false alarms.

Conceptually, all pattern recognition systems can be considered as consisting of three important subsystems: the transducer, the feature extractor, and the classifier. The MSS is our transducer; the classifier is the implementation of the chosen decision rule for discrimination (after training on known signatures in supervised classification) of the hopefully unique and invariant features characterizing the classes of interest. Feature extraction is the step of transforming the transducer output into the features allowing discrimination. Conceptually, feature extraction includes all processing steps from the transducer to the decision rule. Since optimum classifiers are used and fine, stable, relatively noise-free MSS systems are available, the discrimination problem reduces to one of extracting reasonably unique and invariant features. Insufficient care in attacking this problem can lead to poor results. ERIM has consistently shown the gains achievable in performance accuracy by attention to this step.

4.1 DATA PREPARATION

Each step in the processing procedure is potentially information destroying. Unless care is taken from the point of view of information conservation, nonunique and noninvariant features may be presented to the classifier and poor results can ensue. Even the simple step of data preparation and quality assessment is important in achieving accuracy. A study indicating the truth of this too-often-ignored principle was reported in 1971 [61].

Three segments in the 1971 Corn Blight Watch Experiment intensive study area of Western Indiana over which multispectral scanner data were being gathered on a biweekly basis were selected as sites. To support this investigation, ground information in addition to that provided by the county agents was gathered throughout much of the scanner data collection period; it included the location of fields, the crop planted therein, and the condition of the crop.

The need for improved data preparation and processing techniques is dictated by information we have gained through close association with multispectral scanner systems and experiences we have had in processing multispectral data. Our experiences have shown that in each and every data set many potential problems may exist which, if not corrected, could significantly

61. R. F. Nalepka, J. P. Morgenstern, and W. L. Brown, Detailed Interpretation and Analysis of Selected Corn Blight Watch Data Sets, Presented at the 4th Annual Earth Resources Program Review, NASA/MSC, Houston, January 17, 1972, published in Proceedings.

reduce the accuracy of recognition results for that data. Some of these potential problems are instrument-related; others are associated with the radiation environment and the scene being scanned. They include:

- (1) level shifts and gain changes in the recorded data resulting from instabilities in system electronics and tape speed
- (2) misregistration of data between spectral bands due to unequal resolution in all the bands, the lack of optical alignment, either by design or otherwise, of the detectors in all bands, or the imperfect alignment of the tape recorder record and playback heads
- (3) noisy data resulting from a combination of insufficient radiation input and lack of detector sensitivity
- (4) variations in signal levels as a function of scan angle due to nonuniform angular sensitivity of the scanner, the effects of atmospheric scattering, and bidirectional reflectance effects
- (5) changes in the scene illumination level during the data collection mission

Any of the above problems could seriously affect one's ability to generate accurate classification maps and extract useful information. Without going into much detail here, we would like to present one of our approaches to the solution of these problems. Prior to digitizing the data, problems of misregistration or skew are eliminated by aligning the data through the use of electrical delay lines. In this alignment, the reference signal relied upon is one recorded in each band during data collection as the scan mirror views a reference source in the scanner. Level shifts are eliminated by clamping the data for each scan line in each band to the dark level signal (that signal, producing zero radiance input to the system, which is generated when the sensor element scans the dark interior of the scanner housing. Any gain changes and variations in scene illumination which would produce the same effect as changing the gain are accounted for by scaling the data in each band to the "sun sensor" signal. The sun sensor, which is scanned once for every revolution of the scan mirror, monitors the level of radiation incident upon a flat opal glass plate atop the aircraft. Problems with system noise as well as with misregistration of data in the flight direction, can be significantly alleviated by taking advantage of the fact that successive scan lines often overlap. Rather than not digitizing and processing all scan lines (a common approach), we combine the lines containing largely redundant information by averaging.

All of the above operations, which we term data preparation, can be carried out without specific reference to the video data generated when the scene is scanned. One other operation belongs in this category. If the angular responsivity of the scanner is nonuniform, and this nonuniformity is known and fixed, the effect of the nonuniformity can be removed from the data.

Depending on what other operations are planned for eliminating angle effects, this effect may be removed simultaneously with the removal of the other angle effects which, as mentioned earlier, are due to scattering in the atmosphere and bidirectional reflectance. What we call preprocessing includes those operations which are meant to reduce or eliminate external effects—that is, the influence on data of factors lying outside the scanner.

One simple form of preprocessing we have found useful assumes that the scene, over its entirety, contains an approximately equal distribution of all objects of interest at all angles. (We believe that this assumption is valid for most areas devoted to farming.) In this approach, the average signal variation as a function of scan angle is computed for each spectral band; it includes the nonuniform angular responsivity of the scanner if this factor has not already been eliminated.

The effects of scanner angular responsivity, atmospheric transmittance, and bidirectional reflectance are all multiplicative in nature. That is, the radiation incident on the detector is a product of the radiation incident on an object being viewed at a given angle times its reflectance, times the transmittance of the atmosphere between the object and the sensor, and times the scanner responsivity at that particular angle of view. In the absence of significant path radiance (radiation scattered into the receiver by the atmosphere, which is an additive effect), much of the angular variation in the signal can be eliminated by dividing each scan line of data by the normalized averaged signal variation. Since the data of interest were gathered under relatively clear atmospheric conditions, path radiance effects are minimal, thereby justifying this preprocessing approach.

To illustrate the importance of proper data preparation and preprocessing, we now present some examples from data gathered over Segments 203 and 212. The importance of clamping the data to the dark level can be seen in Figure 18 which presents two histograms—one for the first minute and the other for the second and third minutes of data collection for a particular run. It is evident that the dark level varied on the order of $\pm 3\%$ during each of the two periods examined. This variation in itself could seriously affect one's ultimate discrimination capability in processing the data. In addition, however, a further shift in the mean dark level of about 5% also occurred during the run.

In Figure 19, examples are shown of the average angular signal variation for two data sets (43M 203 and 43M 212). It is clear on examining the figure that significant variations in the average angular signal occurred for both data sets, though the amount of variation is more pronounced in Segment 203 data. This may be explained by examining the location of the sun during the two data collection flights. For Segment 203 data, the solar elevation was less and the solar azimuth more easterly than that during the collection of Segment 212 data. With the sun both

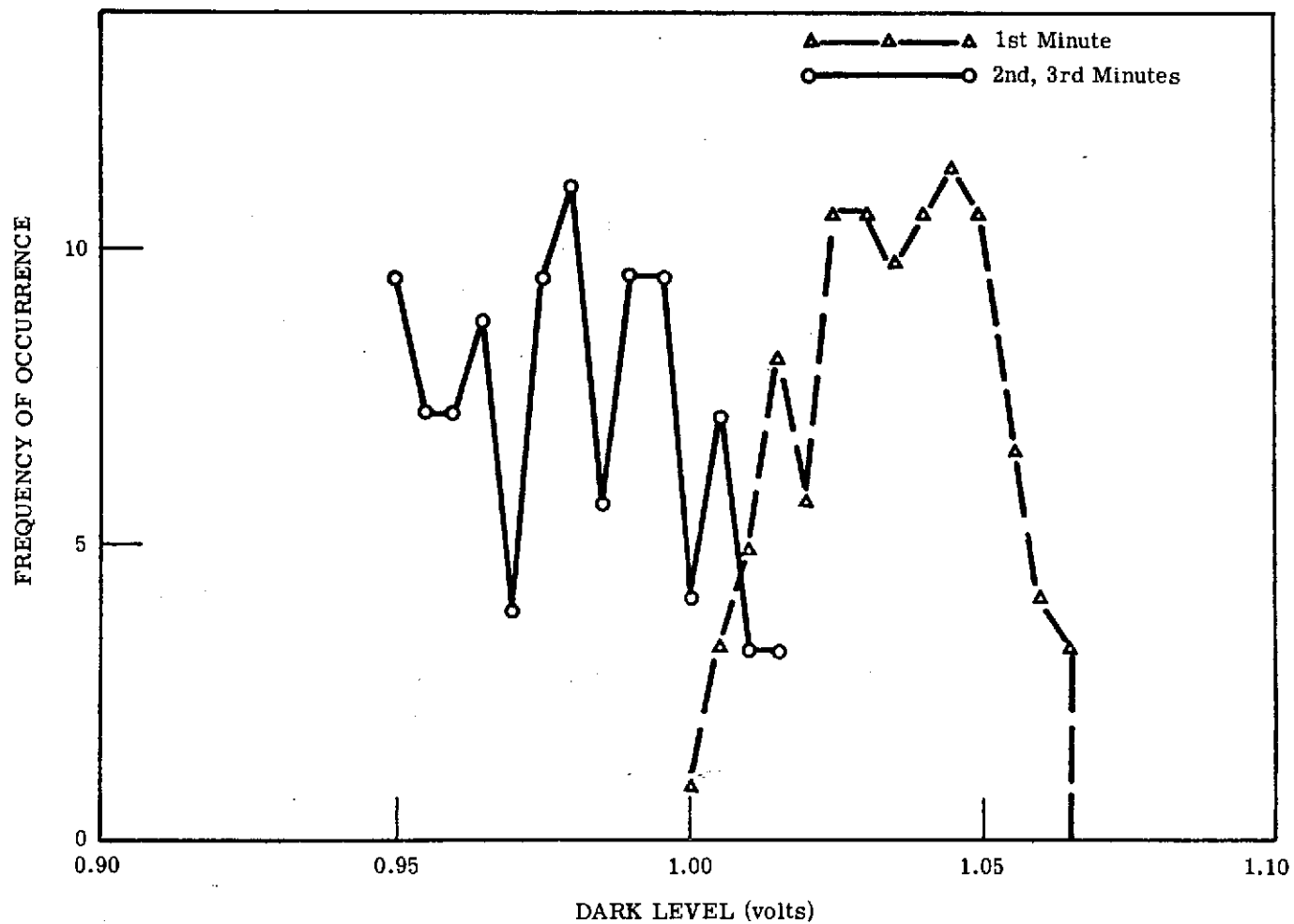


FIGURE 18. DARK-LEVEL VARIATIONS IN UNCLAMPED DATA (ANALOG) FOR SEGMENT 203, MISSION 43

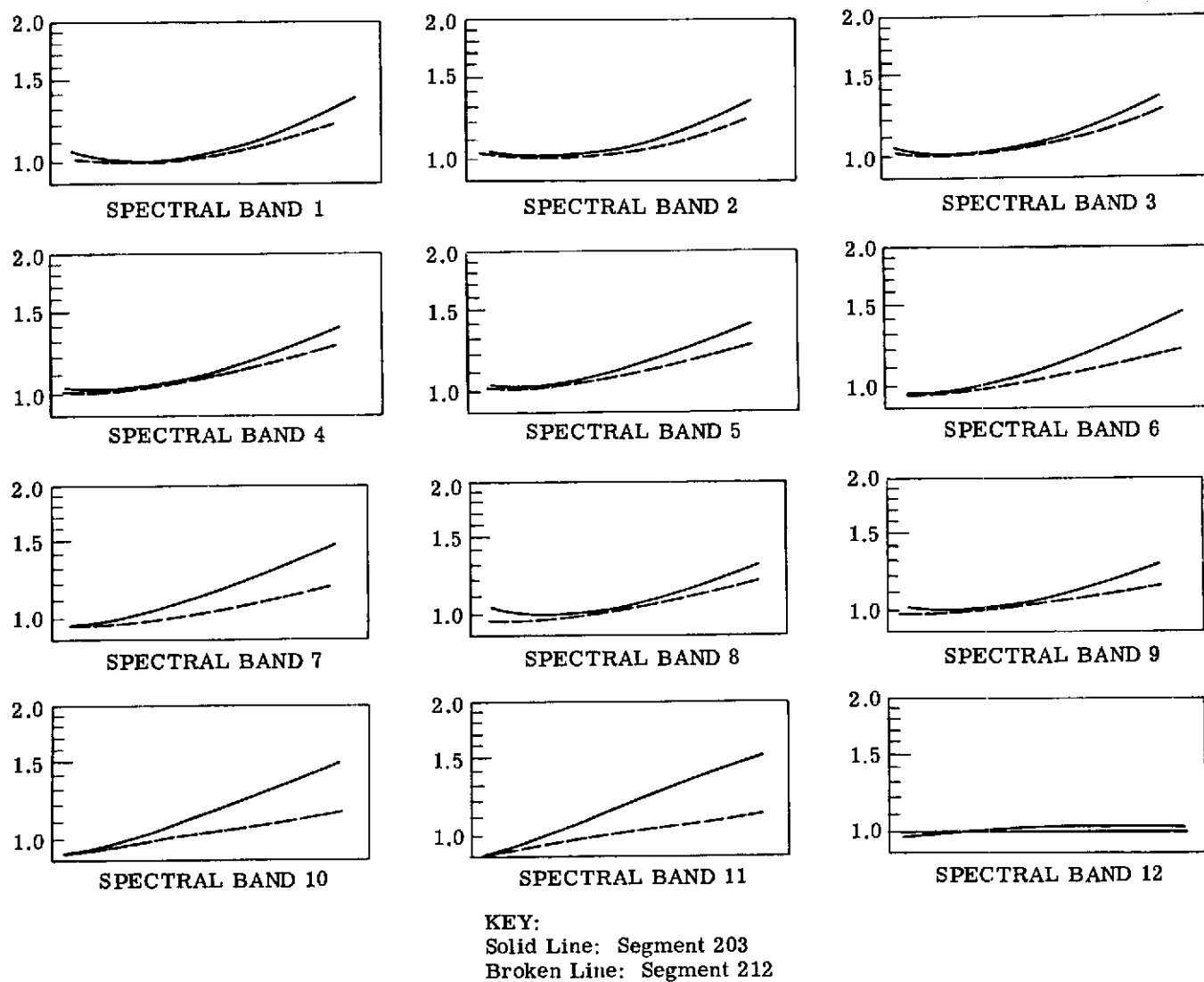


FIGURE 19. AVERAGE ANGULAR VARIATION OF SIGNAL FOR MISSION 43

lower in the sky and more nearly perpendicular to the north-to-south aircraft flight path, a larger variation of reflectance with scan angle resulted.

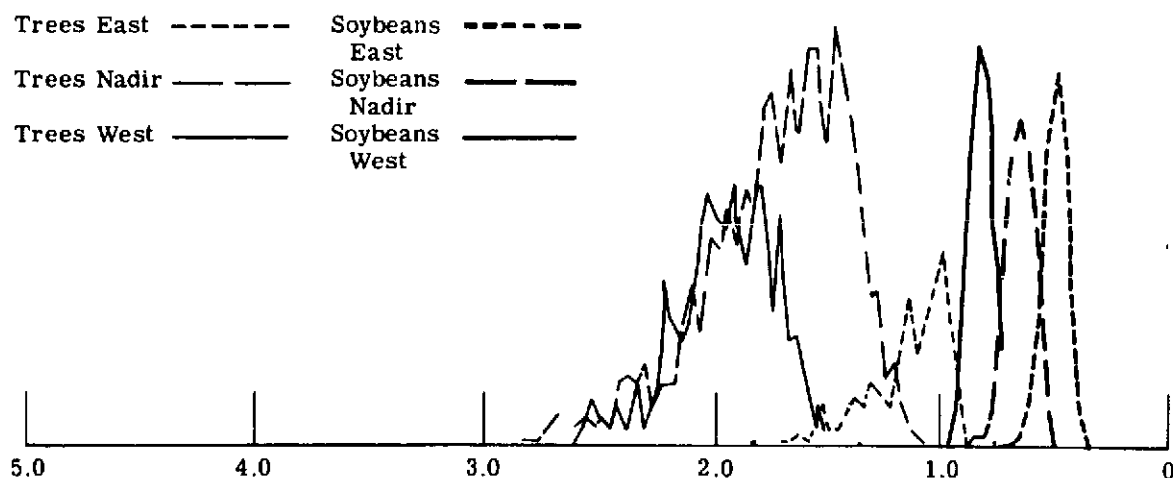
A more specific example of the effects of the angular signal variations is shown in Figure 20. Here, we see histograms in two spectral bands of many samples of soybeans and trees plotted as a function of their location in the scene with respect to the data collection aircraft. The effect on both soybeans and trees is a very obvious shift to higher signal values as the scan mirror rotates from east to west. An important result of this shift, especially noticeable in spectral band 10, is the similarity of signal levels for soybeans on the east side of the aircraft and trees on the west. Obviously, this similarity is a potential source of problems in discriminating between and properly classifying soybeans and trees, independent of their location in the scene. These similarities become even more significant when it is realized that of the four major object classes in this data set (corn, soybeans, pasture, and trees), soybeans exhibit the highest average signal level in all bands while trees exhibit the lowest average signal level. Signals for corn and pasture of course fall between these extremes. So if the data set were to remain unprocessed, one can well imagine the amount of confusion as to identities of the four object classes and the consequent effect on classification accuracy.

The effects of data preprocessing on the range of signal means for corn are shown in Figure 21; a significant reduction in corn signal range is evident. Although not illustrated here, similar reductions were achieved for soybeans, pasture, and trees with the result that these crops, after MSS data preprocessing, exhibited more unique and more easily discriminable signatures.

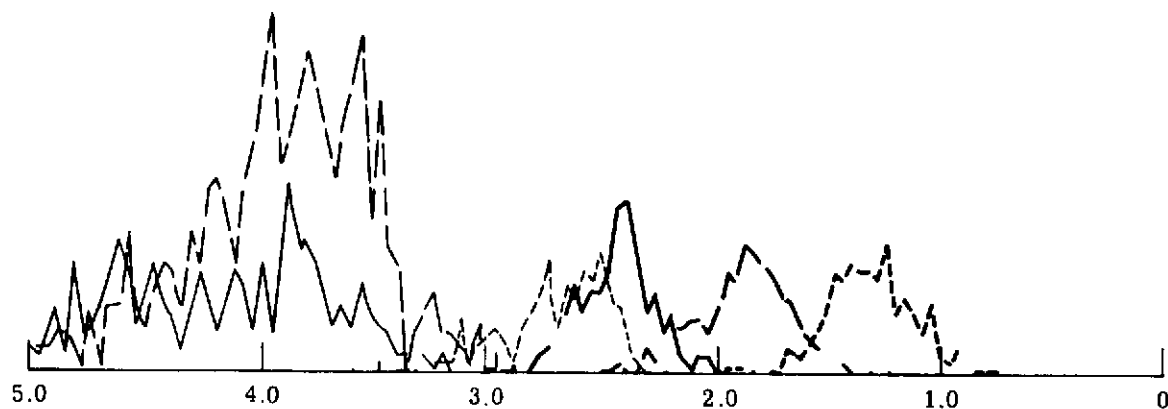
We have attempted, in the foregoing discussion, to illustrate the importance of careful data preparation and preprocessing in order to permit the extraction of the maximum amount of information from any multispectral scanner data set. Upon further research, the approaches and techniques described may prove not to be the best. Even so, we believe that the application of relatively simple techniques can significantly improve one's ability to extract useful information from multispectral scanner data.

4.2 GEOMETRIC CORRECTION, AREA DETERMINATION, AND LOCATION ACCURACY

In computing area of a given class, the usual procedure with MSS data is to sum the pixel areas for each class (these areas may be a function of scan angle). Accuracy is then determined by comparison with an adopted standard of area. Two major efforts undertaken during this contract address the problem of improving the accuracy of area determination: One was concerned with estimating proportions of objects in MSS data, the other with geometric correction, rectification, and mapping of airborne MSS data—including accuracy of geometric location. Our work in estimating proportions began in October 1969; it was based on an idea by Legault



(a) Spectral Band 3



(b) Spectral Band 10

FIGURE 20. HISTOGRAMS OF SIGNALS FROM SOYBEANS AND TREES AS A FUNCTION OF LOCATION IN SCENE

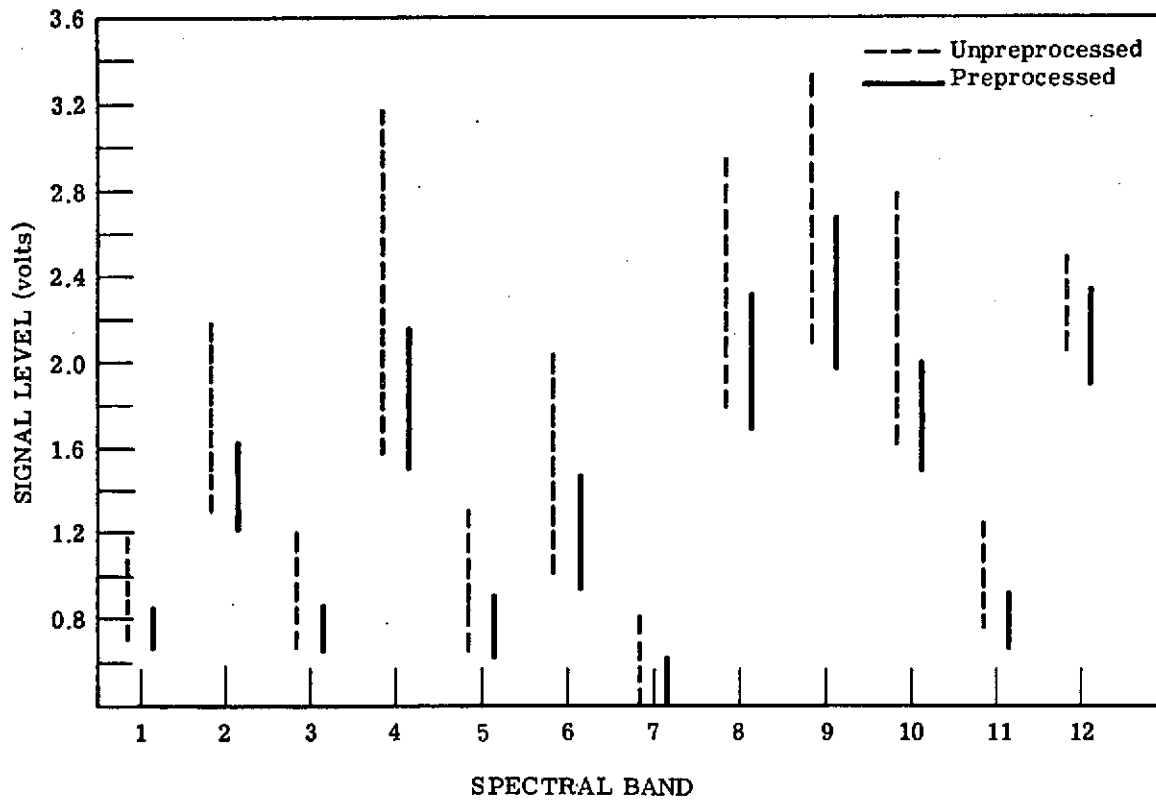


FIGURE 21. RANGE OF SIGNAL MEANS FOR CORN

which he patterned after standard procedures in mass spectrometry. Our present approach to geometric rectification and correction of MSS data began in 1972 although our first efforts at geometric correction go back to 1964 [2].

4.2.1 ESTIMATING PROPORTIONS

The practical utility of multispectral scanner data is often restricted by limited spatial resolution in the sensor employed to gather the data. Multispectral scanners in both the ERTS-1 and SKYLAB satellites impose data restrictions of this sort. These scanners view the ground with an instantaneous field of view (IFOV) covering a ground patch having dimensions of about 300 ft on a side. The radiation detected when scanning portions of a scene containing objects which, *en masse*, are smaller than this size will be composed of a mixture of radiation from all objects within the IFOV. Similarly, when the field of view overlaps the boundary between two larger objects, the radiation detected will be a mixture from the two objects. In both these cases, the signals generated by the sensor will not be representative of any one object. Taking for example ERTS-1 satellite data in which each pixel covers about 1.1 acres, the number of pixels containing more than one material may, for agricultural crops in the corn belt, approach 30% of the pixel total.

The effect of viewing more than a single object class is illustrated in Figures 22 and 23. Figure 22 depicts the reflectance spectra for corn and bare soil as they would appear individually. If the sensor were to simultaneously view both corn and bare soil, the effective reflectance spectrum would be quite different. This is shown in Figure 23 for the combination of 20% corn, 80% bare soil and also for 50% corn, 50% bare soil. These spectra simply comprise weighted combinations of the pure spectra plotted in Figure 22.

The use of standard multispectral recognition processing techniques on data points which result from viewing two or more objects will likely result in the improper classification of those data points. Given a sufficient number of improper classifications of this sort, the results of such efforts as might be applied, for example, in crop acreage determination, would be greatly in error.

Studies [55, 62-71] have been made and are in progress to develop special processing and information extraction techniques which will enable the accurate and timely estimation of the proportions of objects and materials appearing within the IFOV of a remote multispectral sensing device.

62. H. M. Horwitz, R. F. Nalepka, P. D. Hyde, and J. P. Morgenstern, Estimating the Proportions of Objects Within a Single Resolution Element of a Multispectral Scanner, 7th International Symposium on Remote Sensing of Environment, June 1971.

63. R. Nalepka, H. M. Horwitz, and P. D. Hyde, Estimating Proportions of Objects from Multispectral Data, The University of Michigan (WRL) Report 31650-73-T, March 1972.

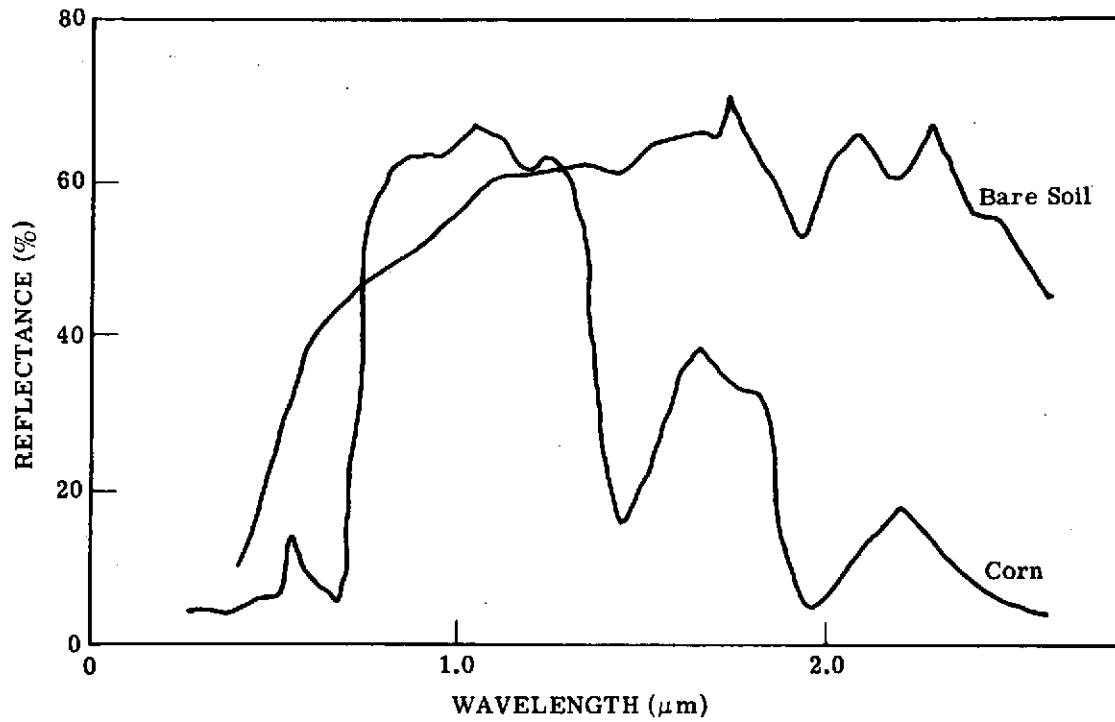


FIGURE 22. REFLECTANCE SPECTRA

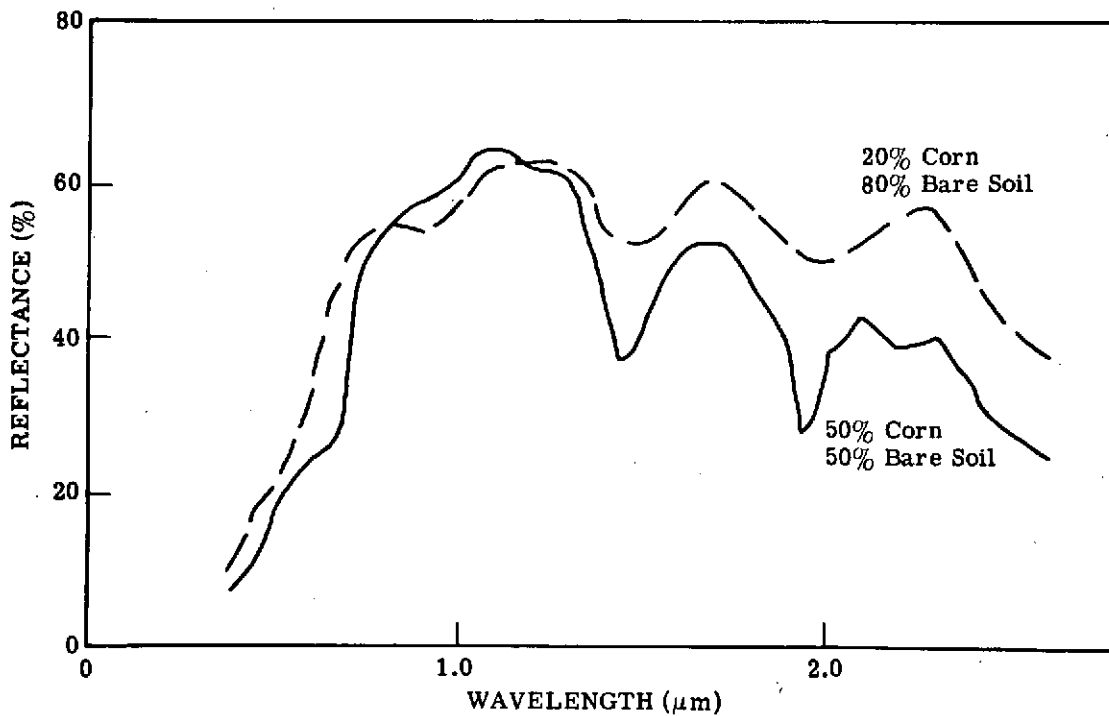


FIGURE 23. REFLECTANCE SPECTRA OF MIXTURES

The fact that the radiation emanating from each scene element is detected simultaneously in several spectral bands opens the possibility of classifying and estimating the proportions of spatially unresolved objects.

As long as the radiation spectra generated by objects within the IFOV are linearly independent—i.e., a unique radiation spectrum results for each combination of objects—a satisfactory solution will usually be possible. This requirement is somewhat more limiting than that imposed for standard recognition processing. In Figures 24 and 25 we present two separate plots of the means and distribution contours (signatures) of three objects as seen in two spectral bands. In each case the signatures of the three objects are sufficiently separate that if any one of them were viewed in its pure state it could easily and properly be classified. For the case depicted in Figure 24, combinations of the three objects would produce points generally falling within the triangle; thus by using the specially developed techniques, we could determine the proportions of these objects. Figure 25, however, depicts a situation in which the pure signature for object A_1 exhibits characteristics very similar to that for a combination of the other two objects. In this case the proportions of a mixture of these objects could not be accurately determined. Although all possible sets of objects and materials of interest may not meet the requirements for linear independence, we believe that the requirements are met often enough to make potentially very useful the solutions now being investigated.

64. R. F. Nalepka, H. M. Horwitz, P. D. Hyde, and J. P. Morgenstern, Classification of Spatially Unresolved Objects, presented at the 4th Annual Earth Resources Program Review, NASA/MSC, Houston, January 17, 1972, and published in Proceedings.

65. R. B. Crane and P. Hyde, Signature Estimation from Satellite Multispectral Scanner Data, Presented at the Second Conference on Earth Resources Observation and Information Analysis System, University of Tennessee Space Institute, Tullahoma, Tenn., March 1973; appeared in Proceedings.

66. R. F. Nalepka and P. D. Hyde, Classifying Unresolved Objects from Simulated Space Data, 8th International Symposium on Remote Sensing of Environment, October 1972.

67. R. Nalepka and P. Hyde, Estimating Crop Acreage from Space-Simulated Multispectral Scanner Data, ERIM, Ann Arbor, Report 31650-148-T, January 1973.

68. W. Richardson and H. Horwitz, A Faster Algorithm for Estimating Proportions, LARS Conference on Machine Processing of Remotely Sensed Data, October 1973.

69. H. Horwitz and P. Hyde, Estimating Proportions of Unresolved Objects from Multispectral Data, 1973 International Symposium on Pattern Recognition, IEEE, Pattern Recognition Society, Am. Soc. of Photogrammetry, Washington, October - November 1973.

70. W. Malila, R. Hieber, D. Rice, J. Sarno, Wheat Classification Exercise Using June 11, 1973, ERTS MSS Data for Fayette County, Illinois, ERIM Report 190100-21-R, September 1973.

71. H. Horwitz, P. Hyde, W. Richardson, Improvements in Estimating Proportions of Objects from Multispectral Data, ERIM Report 190100-25-T, April 1974.

In many applications, proportions for each data point may not be required. Here, a reduction in computation time can be achieved by averaging many data points and then carrying out a single computation of the proportions of the objects appearing in the entire region which was averaged (Figure 26). This approach is not only much faster but can also improve accuracy. Improved accuracy might result since averaging would reduce the effect of the variability of sensor signals due to the natural variation of the radiation received from any object class in the scene. In addition, the effects of random noise would be reduced.

To date, our work on estimation of proportions has included:

- (1) Extension of the signature concept to a mixture of objects
- (2) Development of a statistical and geometric model for sets and mixtures of signatures
- (3) Evaluation of computational methods used to estimate proportions of a mixture by maximum likelihood
- (4) Creation of a computational technique for assessing the expected accuracy of estimation as a function of the signature set
- (5) Development of techniques to identify alien objects
- (6) Testing and evaluating the proportion estimation algorithms on artificial as well as actual multispectral scanner data
- (7) Examining the problem of establishing signatures when pure samples of the objects of interest are not available
- (8) Evaluation of alternative estimators

Since its inception, this effort has consisted of a mix of theoretical model studies and tests with both simulated data and modest amounts of ground-truthed real data. Now that real data sets with adequate associated ground truth are becoming available, we have begun to utilize these in testing and development of mixtures procedures. The past history of the effort is summarized below.

Our work on estimation of proportions was accomplished in several phases. In the first phase [55, 62-64], a mathematical model was constructed which related the multispectral signatures of a mixture to the signatures of component materials. This model permitted the maximum likelihood estimate of the proportion vector to be formulated in terms of the observed data point. The computational aspects of the problem required this simplification: that all of the covariance matrices of the signatures of the component materials be taken as equal to their average. Theoretical and empirical results supported the validity of this assumption. With this simplification, proportion estimation becomes a quadratic programming problem. Several existing computational methods of quadratic programming were adapted and tested on simulated scanner data. Results indicated that this method for proportion estimation was feasible.

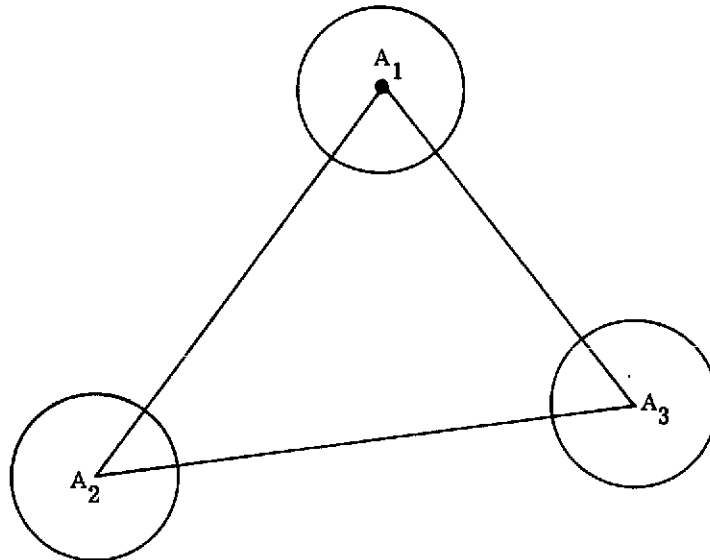


FIGURE 24. WELL-CONDITIONED SIGNATURE SIMPLEX

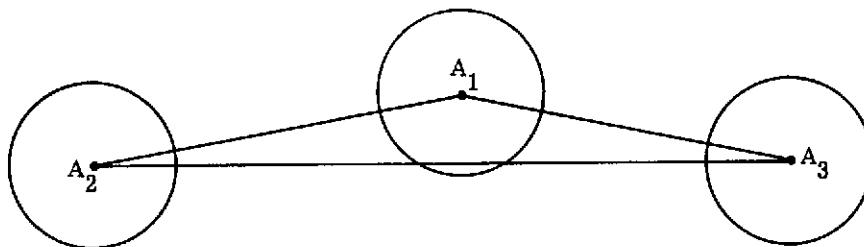


FIGURE 25. ILL-CONDITIONED SIGNATURE SIMPLEX

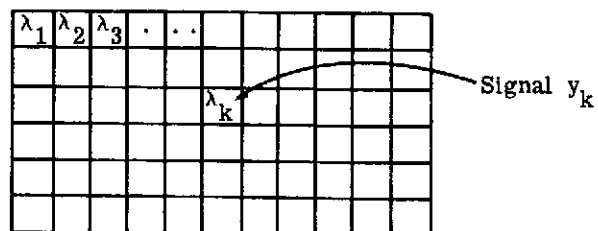


FIGURE 26. SCHEMATIC FOR DATA AVERAGING

The second phase of the program [65-67] included investigating the problem of detecting alien objects—i.e., objects in the scene not representable in the signature set. A procedure was devised for rejecting those pixels probably containing significant amounts of alien materials. In addition, aircraft scanner data were smoothed over ERTS-sized resolution elements to simulate spaceborne scanner data. When proportion estimation techniques were tested on this data, estimates of crop acreage based on the estimated proportions were found to be better than estimates obtained with conventional recognition techniques.

The third phase [68-71] was devoted to investigating problems in proportion estimation that limit its operational usefulness—namely, computation time and inaccuracy stemming from the intrusion of alien objects. In addition, some preliminary trials were made with ERTS-1 data. Increased speed was achieved by an improvement in the basic algorithm, by conversion to a more advanced computer, and by the further development of data averaging prior to estimating proportions. A reduction in computation time by a factor of about seven was attributed to improvements in the basic algorithm; use of the advanced computer contributed a further reduction by a factor of about two. In absolute terms, it took about 20 msec to estimate the proportions of five materials from 12-channel data. Averaging improved the speed of estimation by a factor approximately equal to the number of data points included in the average. (Results of theoretical analyses and simulated tests indicate that averaging may, under certain conditions, even improve the accuracy of proportion estimates.) With the improved proportion estimation algorithm, an ERTS frame containing about 10^7 pixels can be processed in about two hours by averaging signals in groups of 26. It would take over four hours to classify the pixels of the same ERTS frame into seven signature categories by recognition processing using a linear decision rule.

Also, in order to achieve increased speed, we investigated a theoretically less satisfactory but computationally more tractable estimator of proportions. Tests on simulated data indicated that although computation time decreased by about 1/3, the estimate's mean-square error increased by about 1/3 on a pixel-by-pixel basis. A surprising result of tests with simulated space data indicated that the new estimate could improve accuracy when estimates are averaged over a sufficient number of pixels (in the case of these tests, more than 27).

In addition, during this phase, a new procedure was devised for detecting alien objects. This procedure depends upon setting the value of a single parameter called the alien object threshold. Tests with simulated data to determine a satisfactory method of setting this threshold were inconclusive.

During the course of the year the mixtures algorithm was applied to three ERTS-1 data sets. Two of these—involving, respectively, lakes and rice fields—are reported elsewhere

[72, 73]. The third case, a preliminary investigation, considered the use of the mixture algorithm in a general agricultural situation utilizing data gathered under the CITARS (Crop Identification Technology Assessment for Remote Sensing) task (see Section 7.3.2).

The results reported for lakes and for rice fields are most encouraging. These were achieved, however, by employing some special procedures appropriate to the situations. In the case of lakes, a special detection threshold was set to keep slight indications of water in many pixels from accumulating to a large value. In the case of rice, mixtures were calculated only on those elements located on the boundaries between the rice fields.

In the case of CITARS ERTS data for Fayette County, Illinois, the data represent a low-contrast scene relative to the other two cases, so no special procedures were used. The results on this set of CITARS data were not impressive because of the ill-conditioned signatures in the ERTS bands at this time of the growing season. It is evident that in order to develop a mixtures algorithm which will be automatic and effective when the spectral information is limited, or during seasons when contrast is low, additional procedures will have to be devised to complement the present algorithm. The only practical way to achieve this will be by utilizing large data sets with excellent ground truth. The past lack of such data has imposed a major constraint on the development of the proportion estimation technique. We are hopeful that the CITARS data will fill this need.

4.2.2 GEOMETRIC CORRECTION

A system of computer programs referred to as Scanner Imagery Correction and Line-by-line Orientation ProgramS (SICLOPS) has been developed to perform geometrically corrected line-by-line mapping of airborne multispectral scanner data in ground coordinates and to estimate ground areas [74, 75]. As inputs, the system requires aircraft attitude and positional information furnished by ancillary aircraft equipment, plus ground truth information giving the location, in map grid coordinates, of a number of recognizable landmarks on the ground.

72. W. A. Malila and R. F. Nalepka, Atmospheric Effects in ERTS-1 Data and Advanced Information Extraction Techniques, Symposium on Significant Results Obtained from the Earth Resources Technology Satellite-1, Vol. 1, Goddard Space Flight Center, Greenbelt, MD, 1973.

73. F. J. Thomson, Crop Species Recognition and Mensuration in the Sacramento Valley, Symposium on Significant Results Obtained from the Earth Resources Technology Satellite-1, Vol. 1, Goddard Space Flight Center, Greenbelt, MD, 1973.

74. M. Spencer, J. Wolf, and M. Schall, SICLOPS: A System of Computer Programs for Rectified Mapping of Airborne Scanner Imagery, 9th Symposium on Remote Sensing of Environment, Ann Arbor, April 1974.

75. M. Spencer, J. Wolf, and M. Schall, A System to Geometrically Rectify and Map Airborne Scanner Imagery to Estimate Ground Area, ERIM, Ann Arbor, Report 190100-28-T, May 1974.

The effects of aircraft motion are first partially compensated by applying the navigational data to the data points corresponding to the landmarks in the scanner imagery. After this preliminary geometric correction, the correct data points and the ground truth information are used in a two-stage fitting process. The first fit is special, designed to eliminate errors not handled by the second, which is a standard cartographic fit. Final data processing does the actual mapping; applied to all data points, it combines the preliminary geometric correction and the fitting corrections into one operation, converting line or pixel locations into map grid coordinates. To obtain ground area values for individual pixels or for predesignated parcel specified in graymap coordinates, the area algorithm (area estimation procedure) is used in the data processor.

The system was exercised with simulated data to demonstrate its feasibility. Results show a dramatic improvement in location accuracy in the corrected over the uncorrected imagery. Area measurements were also made on the simulated data which included simulated errors; these errors are round-off and quantization errors (which are characteristic of the real input data) and systematic errors. In the presence of significant simulated errors, the area estimates were accurate to better than 99.7%.

Real input data have been prepared for the system but, pending generation of ground truth information, have not as yet been used.

In the initial study of the scanner cartography problem, the quantitative effects of aircraft instabilities and scanner geometry on scanner data were identified, correction techniques utilizing information from ancillary sensors and ground truth data were specified, and an area algorithm was developed. The results of this study led to the development of a system of computer programs referred to as SICLOPS. The system of computer programs as developed under this contract has been tested with simulated data. Results indicate that the SICLOPS System works. The demonstration of corrected imagery supported by the area measurements results strongly verifies the feasibility of this approach for post-flight processing of scanner data. The SICLOPS System still needs exercising with real data.

Those system programs presently devoted to data preparation are specially designed to accept certain data provided by NASA's NC130B airborne system. These data come from the Multispectral Scanner, the Litton LTN-51 Navigation System, and the radar altimeter. The main programs of the SICLOPS System, however, apply to any imaging airborne scanning system and can be utilized as long as the necessary attitude and position information is furnished in time-synchronization with the scanner data.

The first real data assembled for processing by the SICLOPS System do not have the preferred MSS data format. The system was designed in the expectation that the data would be in the Universal format which includes a reference time for each scan. Instead, the real data

actually to be processed (MSDS format) has no such reference time; its estimate by an auxiliary operation will thus be necessary. Results obtained on the same flight line for these two different MSS inputs to the system should be compared.

Combination of the SICLOPS System with the EDGES program and a recognition algorithm is an obvious next step. To estimate the area of a crop in a particular field by automatic means would then be within reach.

Elevation variations within the scanned scene are not handled in the present SICLOPS System; the severity of the problem should be studied. Possible methods of providing elevation information to the system should also be studied. One approach would be to use topographic information as it is known with respect to a geographic grid system. Another approach would be to consider modifying the scanner system to include a pulse laser to provide the slant range in time-synchronization with the scanner data.

Practical means for supplying the ground truth (control) data should be considered. To work from visicorder pictures, etc., rather than from digital graymaps, may prove possible.

Finally, experience could be gained toward the ideal of calibrating the static errors out of the data-taking equipment. If that were possible, the requirement for ground truth would shrink to the minimum necessary to adjust the coordinate zero, adjust scale, and rotate to grid north.

The SICLOPS System as developed thus far is not a final product. Its programs were developed sequentially as a programming convenience and thus provided an economy in computer usage. In consequence, some of the later programs have good features not found in the earlier ones. The present programs merit further clean-up to improve speed and ease of processing. Telescoping of several programs into one is possible, and the ease of operating the programs could be improved. Further development should be forthcoming as experience is gained in handling real data. The simulators will continue to be useful tools in ensuing development stages.

Because of the uncertainty in timing and the infrequent rate of the LTN-51 data which furnish the SICLOPS System with aircraft heading, track angle, and velocity, we suggest that three similar and available outputs from the Litton navigation system be incorporated in the ADAS recording system. These three outputs are true heading, which is available in the Litton analog output as synchro data, and the north and east components of velocity which are available as binary outputs. All three of these outputs are updated every 50 msec by the Litton system with a timing uncertainty of 12 msec. The increased data rate of the heading information would then provide the SICLOPS System with adequate yaw data. The binary outputs (the two velocity components) would have resolutions of 0.1 knot, as compared to a resolution of 1 knot in the current LTN-51 velocity record. Executing this change would eliminate the timing uncertainty

and also reduce the data preparation effort since the LTN-51 record would no longer be needed. A smoothing technique to reduce the effects of noise, as now used on current ADAS data, could then be applied to these three new inputs.

Another suggestion is to bring (relocate) the LTN platform closer to the scanner on-board the aircraft. The Litton unit is presently mounted well aft while the scanner occupies a forward position. This dynamic deformation of the aircraft fuselage in flight can produce occasional misalignment possibly amounting to several degrees. Surveying the LTN platform to the scanner platform would be very desirable.

4.3 SPATIAL—SPECTRAL INFORMATION

It is natural to seek methods for increasing accuracy which use more of the information collected by a MSS than simply the spectral measurements from each pixel to make a decision. Under other contracts [76] ERIM has tested approaches which extract spatial/spectral features related to texture or spatial frequency attributes of various classes. These promising approaches generally require large numbers of pixels to be grouped (thereby reducing significantly the effective spatial resolution of the system) and also require time-consuming transformations such as the fast Fourier transform to accomplish feature extraction.

Another way of using data from neighboring pixels is to define boundaries by a boundary-detection rule and then carry out a single recognition for each area enclosed. This approach, referred to as sample or per-field classification, is being investigated currently but has certain potential difficulties:

- (1) Human touch-up may be needed to insure that gaps in the boundaries are filled up
- (2) Some data sets would not conform to the pattern of homogeneous areas surrounded by boundaries, as, for example, when water depth is mapped by multispectral recognition
- (3) If the shapes of homogeneous areas are more complicated than simple quadrilaterals, a time-consuming algorithm may be required to collect the data from a single field. Hypothesis testing and clustering approaches to this problem are being pursued because of difficulties with various heuristic approaches such as gradients in boundary detection.

76. R. J. Kauth, R. B. Crane, W. Richardson, Feasibility Demonstration of Processing ERTS Data for Global Terrain Clutter Mapping, ERIM Report 106600-1-L, January 1974.

In the many applications where a pixel is likely to represent the same material as its immediate neighbors, a contextual rule taking neighboring data into account would be expected to perform better in terms of recognition accuracy than a single-element rule.

Nine-element rules are designed to gain the advantage of using spatial information while preserving the virtues of simplicity and speed since there is only a slight extra cost in processing time. Such rules are applied to each pixel of the scene, in turn, in the context of a 3×3 grid in which eight immediate neighbors surround one pixel in the center. The rules assume that most or all of these nine pixels represent the same material and they assign to the center pixel this majority material. The modest storage requirements and small number of pixels playing a part in each decision make these rules practical.

The nine-element rules are most effective in those contexts where the assumption of similarity of neighbors is most realistic. For this reason, one would expect nine-element rules to be more reliable within homogeneous areas and less precise along boundaries than a single-element rule. Nine-element rules are thus most applicable to MSS data on agricultural fields collected at aircraft altitudes or to surveys of lakes and rivers; they are not at all applicable when, as in some geological data, the materials are "salted and peppered" across the scene. When neighboring pixels are likely to represent different materials, then it is also likely that many pixels represent more than one material and a mixture rule would be appropriate.

Three rules were implemented and tested [77]. The nine-point likelihood rule is the maximum likelihood decision rule derived from the assumption that the nine elements are an independent random sample from a multivariate normal distribution. It amounts to adding, for each material, the nine multivariate normal exponents and choosing the material with the smallest such sum. To prevent occasional alien points from disturbing the decision rule, we have modified it to sum only the m smallest exponents, where $m = 1, \dots, 9$.

The moving average rule averages the nine data points and then applies the one-point rule. We have modified this rule to lessen its sensitivity to alien points by deleting the t largest and t smallest of the nine values in each channel, where $t = 0, \dots, 4$.

The voting rule is applied after one-point decisions have been made on the nine pixels. It assigns to the center pixel the material most frequently recognized among the nine pixels. In cases of tie, the conventional one-point decision on the center pixel is used.

77. W. Richardson, A Study of Some Nine-Element Decision Rules, ERIM Report 190100-32-T, July 1974.

For purposes of quantitative comparison, these three rules and the one-point rule were tested by counting the number of points misclassified within the interiors of 42 fields from the Imperial Valley, California. Test results showed an improvement in classification accuracy over the usual one-point rule, with the following ranking of rule performance from best to worst:

- nine-point likelihood rule with $m = 9$
- voting rule
- moving average rule with $t \neq 0$
- moving average rule with $t = 0$
- one-point rule
- nine-point likelihood rule with $m = 1$

The nine-point likelihood rule performed steadily better as m went from 1 to 9. The error rate for $m = 9$ was about one-half that of the one-point rule on the training sets; on the test sets it was about three-fourths that of the one-point rule.

To supplement the results on field interiors, we made qualitative comparisons of maps generated by the different rules. We implemented an option to allow each rule to decide against all the alternative materials and display such decisions by blanks on the map. Such null decisions leave a white framework of roads, rivers and other extraneous materials, against which materials of interest are located, and thereby help to produce a readable map.

Application of the $m = 9$ rule in conjunction with the null test splotted the map with white rectangles because a single unusual point produces higher than normal exponent sums for a 3×3 rectangle around it. The rectangles disappeared for $m = 7$. Fine detail such as small roads seem to be lost by the nine-point rules. The voting rule null test was to decide null if the winning vote total fell below a prescribed level. This null test worked well in locating narrow boundaries but failed to discard points distant from the material signatures but consistent with each other.

For some fields, the nine-point rules brought out an underlying pattern not readily apparent in a mixture of individual recognitions. For others, the nine-point rules seemed to find order where there was none. In either case, the contradictory character of the data was suppressed.

The null test can be used as a boundary detector by displaying each null point as a dark symbol and leaving everything else blank. Neither the $m = 7$ rule nor the voting rule succeeded well as a boundary detector. The $m = 7$ rule lost many small boundaries and the voting rule lost the large extraneous areas.

The experiment comparing the nine-point rules and the one-point rule is based on one data set. The conclusions from it are therefore tentative, and the ultimate impact and utility of the nine-point approach have yet to be established. The more successful performance of the nine-point rules as compared to the one-point rules in the experiment warrants their quantitative and

qualitative testing on other data sets and encourages the implementation and comparison of other promising nine-point rules. The development of a better boundary detector, combining the principle of distance from known signatures with the principle of divided allegiance, is indicated.

4.4 GEOLOGICAL AND NATURAL RESOURCE SIGNATURES AND APPLICATIONS

Photographic remote sensing in geological applications has historically dealt primarily with structural geology (e.g., finding faults, lineaments, etc.). MSS surveys allow lithologic surveys of rock type and chemical composition to be accomplished. Geologists are continually mapping rock types in order to better understand the geological history of the earth's crust. Although aerial photography has assisted the geologist greatly, the burden of final rock identification is still with the field geologist. An ability to map rock type by aerial remote-sensing and automatic-recognition methods would allow such mapping to be done more quickly at less cost.

A benefit of an imaging system which could discriminate rock types is that mineable ore deposits are often associated with certain types of surface rocks. For instance, the diamond-producing kimberlites are ultrabasic (silica-poor) rock formations. Also, the rare, high-temperature carbonates, called carbonatites, are associated almost exclusively with alkalic basic rock complexes. Carbonatites are most valuable for their high concentrations of rare-earth elements and are primary sources of niobium, used in high-temperature alloys, and thorium, important as a natural radioactive isotope. Therefore, from a natural-resource aspect, the ability to discriminate between at least acidic and basic silicate rocks in a quick and economical manner is quite advantageous for identification of potential exploration sites.

Geological remote sensing differs in several aspects from vegetative surveys. First, temporal effects are much slower for geological than for vegetative objects. Second, for rock-type identification the spectral emittance or reflectance variations are much more important than geometrical variations (shapes, shadows, look angle), whereas both are relatively important for the identification of vegetative classes. Third, the thermal IR spectral region contains more chemically diagnostic information about rocks than do the visible-reflective IR wavelength regions, whereas the converse is true for vegetative classes.

Development of special techniques for geological discrimination has been pursued at ERIM. These efforts began in 1970 as a demonstration that more accurate automatic information extraction techniques could be developed by examining the spectral characteristics of the classes (as from ERSIS).

A scheme for the broad-scale spatial mapping of compositional differences in the SiO_2 content of igneous silicate rocks is actually an innovation on an old theme, because the physical basis for the method depends on two properties of silicates first noticed by R. J. P. Lyon in

1964 [28]. First, unlike vegetation, other types of rocks, and most minerals, all silicate rocks characteristically display broad emissivity minima (reststrahlen bands) in the 8.0- to 12.0- μm wavelength region. These minima are caused by the silicon-oxygen stretching modes of the SiO_2 molecule. Secondly, the position of the silicate emissivity minimum shifts to longer wavelengths as the content of SiO_2 decreases—i.e., the emissivity minima for basic and ultrabasic rocks occur at longer wavelengths than do the emissivity minima of acidic rocks. The reason for this shift is that oxygen-silicon bonds are replaced by oxygen bonds to heavier ions such as iron and magnesium in the basic and ultrabasic rocks. A demonstration of both the silicate properties just mentioned is given in Figure 27, a rearranged plot of Lyon's data, which shows the emissivity spectra of 25 silicate rocks that vary in SiO_2 content from approximately 68 to 36%. The rock samples examined by Lyon were natural specimens with varying surface roughness.

From these experimental data, it was possible to devise a ratio method for imaging differences in SiO_2 content. At least three wavelength channels—two inside the reststrahlen region and one outside—are required to do the job properly. The outside channel could be located in the 11.5- to 13.0- μm region, where silicates exhibit little departure from unit emissivity. If signal-to-noise were not a problem, 11.5 to 12.0 μm would be a preferable region because the small, 13.0- μm , silicate bands would then be eliminated; however, the energy gained by making the upper limit 13.0 μm instead of 12.0 μm may, for most practical systems, be worth the relatively small degradation of useful information. The purpose of this channel (11.5-13 μm) outside the reststrahlen band region is to act as a reference for two operations: one to ascertain the true temperature of the target; and the other to determine, when this channel is ratioed with the sum of the two channels inside the reststrahlen region, whether the target is a silicate.

The remaining two channels inside the reststrahlen region can be ratioed as the next step in determining the approximate silica content of the silicate target. As reported in Ref. [22] in April 1971, this method was applied to July 1970 MSS data from Mill Creek, Oklahoma, which resulted in the first successful geological compositional recognition map discriminating quartz sand and sandstone from the background (see Figure 28).

At least 12 additional reports [31, 32, 78-97] of work which is an outgrowth of this initial research have resulted from this contract (NAS9-9784). Additional band-ratio schemes using visible green and reflective IR bands for mapping iron oxides and alteration patterns associated with mineral deposition have also been developed [86] with significant results reported in the ERTS program. These contributions over a four-year period have taken geological and natural resources MSS sensing out of the realm of what was at first mildly interesting to those in the field, to a stage verging on resource discovery, mining site location, and operational use. Moreover, some of these techniques are useful in soils mapping as well [98-104]; the interested reader may pursue further details in these references.

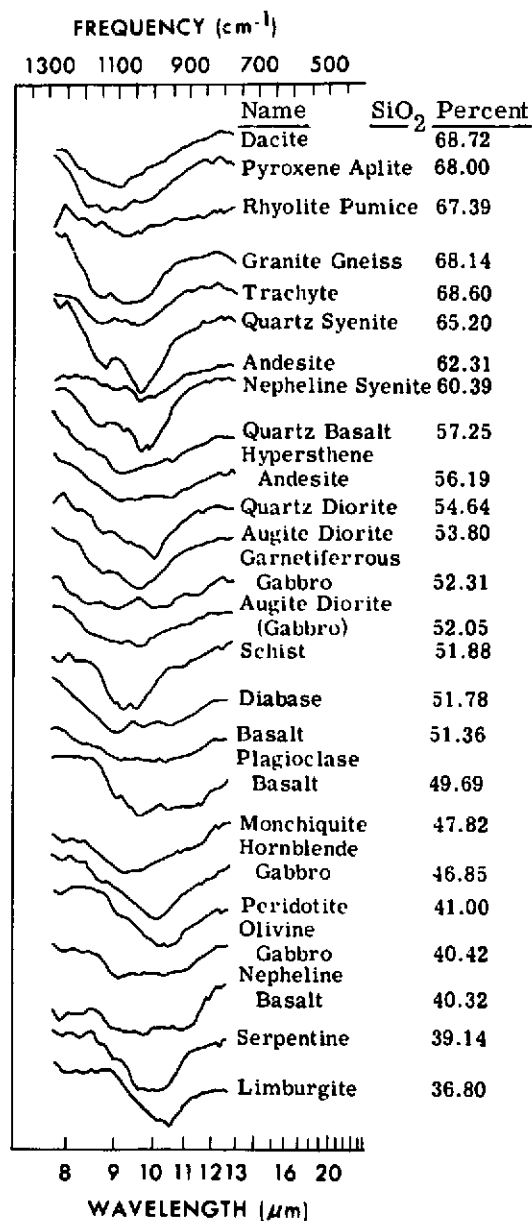


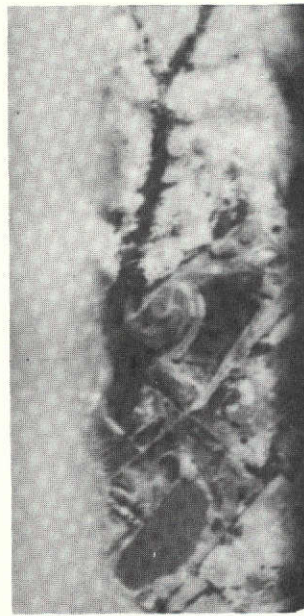
FIGURE 27. EMISSIVITY SPECTRA OF SILICATE ROCKS (From Lyon Data)

ORIGINAL PAGE IS
OF POOR QUALITY

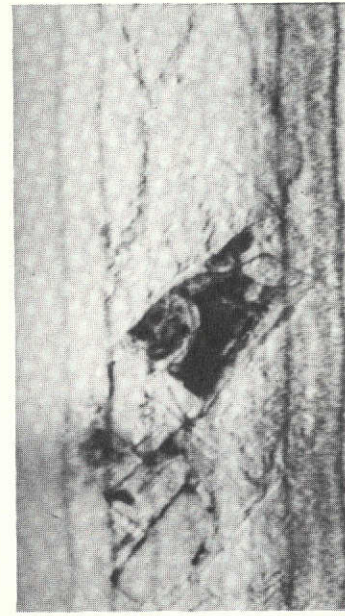
87



(a) 8.2 to 10.9 μm



(b) 9.4 to 12.1 μm



(c) Ratio Image

FIGURE 28. ANALOG-PROCESSED IR IMAGES OF SAND QUARRY FROM 25 JULY 1970 FLIGHT OVER MILL CREEK, OKLAHOMA. Dark represents cool in left and center single-channel images; dark corresponds to quartz sand and quartz sandstone in ratio image on the right.

78. R. K. Vincent and F. J. Thomson, Discrimination of Basic Silicate Rocks by Recognition Maps Processed from Aerial Infrared Data, 7th International Symposium on Remote Sensing of Environment, June, 1971.
79. F. Thomson, Processing of Pisgah Crater Thermal and Multispectral Data, ERIM Report 3165-64-T, July 22, 1971.
80. R. Vincent, Rock-Type Discrimination Ratio Images of the Pisgah Crater, California Test Site, ERIM Report 31650-77-T, June 1972.
81. R. Vincent, F. Thomson, Rock-Type Discrimination from Ratioed IR Scanner Images of Pisgah Crater, California, SCIENCE, March 1972.
82. R. K. Vincent, Experimental Methods for Geological Remote Sensing, presented at the 4th Annual Earth Resources Program Review, NASA/MSR, Houston, January 17, 1972, and published in Proceedings.
83. R. Vincent, F. Thomson, Spectral Compositional Imaging of Silicate Rocks, Journal of Geophysical Research, Vol. 77, No. 14, pp. 2465-72, May 1972.
84. R. Vincent, F. Thomson, K. Watson, Recognition of Exposed Quartz Sand & Sandstone by Two-Channel Infrared Imagery, Journal of Geophysical Research, Vol. 77, No. 14, pp. 2473-77, May 1972.
85. R. Vincent, An Emission Polarization Study on Quartz and Calcite, Submitted to Applied Optics, September 1972.
86. R. K. Vincent, An ERTS Multispectral Scanner Experiment for Mapping Iron Compounds, 8th International Symposium on Remote Sensing of Environment, October 1972.
87. R. Vincent, Spectral Ratio Imaging Methods for Geologic Remote Sensing from Aircraft and Satellites, Management and Utilization of Remote Sensing Data Conference, 29 Oct—1 Nov 1973.
88. R. K. Vincent, Infrared Recognition Maps of Silicate Rock Types—A New Tool for Mineralogical Exploration, 1971 Annual Meeting of the Geological Society of America, Washington, p. 739, 1971.
89. L. Rowan and R. K. Vincent, Discrimination of Iron-Rich Zones Using Visible and Near-Infrared Spectral Analysis, in ABSTRACTS of 1971 Annual Meeting of the Geological Society of America in Washington, p. 691, 1971.
90. R. K. Vincent and F. Thomson, Spectral Compositional Imaging of Silicate Rocks, Journal of Geophysical Research, Vol. 77, pp. 2465-71, 1972.
91. R. K. Vincent, Ratio Maps of Iron Ore Deposits, Atlantic City District, Wyoming, Symposium on Significant Results Obtained from the Earth Resources Technology Satellite-1, Vol. 1, pp. 379-86, 1973.
92. R. K. Vincent, Ratio Techniques for Geochemical Remote Sensing, Proceedings of the Fourth Annual Conference on Remote Sensing in Arid Lands, Tucson, November 1973, (to be published in 1974).
93. R. K. Vincent, A Thermal Infrared Ratio Imaging Method for Mapping Compositional Variations Among Silicate Rock Types, Ph.D. Dissertation, Department of Geology and Mineralogy, The University of Michigan, Ann Arbor, 1973.
94. B. Salmon and R. K. Vincent, Surface Compositional Mapping in the Wind River Range and Basin, Wyoming by Multispectral Techniques Applied to ERTS-1 Data, Proceedings of Ninth Symposium on Remote Sensing of Environment, Ann Arbor, Michigan, 1974 (In Press).
95. R. Dillman and R. K. Vincent, Unsupervised Mapping of Geologic Features and Soils in California, Proceedings of the Ninth Symposium on Remote Sensing of Environment, Ann Arbor, Michigan, 1974 (In Press).

The most recent report [87] describes four independent investigations concerned with improving and utilizing correlations between the physical properties of natural materials as evidenced in laboratory spectra and spectral data as collected by multispectral scanners. The first investigation resulted in the presentation of two theories which permit the calculation of spectral emittance spectra for rock and mineral surfaces of various particle sizes. The inputs to the simpler model are a near-normal-incidence infrared reflectivity curve of a polished surface of the rock or mineral of interest and a specified particle size that is typical of the rock or mineral surface under natural conditions. The calculated results for quartz, calcite, chert, and limestone were qualitatively accurate. The major conclusion was that for most silicate rock surfaces, texture does not have as much control as chemical composition over the spectral emittance, as long as the diameters of particles comprising the surface are on the order of 30 μm or larger (which is the case for most rocks not covered with products of weathering). The relevance of these results for geological remote sensing is that variations of texture indigenous to silicate rock genesis will most likely not mask the effect of rock composition on spectral emittance in the 8-14 μm wavelength region. For carbonate rocks, however, textural effects on spectral emittance can be appreciably large, though not of such a nature as to cause

96. R. K. Vincent and W. W. Pillars, Skylab S-192 Ratio Codes of Soil, Mineral, and Rock Spectra for Ratio Image Selection and Interpretation, Proceedings of the Ninth Symposium on Remote Sensing of Environment, Ann Arbor, Michigan, 1974 (In Press).

97. T. Wagner, R. K. Vincent, B. Drake, R. Mitchell, and P. Jackson, Tunnel-Site Selection by Remote Sensing Techniques, The University of Michigan Technical Report 10018-13-F, U.S. Bureau of Mines Contract H0210041 (ARPA Order No. 1579, Amendment 2, Program Code IF10), 1972.

98. R. K. Vincent, T. Wagner, B. Drake and P. Jackson, Geologic Reconnaissance and Lithologic Identification by Remote Sensing, ERIM Technical Report 191700-8-F, ARPA-USBM Contract No. H022064, 1973.

99. P. G. Hasell, Jr., et al., Investigation of Multispectral Techniques for Remotely Identifying Terrain Features and Natural Materials, ERIM Report 196200-12-F, May 1974.

100. T. W. Wagner and P. G. Hasell, Jr., Remote Identification of Terrain Features and Materials at Kansas Test Sites: An Investigative Study of Techniques, Federal Highway Administration, Washington, Report FHWA-RD-73-53, 1973.

101. F. G. Sadowski, T. W. Wagner, F. J. Thomson, and P. G. Hasell, Jr., The Remote Identification of Terrain Features and Materials at Pennsylvania Test Sites: An Investigative Study of Techniques, Federal Highway Administration, Washington, Report FHWA-RD-74-9, 1974.

102. T. W. Wagner and P. G. Hasell, Jr., The Remote Identification of Terrain Features and Materials of Virginia Test Sites: An Investigative Study of Techniques, Federal Highway Administration, Report FHWA-RD-74-10, Washington, 1974.

103. R. K. Vincent, R. D. Dillman, and P. G. Hasell, Jr., The Remote Identification of Terrain Features and Materials at a California Test Site: An Investigative Study of Techniques, Federal Highway Administration, Washington, Report FHWA-RD-74-27, 1974.

104. Remote Sensing in Michigan for Land Resource Management: Highway Impact Assessment, Report 190800-1-T, Infrared and Optics Division of Environment Research Institute of Michigan, Michigan State University, and Michigan Department of State Highways, 1972.

misidentification of carbonates as noncarbonates. These rock surface models also have utility for atmospheric aerosol problems. NASA scientists working on Mariner Mars data have already calculated results for atmospheric aerosol models.

In the second investigation, optimum filters for implementing a two-channel thermal infrared region ratio technique with low altitude aircraft scanner data were selected for the purpose of discriminating among silicate rock types on the basis of an $\%SiO_2 - \%Al_2O_3$ chemical parameter. The best filter combination for this purpose is 8.1-10.1 μm for the lower wavelength filter and 9.2-11.2 μm for the higher wavelength filter. When only two infrared channels are considered, the 2 μm filter width is for all practical purposes as good as or (considering signal-to-noise improvement) better than narrower filters on the order of 0.5 μm wide.

The third investigation involved the compression of approximately 235 laboratory spectra into 11-digit ratio codes, for use with the ERIM M7 aircraft scanner. These M7 ratio codes can be used in three ways: to determine which ratios are best for discriminating a given target from other targets and background, to predict which materials have similar enough spectral properties to be confused with a given target, and to eventually be used as training sets from which automatic recognition maps can be made. Before the latter long-term goal can be accomplished, many more laboratory and field spectra will be needed to make the collection of ratio codes more complete.

In the fourth study, reported in Ref. [87], we outlined a system for producing automatic recognition maps aboard space shuttle and high altitude aircraft. Ratio preprocessing steps were described for both reflective and thermal-infrared scanner channels. The reflective channel signals would undergo dark object subtraction and ratio normalization to an easily identifiable reference in the scene. Thermal-infrared channel signals would be corrected for atmospheric effects by an atmospheric model. A thermal channel in a spectral region where silicate targets show little emittance contrast would be used with an atmospheric model to correct the single-channel thermal radiances for temperature variations across the scene. Corrected spectral ratios for both reflective and thermal channels would result from these preprocessing steps. Different data processing methods were recommended for two different types of remote sensing problems. For targets of interest preselected by the user, a ratio gating logic (RAGAL) procedure was suggested and a method described for finding the most efficient logic sequence for RAGAL. Stored laboratory and field spectra of target materials would be used for training sets. For the type of remote sensing problem in which there are no preselected targets, three types of logic were suggested, all of them involving the use of laboratory and field spectra as training sets: One is RAGAL, performed in reverse to the preselected target case. A second is unsupervised clustering in ratio space, with stored lab and field spectra used to identify the clustered targets. The third is a parameterization method whereby a linear combination of ratios is used to predict a physically meaningful index related to target composition.

IMPROVING EFFICIENCY OF EXTRACTED INFORMATION

In order for any information system to become operationally acceptable to potential users, the information extraction process must be relatively efficient so the cost-effectiveness of the data collection operation will not be compromised. In this section we briefly discuss a number of approaches and techniques developed and investigated by ERIM under this contract for decreasing, through powerful automatic procedures, the cost and time required for information extraction.

5.1 FEATURE EXTRACTION

In Section 4 we discussed the main purposes of feature extraction as providing unique and invariant features for classification. In the context of spectral discrimination and efficiency, feature extraction is concerned with developing dimensionality reduction by selecting subsets of spectral bands or linear combinations of spectral bands as means of reducing time and cost on general purpose computers without significant loss of accuracy.

On general purpose computers, computing time increases as the square of the number of spectral bands for quadratic decision rules. Thus, if the time spent selecting a subset of bands or linear combination of bands is less than the time difference between processing all bands or, alternatively, only a selected few, the feature extraction approach described below may be a substantial improvement in terms of time and money savings. The key is whether essentially equivalent performance can be achieved as far as classification accuracy is concerned.

A greater reduction in dimensionality may be obtained by use of a subset of linear combinations which can be used in recognition processing just as if they were a subset of spectral bands. The training data are examined to determine which linear combinations of bands to use, but accuracy testing should not be done on training data but rather on test data of known classes. In many applications, it may be that a subset of 2 or 3 linear combinations will give the same recognition information as the use of all pure channels.

ERIM achievement in this area of subset selection has evolved from a channel selection with a quadratic average pairwise probability of misclassification criterion, through channel selection with a best Bayesian linear average pairwise probability of misclassification, to a linear combination of channels subset selection with average pairwise probability of misclassification.

It is of interest to note that even the 1967 quadratic channel selection criterion employed the time-saving Cholesky decomposition of the inverse of the covariance matrix [105].

105. P. G. Hasell, et al., Investigations of Spectrum-Matching Techniques for Remote Sensing in Agriculture, Report for March-December 1967, The University of Michigan (WRL), Ann Arbor, Report 8725-13-P.

5.1.1 CHOOSING SUBSETS OF CHANNELS

In order to choose subsets of channels, it is necessary to have a criterion for doing so. The Bayesian criterion, average expected loss (which can be formulated as an average probability of misclassification), is an excellent one for classification performance evaluation and channel selection. It has direct physical interpretation, and can be applied when the objective is to optimize performance either in choosing between a few material classes in a scene or between all material classes.

In the context of multispectral recognition, the average expected loss is defined as follows. Let us suppose that a decision is being made as to which of k materials is being observed. One specifies in advance a rule for making this decision (for example, the rule that the material chosen is the one with the largest normal likelihood function). Let p_{ij} be the probability that the rule will choose material i , given that the material really is j . If L_{ij} is a cost factor that measures how much you lose by making this erroneous decision, then

$$L_j = \sum_{i=1}^k p_{ij} L_{ij}$$

is the expected loss incurred when material j is being observed.

It is not possible to construct a rule for minimizing L_1, L_2, \dots, L_k simultaneously. For example, L_1 would be minimized by using the rule "always choose material 1," but then L_2, \dots, L_k would all be maximized. Bayesian theory strikes a balance between these expected losses by minimizing a weighted average of them, i.e.,

$$L = w_1 L_1 + w_2 L_2 + \dots + w_k L_k$$

The rule that accomplishes this minimization is called the Bayesian decision rule.

The weights, w_i , play the role of prior probabilities. Suppose that there were a chance mechanism for assigning materials to resolution elements and w_i were the probability that material i would be assigned to the resolution element, then $\sum w_i L_i$ would be the total expected loss, which the decision maker would seek to minimize. Thus when weights, w_i , are specified in a Bayesian decision rule, the decision maker is in effect estimating the prior probabilities of the materials. A conventional procedure when the prior probabilities are not known is to make the weights equal. If the losses are also assumed equal, it can be shown that the Bayesian decision rule is the same as the maximum likelihood decision rule.

Ideally, then, questions about channel selection are answered by computing the average expected loss. The best subset of size s is the one with the smallest average expected loss. You find the best subset of size 1, the best subset of size 2, and so on for all $s \leq n$, the number of

channels. The average expected loss for each subset is a decreasing function of s . You look at this function and weigh the decrease in loss against the increased cost of processing, which goes up as the square of the number of channels, and reach a decision about the optimal value of s .

But the calculations required for this ideal procedure are so formidable that it would not be practical to carry them out. To make the implementation worthwhile, the selection of the subset of channels must be significantly less time consuming or costly than the processing would be without selecting a subset. The probabilities, p_{ij} , as heretofore defined, can be calculated only when $k > 2$ and a normal maximum likelihood decision rule is used by an n -dimensional quadrature or Monte Carlo. If $n \geq 6$, the quadrature is impossible on even the largest computers, and the Monte Carlo estimates become so imprecise and time-consuming that they are worthless for discerning small differences between subsets. Therefore, a number of approximations and assumptions have been made to simplify the task.

First, p_{ij} is approximated by the pairwise p_{ij} —that is, the p_{ij} that one would get if material i and material j were the only materials present. Monte Carlo checks of this approximation have given very satisfactory agreements. The pairwise p_{ij} can be calculated by a quadratic method.

Second, L_{ij} is assumed equal to L_{ji} , and the loss constants are so normalized that $\sum_j L_{ij} = 1$. The average expected loss is, therefore, a weighted average of p_{ij} 's and can be considered an average probability of misclassification. Thus, as a performance measure, the average expected loss has an intuitive meaning that provides a basis for choosing the subset size, a choice that requires weighing performance of the decision rule against cost of processing. (At present, this choice is made by an individual user based on his experience and judgement.) Equal weights, w_j , are normally assumed but there may well be some good reason for making the L_{ij} 's different. Suppose, for example, the signatures are barley, two kinds of wheat, and oats, and you want to be able to recognize the different crops but care nothing about discriminating between the two kinds of wheat. Equal L_{ij} 's would give the wheat-wheat p_{ij} equal weight with the other p_{ij} 's. Moreover, the wheat-wheat p_{ij} would probably be by far the largest, so the channels would be selected mostly on the basis of how well they distinguished between the two kinds of wheat. This unwanted result is avoided by making the wheat-wheat L_{ij} equal to zero. Or suppose one is making a map of bodies of water and has signatures for shallow water, deep water, forest, crops, swamp, and bare soil. The only errors that matter are those between a water and a land signature, and these are the pairs for which L_{ij} should be nonzero. For the water-water and land-land pairs, L_{ij} should be zero.

A third approximation is that the subset is chosen by a stepwise without replacement procedure, that is, by choosing the best channel, then the channel which, along with the one chosen, is best, then the channel which is best along with the two previously chosen, and so on.

In choosing a subset of size 5 from 10 channels, the time saving by the stepwise approximation is by a factor of 8.4. This approximation was tested [48] on seven pairs of 10-channel signatures which were close together, had produced a confusing recognition map, and which, therefore, are believed to represent a demanding test of the approximation. All subsets of size 3 (and later of size 5) were ranked according to probability of misclassification. For all of the subsets of size 3 and all but one of the subsets of size 5, the stepwise procedure found the best subset. In the one exception, the procedure picked the second of two subsets that were nearly tied for first place. It appears, therefore, that use of the stepwise procedure is justified.

Ways of speeding up the calculations have been studied [106, 107] and a fourth approximation is used: this is to assume a best Bayesian linear approximation to the quadratic decision rule, thereby making it much simpler to calculate the probability of misclassification. Using this approximation results in a fifty-fold saving in time. Table 4 shows how the results compare. The probabilities computed by the two methods are comparable. The orderings are the same except that the linear method interchanges the last two pairs of channels as compared to the ordering produced by the quadratic method. The use of channel 2 rather than channel 8 in a subset of seven channels would increase the average probability of misclassification by only 0.00001, according to the quadratic calculations. Similarly, the interchange of the ordering of the last two ranked channels would increase the average by 0.00003 for a subset of nine channels. The accuracy of the calculation of average probability of misclassification depends upon the representativeness of the training data.

The seven close pairs of signatures referred to earlier were used to test the performance of three forms of the linear approximation. All subsets of size 3 (and later all of size 5) were ranked by the quadratic and the three linear criteria, and the quadratic probability of classification for each subset was retained as a measure of performance. By this measure, the performance of all three linear methods was virtually identical and nearly as good as the quadratic method.

Table 5 gives, for each of the pairs of signatures: (a) the rank of the subset chosen by the fastest linear method, (b) the difference between the quadratic p.m. (probability of misclassification) of that subset and the p.m. of the best subset, (c) the p.m. of the best subset, and (d) the difference between the p.m. of the worst subset and the p.m. of the best subset. The table shows

106. R. Crane, W. Richardson, Rapid Processing of Multispectral Scanner Data Using Linear Techniques, in Remote Sensing of Earth Resources, Vol. I, containing selected papers from Earth Resources Observation & Information Analysis Systems Conference of 13-14 March 1972, May 1972.

107. R. B. Crane, W. Richardson, Performance Evaluation of Multispectral Scanner Classification Methods, 8th International Symposium on Remote Sensing of Environment, Ann Arbor, October 1972.

TABLE 4. COMPARISON OF CHANNEL SELECTION METHODS FOR NINE SIGNATURES

(a) Quadratic Channel Selection										
Order of Channels	4	10	1	9	7	5	8	2	3	6
Average Probability of Misclassification	0.119	0.054	0.031	0.025	0.023	0.021	0.019	0.018	0.017	0.016
(b) Linear Channel Selection										
Order of Channels	4	10	1	9	7	5	2	8	6	3
Average Probability of Misclassification	0.122	0.059	0.034	0.028	0.025	0.024	0.023	0.021	0.021	0.020

TABLE 5. PERFORMANCE OF LINEAR CHANNEL SELECTION FOR SEVEN PAIRS OF SIGNATURES

(a) Subset Size 3 (120 subsets)			
rank of subset chosen by linear	linear p.m. - best p.m.	best p.m.	worst p.m. - best p.m.
4	0.009	0.110	0.32
1	0	0.081	0.27
1	0	0.110	0.13
1	0	0.023	0.08
1	0	0.006	0.13
1	0	0.010	0.25
1	0	0.035	0.29
(b) Subset Size 5 (252 subsets)			
rank of subset chosen by linear	linear p.m. - best p.m.	best p.m.	worst p.m. - best p.m.
9	0.006	0.090	0.24
1	0	0.072	0.23
2	0.000	0.082	0.10
1	0	0.013	0.04
1	0	0.004	0.07
3	0.000	0.006	0.04
2	0.000	0.022	0.15

that the linear method picked the best subset in 9 cases out of 14, did no worse than third for all but 2 of the cases, and, in the worst case, chose a subset with a p.m. only negligibly greater than the best p.m. The fourth column of the table shows how badly a poorly chosen channel selection method might perform. When one considers that time spent in a lengthy calculation of optimum channels would be better spent in adding more channels to the decision process, the linear approximation in channel selection and ordering appears useful. A typical calculation takes a minute or less.

5.1.2 CHOOSING LINEAR COMBINATIONS

The problem of finding a good method of choosing linear combinations [108-112] is primarily one of finding a workable algorithm in three distinct steps: (1) develop a measure of performance, (2) develop a minimum seeking technique, and (3) find suitable starting points for initiating the minimum seeking technique. In addition, the algorithm should not require an excessive amount of computational time.

The performance measure used to evaluate both subsets of linear combinations and subsets of pure channels can be expressed as:

$$M = \sum_{i,j} \phi \left\{ \frac{1}{2} \left[(\mu_i - \mu_j)^t A^t A \frac{R_2 + R_1}{2} A^{t-1} A (\mu_i - \mu_j) \right]^{1/2} \right\}$$

where the summation is for all signatures, the i -th class is distributed normally with mean vector μ_i and covariance matrix R_i , and $\phi(X)$ is the normal distribution function. The row vectors of the $m \times n$ matrix A represent the linear combinations in question (n is the number of pure channels and m is the number of linear combinations). When this expression is used to

108. R. B. Crane, Linear Combinations, Quarterly Supporting Research and Technology Review, JSC, Houston, 26 September 1972, and (WRL) Report 31650-147-L, October 1972.

109. R. Crane, W. Richardson, R. Hieber, and W. Malila, A Study of Techniques for Processing Multispectral Scanner Data, ERIM Report 31650-155-T, January 1973.

110. R. B. Crane, Feature Extraction of Multispectral Data, LARS Conference on Machine Processing of Remotely Sensed Data, Purdue University, October, 1973.

111. R. Crane and P. Hyde, Adaptive Processing Using a Decision Directed Kalman Filter and Feature Extraction of Multispectral Scanner Data, ERIM Report 190100-31-T, July 1974.

112. R. B. Crane, T. Crimmins, J. Reyer, and R. Kauth, Feature Extraction of Multispectral Data, IEEE Transactions on Geoscience Electronics, 1973.

evaluate a subset of pure channels, the matrix A becomes an array of 0's and 1's. Notice that if the distance between means, $\mu_i - \mu_j$, is increased, the argument of the normal distribution function associated with that pair is increased, resulting in an increase of the expression M . M is thus an approximate measure of the total number of correct classifications. The average probability of misclassification is then approximately 1 minus a term proportional to M .

If R_i and R_j increase, then the average probability of misclassification would be expected to increase. We see, by following through the expression for M , that this is so. The measure M is an accurate measure of the results actually obtained in using a maximum likelihood linear rule with two specific approximations: First, M gives added weight to regions which can be misclassified in more than one way, while a decision rule used on actual data partitions all the data uniquely into separate classes. Second, the linear decision rule actually used on data takes account of both of the covariance matrices $R_i + R_j$, whereas M merely averages them together. M is, however, a more accurate measure than some others which have been suggested. For example, $(R_i + R_j)/2$ could be replaced by the average of all the covariance matrices in the signature set, rather than using the appropriate pairwise average. Also, the function ϕ could be replaced by its argument, resulting in what has been designated [113-115] a "divergence criterion." This is clearly an inferior criterion since it continues to force more separation between means even after they are several sigma apart. An advantage of M as defined above is that it can be developed directly from the maximum likelihood decision rule, so the approximations used can be enumerated and evaluated; in fact, it is approximately proportional to a constant minus the average probability of misclassification that would be measured.

A method has been developed to find a local minimum of a function of several variables by starting at a point and following a path of steepest descent by steps of variable but controllable size. Both the local gradient and the local curvature are used to estimate the path of steepest descent.

There is one additional problem concerning the determination of A that should be mentioned. If A is an $m \times n$ matrix, there are mn components to be determined. This number of components can be reduced to $m(n - m)$ by the choice of a suitable canonical form of A . A canonical form is possible because the value of M obtained for any A is not changed if PA is substituted for A ,

113. W. S. Hsia and J. P. deFigueiredo, Optimal Feature Extraction—The Two-Class Case, ICSA-275-025-010, Rice University, Houston, May 1973.

114. D. J. Jegewski, Optimal Feature Extraction by a Linear Transformation, Revision 1, MSC Internal Note No. 73-FM-19, March 1973.

115. J. A. Quirein, An Interactive Approach to the Feature Selection Classification Problem, TRW Systems Technical Note 99900-H019-RO-00, Houston, December 1972.

where P is any nonsingular matrix. We actually use PA , where P is chosen to scale the average covariance matrix and the mean vectors of the materials to our data format. The canonical form we chose is:

$$A = \begin{bmatrix} \tan \theta_{11} & \tan \theta_{12} & \dots & \tan \theta_{1(n-m)} \\ \tan \theta_{21} & & & \\ \vdots & & & \\ \tan \theta_{m,1} & & & \end{bmatrix}$$

where I_m is the identity matrix with rank m . (For a specific example see Table 8, where $m = 3$, $n = 10$, and the 10 pure channels have been rearranged in order of the wavelength.)

The canonical form with the θ_{ij} has two advantages. The first is that, in general, a minimum number of unknown scalars must be found. The second advantage is that the minimization process can be accomplished by varying the θ_{ij} with a nearly uniform step size. It is not necessary to have large jumps in the values of the unknown scalars, which occur if the $\tan \theta_{ij}$ are considered to be the unknown scalars.

Finding starting points, the third step, is more difficult. The following are suggested starting points.

Best Subset of Channels Starting Point

Each individual channel can be thought of as a linear combination of channels. (The vector representing this combination has a 1 in the appropriate coordinate and 0's elsewhere.) Therefore, a subset of m channels can be thought of as a set of m linear combinations. Since the number of subsets of m channels can be large, rather than check through all of them to find the best one, we use a stepwise procedure to find a "good" one. This stepwise procedure successively adds the one channel which gives the lowest average probability of misclassification when used with the channels already selected. The linear combinations represented by this subset are then used as a starting point.

Norm-Squared Starting Point

By replacing each covariance matrix with the average of all of them, the problem is reduced to minimizing the function

$$M(P) = \sum_i \phi(1/2 ||Pw_i||)$$

where the w_i are a fixed set of vectors and P ranges over all orthogonal projections of rank m . The number of vectors w_i is the total number of pairwise combinations of signatures. Each

projection P corresponds in a simple fashion to a matrix A in the original formulation. The projection P which maximizes

$$\sum_i ||Pw_i||^2$$

is found analytically and the corresponding A is used as a starting point.

Principal Eigenvector Starting Point

First calculate the average of all the covariance matrices. Then transform the data so that the average covariance matrix is the identity matrix. Let $N(\mu, R)$ be the distribution that can be calculated from the distributions of the various materials if we can estimate the frequency of occurrence of each material. The starting point A is then taken as the matrix whose row vectors are the m orthogonal eigenvectors corresponding to the m largest eigenvalues of the covariance matrix R .

Clustered Starting Point

This method is based on the fact that if there are only two signatures and we are using linear discrimination, then there always exists a single linear combination channel which distinguishes exactly as well as all n channels no matter what the value of n . If there are many signatures, then for each pair $S_i, S_j (i \neq j)$, v_{ij} can be the unit vector corresponding to this best single linear combination. In general, the number of vectors $v_{i,j}$ will be greater than m . The $v_{i,j}$ are then clustered into m clusters. For each cluster $C_k, k = 1, \dots, m$, we compute a weighted average, w_k , of the $v_{i,j}$ in that cluster. The starting point A (a matrix) has rows which are formed from the w_k . The weights can be made to reflect the sensitivity of the recognition accuracy to the decision rule.

We compared subsets of linear combinations with subsets of pure channels. The data used were from one of the sets previously employed to test our linear decision rule. We chose this particular set because of the difficulty we have noticed in obtaining satisfactory recognition with it. We felt that with relatively poor recognition accuracy, the test results would represent greater statistical accuracy. If only a few data points were incorrectly recognized, the test results would be too dependent on those few points.

The test procedure we used was to first select data that corresponded to 20 training fields. From these fields we developed statistics (mean and covariance) for each of the 7 classes of materials. The statistics or signatures were then used to develop the decision rules which were applied to data that corresponded to 23 test fields different from the training fields. We then found the average correct recognition for each field, and then the average for each material. Finally we averaged recognition accuracies for the materials to obtain an average recognition

accuracy for the data set. The computer programs were merely functional, not optimized for minimum computation time, so meaningful comparisons of computation times were not made.

The material classes consisted of bare soil and six vegetative species: alfalfa, barley, lettuce, sugar, safflower, and rye. The bare-soil data tended to be atypical, because three or more pure channels of data provided almost perfect recognition, whereas all of the subsets of 3 linear combinations of channels provided reduced accuracy. Note that the various subsets of linear combinations were chosen to optimize over all the species; therefore, it is not surprising that they did less well for one of them. There is some evidence that one infrared channel or ratio of channels can be used to separate vegetative and nonvegetative materials. Thus, for some applications of layered or sequential classifiers, bare soil may not be considered as a class to be recognized when discriminating among vegetation types. However, for this study, we retained bare soil as a class.

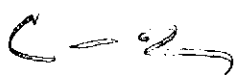
The test results are shown in Figure 29. The entire bar indicates the average recognition accuracy obtained for the 7 classes. The unshaded portion indicates accuracies for the 6 vegetative classes. Note that the recognition accuracy for the subset of 3 linear combinations was better than that obtained when subsets of either 3 or 4 best pure channels were used. In fact, the accuracy approached that obtained for all 10 channels, especially when only the 6 vegetative materials are considered.

Figure 29 shows the average recognition accuracy obtained for one subset of 3 linear combinations only. We actually tested three subsets of 3 linear combinations. Two of the subsets resulted from minimizing our measure function with two different starting points (the first of these was used for Fig. 29); the third subset was an unweighted addition of channels. We obtained approximately the same average recognition accuracy for each of the subsets of linear combinations [111].

5.2 LINEAR DECISION RULE

A number of possible linear decision rules could be used for classifying multispectral scanner data. We chose to evaluate rules that can be put in the form of a series of pairwise decisions; the linear discriminant method is such a decision [116]. Another common feature of the selected rules is that the same data channels are used for each series of pairwise

116. T. W. Anderson and R. R. Bahadur, "Classification into Two Multivariate Normal Distributions with Different Covariance Matrices, *Annals of Mathematical Statistics*, Vol. 33, 1962, p. 420.



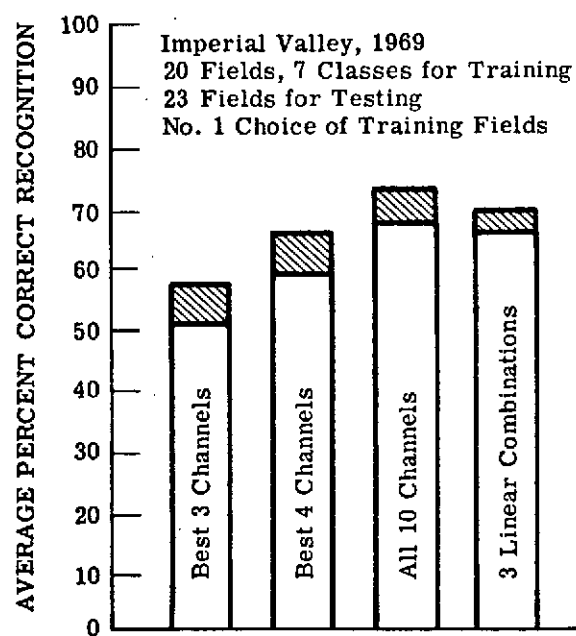


FIGURE 29. COMPARISON OF LINEAR COMBINATIONS WITH SUBSETS OF CHANNELS FOR TEST FIELDS

decisions. We felt that, while choosing different channels for each pairwise decision should be advantageous when classifying the training data, the advantage would tend to be lost when nontraining data were classified.

Five linear decision rules were tested and compared with the quadratic decision rule. One rule, optimistically labeled "best linear," uses the pairwise linear rule that best classifies data from two normal distributions [116]. The best linear decision rule proved to be the best of the linear rules that we tested.

The maximum likelihood decision rule becomes linear when the assumption is made that all covariance matrices are the same. Therefore, we call it the equal covariance rule, although it is sometimes referred to as the linear discriminant rule. To develop another rule we tested, the modified equal covariance rule, we found the linear function and the additive constant which, when added to the quadratic function formed from the common covariance matrix, best approximated the likelihood function in the mean square sense. To be more precise, if the quadratic decision rule based its decision on the maximum of

$$g_i(y) = (y - \mu_i)^t Q_i^{-1} (y - \mu_i) + \ln |Q_i|$$

and we wished to see

$$h_i(y) = (y - \mu_i)^t Q_0^{-1} (y - \mu_i) + y^t C_i + D_i$$

where the same covariance matrix Q_0 is used for all processes, then we found the C_i and D_i that minimized

$$\int [h_i(y) - g_i(y)]^2 P_i(y) dy$$

where the integral is n -dimensional. The use of $h_i(y)$ involves a linear function of y only, since the quadratic function $y^t Q_0^{-1} y$ is common to all processes and hence plays no part in the decision. This rule we labeled modified equal covariance. It proved to be no more accurate than the unmodified rule.

We tested two additional decision rules. In one, we used the diagonal terms of the covariance matrices, letting the remaining elements be zero. We labeled this rule the zero covariance rule. The nearest neighbor rule, derived by setting the covariance matrices equal to the unit matrix, chooses the distribution with the nearest mean. These last two rules, as well as the equal covariance rules, are convenient for both serial and parallel computers. The best linear rule is used most easily on a serial digital computer.

We performed a series of tests designed to evaluate the performance of the various decision rules [106, 107, 109]. Our desire was to devise a quantitative comparison, and thereby to eliminate such qualitative procedures as a visual comparison of recognition maps. We also wanted to make comparisons in a manner directly applicable to the classification problem. We programmed the decision rules for a digital computer, counting the number of correct and incorrect recognitions within fields for which we had corroborative ground observations, and measuring the time taken by the computation. A probability of misclassification was computed for each field by finding the number of incorrect recognitions, and dividing by the sum of the number correct and the number incorrect. An average error rate was then found by establishing the average probability of misclassification. The time measurement included not only that time needed to make the actual decisions and test for possible rejection, but also the time to read the data from tape, construct each datum vector, and write the decision on the output tape in our normal format. Therefore, only relative processing times are presented on the graphs that follow. We varied the number of channels in order to generate the results.

The results of our classification studies are twofold: first, the quadratic and best linear decision rules are compared, after which the various linear decision rules are evaluated. In Figure 30 we show the results with data from the Imperial Valley. The points indicate the measured results; the lines between adjacent points were drawn for convenience in identifying the trends. For the quadratic decision rule, the points from left to right were obtained with two, four, and six channels of data. For the best linear decision rule, the points correspond to two, four, six, eight, and ten channels of data. The choice of channel subsets to use was determined by our normal channel selection procedure (Section 5.1).

In Figure 30, the bottom two curves were obtained from tests of the training data from which had been derived the mean vectors and covariance matrices used in the decision rules. The two decision rules may be compared by noting that the curve for the quadratic decision rule lies above and to the right of the curve for the best linear decision rule, showing that for a fixed processing time the quadratic decision rule had a higher error rate. Alternatively, for a fixed error rate, the quadratic decision rule required more processing time. When the same number of channels were used, the quadratic decision rule required more computer time and produced a slightly lower error rate.

Nontraining or test data provided the top two curves, so they are probably more representative of an actual classification of data for recognition. The most obvious difference between these curves and those taken from the training data is that here the error rates are considerably greater. The quadratic decision rule curve is again above and to the right of the linear decision rule curve. Also, it is no longer true that for the same channels, the quadratic decision rule produces a lower error rate. The same observations hold for all of the data sets that we tested.

In order to determine whether the particular choice of training data determines the test results, we decided to use one half of the fields for training data and the other half for test data. After testing in this manner, we reversed the roles of the data so that the data that had been training fields became test fields. Three of our classes had an odd number of fields, so one field from each of these classes was always used as a test field. The results of these tests can be seen in Figures 31 and 32. Comparing these figures with Figure 30, we see that the error rates are reduced for the test fields and increased for the training fields. One might conclude from this that for recognizing unknown data, one should use multiple training fields for each class. We can also see from the curves that the best linear decision is preferred whenever both error rate and processing time are important considerations.

To see whether our conclusions regarding the comparison of the two decision rules were only valid for the one data set, we repeated our tests for three other sets with the same results.

To compare the performance of the five different linear decision rules, we used the data sets identified in Figures 31 and 32. After examining and evaluating the results, we reached the following conclusions:

- (1) When only two channels of data are used, there is no particular preference to be had among the linear decision rules. The quadratic decision rule required more processing time with no noticeable decrease in error rates.
- (2) When four or more channels were used, the "best linear" rule had the lowest error rates of the linear rules. For equivalent processing time, it had lower error rates than did the quadratic rule. For the same number of channels processed, the linear rule did as well as or better than the quadratic rule on the test fields but slightly worse on the training fields.
- (3) The nearest neighbor and zero covariance decision rules gave the largest error rates. In fact, there was no clear choice between the two.
- (4) The modified equal covariance decision rule was no better than the equal covariance decision rule and, for one of the data sets, was much worse.
- (5) Of the rules suitable for parallel computation, the quadratic rule gives the best performance and the equal covariance rule follows. The equal covariance rule has the advantage of requiring far fewer coefficients; however, an assessment of the relative costs of their implementation on parallel processors was not made.

5.3 SIGNATURE EXTENSION

One of the requirements for an operational multispectral scanner survey system is that it provide the required information in an efficient, timely, and cost-effective manner. The

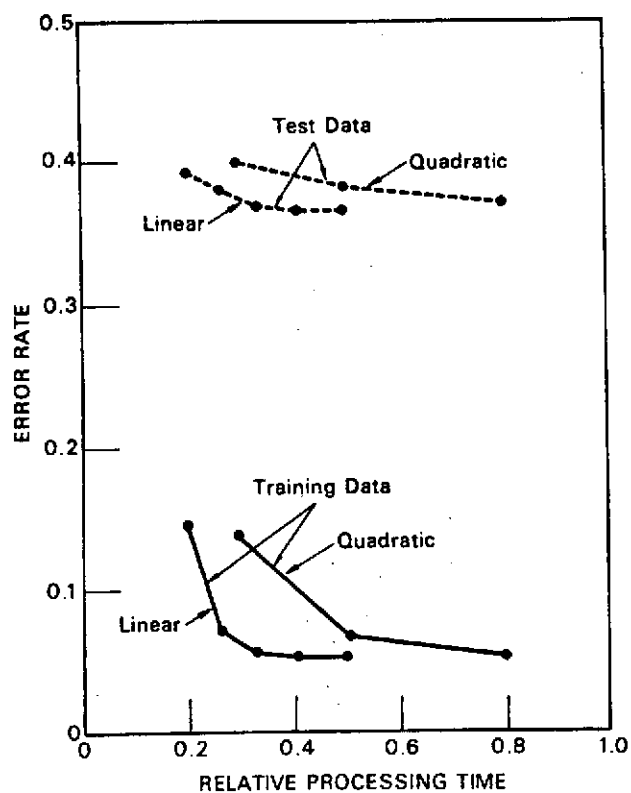


FIGURE 30. LINEAR VERSUS QUADRATIC DECISION RULES FOR SINGLE TRAINING FIELDS

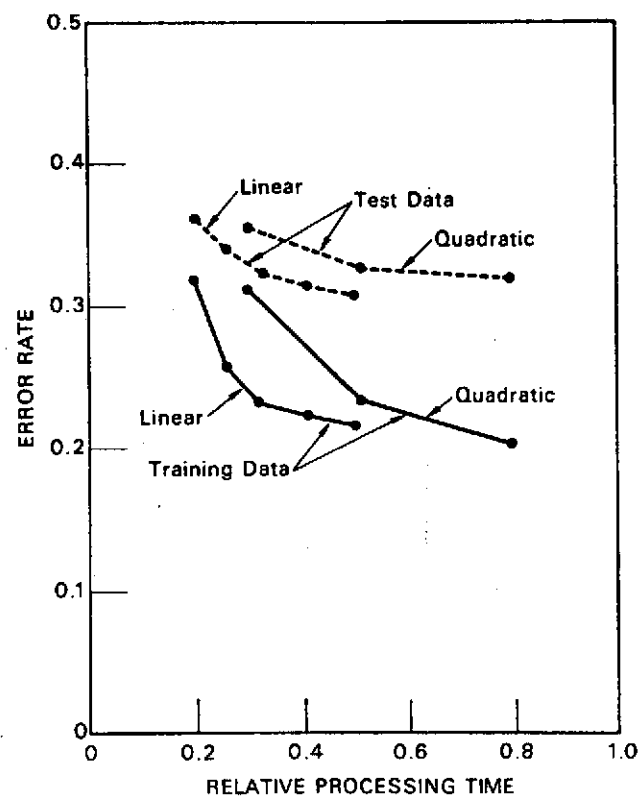


FIGURE 31. LINEAR VERSUS QUADRATIC DECISION RULES FOR COMBINED TRAINING FIELDS NO. 1

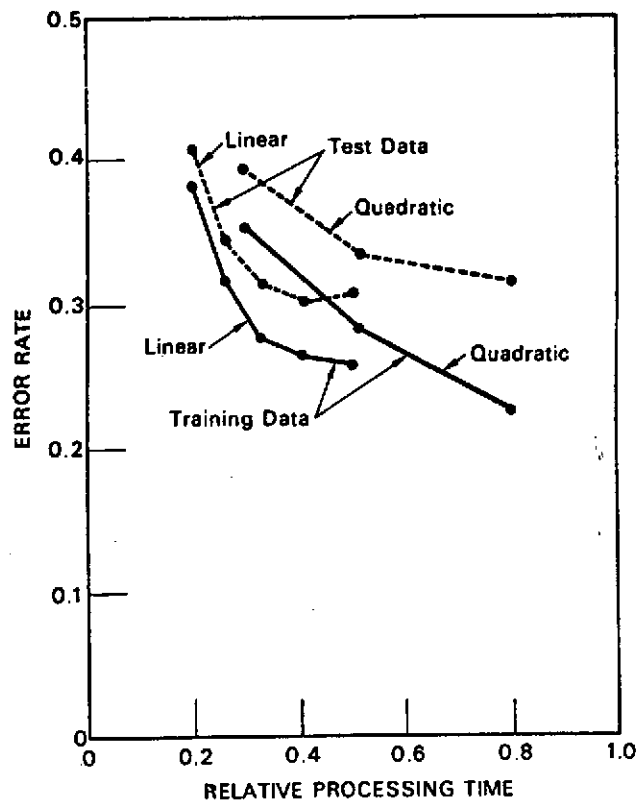


FIGURE 32. LINEAR VERSUS QUADRATIC DECISION RULES FOR COMBINED TRAINING FIELDS NO. 2. Imperial Valley, 1969; 20 fields, 7 classes for training; 23 fields for testing.

processing approach which has been employed by most investigators during the feasibility demonstration stage has required large amounts of ground truth information. This information has been needed to establish the signatures of the object classes of interest in the scene in order to train the computer to recognize those objects. The three processes—gathering ground information, establishing signatures and training the computer—can be costly and time-consuming, especially if these operations need to be carried out repeatedly over the area being surveyed. Under those circumstances it may become too costly to process large volumes of data using current methods.

The goal of signature extension is to help bridge the gap between feasibility studies and operational systems. Whereas the feasibility studies were characterized by the need for large amounts of ground truth, large numbers of signatures to represent the subclasses of the object classes of interest, large amounts of computer time, and a necessity to retrain the computer for every 10-20 miles of flight line data, the operational system, to be cost-effective, must be characterized by small amounts of ground truth, a small group of signatures representative of all objects of interest and a minimization of retraining and processing time for the computer.

The methods studied to minimize the computer training and ground data collection effort required for an operational system fell into two broad categories. One approach was to use unsupervised classification techniques (clustering). The other approach was to devise processing techniques which required only one set of signatures gathered from an isolated area to process many data sets. Thus, as the end result of this study, our goal was to identify data processing methods which would allow processing of large amounts of data within an acceptably small time/cost frame.

Investigation into the sources of signal variability was carried out. It has shown that atmospheric attenuation and scattering are prominent causes of signal variation. Additional sources of variation include changes in solar conditions, bidirectional reflectance, and scanner electronics.

Two data processing techniques had been suggested as applicable to the large-area survey problem. One suggested approach was to use unsupervised classification (clustering) techniques. Investigation of this method showed that, since the method did nothing to reduce the signal variability, the use of this method would require large amounts of processing time in order to obtain reasonable classification accuracy. The conclusion is that clustering techniques, of themselves, are not a solution to the large-area survey problem.

The other method investigated was the use of signature extension techniques. Generally speaking, such techniques function by normalizing the data to some reference condition, hence reducing the variability of the data. Thus signatures from an isolated area could be used to process large quantities of data. This minimizes ground information requirements and computer training.

Several signature extension techniques were devised and tested. The first of these, the ratio of adjacent channels transformation, yielded fair to good results. However, it was decided that classification accuracy for this transformation could be increased if the path radiance effects could first be eliminated from the data.

Accordingly, attempts were made to estimate the path radiance effects in the data. One method used the ERIM radiative transfer model to calculate the path radiance. Because of problems associated either with the calibration of the data or with the specification of parameters to the model, this approach was unsuccessful. A second, empirical approach was devised. In this approach, the smallest signals at each scan angle were used as an estimate of path radiance. Results of classifying data modified in this manner were inconclusive. These two approaches should have, theoretically, improved classification accuracy. We feel that these initial test results may not be indicative of the ultimate utility of these approaches.

Other signature extension techniques tested were the U-V transformation and the average signal versus angle transformation. The U-V transform yielded good results in a limited test. Results of the average signal versus angle transform were excellent.

The best signature extension technique tested was the average signal versus angle approach. This technique allowed signatures to be extended over a 90° scanner field of view and between data sets collected four days and 80 miles apart with an average accuracy of better than 90%.

5.3.1 UNSUPERVISED CLASSIFICATION APPROACH

The use of unsupervised classification techniques (i.e., clustering) has been mentioned in several quarters as the solution to the problems posed by an operational remote sensing system [117].

In the clustering approach, the set of multispectral scanner data points to be processed are examined and distinct groupings or clusters of data points are identified. These clusters are then used to establish training signatures for the computer. Only after the data set has been classified into the many clusters is the ground information gathered to associate a real object with each of the clusters [117-120]. As the theory goes, only a minimal amount of ground

117. G. Nagy, G. Shelton, and J. Tolaba, Procedural Questions in Signature Analysis, published in Proceedings of the Seventh International Symposium on Remote Sensing of Environment, Ann Arbor, May 1971.

118. G. Nagy and J. Tolaba, Nonsupervised Crop Classifications Through Airborne Multispectral Observations, IBM Journal of Research and Development, v. 16, No. 2, March 1972, pp. 138-53.

119. Dennis A. Johnston, Statistical Consideration in an Interactive Graphics Pattern Recognition System, NASA-MSC Internal Note 72-FD-019, September 1972.

120. M. M. Su, An Unsupervised Classification Technique for Multispectral Remote Sensing Data, Proceedings of the 8th International Symposium of Remote Sensing of Environment, Ann Arbor, October 1972.

information need be gathered since the cluster classification results can be used to direct the ground truth team to only a few locations in the survey area to determine the correspondence between clusters and real objects. We feel that this approach is a very reasonable one, except that it seems to overlook the very real problem of signal variation.

As an example, we chose data points from one data set (Segment 204) representing the three object classes at five different scan angles: 0° , $\pm 25^{\circ}$, $\pm 40^{\circ}$ from Nadir. Attempts to generate three clusters (after all, there are only three classes represented) resulted, as Table 6 shows, in the points being clustered according to their location in the scene, rather than according to object class.

Obviously, the variation in signals caused by the environmental and/or scanner-related effects overshadowed any differences in the basic reflectance spectra of these ground covers. Further experiments revealed that it took eight clusters to correctly separate the three object classes as shown in Table 7; the resultant error rate (points assigned to the wrong cluster) was about 3%.

Now the question is asked, is it cost-effective to use eight signatures (as represented by the clusters) to classify three object classes? This is roughly a threefold increase in time to train the computer and at least a threefold increase in processing time and ground truth necessary to accurately classify the data. The answer to the question appears to be that such an approach is not cost-effective.

Nor is the clustering approach to be faulted only on this score. This approach proves to be cumbersome on many other counts as well. Because of its nature, the clustering process must be carried out for each of the data sets to be processed. Also, the clustering process itself is fairly time-consuming because the algorithms used tend to be complicated, frequently involving several passes through all the data to be classified, with tentative merging and partitioning of the data sets. In addition, most of the current clustering algorithms require additional information, such as the expected number of clusters or the size and shape of the clusters, that may not be available in an operational environment. One last, perhaps minor, fault is that the ground truth is gathered only after classification. In some instances the characteristics of certain areas may be different at ground information collection time than they were at data collection time. For example, in an agricultural scene, fields may be cut, harvested, plowed, or

TABLE 6. RESULTS OF CLUSTER ANALYSIS USING THREE
CENTROIDS FOR CORN, SOYBEANS AND TREES AT
SCAN ANGLES 0° , $\pm 25^{\circ}$, $\pm 40^{\circ}$

Class	Scan Angle ($^{\circ}$)	% of Category in Cluster		
		Cluster Number		
		<u>1</u>	<u>2</u>	<u>3</u>
Corn	-40	100		
Soybeans	-40	100		
Trees	-40	40	60	
Corn	-25	100		
Soybeans	-25		100	
Trees	-25		100	
Corn	0	95	5	
Soybeans	0		100	
Trees	0		100	
Corn	25			100
Trees	25			100
Corn	40			100
Soybeans	40			100
Trees	40			100

TABLE 7. RESULTS OF CLUSTER ANALYSIS USING EIGHT CENTROIDS
FOR CORN, SOYBEANS AND TREES FOR SEGMENT 204
AT SCAN ANGLES 0° , $\pm 25^{\circ}$, $\pm 40^{\circ}$

Class	Scan Angle ($^{\circ}$)	% of Category in Cluster Cluster Number							
		1	2	3	4	5	6	7	8
Corn	-40	-	100	-	-	-	-	-	-
Corn	-25	-	100	-	-	-	-	-	-
Corn	0	-	100	-	-	-	-	-	-
Corn	25	100	-	-	-	-	-	-	-
Corn	40	100	-	-	-	-	-	-	-
Soybeans	-40	-	-	-	100	-	-	-	-
Soybeans	-25	-	-	-	-	100	-	-	-
Soybeans	0	-	-	-	-	100	-	-	-
Soybeans	40	-	-	100	-	-	-	-	-
Trees	-40	-	42	-	-	-	58	-	-
Trees	-25	-	-	-	-	-	100	-	-
Trees	0	-	-	-	-	8	92	-	-
Trees	25	-	-	-	-	-	-	52	48
Trees	40	-	-	-	-	-	-	57	43

Error Rate = 3.6%

exhibit (early in the growing season) a marked increase in ground cover—all these changes occurring during the time the data set is being processed.

Thus, the unsupervised classification approach by itself does not appear to meet the requirements for an operational processing system. It requires retraining for every data set; the process of extracting the signatures (clusters) is a time-consuming process requiring additional information that may not be available. Because of variation in the scanner-generated signals, it requires many more times the number of signatures than there are object classes, with a resulting manyfold increase in actual processing time. Finally, the accuracy of the ground truth may be in doubt.

5.3.2 SIGNATURE EXTENSION TECHNIQUES

The signature extension techniques that have been developed are discussed in this section.

In one technique the signals from a known target in a new data set are used as a transfer standard to derive a set of multiplicative factors to correct the new data to the old data set signal levels. This method allows signatures from one data set to be extended to another data set, provided that the location of a transfer standard in the new data set is known. This method will not reduce angular variation from changes in atmospheric or irradiance during collection of a single data set.

Another technique is similar to the one above except that the signals from the scanner's sky sensor are used as the transfer standard. This method reduces the effects of atmospheric and irradiance changes along the data collection flight path and allows signatures to be extended to other data sets.

Another technique employs a class of transforms which attempt to reduce the variation by taking advantage of certain properties of the environment which are evident in the data itself. For example, if the sum of all data channels associated with a data point is considered a good measure of irradiance and transmittance, then transforming the data point by dividing each channel by this sum will reduce variability.

Another example is the ratio of adjacent channel transform. We know that, for any given set of conditions, the values of E and T in adjacent spectral regions exhibit variations which are highly correlated so that the ratio

$$\frac{E_i T_i}{E_{i+1} T_{i+1}} \approx \text{constant}$$

This permits us to derive correction functions for a data set by using the average signal at each scan angle as a measure of the average angular variation inherent in the data. The resulting corrections may be implemented by subtraction (correcting for the additive term), or by

division (correcting for variation due to multiplicative effects). This approach reduces the effects of angular variation. In addition, a method to allow signature extension has been developed; it involves modifying the means of the signatures from the original data set to match the signal levels in the new data set. The correction factors are calculated by comparing the level of the corrected averaged signals for the two sets of data. One requirement for the average signal versus angle method is that each scene must contain a quasi-random distribution of all object classes.

Another method uses the average signal level and the standard deviation from that signal from each scan angle as an average measure of the additive and multiplicative effects inherent in the data.

A method for empirically estimating the additive component at each scan angle is also used. If the reflected radiance at any point is close to zero, either because the reflectance is close to zero or the object is in a deep shadow, the signal received at the sensor is essentially all path radiance. Thus the lowest signal level at each scan angle may be used to estimate the additive correction function. This method assumes that there exist sources of low reflected radiance in the data at many angles, and that the atmospheric state does not change during the time of data collection. If the path radiance term is sufficiently small, the ratio of adjacent channels yields new information channels that are approximately the ratio of the reflectances from the original data point. Such transformations as these will reduce the effects of angular variation, along-path variation, and variation from data set to data set.

A new transformation has been developed on the basis of information extracted through use of the ERIM radiative transfer model. Our calculations indicated that, under certain sets of conditions, the shape of the path radiance spectrum is essentially constant, so a data transform was developed which would take advantage of this fact. This transform utilizes these adjacent spectral bands and calculates the ratios of weighted differences. In theory, this transform will simultaneously handle both additive and multiplicative effects and, hopefully, will reduce angular, along-path and data set to data set variability.

In the "U-V" transform, a pair of fields or regions exhibiting different reflectances are utilized to calculate scan-angle-dependent multiplicative (U) and additive (V) correction coefficients to correct the data to the conditions existing at a selected reference angle. Signature extension to other data sets is accomplished by utilizing secondary standards.

In the above method the signatures are continually updated during the classification operation in order to account for changes occurring along the flight path.

5.3.3 COMPARISON OF SIGNATURE EXTENSION TECHNIQUES

In Figures 33, 34, and 35, the results for the various signatures extension techniques are compared for Segments 204, 203, and 212, respectively. As one can see in examining those figures, the best results are obtained for the average signal versus angle transform. Results for the ratio of adjacent channel transform were not quite as good. The results of experiments to estimate the path radiance and thus correct the data for both additive and multiplicative effects were unsuccessful. However, this may have been due to subsidiary influences and hence not a true indication of the value of these approaches.

The untransformed results for Segment 204 show how variation in the data as a function of scan angle can affect classification performance. Most of the data viewed with scan angles greater than 30° was not correctly classified for this test case. However, use of preprocessing transforms for Segment 204 produced results for edge areas at the same level of accuracy as that obtained in the middle areas. As previously noted, there is some fall-off of recognition at the edges of Segment 204 for the ratio of adjacent channels transform. The average signal vs. angle transform yields results that do not fall off as much in the edge areas. For Segments 212 and 203 there was not much distinction between middle and edge results.

In reviewing the false alarm rates quoted earlier in this section, we noted a very high false alarm rate associated with the tree category for both Segments 203 and 212. But aside from the trees, the false alarm rates for all the transformations were low, especially for the average signal versus angle transformation.

In summary, the point to be made here is that the accuracy of classification increases substantially with the use of signature extension techniques. One small group of signatures extracted from an isolated area can be used to successfully process many data sets, despite the fact that these data sets may be 50-100 miles distant and collected several days apart.

We have shown that for multispectral scanner survey systems to be effective in an operational environment, approaches other than those employed during the feasibility demonstration stage will be required. We have discussed two suggested approaches: the use of clustering, and the development and use of signature extension techniques. Based on evidence we have presented, it is our feeling that the clustering approach alone will not provide for both cost reductions and accuracy in an operational situation. The use of signature extension techniques, perhaps, but not necessarily, in concert with clustering, seems to show a great deal of promise for satisfying the requirements of an operational multispectral scanner resource survey system.

Several of the signature extension techniques tested yielded good to excellent results. At the present time, we do not have a universally applicable and optimum signature extension technique. We have found that not all the techniques yield good results on all data sets; we have a

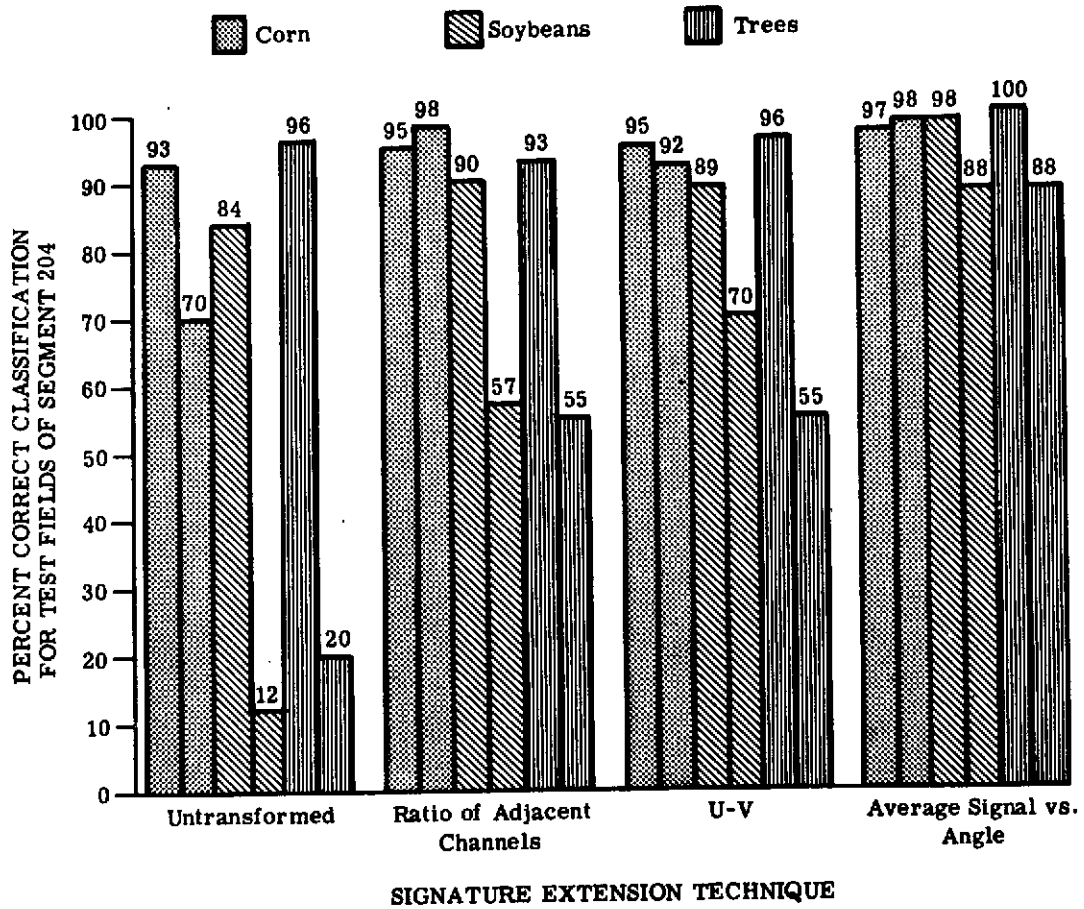


FIGURE 33. COMPARISON OF CLASSIFICATION ACCURACY FOR FOUR SIGNATURE EXTENSION TECHNIQUES FOR SEGMENT 204, MISSION 43M, 1971. For each category, left bar refers to middle fields and right bar refers to edge fields.

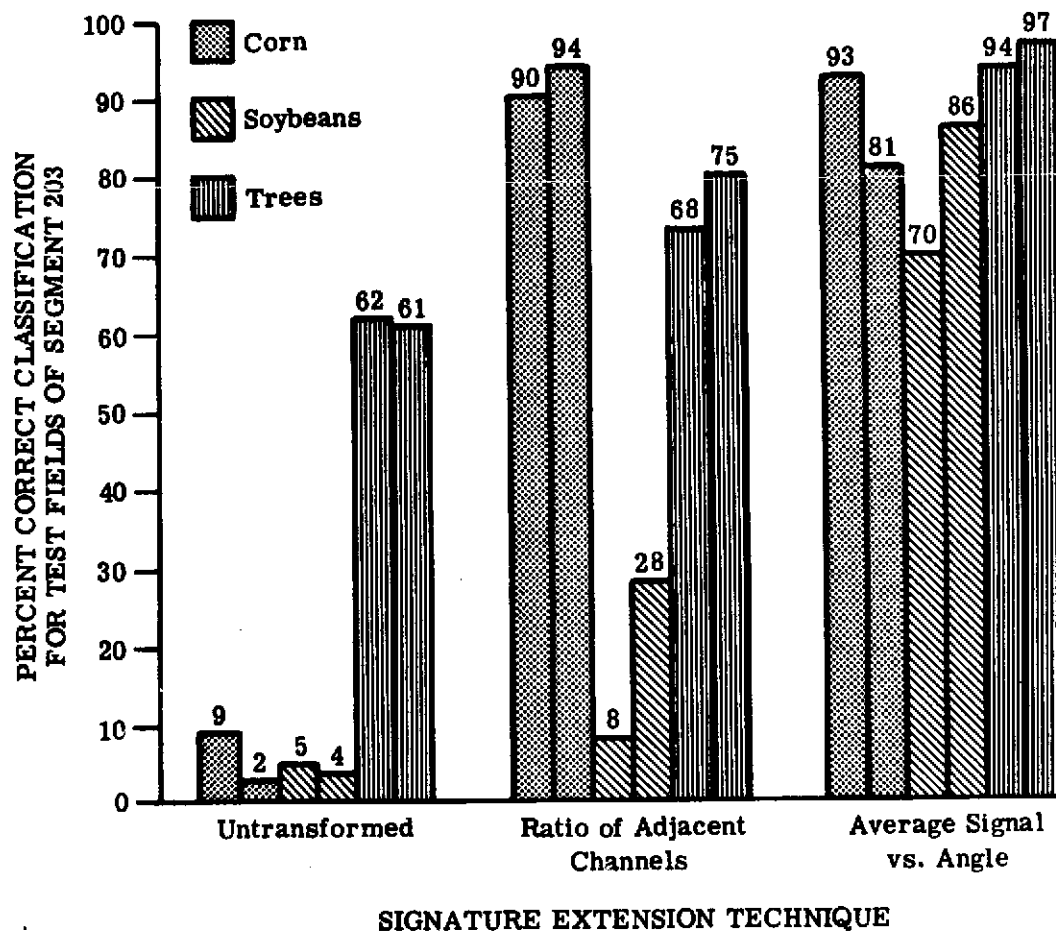


FIGURE 34. COMPARISON OF CLASSIFICATION ACCURACY FOR THREE SIGNATURE EXTENSION TECHNIQUES FOR SEGMENT 203, MISSION 43M, 1971. For each category, left bar refers to middle fields and right bar refers to edge fields.

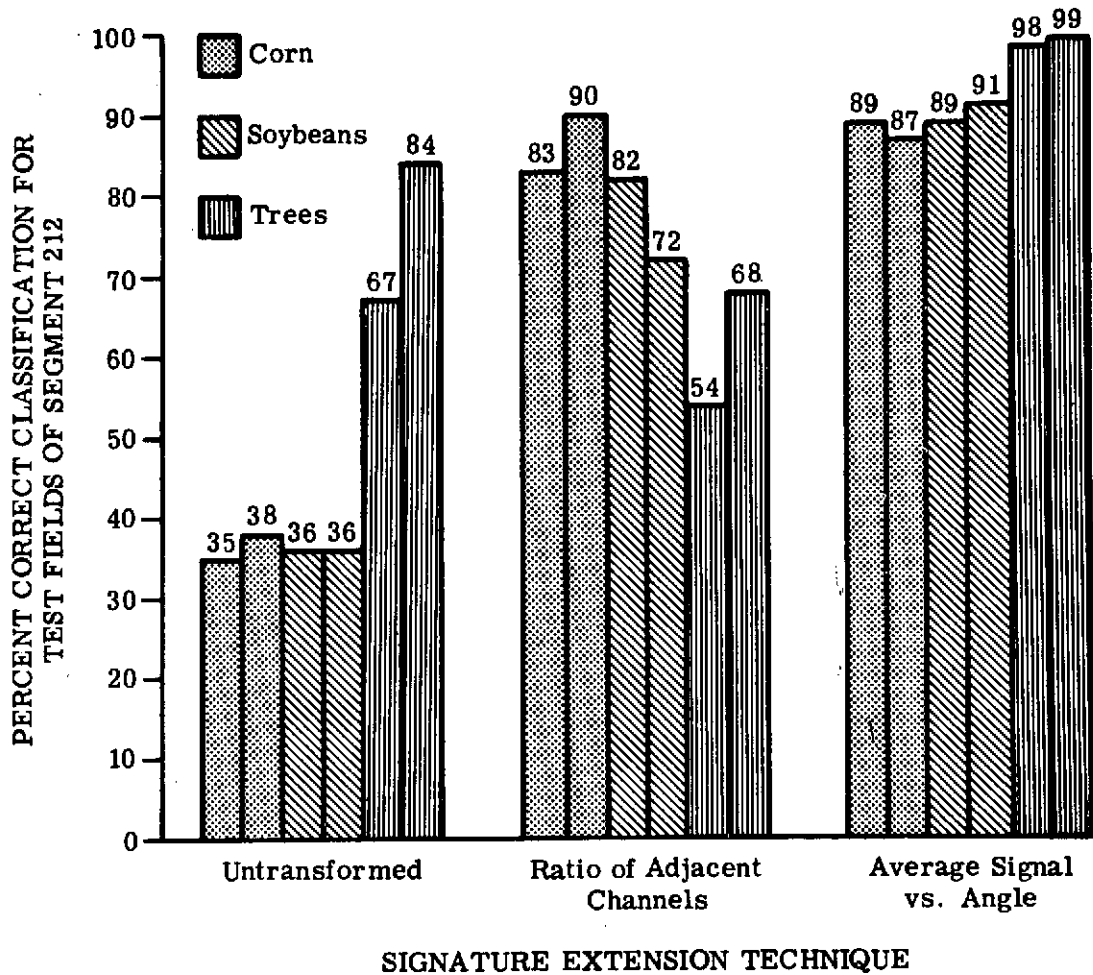


FIGURE 35. COMPARISON OF CLASSIFICATION ACCURACY FOR THREE SIGNATURE EXTENSION TECHNIQUES FOR SEGMENT 212, MISSION 43M, 1971. For each category, left bar refers to middle fields and right bar refers to edge fields.

need to establish criteria for determining when a given technique is useful and when it is not. Further research on this topic should address itself to these points. We hope eventually to establish a universally applicable signature extension technique.

ERIM documents which address the problem of signature extension include Refs. [45], [47], [48], [51], [52], [110], and [121-130].

5.3.4 ADAPTIVE PROCESSING

One research effort being carried out at ERIM to develop methods to compensate for the variations in the means and covariances is that of making adaptive corrections [131, 132]. In this approach, the mean vectors are slowly updated based on the decisions made by the classifier as well as on the actual values of the individual data vectors which are classified. The approach has its basis in the following idea. Suppose a sequence of observations (data

121. F. J. Kriegler, Implicit Determination of Multispectral Scanner Data Variation over Extended Areas, 7th International Symposium on Remote Sensing of Environment, June 1971.

122. R. B. Crane, Preprocessing Techniques to Reduce Atmospheric and Sensor Variability in Multispectral Scanner Data, 7th International Symposium on Remote Sensing of Environment, June 1971, Ann Arbor.

123. H. Smedes, M. Spencer, F. Thomson, Preprocessing of Multispectral Data and Simulation of ERTS Data Channels to Make Computer Terrain Maps of a Yellowstone National Test Site, 7th International Symposium on Remote Sensing of Environment, June 1971, Ann Arbor, ERIM Report No. 31650-49-S/SA.

124. M. Spencer, F. Thomson, Experimental Study on Preprocessing of Multispectral Data of a Yellowstone National Park Site, ERIM Report No. 31560-79-L, September 1970.

125. R. Nalepka, The Application of Data Preprocessing and Signature Extension Techniques to Multispectral Scanner Data, December 1971, ERIM Report No. 31650-9/S.

126. F. J. Thomson and R. F. Nalepka, Contribution to the Corn Blight Watch Final Report, January 1972.

127. R. F. Nalepka, J. P. Morgenstern, Signature Extension Techniques Applied to Multispectral Scanner Data, 8th International Symposium on Remote Sensing, October 1972.

128. R. S. Driscoll and M. M. Spencer, Multispectral Scanner Imagery for Plant Community Classification, 8th International Symposium on Remote Sensing of Environment, October 1972.

129. R. Nalepka and J. Morgenstern, Signature Extension: An Approach to Operational Multispectral Surveys, ERIM Report 31650-152-T, February 1973.

130. R. K. Vincent, G. Thomas, and R. Nalepka, Signature Extension Studies, ERIM Report 190100-26-T, July 1974.

131. R. E. Marshall, F. J. Kriegler, W. Richardson, Adaptive Multispectral Recognition of Wheat, presented at the 1971 IEEE Decision and Control Conference, 15-17 December 1971, Miami.

132. R. E. Marshall, F. J. Kriegler, W. Richardson, Adaptive Multispectral Recognition of Wheat Fields, Presented at the EAI Symposium on Automatic Photointerpretation, Washington, 7-8 December 1971.

vectors), a_j, z_{j+1}, \dots were all recognized as material class A by the classifier, but that these observations tended to cluster to one side of the current estimate of the mean, μ_A , of that material class. This would provide us with some evidence that the mean of the material class A had shifted. A decision-directed adaptive classifier is one which automatically adjusts the value of μ_A to bring it closer to the current observations which were classified as material A.

We would like our decision-directed adaptive classifier to take account of some additional considerations. The amount by which we allow a signature to be modified in any particular updating cycle may be different in different spectral channels. Also, a particular crop may not be observed for some time, and during that time the true mean of that crop, along with the means of other crops, may shift. Hence we would like to be able to adapt all signatures based upon the observations and classifications of one or a few of them.

In practice, resolution elements often overlap two or more different crop types, producing an observation far from the mean of any particular crop class. We would like to avoid using these observations as well as "wild" observations from any other cause.

Kalman filter theory provides a framework within which these considerations and others can be combined into one systematic approach [133].

The Kalman filter is an iterative filter, especially useful for digital computation, that produces an estimate of a time sequence of state vectors from a corresponding time sequence of measurement vectors. In the simplest applications, five elements must be defined. These are: (1) the state vector, (2) the measurement vector, (3) an observation matrix relating the state vector to the measurement vector (assuming no measurement noise) by a linear transformation, (4) a covariance matrix describing additive noise in the measurement, and (5) a covariance matrix describing the statistics of the successive differences in the state vector.

In order to apply the Kalman filter to remote sensing data, we must make an association between the elements of the Kalman filter and elements of the classifier. This can be done in a number of ways, one of which is described below.

Assume that the most important statistics to update are the components of the mean vector of each material class, and that we will update after each single observation. Then we make the following identifications.

133. H. W. Sorenson, *Talman Filtering Techniques*, in *Advances in Control Systems*, Vol. 3, C. T. Leondes, ed., Academic Press, 1966.

- (1) The mean vectors of each material are combined into a single vector identified as the state vector, x_t . The initial condition, x_0 , is given by the initial training data for each crop.
- (2) The observed data vector is identified as the measurement, z_t .
- (3) The classified output (a recognition vector) is used to produce a matrix, H_t , of zeros and ones (a spotting function) which selects the correct components of the state vector to provide a relationship between the state vector and the noise-free measurement.
- (4) The covariance matrices of all the signatures are averaged. This result is identified as an average estimate of the measurement noise covariance, R , as required for the Kalman filter.
- (5) By replicating and scaling the matrix R , an augmented matrix is formed which is identified as the covariance, Q , of successive differences in the state vector. Covariance Q is assumed to be a simple function of R . (This assumption results in significant savings in computation time, since matrix inversions are not required for each update, and the computer memory requirements are minimal.)

A general linear theory can be used for adapting the means of class signatures. The theory can accommodate the use of known additive and multiplicative changes to the means, use of uncertain decision results or proportion estimates, a method to use auxiliary ground truth, and a method of adapting scan angle corrections. The general theory, which is essentially a decision-directed Kalman filter, includes as special cases the adapting algorithms which had been derived empirically and tested earlier [131, 132].

Two limiting features of the Kalman filter can be avoided simultaneously: (1) the requirement that first- and second-order statistics of the variations of the means be known, and (2) the large memory and computation requirements generally associated with a Kalman filter containing many states. Because the Kalman filter model is only an approximation to a description of remotely sensed data, the use of the more accurate statistics may not produce a significant improvement in the accuracy of the mean estimates.

The development and testing program was devoted to finding simple, practical methods, rather than to the full utilization of the generality of the theory. The test results provided confirmation of the Kalman filter model's usefulness. They showed that processing accuracy could be improved over that obtained previously with empirically derived algorithms, as well as that obtained when the means were held constant.

We conclude from these limited tests that the Kalman filter algorithm can improve classification accuracy in two ways: The updated means can be made to follow variations in the data caused by inter- and intra-field changes in the ground covers. Or, the updated means can be

restricted to show variations which would follow slow changes resulting from atmospheric variations, varying sun position, or varying ground cover reflectances in the data.

The ability of the Kalman filter to adapt to rapid changes in the data may have an important operational consequence. It should be possible to better delineate fields and field boundaries. This may improve the accuracy of estimating acreage—e.g., specific agricultural crops—as well as increase the probability of a correct decision as to the ground cover on a given field.

From these test results, one conclusion must be that adaptive processing is capable of improving recognition accuracies, at least for some data sets. Additional testing should indicate the general usefulness of the technique and the parameters to be used. There are indications that the linear, rather than quadratic, decision rule would increase classification accuracy and decrease processing time. We believe that the filter should be implemented so that auxiliary training fields can be used to decrease the probability of capture.

From observing the test results, we have concluded that the Kalman filter model should be changed so that the means adapt simultaneously to both slow and rapid changes in the data. If this change is made, the updating rate should increase without increasing the probability of capture.

We did not try to update the signature means while estimating proportions of unresolved objects. Nor did we try using any auxiliary information. The sun sensor in the ERIM M7 multispectral scanner is one source of auxiliary information presently available.

We believe that adaptive processing is a useful method of classifying multispectral data. Additional testing with other data sets should be performed so that its capabilities and limitations may be better understood and the method can come to be used routinely. The Kalman filter processor can fulfill many functions simultaneously. In fact, it appears that many practical adaptive algorithms can be shown to be equivalent to a Kalman filter.

References [134-137] cite other documents which address adaptive processing.

134. F. J. Kriegler, Adaptive Multispectral Recognition of Agricultural Crops, 8th International Symposium on Remote Sensing of Environment, The University of Michigan, October 1972, Ann Arbor; appeared in Proceedings.

135. F. J. Kriegler, H. Horwitz, Investigations of Adaptive Processing of Multispectral Data, ERIM Report 31650-151-T, January 1973.

136. R. B. Crane, A Kalman Filter Approach to Adaptive Estimation of Multispectral Signatures, presented at 12th Symposium on Adaptive Processes, San Diego, December 1973.

137. R. Crane, Adaptive Processing of Multispectral Scanner Data Using a Decision Directed Kalman Filter, 9th Symposium on Remote Sensing of Environment, Ann Arbor, April 1974.

5.4 EFFICIENT PROCESSING SYSTEMS [11]

A particularly important and easily overlooked aspect of applying a remote sensing, multi-spectral system to aid in mapping crops, detecting pollution, or locating some ecological disturbance is that of processing the data to provide the proper information to someone in a time short enough to meet his needs. Unfortunately, ongoing programs do overlook this aspect of the system design problem, for reasons which are rarely clear.

Knowing the utility of these techniques, one would think that the data, gathered as it is at very high rates and over very large areas, must be processed before it can be useful. And when the time allowed to produce such results is relatively short, as it invariably is, then it becomes clear that a major problem exists and requires a solution.

The magnitude of the discrepancy between the ability of a sensor to gather this data and the ability of a general purpose computer to process it becomes the next aspect of the problem to be assessed. This enormity can probably be best appreciated by considering a brief numerical example. An airborne scanner will, typically, gather data over a 20- to 30-mile flight line in about 15 minutes on one reel of magnetic tape. A general-purpose digital computer can process this raw data in a period about 1000 times as long. Thus, the data collected in 15 minutes will require 15,000 minutes of processing. This means 6 weeks of processing, assuming a 40-hour week. Given one such computer to process this data, this aircraft could only be used for eight 15-minute sorties per year. Clearly, the discrepancy in capabilities is unacceptable.

At this point, one must examine the problem more carefully. We should point out that the above discrepancy of 1000 to 1 is actually rather conservative, possibly by as much as a factor of 10, but editing of the data should alleviate the problem to this extent. We should also point out that this form of processing yields a map containing the color-coded identification of each element of the scene at the time of the overflight, but also containing errors in this color-coding and geometrical errors resulting from the sensor and motions of the sensor platform. And it is important to note that the scene is not at all unchanging as one flies along: ground conditions vary, the atmosphere varies, the sensor stability varies and, in short, there is a spatial-temporal uncertainty about the data. Processing, as it becomes better understood, will require even more computation to remove these errors and to improve the results finally provided.

From another point of view, the objective of providing greater speed also includes much lower cost. This is true not only for the operational situation but also research and development. Given the limited resources for research, more investigations can be conducted. It has been estimated that processing costs in an operational system can be reduced by about a factor of 20 or more as compared to some processing costs based on present day feasibility. For example, the typical data set described earlier could be processed at a cost of less than \$400 instead of recent typical costs of about \$8000.

Another important objective is to facilitate control by the user. Classification of remotely sensed data is an interactive process in which the man and machine must, in fact, be considered as the real processing system. This is not apparent in some processing systems since the machine is so slow that an operator is easily able to keep pace with the task. In any system in which the processor is substantially faster, the time required by an operator may run three or four times longer than that taken for processing. Increases in processor speed will then provide little improvement in throughput. It thus becomes evident that well designed, interactive display and control subsystems will, in reality offer the greatest gains in throughput. As should also then be evident, the development process must inherently involve an evolutionary refinement of the display and control interface. This, to some extent, is an experimental task initially addressed in the second phase of this development program. It is a task which can be bypassed only at the risk of seriously impaired throughput. This task also implies that the system should be considered as a prototype from which further refined systems may be derived for specific programs. To allow this tailoring of the operational system the user requires, modular design becomes an important aspect.

One final motivation exists in addressing this problem: Proper configuration of an operating system almost always necessitates experience in the use of a system similar to the one required.

One must, therefore, see this problem as one of great and, indeed, critical importance to the objective of making remote sensing a useful, cost-effective tool. It is thus necessary to pursue a course which, in the development of these methods, provides assurance that processing methods are available to meet the demands of those who would use them. The above rationale is from Ref. [11].

From the first MSS designs in 1964, it was apparent that operational systems would require accurate but fast and cheap processing systems. SPARC, built in 1967 [9, 10], was a demonstration that likelihood ratio and maximum likelihood classifiers making decisions on 200,000 data vectors per second could be built cheaply. It was a limited demonstration in that manual programming was required, but a natural next step in the development was to interface a mini-computer for automatic programming and control and higher average throughput.

Studies carried out under this contract addressed the design of such a hybrid processor [138, 139]. But by 1973 a cheap digital implementation was feasible.

138. F. J. Kreigler and R. E. Marshall, A Prototype Hybrid Multispectral Processor (SPARC/H) with High Throughput Capability, WRL Report 31650-23-T, March 1971.

139. R. E. Marshall and F. J. Kriegler, Study of a Hybrid Multispectral Processor, ERIM Report 31650-154-T, January 1973.

MIDAS, which stands for Multivariate Interactive Digital AnalysSystem, represents a breakthrough in the field of multispectral scanner image analysis by providing a low-cost capability for user-oriented, interactive, near-real-time, digital analysis to produce thematic mapping with instantaneous or multi-temporal data. MIDAS accepts data from multispectral scanners in the form of high-density digital tape, computer-compatible tape, or analog tape, and makes use of proven multispectral processing techniques (including signature extension) within an innovative hardware approach resulting in a cost-effective, user-controlled system for multispectral analysis and recognition. Its hardware and software are designed to require only a minimal amount of instructional training for successful operation. MIDAS is intended to provide multispectral analysis for applications in disciplines such as agriculture, urban planning, forestry, geology, pollution detection, hydrology, and others. Features may be extracted that are spectral, spatial, temporal, and (possibly) polarization-dependent, thus giving a very general and powerful capability.

A report [11] describes the status achieved at the end of the first phase of a two-phase, 2-1/2 year program to demonstrate the unique advantages of a special-purpose multispectral processor. In this machine the parallel digital implementation capabilities of a low-cost processor are combined with a mini-computer to achieve near-real-time operation of a complete processing system that includes multiple, user-selectable, preprocessing functions and color displays.

The overall system hardware is shown in Figure 36. The MIDAS system consists of several principal subsystems: the general purpose computer (DEC-PDP-11/45), the classifier, the preprocessor, the input subsystem, the control subsystem, and the output displays. Of these, the PDP-11/45 computer, the classifier, the control system, and part of the input system have been designed and tested in the Phase I first year of the program. The remaining units to be added during Phase II are indicated as cross hatched blocks in Figure 36. The various subsystems are described below.

Input Subsystem

The input subsystem contains the necessary circuitry and hardware to input data stored on (1) high-density digital tape (HDDT), (2) computer-compatible tape (CCT), and (3) analog tape. The HDDT input is viewed as the principal input medium because of its high data rate and digital format. Data stored on HDDT's at 20,000 bits per inch and played back at 120 inches per second gives a data rate of 2.4 megabits per second per channel. For 8-channel data, this is a bit rate of 20 megabits per second. This is an excess of the present classifier bit rate of 12 megabits per second but will be below the Phase II system which, at 24 megabits per second, has twice the bit input rate. Another advantage of HDDT is the efficient storage of data. As much data may be contained on an HDDT as on 50 CCTs.

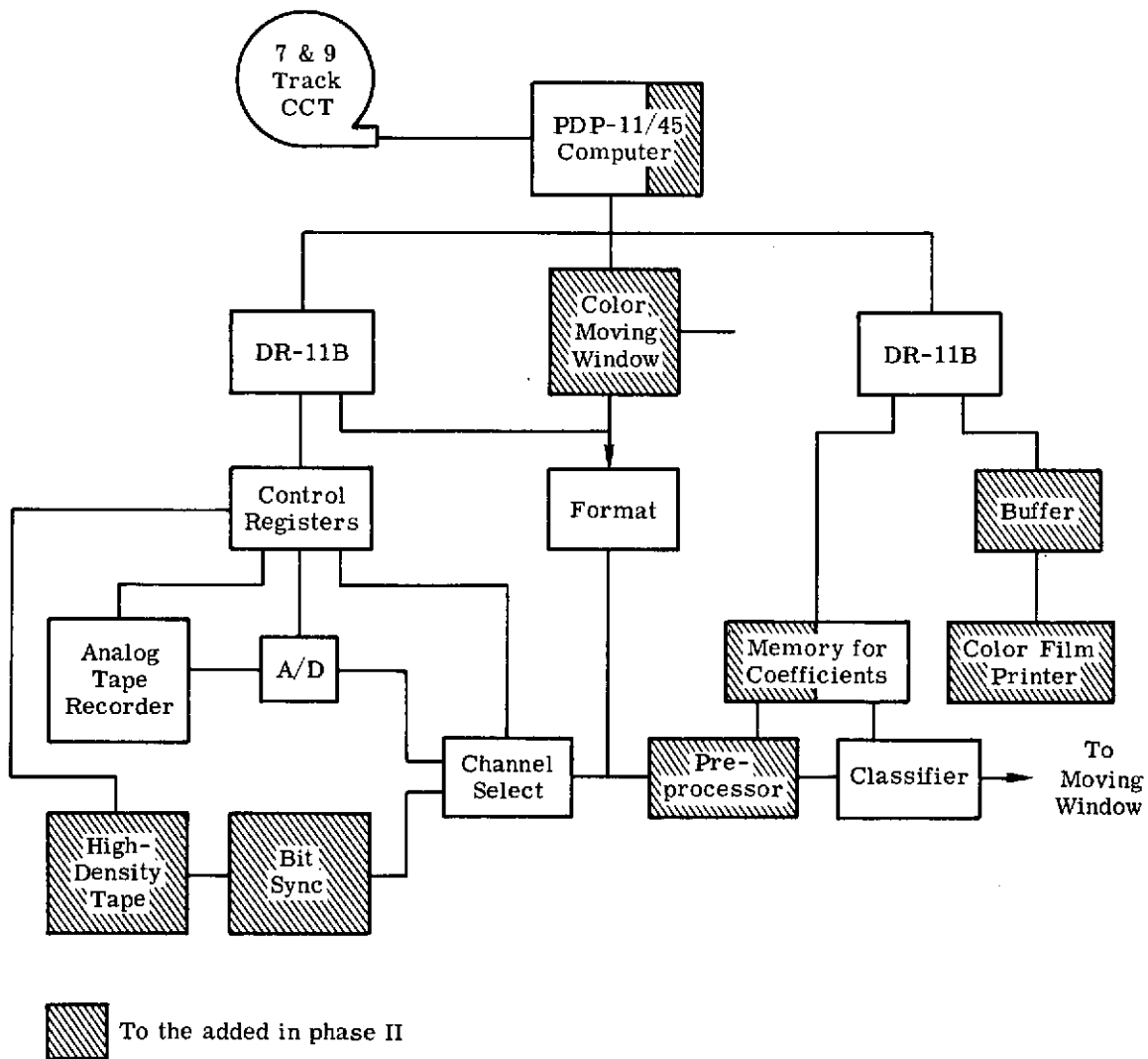


FIGURE 36. OVERALL MIDAS SYSTEM BLOCK DIAGRAM

The second input medium is a CCT. The availability of data from many sensors on a common format is desirable, however past experience has shown that the turn-around time to produce such tapes from the original data (usually HDDTs) is quite long and may make the data out of date. Although faster tape drives may somewhat increase the data rate, they still would be an order of magnitude below the system capacity.

The third medium of data input is from analog tape through the use of multiple A/D converters. Although this is an efficient data storage medium capable of maximum data rate for the MIDAS system, it appears as the third choice because data from this source is not completely repeatable.

The preprocessor will have the capability of performing signature extension, making the following calculations as needed: (1) calculation of scan angle correction functions, both additive and multiplicative; (2) selecting and calculating channel ratio transforms, and (3) calculating a linear dimension reduction transform. These options or steps are performed in this sequence since each step provides modified data for the next step and serves to provide improved data for classification at each step.

Classifier

The Classifier is designed to perform a maximum-likelihood decision, assuming a multimodal Gaussian multivariate distribution. This assumption has been well justified at this time by over 100 experiments using multispectral data at ERIM by a similar number at LARS and, as time goes on, by more and more experience at NASA and other agencies. Although simpler algorithms can perform well for some data sets, a significant percentage of applications demand this powerful decision rule. For example, a test of the hypercube decision rule indicated that it was not useful for the Imperial Valley data set although maximum-likelihood performed acceptably. No penalty in speed and only a small additional cost occurs for using this algorithm, hence it is employed.

The actual computations are performed by a set of time-shared arithmetic units arranged in a sequence allowing a set of operations whose execution is less than 5 μ sec before the outputs are latched. Each stage supplies its results to a subsequent stage for further processing. Precision varies between 8 and 16 bits as the data progresses through the pipeline and acquires greater significance.

The machine will accept 8 input signals and can classify the results into one of 9 classes (including the null class) at its output on one mode of operation. In another mode of operation it can accept 4 input signals and classify the results into one of 17 classes at its output. The decision rate is 200×10^3 /sec.

Internal arithmetic operations are conservatively derated to less than 50% of rated component needs. For example, an 8×8 bit multiply is allowed 300×10^{-9} sec, but could take less than 200×10^{-9} sec. As a result, the system would be able to operate at higher speeds later, if needed.

Output Subsystem

a. Interactive Color (Image) Display

This display is a three-color video display using high resolution, a shadow-mask CRT, and a MOS storage for display refresh. The unit chosen is the RAMTEK GX-100/200 series configured to hold a 5-bit color vector with 5.2×512 elements on the display. The unit will allow direct data input from the MIDAS as well as the normal input from the PDP-11/45.

The display offers image display, alphanumerics, vector generation, two movable cursors, moving window display and table look-up of predetermined colors. This color display provides the major interface for a fast man-machine interface. A scene or portions of a scene, as the user may request, can be displayed almost immediately from disc. Once the display memory is loaded, the computer can perform other operations. The ability to change colors quickly on the CRT through use of the table look-up means that enhanced pictures can be viewed to help locate training sets. These enhanced pictures may also be put in hard-copy form.

For alphanumeric information display, a second interactive CRT is part of the system.

b. Hard-Copy Color Output

An extremely important output device for the MIDAS system is a fast color-printer. Methods proposed for this function include CRT color filter camera devices, multi-laser film devices, LED color array systems for printing on film, and colored-ink printers. Of these, the most attractive one is the ink-jet printer since it produces a usable output immediately with no delay for color processing. Printers of this type have been developed by several sources and appear capable of producing a picture consisting of about 10^7 elements in 15 minutes or less.

This fact turnaround for intermediate or final recognition results will permit the user to be much more efficient, particularly since enhanced false-color maps of training areas can be made quickly. (Present ERTS data sets, because of poor quality and low contrast on available single-channel black and white hardcopy, can take up to 40 manhours of analysis to locate training sets.)

Computer Peripherals

a. Large-Capacity Disk

Upon ERIM's acquisition of the DIVA DD-14/2 disk system, it will be possible to initiate high-speed, random-access, digital processing of up to a full ERTS frame of multispectral data

(4-channel, 8-bit data) using the MIDAS classification hardware. Specifically, the following modes of operation will become feasible:

- (1) Signature extraction of data in a high-speed one-pass calculation from different quarter frames, by virtue of the direct random-access nature of disk storage. Previously, this task has been extremely cumbersome because of tape searching, multi-tape data, etc.
- (2) High-speed digital classification of ERTS data over quarter-frame boundaries, due to the merging capability available with the dedicated disk system. Storage of classification results is performed on the disk drive not dedicated to input storage. The two-drive system implies that read/write head-move time becomes insignificant, whereas previously this was not the case.

b. Printer/Plotter

The high-speed printer/plotter system provides extensive capability in two important areas of the MIDAS system. First, by decreasing turnaround time, an important factor in software programming efficiency, it allows the efficient development of software by the programming staff. Second, the plotting feature provides hard-copy output for such functions as graphing, histogramming, cluster-plotting, etc., as well as binary (black or white) reproduction of display maps from the CRT display system, if desired.

Additional information on this subject is contained in Refs. [140-142].

140. R. E. Marshall and F. J. Kriegler, Data Display Requirements for a Multispectral Scanner Processor with High Throughput Capability, WRL Report 31650-28-L, July 1971.

141. F. J. Kriegler and R. Marshall, An Operational Multispectral Survey System, 7th International Symposium on Remote Sensing of Environment, Ann Arbor, June 1971.

142. F. Kriegler, Extension of ERIM Multispectral Data Processing Capabilities Through Improved Data Handling Techniques, ERIM Report 31650-158-T, January, 1973.

ADDITIONAL APPLICATIONS FOR AND MODIFICATIONS TO SCANNER SYSTEMS

Besides endeavoring to improve the understanding, accuracy, and efficiency of information extraction for the more usual and common applications (e.g., agriculture surveys), we undertook to develop additional applications for multispectral scanner systems. We also examined modifications to such systems which may be useful for reducing their limitations or improving the quality of information contained in the data gathered by them. All of these subjects are discussed in this section.

6.1 RADIATION-BALANCE MAPPING

The ability of multispectral scanners to map radiances emanating from the Earth's surface in various spectral bands has been demonstrated many times, and multispectral pattern recognition techniques have been used to identify the classes of surface materials present in scenes. Heretofore, little attention has been directed toward use of attributes derived from the multispectral signals for interpretation of scene conditions. Surface exitance* and surface radiation balance were derived attributes considered during this contract. Radiation is the principal form in which the sun transmits energy to Earth for the sustenance of life. While ground instrumentation can provide point measurements of incident radiation and radiation balance, only airborne and spaceborne multispectral scanners can provide synoptic and quantitative measurements over large areas. Such measurements are applicable to many disciplines—agriculture, forestry, hydrology, meteorology, physical geography, and urban climatology. This universality results in large part from the linkage between radiation balances and water balances of terrestrial ecosystems, and the energy budget relationships implicit therein.

As a planet, the Earth maintains a constant average annual temperature because the radiation output at the top of the atmosphere just equals the incoming radiation when both are averaged globally for a year over all wavelengths [143]. This is not the case, in general, for any specific latitude or for any shorter period such as a season, month, day, or minute. Furthermore, incoming and outgoing radiation streams generally would not be expected to balance or equal each other at the interface between Earth's surface and the atmosphere. Net radiation (incoming minus outgoing) and its partitioning into components of energy budgets are of interest here, including radiation at both long and short wavelengths.

In radiation balance and energy budget studies [144, 22], it is conventional to discuss two broad wavelength categories of radiation. These categories comprise: (1) short-wavelength

*Exitance is the outgoing radiant flux density, e.g., W/m^2 leaving surface.

143. William D. Sellers, Physical Climatology, University of Chicago Press, 1965.

144. David M. Gates, Energy, Plants, and Ecology, Ecology, Vol. 46, Nos. 1 and 2, 1965.

solar radiation from 0.3 to about $3\text{ }\mu\text{m}$ and (2) long-wavelength thermal radiation from about 3 to $30\text{ }\mu\text{m}$. These divisions come about for at least two reasons. First, the direct contribution of solar radiation is insignificant in the long-wavelength interval as compared to that from the atmosphere. Second, measurement instruments (e.g., pyrometers) incorporating glass domes are effective only in the short-wavelength interval.

The short-wavelength solar radiation that reaches the Earth's surface has both a direct component and an indirect or diffuse component. The direct component is reduced as it passes through the atmosphere because of transmission losses along the path. The diffuse component occurs because of scattering by aerosols and molecules in the atmosphere; clouds also can produce indirect radiation by reflection. The radiant flux density on a horizontal unit area is the incidence, E ; it is measured in units of $\text{watts}\cdot\text{m}^{-2}$ which are gaining acceptance over another common unit, $\text{cal}\cdot\text{cm}^{-2}\cdot\text{min}^{-1}$, sometimes called langleys $\cdot\text{min}^{-1}$.

At the top of the atmosphere, the normal incidence of the sun is approximately $1396\text{ W}\cdot\text{m}^{-2}$ or $2\text{ ly}\cdot\text{min}^{-1}$. The total (direct and diffuse) amount reaching a horizontal surface on the Earth is typically 700 to $900\text{ W}\cdot\text{m}^{-2}$ at midday at mid-latitudes. A substantial amount of thermal radiation from the atmosphere also reaches the Earth's surface. It results from thermal emission by air molecules, aerosols, and any clouds present. On a typical summer day at mid-latitudes, the thermal incidence from the atmosphere might be 300 to $400\text{ W}\cdot\text{m}^{-2}$.

Radiation at short wavelengths leaves the Earth's surface by reflection and, at long wavelengths, primarily by thermal self-emission. Typical values are 140 and $420\text{ W}\cdot\text{m}^{-2}$, respectively.

For an opaque, diffusely reflecting surface, we can write a simple equation for the net incoming radiant flux density (that is, for the balance of radiant flux on a surface of unit area):

$$E_{\text{Net}} = (1 - \rho)(E_S + E_s) + \epsilon E_T - M_T \quad (7)$$

where E_{Net} is the net radiant incidence

E_S is the direct solar incidence

E_s is the indirect, or diffuse, solar incidence

ρ is the diffuse hemispherical reflectance (sometimes called albedo) of the surface (values between 0.05 and 0.30 in the absence of snow [144, p. 21])

E_T is the thermal incidence

ϵ is the thermal absorptance (emissivity) of the surface (a value between 0.90 and 0.96 for most natural objects)

and M_T is the thermal exitance of the surface [i.e., self-emitted thermal radiation which depends on both the temperature, T_s , and the emissivity of the surface;

$M_T(T_s) = \epsilon \sigma T_s^4$, where the Stefan-Boltzmann constant $\sigma = 5.67 \times 10^{-8}\text{ W}\cdot\text{m}^{-2}\text{ }^\circ\text{K}^{-4}$].

All quantities except ρ and ϵ , which are dimensionless, have units $\text{W}\cdot\text{m}^{-2}$ (or $\text{ly}\cdot\text{min}^{-1}$).

Equation (7) can be rewritten as follows:

$$\begin{aligned} E_{\text{Net}} &= [E_{\text{S}} + E_{\text{S}} + \epsilon E_{\text{T}}] - [\rho(E_{\text{S}} + E_{\text{S}}) + M_{\text{T}}] \\ &= [\text{Incoming radiant flux density}] \\ &\quad - [\text{Outgoing radiant flux density}] \end{aligned} \quad (8)$$

$$E_{\text{Net}} = E_{\text{Total}} - M_{\text{Total}} \quad (9)$$

Here, E_{Total} is the total incidence, while M_{Total} is the total exitance. When the surface is not a diffuse reflector and emitter, Eqs. (7) and (8) become more complex. For example, the reflected radiation from a nondiffuse surface depends on the spectral distribution of the incoming radiation, so the same reflectance term should not be applied, in general, to the direct and indirect components of solar radiation in Eqs. (7) and (8). These factors are considered in more detail in Refs. [145-147].

In these documents the use of multispectral scanner data for mapping exitance and radiation balance are discussed as an initial step in the quantitative interpretation of physical and/or biological differences in scene materials through computer processing of remote sensor data. Example maps of apparent exitance and radiation balance are presented for agricultural and urban applications; the results encourage further study of their use for assessing scene material conditions. Additional analysis is required to compensate for atmospheric effects, account for the bidirectional reflectance properties of surface materials, correlate the instantaneous remote sensor data with time-integrated phenomena, and evaluate energy budget components. The technique should be useful for other applications as well. Specialized computer programs which were developed to generate and display the exitance and net radiation attributes derived from multispectral scanner data are described. Although specialized in application, these programs are general in concept and can be adapted to other uses.

6.2 WATER DEPTH DETERMINATION

The purpose of the investigation summarized herein was to determine how changes in local sea state and differences in spectral reflectances could be used to detect and measure shallow-

145. W. Malila, Discrimination Techniques Employing Both Reflective and Thermal Multispectral Signals, ERIM, Ann Arbor, Report 31650-75-T, January 1973.

146. W. A. Malila, Radiation Balance Mapping with Multispectral Scanner Data, Remote Sensing of Earth Resources, Vol. I. Selected Papers from Earth Resources Observation & Information Analysis Systems Conference (13-14 March 1972), May 1972.

147. W. Malila and T. Wagner, Multispectral Remote Sensing of Elements of Water and Radiation Balances, presented at 8th International Symposium on Remote Sensing of Environment, The University of Michigan, Ann Arbor, (WRL) October 1972; appeared in Proceedings.

water features. More specifically, we were interested in relating the measurable changes in observable quantities, such as wave length* and spectral intensity. In this research, we used aerial photography and multispectral scanner imagery to record the wave surface and radiance at various locations. The photographic transparencies were then analyzed via an optical processor to produce measurable Fourier transform frequencies which are related to the wave surface. Comparisons of deep- to shallow-water wave lengths at probable sites were then made in order to compute shallow-depths.

In the second technique for measuring depth, we use the signals collected by a multispectral scanner. These signals were recorded on analog tapes during the data-collection missions, subsequently digitized, and finally analyzed via a digital computer. The signals, carried in 12 separate tape channels, represent the relative intensity of the scene on a point-by-point basis; they enabled us to determine (with the use of a calibrated sun sensor) the spectral reflectances on a high-resolution basis.

Depth Measurement from Wave-Refraction Analysis

The detection of shallow water by changes in wave state has been attempted by a variety of techniques. Interpretation of aerial photography allowed researchers to detect and measure the influence of shallow water on wave action [148, 149]. It is well known that this influence is primarily on the wave length and wave direction. More specifically, as a set of waves approaches shallow water, the wave length will decrease as it feels bottom. If the wave train is approaching the shallow area at an angle, the longitudinal orientation of the wave train will refract, causing the wave train to approach the shoreline in a mode parallel, or nearly parallel, to the shoreline.

Recent studies have made use of another approach for detecting the presence of shallow water. Polcyn and Sattinger [150] analyzed wave motion via optically generated Fourier transforms. This procedure uses photographic imagery, collected via aircraft or spacecraft, of reflected sun-glitter patterns on water surfaces. The technique makes use of the observable

*Care must be taken to distinguish the two-word term "wave length," referring to the water surface, from the one-word term "wavelength," referring to the radiation spectrum.

148. Breakers and Surf, Principles in Forecasting, U.S. Naval Oceanographic Office, H. O. Publication No. 234, 1958.

149. J. W. Johnson, et al., Graphic Construction of Wave Refraction Diagrams, U. S. Naval Oceanographic Office, H. O. Publication No. 605, January 1948.

150. F. C. Polcyn, W. Brown, and I. Sattinger, The Measurement of Water Depth by Remote Sensing Techniques (Final Report), The University of Michigan (WRL) Ann Arbor, Report 8973-26-F, November 1970.

151. N. F. Barber, A Diffraction Analysis of a Photograph of the Sea, Nature, Vol. 164, p. 485, 1949.

changes in wave motion as a set of waves moves from a deep-to shallow-water location. Both wave-length changes and wave-refraction angles are detectable when a coherent light source (laser) is used in an optical processor to generate a Fourier transform to give frequency and directional characteristics.* The deep-water transform is compared to the shallow-water transform to derive changes in wave state. The results of the comparison lead to measurements of the change in depth.

The sea-state condition at the time of imagery collection is extremely important for optical processing techniques. "The simplest model consists of a set of sinusoidal waves, having one frequency and one direction" [152]. The wave train in Jobos Bay, along the southern coast of Puerto Rico, closely duplicates this model. This area and its transform are shown in Figure 37.

The diffraction pattern discloses several important features about the sea state. In the transform process, the lowest frequencies occur closest to the center of the pattern and increase with the radial distance from the center. Thus, the low-frequency wave set (swell) appears near the center of the diffraction pattern as opposing dots. The cluster farther out discloses a higher frequency wave set in the bay. The linearity of the total pattern indicates that all the wave sets are moving either in the same direction (SW to NE) or in directions exactly opposite to each other. Close inspection of the imagery substantiates the former interpretation.

Most of the wave imagery collected for this mission does not have this simple, well defined character. It is much more complex than the ideal, revealing wave sets which have differing propagation directions, wave lengths and wave heights. The result is a reflected sun-glitter image which, in many cases, is devoid of obvious pattern. Furthermore, the sun-glitter pattern may not display the important, longer wave lengths to best advantage.

The importance of collecting imagery which displays waves of very great length is substantiated by the relationship of detectable depth versus wave length. This relationship is illustrated in Figure 38, which was first presented in [153]. From the wave-length ratio of shallow water to deep water (L/L_d), a corresponding relative depth can be extracted from the

*This is not a new process. In 1949, Barber [151] used an arc lamp as a light source and successfully produced diffraction patterns of wave state which showed both low and high frequency components.

152. C. Cox and W. H. Munk, Statistics of the Sea Surface Derived from Sun Glitter, J. Marine Res., Vol. 13, No. 2, pp. 198-227, 1954.

153. F. C. Polcyn, and R. A. Rollin, Remote Sensing Techniques for the Location and Measurement of Shallow-Water Features, The University of Michigan (WRL), Ann Arbor, Report 8973-10-P, January 1969.

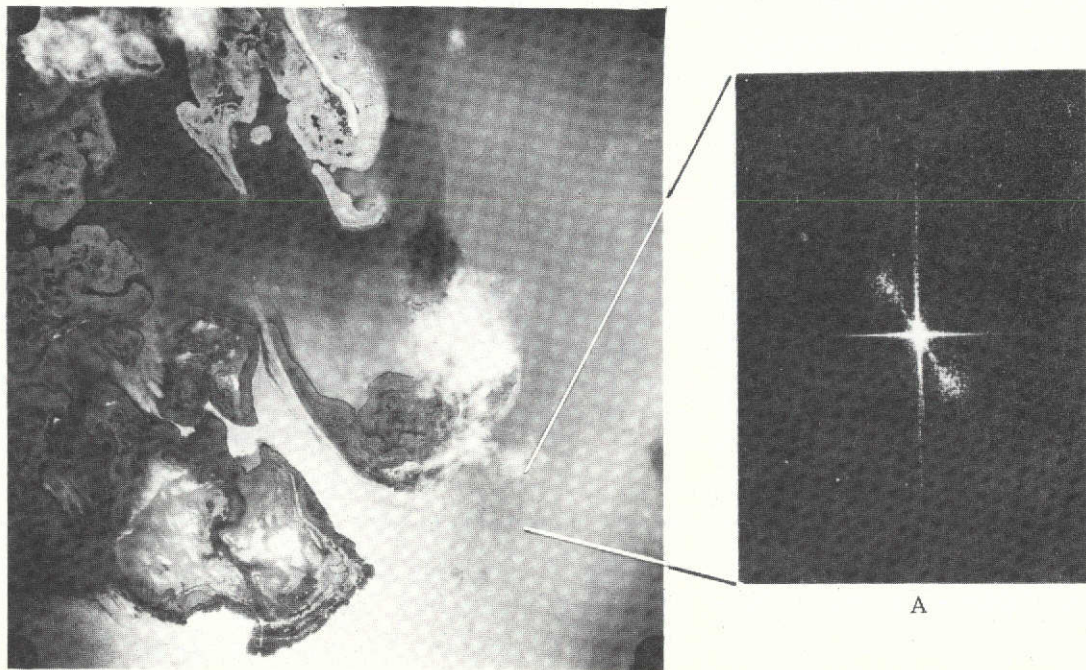


FIGURE 37. SEA STATE OF A MODERATELY WELL DEFINED SWELL AND ITS FOURIER TRANSFORM, PUERTO RICO

*This is not a new process. In 1949, Barber [151] used an arc lamp as a light source and successfully produced diffraction patterns of wave state which showed both low and high frequency components.

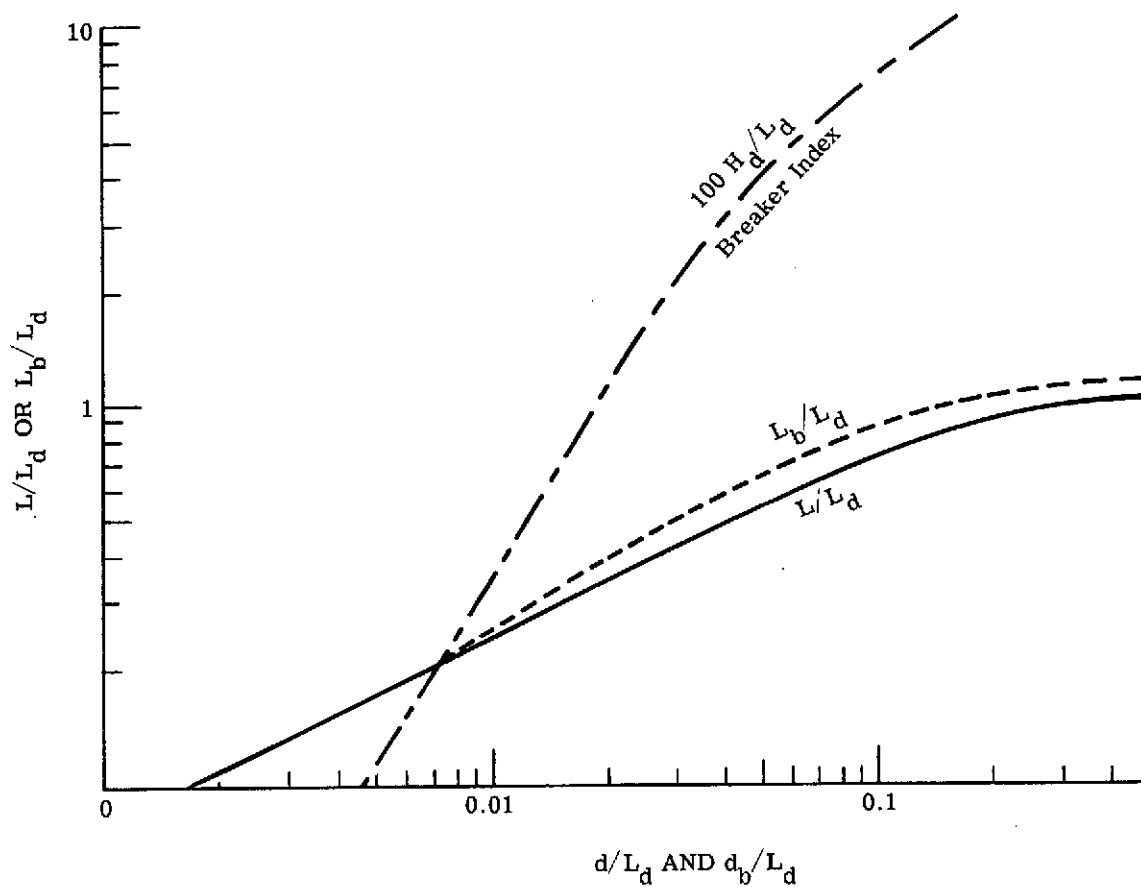


FIGURE 38. CHANGE DURING SHOALING IN WAVE-LENGTH RATIO VERSUS RELATIVE DEPTH

abscissa (d/L_d). Shoal depths are then calculated by multiplying the relative depth by the deep water wave length. Potentially, the longer the wave length, the deeper one can detect. Thus, the use of changes in detectable wave length to measure shoal water depths is most successful when we use imagery of waves which are simplest in form and relatively long at the depth locations to be measured.

Determination of Water Depth by Use of Remotely Sensed Multispectral Data

A remote sensor oriented toward a shallow body of water receives electromagnetic radiation from sunlight scattered by the water and atmosphere and from sunlight reflected from the ocean floor and the air-water interface. Because that portion which has been reflected from the ocean floor must pass through an intervening, absorbing water layer, the power received by the sensor will be dependent upon the extent of the attenuation and, thus, upon the depth of the water.

Quantitatively, this process can be described essentially by the following relationship:

$$P(\Delta\lambda) = \int_{\lambda}^{\lambda+\Delta\lambda} \left[\rho(\lambda)L_{\lambda} e^{-(\sec \theta + \sec \phi)\alpha(\lambda)Z} + \rho(\lambda)_{a/w}L_{\lambda} \right] d\lambda + P(\Delta\lambda)_{sc} \quad (10)$$

where $P(\Delta\lambda)$ = power received in the spectral band

$P(\Delta\lambda)_{sc}$ = scattered sunlight

$L(\lambda)$ = incident solar spectral radiance

$\rho(\lambda)$ = bottom reflectance

$\rho(\lambda)_{a/w}$ = air-water interface reflectance

$\alpha(\lambda)$ = water's attenuation coefficient

θ = viewing angle (from the nadir)

ϕ = solar-illumination angle (from the vertical)

Z = water depth

For very deep water, the exponential term of Eq. (10) goes to 0, and yields the following deep-water expression:

$$\lim_{Z \rightarrow \infty} [P(\Delta\lambda)] = \int_{\lambda}^{\lambda+\Delta\lambda} \rho(\lambda)_{a/w}L_{\lambda} d\lambda + P(\Delta\lambda)_{sc} = P(\Delta\lambda)_{\infty} \quad (11)$$

Although the light scattered by the water will increase with depth, the effect is slight. Thus, combining Eqs. (10) and (11) we obtain

$$P(\Delta\lambda) - P(\Delta\lambda)_{\infty} = \int_{\lambda}^{\lambda+\Delta\lambda} \left[\rho(\lambda)L_{\lambda} e^{-(\sec \theta + \sec \phi)\alpha(\lambda)Z} \right] d\lambda \quad (12)$$

On the assumption that both P and P_{∞} can be measured, Eq. (12) enables us to calculate water depth. In practice, P_{∞} is determined when we scan over very deep water. By averaging the signal over many scan lines for each spectral band, we obtain P_{∞} as a function of the scan angle (θ) and the spectral band. This function is then subtracted from the shallow-water signal (also a function of θ and λ) and leaves, to a first approximation, only the bottom-reflection term.

Conclusion

Additional details and considerations are discussed in Ref. [154] where some preliminary results are also provided. Further development of these techniques has been supported by the Naval Coastal Systems Laboratory and other NASA contracts in recent years and the interested reader is referred to Refs. [155-157] for more information.

6.3 MULTI-ASPECT REMOTE SENSING TECHNIQUES

The trend in the development of remote sensing technology has been toward the inclusion of additional information channels or recording media. For example, early aerial cameras used black-and-white film with a single spectral filter function. Though single film-filter combinations are still employed, we now have color film with dyes sensitive to three different spectral bands of light in common use. Today's multispectral cameras and scanners collect data in even more spectral bands. Yet another example of this trend is the past development of stereographic techniques whereby overlapping photographs of terrain taken from different camera stations and resulting in different angles of view permit the measurement of terrain elevation differences not easily measured in individual aerial photographs.

This section briefly describes remote sensing techniques for collecting multispectral scanner data at two or more different view (or aspect) angles over the same scene. (More details are available in Refs. [56] and [158].) These multi-aspect remote sensing techniques

154. W. L. Brown, F. C. Polcyn, A. N. Sellman, and S. R. Stewart, Water-Depth Measurement by Wave Refraction and Multispectral Techniques, The University of Michigan (WRL), Ann Arbor, Report 31650-31-T, August 1971.

155. F. C. Polcyn and D. R. Lyzenga, Calculations of Water Depth from ERTS-MSS Data presented at the 5-9 March 1973 ERTS-1 Symposium on Significant Results, New Carrollton, Maryland, and published in the Proceedings of that Symposium.

156. M. Bair, Reconnaissance in Support of Amphibious Operations: Bathymetry and Land Trafficability, ERIM, Ann Arbor, Report 194600-25-T, June 1974.

157. Dr. R. Lyzenga and F. C. Polcyn, Remote Bathymetry and Shoal Detection with ERTS, ERIM, Ann Arbor, Report 193300-51-F (In Press).

158. W. Malila, Multi-Aspect Techniques in Remote Sensing, 9th Symposium on Remote Sensing of Environment, Ann Arbor, April 1974.

are directed toward the improved extraction from scanner data of two major types of information: (a) accurate classification information, and (b) useful information about the condition or state of surface materials.

General observation and experience show that the observed color and brightness of vegetation canopies and other surface materials depend of the angle of view, as well as on the location of the sun relative to the observer. Calculations made with a vegetation-canopy reflectance model developed at ERIM substantiate that there are spectral differences at different view angles, and that these differences can be linked to the canopy structure as well as to the spectral reflectance and transmittance characteristics of the canopy components. To enable study of techniques for exploiting such differences in remote sensing, the ERIM M7 multispectral scanner installation in the C-47 aircraft was modified so that it can be tilted forward at angles up to 55° .

Figure 39 illustrates typical data collection geometry for a multispect mission. Two or more passes are made over the flight line, the first with the scanner in its normal position; the second and any succeeding passes are made with the scan plane tilted forward to a selected tilt angle (e.g., 45°). Differences will be produced in signals by differences in both tilt angle and flight heading. In flying the tilted-scanner passes, there are two altitude options. One is to fly the tilted scanner at the same altitude as that of the standard pass; the other option is to fly at that lower altitude which gives both the standard and the tilted-scanner passes the same slant range to the ground for a 0° scan angle. The latter case produces the same atmospheric path length for the received radiance signals and results in ground spatial resolution elements approximately equal in size. Obviously an operational system could be designed to record both aspects simultaneously, thus requiring only a single pass over the ground area being scanned.

In describing the geometry of tilted scanner data, several angles are important. Three are of principal interest for modeling studies: the zenith angle of the sun, the zenith angle of the scanner's view direction, and the difference between the sun and the view azimuth angles. These angles, in turn, depend on angles that describe the operational configuration of the scanner—namely, the tilt angle, the aircraft heading angle, and the scan angle which is measured from the nadir ground track within the scan plane.

Multi-aspect scanner data collected over two areas are discussed in Ref. [56]. One is an agricultural site in Eaton County, Michigan, southwest of Lansing; the other is a forested site, The University of Michigan School of Natural Resources' Saginaw Forest near Ann Arbor. The agricultural data were collected on 13 August 1972, the latter part of the growing season, while the forest data were collected on 20 March 1973 when deciduous trees were leafless and ground and forest litter were snow-covered.

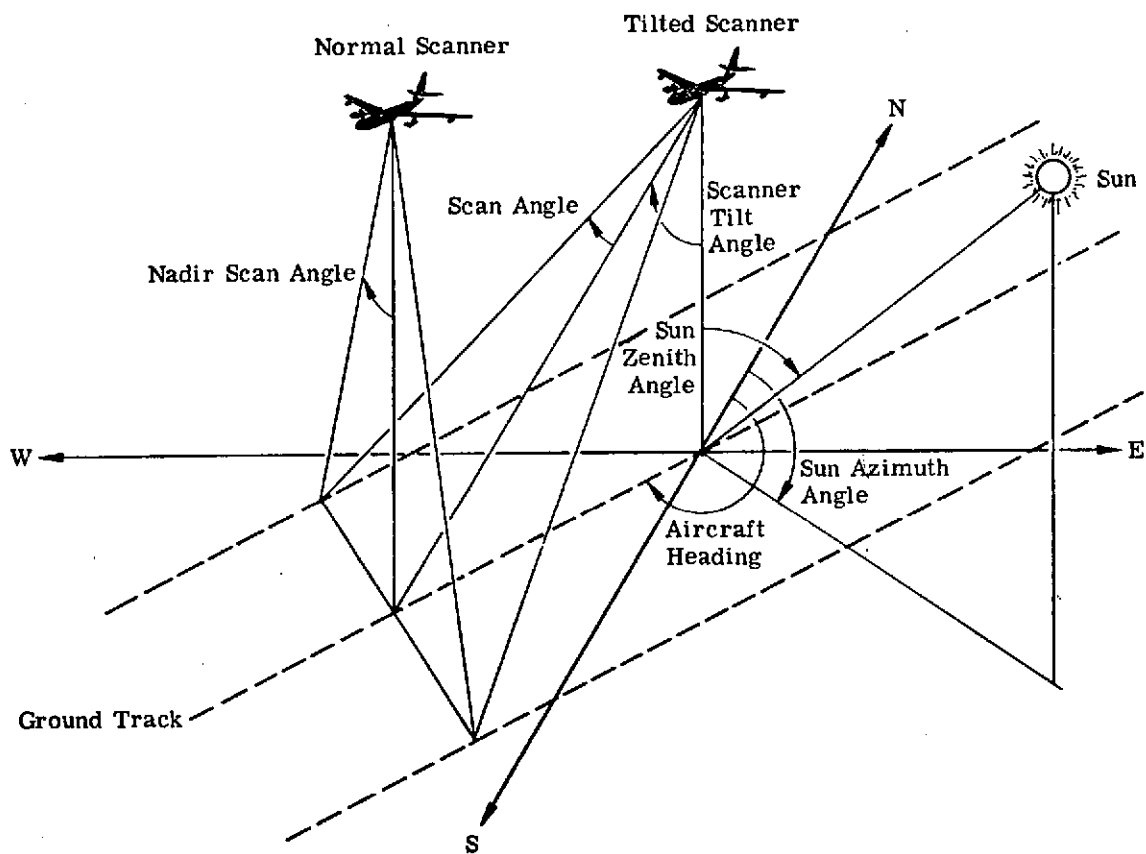


FIGURE 39. NORMAL AND TILTED GEOMETRIES

In addition to empirical analyses of multi-aspect scanner data, complementary theoretical analyses were carried out using radiation transfer as well as canopy reflectance models both to predict and simulate scanner signals and to explore the correlation between canopy biological characteristics and observable radiation.

The majority of our theoretical analysis was devoted to calculation of canopy characteristics using the bidirectional canopy reflectance model developed by Dr. Gwynn Suits of ERIM [34]. The computer program that implements his model was modified in several ways as a part of this study. The principal modification was the addition of operational scanner geometry to the input section, including the capability for specifying a scanner tilt angle and for computing the angles needed for reflectance calculations.

Suits assumes a multilayered canopy model, each layer being of infinite extent and characterized by randomly distributed and homogeneously mixed constituents with different spectral properties. Both the spectral transmittance and spectral reflectance for each constituent are required inputs to the computer program. Also, the physical structure of the canopy can be characterized by specifying optical cross-sections for horizontal and vertical components of each constituent material in each layer. The bottom layer of the canopy is bounded by the ground surface—bare soil or snow, for example. The important feature of the model is that it predicts the bidirectional reflectance properties of a canopy in a way that can be traced to the geometric and spectral properties of identifiable canopy components while still allowing the parametric variation of canopy constituents and observation geometry.

Multispectral classification algorithms depend on the differences between signals received from scene materials in various spectral channels. In a more general context, the spectral channels are merely information channels upon which the classifier operates, and the fact that the observed differences have spectral origins is of little or no consequence. An information channel that differs from another one could just as well do so because of viewing geometry, temporal, or polarization differences.

This study was carried out on the data gathered in 1972 and 1973 to determine the utility of multi-aspect remote sensing techniques for improving agricultural crop classification accuracies and for extracting forest stand information (such as stand volume). The conclusions resulting from this investigation are:

(1) The use of multi-aspect data offers some promise for improved classification performance over that obtainable with conventional multispectral scanner data. The following results were obtained with multi-aspect data collected over an agricultural area in mid-August.

- (a) Results with manually registered data from 69 agricultural fields showed slightly more accurate and more consistent classification performance for multi-aspect

data than both tilt-only and no-tilt data for one selection of training and test fields.

- (b) Results for switched roles of training and test fields in the manually registered data were not as consistent, but the switch in roles was complicated by the use of combined, instead of multi-modal, signatures.
- (c) A classification map produced from six channels of machine-registered multi-aspect data was examined and found to exhibit better overall qualities than six-channel maps from either no-tilt or tilt-only data. Classification patterns were most spotty on the no-tilt map; mature trees appeared to be most accurately delineated on the multi-aspect map; and overall delineation of corn fields was best on the multi-aspect map. (Although corn fields were slightly better recognized on the multi-aspect map, the tilt-only map had more false corn detections in trees. In several no-tilt corn fields there were numerous false tree detections.)
- (d) A rank-ordering of the multi-aspect channels, based on average pairwise probability of misclassification between signatures, showed a balance between the tilt and no-tilt channels: two tilt channels were assigned the highest rank while no-tilt channels placed in the next several ranks.

(2) Maps of the difference between tilt and no-tilt signals in several channels and corresponding scatter diagrams of class mean signals exhibited interesting characteristics.

- (a) On the 0.55- to 0.60- μ m difference map, bare soil exhibited the greatest relative signal increase in going from no-tilt to tilt geometry. The effect appears to decrease progressively as the fields contain more and more vegetation biomass (and/or green vegetation).
- (b) On the 0.62- to 0.70- μ m difference map, vegetation signatures have more nearly equal difference values, but bare soil has a markedly lower difference value.

(3) Theoretical multi-aspect reflectance calculations for corn canopies show that variations in canopy physical characteristics produce substantial changes in reflectances (although extraction of such information from empirical data has not yet been attempted).

- (a) The greatest effect was produced by the combination of a stressed canopy with 50% chlorotic leaves.
- (b) Soil-color differences became important only when coupled with low plant densities.
- (c) Corn-tassel effects were discernible on multi-aspect diagrams, and the dispersion pattern of different tassel, soil, and density conditions in healthy corn

came closest to matching empirical scatter plots for tilt channel 9 (760 nm) versus tilt channel 5 (570 nm).

(4) The canopy reflectance model predicted trends found in empirical data for a leafless deciduous tree stand with snow-covered ground. The analysis was not completed, so the feasibility of extracting information on forest stand characteristics (such as stand volume) was neither established nor rejected; further work is recommended.

6.4 APPLICATIONS OF ACTIVE/PASSIVE SCANNER FOR VEGETATION ANALYSIS

All vegetative canopies interact with incident electromagnetic radiation, modify that radiation, and direct a portion of that modified radiation towards a remote sensor. The modification of the incident radiation contains the information with which vegetation analysis is to be achieved.

Two major categories of canopy properties produce the modifications upon incident radiation: (1) the spectral properties of the canopy parts such as leaves, stalks, and soil and (2) the structural arrangement of these parts such as the number, orientation, and sizes of those parts. The manner and extent of the influence of these two properties are described in a series of publications by Suits [34, 36] and Suits and Safir [35]. The reflectance calculations presented in the first two publications provide an analytical connection between the remotely measured directional reflectance of a vegetative canopy and the character of the two major canopy properties. The third publication shows that the calculations are valid by comparing experimental results with calculated predictions. In addition, the third publication illustrates the analytical capabilities of the approach as applied to the detectability of Southern Corn Leaf Blight. The third publication also illustrates the difference between the analytical properties of two different geometries of measurement—the bistatic reflectance measurement which is the usual geometry of measurement employed by passive reflected light systems using sunlight, and the monostatic geometry of measurement (the usual geometry of measurement of active scanners) where the source and receiver are situated on the same platform.

Generally, the bistatic geometry of measurement produces results that are primarily governed by the properties of the uppermost canopy components and structure. The dominance of the upper structure in influencing the result increases as the solar altitude angle decreases toward the horizon. On the other hand, the monostatic geometry of measurements produces results that are independent of sun angle and are due to both upper and lower canopy structure properties. Indeed, according to the theory of Ref. [36] the maximum possible influence of the lower canopy structure is obtained with this geometry. A simple heuristic argument can be used to explain the above differences. In order for a remote object to influence or modulate the reflectance value of a given area, a complete electromagnetic communication link must be established—source to

object to receiver. In the bistatic case using solar illumination the upper structure is always best illuminated by the sun because it is in direct line of sight to the sun. However, the upper structure seldom completely obscures the lower structure from the sun so that sun flecks or shafts of sunlight penetrate deep into the canopy, though with steadily diminishing size and number as depth increases. Except for the presence of sky light and diffuse flux scattered within the canopy, the illuminated area of the lower structure and soil lies in considerable shadow. If, now, this canopy were viewed bistatically, those parts of the canopy which are simultaneously in line of sight to the sun and in line of sight to the receiver would produce the major modulation in the link. The upper structure is in direct line of sight to both at all times, so an upper structure contribution can be substantial. However, suppose that the fractional area illuminated by the sun on the lower structure and soil were, say, only 0.1, then the probability of achieving line of sight through the upper structure to the lower structure is 0.1. A bistatic view through an independent path through the upper structure would likewise bring to view a fraction (0.1) of lower structure but not entirely the same areas that are illuminated. The average fractional area which would be both illuminated and in view would be 0.1×0.1 or only 0.01. In monostatic viewing, the direction of view is identical to the direction of illumination. Therefore, if light reached and illuminated a component in the lower structure, that component must necessarily be in line of sight for viewing. The fraction of directly illuminated lower structure which is both illuminated and in view must be 0.1—or a factor of 10 greater than in the bistatic viewing geometry. A low altitude sun angle emphasizes the contribution of upper structure as compared to lower structure since direct illumination must now pass through a far greater number of components of the upper structure to reach the lower structure by mixture of the oblique path. Consequently, the lower structure, even though it may be in easy view from the nadir, will be primarily in shadow.

From the foregoing argument, one may anticipate important new information for vegetation analysis, especially of agricultural crops, by employing a combination of active and passive scanning systems. Every crop has a genetically controlled morphological sequence which may be only partly modified by environmental factors. This morphology is frequently expressed in a layered canopy structure. For example, wheat heading is to be expected in the uppermost structure of a wheat canopy; corn plants tassel at the top of the plant; and many plants flower at specified locations within the canopy. Many pathological conditions favor a particular canopy level and location; for example, the first sign of senescence for many plants is necrosis of old lower canopy leaves. Although the signals from combined active/passive systems will not directly measure each structural property, the combined signals must be significantly correlated with these structural properties so that suitable data calculations should produce measures of these separate properties.

In the multispectral remote sensing of vegetation, two effects are known to be of great importance [159]. The first is the effect of absorption by chlorophyll in the red, which reduces the transmission and reflection of green leaves at these wavelengths. The second is the strong water-absorption band centered at $1.9 \mu\text{m}$, which again reduces the reflectance of leaves markedly in this region of the spectrum. Figure 40 illustrates these two effects. There is also a third effect that is less well known, namely, the effect of plant health on the cellulose absorption band at $2.1 \mu\text{m}$.

Passive techniques to make use of these effects suffer from the limitation that the vegetation to be studied must be suitably illuminated by sunlight. Thus, observation of the chlorophyll band is dependent on clear skies and a reasonably high sun angle. Observation of the $1.9 \mu\text{m}$ band is difficult in any case because of the strong overlapping water-vapor absorption in the clear atmosphere. The cellulose band at $2.1 \mu\text{m}$ is in a moderately good atmospheric window, but the reflected solar energy in this region suffers the same kinds of problems as the chlorophyll band, though the magnitudes of the problems are even greater, because at $2.1 \mu\text{m}$ there is less energy available than in the visible region.

In order to avoid these limitations, the use of active scanners with suitable laser lines as sources has been suggested. Active systems offer the advantage of narrow bandwidths (for better discrimination) at much larger power levels than are offered by reflected solar radiation in similar bandwidths. To look into this possibility, and at the same time to exercise the data in ERSIS, the following investigation was carried out.

(1) Four vegetation types were chosen:

- healthy wheat
- wheat afflicted by rust
- dry corn leaves
- aspen forest and leaves in various conditions

(2) Six wavelengths related to the chlorophyll, $1.9 \mu\text{m}$ water, and cellulose bands were chosen which are at (or close to) strong laser lines:

- $0.50 \mu\text{m}$ (Argon)
- $0.57 \mu\text{m}$ (Krypton)
- $0.65 \mu\text{m}$ (Krypton)
- $1.06 \mu\text{m}$ (Neodymium)
- $2.00 \mu\text{m}$ (Tm^{3+} :YAG)
- $2.10 \mu\text{m}$ (Ho^{3+} :YAG)

159. V. I. Meyers, et al., Remote Sensing, National Academy of Sciences, Washington, p. 253, 1970.

- (3) For about 15 specimens of the four vegetation types, the following ratios, r , of the spectral reflectances, R_λ , were formed:

$$r_1 = R_{0.50}/R_{0.57}$$

$$r_2 = R_{0.57}/R_{0.65}$$

$$r_3 = R_{0.57}/R_{1.06}$$

$$r_4 = R_{2.0}/R_{2.1}$$

One would expect r_2 to be larger than unity for a healthy plant but to become less than unity as the chlorophyll disappears, whereas r_4 should be appreciably less than unity if the leaves are healthy but otherwise close to or somewhat larger than unity. In general, the results followed these expectations.

(1) We found that r_1 was uniformly high (0.7) for the dry corn and also high for two exceptional cases of aspen—a blackening leaf (0.7) and a winter forest (0.85); this was hardly surprising. Otherwise, r_1 values for the wheat and aspen ranged from 0.4 to 0.7 with perhaps some tendency for diseased wheat to show a higher value than the normal wheat. To relate the values to the detailed descriptions, however, was not found possible.

(2) For r_2 , the dry corn showed values close to 0.7 while, as expected, most other samples were higher. The blackening aspen leaf and winter aspen leaf were also low, but so are two samples of normal wheat. The values for wheat and aspen vary considerably (from ~ 1.0 to ~ 2.7).

(3) As might be expected, the values for r_3 varied a good deal from about 0.15 to about 0.67. Apart from a slight tendency for the values for the diseased wheat to be at the higher end of this range and for the normal wheat to be at the lower end, the variations appeared random.

(4) The values of r_4 for the dry corn were all close to unity (0.977 to 1.105) while, as expected, five samples of healthy aspen leaves showed lower values (0.433 to 0.750). No values were available for the wheat or for the remaining aspen.

An exercise in forming ratios of selected spectral radiances has supported the view that an active scanner based on existing strong laser lines could be used to monitor the chlorophyll, water, and cellulose bands in vegetation. For instance, if r_2 and r_4 were monitored simultaneously, the quantity r_2/r_4 would have large values for healthy vegetation and small values for dying vegetation. Therefore, an active scanner with four laser lines at 0.57 μm (krypton), 0.65 μm (krypton), 2.0 μm (Tm^{3+} :YAG), and 2.1 μm (Ho^{3+} :YAG) could be used to monitor plant health.

It is obvious that the above effort only scratches the surface as far as active scanners are concerned. Perhaps the most important potential advantage of active scanners is that they permit the collection of data day or night and, as a result, overcome a serious restriction of conventional scanning systems. An active scanning system is presently being developed at

ERIM under Air Force funding. We recommend that such systems be used to empirically investigate the utility of active scanning systems for remote sensing of earth resources.

6.5 MULTISPECTRAL PARAMETER MAPPING

In the survey and analysis of soil conditions there has been an interest in the use of vegetation in an area affected by some chemical agent as an indicator or sentinel of the extent and concentration of the agent. It has also been proposed that such techniques be tested as a means of locating other sub-surface agents such as ore bodies. Finally, after some experimental tests of techniques developed for the above problems, it was proposed that an important application of the technique could also be found in the selective mapping of any parameter affecting a recognizable surface object. This was proposed specifically as a means of investigating the thermal characteristics of a set of surface objects such as plants of a particular species.

A simple description of multispectral parameter mapping as implemented on our SPARC processor is given in the remainder of this treatise. Suppose all samples of a species of plant as observed by a multispectral scanner have a radiance distribution in two spectral bands (λ_1, λ_2) as shown in Figure 41 and the normal plant is distributed as a subset in the space with a mean, $\bar{P}_N(\lambda_1, \lambda_2)$. Another species of plant is similar and is shown as a possible interfering background distribution. The object decision bound is determined by a likelihood ratio function of the two distributions. A distance $\{D[P(\lambda_1, \lambda_2)]\}$ is continuously calculated for each point $[P(\lambda_1, \lambda_2)]$ and is defined as the sum of squared distances from the mean

$$\sum_{i=1}^k [P(\lambda_i) - \bar{P}_N(\lambda_i)]^2$$

If $P(\lambda_1, \lambda_2)$ is classified as a member of the object set, the distance is printed on a CRO film printer with an intensity proportional to the distance as shown in Figure 41. The printing process proceeds at a real-time rate, about 10^5 elements/sec, and provides a map of the parameter.

The technique of parameter mapping should prove useful in processing a variety of data involving the mapping of effects of various substances on plants. Among these are the effects of water privation, soil salinity, chemical pollutants and disease affecting several species or maturities of plants. Parameter mapping (or scene attribute estimation) is discussed in more detail in Refs. [145-147], [158], and [160-161].

160. W. A. Malila, R. H. Hieber and A. P. McCleer, 1973. Correlation of ERTS MSS Data and Earth Coordinate Systems, Proceedings of Conference on Machine Processing of Remotely Sensed Data, Purdue University, W. Lafayette, 16-18 October 1973.

161. A. E. Coker, R. Marshall, and F. Thomson, Discrimination of Fluoride and Phosphate Contamination in Central Florida for Analysis of Environmental Effects, 4th Annual Earth Resource Program Review, Section 79, January 1972.

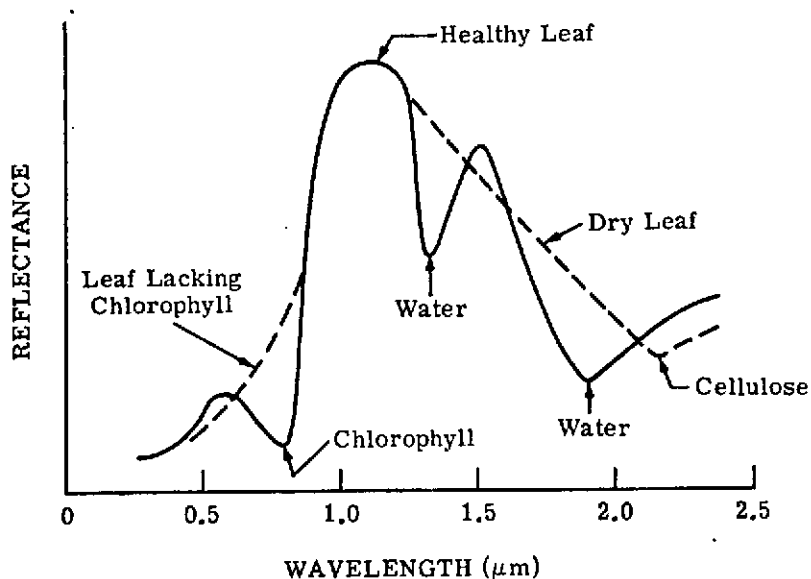


FIGURE 40. TYPICAL LEAF REFLECTANCE SPECTRA

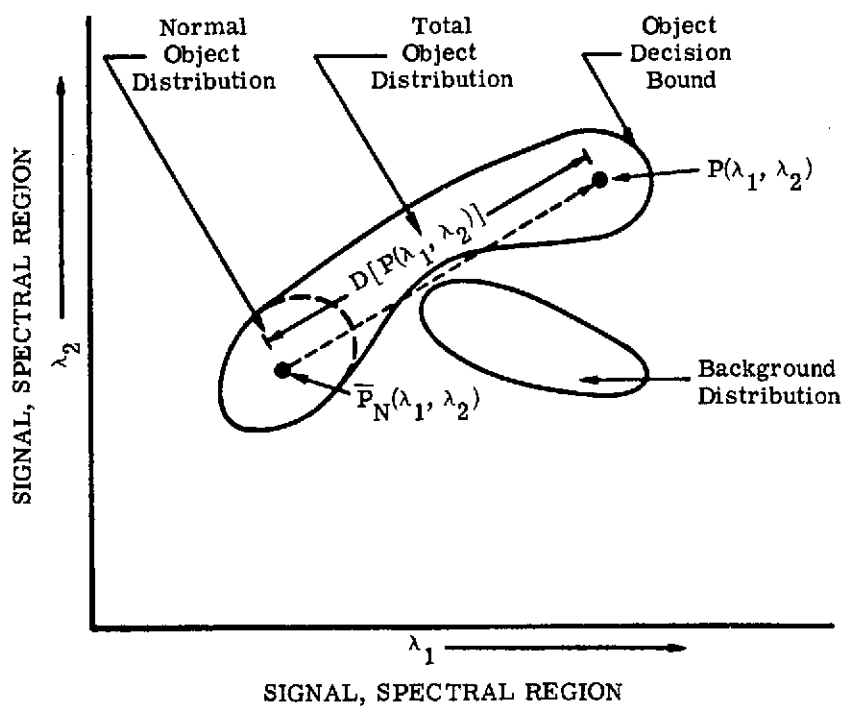


FIGURE 41. ILLUSTRATION OF MULTISPECTRAL PARAMETER COMPUTATION

TECHNOLOGY: APPLICATION AND TRANSFER

In this section we describe ERIM's efforts under this contract to apply and measure the state-of-the-art of multispectral remote sensing technology and to transfer to NASA and the user and remote sensing communities the technology developed in this program for purposes of design of operational earth resources survey information systems. In addition to the standard methods of technology transfer between contractor and sponsor (monthly progress reports, annual technical reports, and frequent program reviews) several other efforts were undertaken during this contract which resulted in the application and transfer of technology. These efforts are described in the following sections.

7.1 SCANNER DESIGN, DEVELOPMENT, AND EVALUATION

Because of our successful experience in designing, constructing, and operating the first multispectral scanner, ERIM was asked to participate in specific aspects of the design, development, and evaluation of new multispectral scanner systems. These efforts are briefly discussed below.

Optical Transfer Techniques for Orbital Scanners

During 1966 a 12-channel spectrometer, which could be used in place of one of the regular detectors in an AN/AAS-5 scanners, was designed and built at ERIM. Using this spectrometer, 12 parallel video signals corresponding to 12 wavelength bands spread over the 0.4- to 1.0- μm region could be tape-recorded for subsequent processing.

However, it was obvious that the value of this system was limited both by the restricted wavelength coverage and by the impracticability of flying the system in other than a low-performance aircraft. It was also apparent to those directly associated with the design and fabrication of the spectrometer that designs suitable for wider wavelength coverage and for use in high-performance aircraft or spacecraft would depend on much more sophisticated technology than that used in the 12-channel system.

Subsequent studies demonstrated that it is indeed difficult to combine appropriate spectral resolution over a wide range with high optical efficiency and practical, efficient detector arrays. This study was, therefore, aimed at evolving techniques which might be used to overcome these difficulties, with a view to finding optimum solutions.

A previous study [162] on multispectral scanners for manned orbital operations recommended that a conical scan be used in order to achieve a relatively efficient duty cycle with a relatively

162. J. Braithwaite, L. Larsen, and E. Work, Further Infrared Systems Studies for the Earth Resources Program, Report No. NASA CR-WRL 2122-14-F, The University of Michigan (WRL), Ann Arbor, December 1969.

simple scanner. A preliminary layout for such a scanner was given and its feasibility demonstrated in a general way.

Early in the performance of this task, NASA began planning an Earth Resources Experiment Package (EREP) to be flown in the AAP/Dry Workshop (now known as the Skylab), scheduled for launch in the spring of 1972. During these preparations, the specifications for the EREP scanner were solidified. It was natural to use these specifications, particularly those concerned with spatial and spectral resolution and coverage, as a basis for the scanners considered here. However, the work discussed here and in [163] is restricted to that carried out in this laboratory, independent of any efforts relating directly to the EREP scanner development.

The success of a system of this sort would depend on the performance of the optical system with respect to throughput and absence of aberrations and, more importantly, on the way in which the optical design allows the use of optimized detectors. Although the latter factor was considered briefly here, a restricted study like this one prevented taking detector properties into account as fully as would be desirable. In fact, at a time when detector technology was changing rapidly, any approach to a system of this sort was likely to be made obsolete by a new development in detector technology, or even by an unforeseen willingness on the part of a detector manufacturer to extend the state of the art in a particular direction.

Feasible designs of optical scanners employing conical scan patterns suitable for operation from earth orbit were studied in this investigation. Various possible optical scanner layouts were considered to determine which to recommend. The detailed optical performance of the preferred optical scanner layout was analyzed by means of computer ray-trace techniques and it was concluded that scanners with apertures of 12 to 18 in. and spatial resolution of the order of 1/10 mrad were practicable, from the point of view of optical design and fabrication, for spectral resolution appropriate for earth resources measurements.

Calibration of Multispectral Scanners

The internal calibration systems of the 24-channel multispectral scanner and the RS-14 dual-channel scanner were studied and evaluated by ERIM for NASA. On the basis of measured results obtained by NASA, a series of specific recommendations were made to ensure accurate calibration of these instruments. Both scanners were provided with internal calibration sources which are viewed by the scanner at times when the external scene is not being viewed. Accurate calibrations can then be ensured, if both the power radiated into the scanner optics by the calibration sources and the performance of the scanner and data handling system can be accurately predicted. These must be ensured for all pertinent variables such as ambient temperature, scan angle, and signal level.

163. J. Braithwaite and E. Work, Optical Transfer Techniques for Orbital Scanners, The University of Michigan (WRL), Ann Arbor, Report 31650-21-T, March 1971.

The RS-14 has the four-sided prism scan mirror viewed by split optics used in many of the Texas Instruments scanners. As a result, its response as a function of scan angle is probably nonuniform. Further, the internal calibration sources are small blackbodies viewed through collimating optics and windows in their housings. These windows and the apparent radiance of the sources as seen by the scanner will be a function of the temperature of these optics as well as of the temperature of the source.

Following analysis of some results obtained during environmental chamber tests to verify performance as a function of scan angle and ambient temperature, we submitted written recommendations to NASA. These covered suggestions for verifying the performance of the external thermal source and the electronic subsystems, for facilitating environmental chamber tests, and for methods for reducing test data.

We were invited to attend periodic formal and informal design review and test program meetings relating to the 24-channel multispectral scanner. The bulk of our inputs consisted of oral recommendations made during such meetings; in addition, written comments and recommendations were often submitted, following further study of problems or as a critique of documents submitted by Bendix.

While we hope and believe that these recommendations regarding various aspects of calibration have been of significant value, our impact on these programs has undoubtedly been less than it might have been because of the intermittent nature of our association with the programs. A more detailed discussion is presented in Ref. [164].

Evaluation of the NASA MSDS

During this contract ERIM personnel participated in an evaluation of the NASA 24-channel multispectral data system (MSDS). In order to provide data for the evaluation, the MSDS was flown over the Willow Run Airport area in Southeastern Michigan during August 1971 and June 1972.

On the ramp at the time of the August overflight we had deployed 20×40 ft calibration panels of standard gray reflectance and standard colors. These panels were deployed near spatial resolution charts which had been painted on the ramp with glass beaded traffic marking paint.

A collection of instruments were set up to obtain measurements of the radiation incident upon the earth's surface around the test site. Both the sky background radiation contribution and that of the solar disk were of interest. The instruments used included: (1) an Isco SR

164. J. Braithwaite, Calibration of Multispectral Scanners, The University of Michigan (WRL), Ann Arbor, Report 31650-27-L, September 1970.

Spectroradiometer used to measure the spectral irradiance in the wavelength region 0.4 through 1.35 μm , (2) a Skyometer used to measure the irradiance of selected sky quadrants in three narrow spectral regions centered at 0.488, 0.633, and 1.06 μm , (3) a Gamma Scientific Model 2000 Telephotometer mounted so that sky background radiance measurements could be made at various zenith and azimuth angles at 0.433, 0.533, and 0.633 μm , and (4) a Kahlsico Mechanical Actinograph which measured the total hemispherical radiation of both the solar disk and the sky background.

A Spectra-Pritchard Photometer modified to a spectroradiometer was used to measure the amount of radiation reflected from selected surfaces at center wavelengths of 0.400, 0.433, 0.466, 0.500, 0.533, 0.600, 0.666, 0.700, 0.800, 0.900, and 1.0 μm . A Barnes Radiation Thermometer (PRT-5) was used to determine the apparent temperature of selected targets (including a nearby lake) in the 8-14 or the 3-5 μm spectral regions. Other instruments used include: (1) a Field Infrared Spectral Radiometer (FISR) which is used to measure target radiance over the spectral range 6-14 micrometers, (2) a Net Radiometer which is used to obtain the radiant flux (i.e., the difference between the incident radiation energy on an area and the radiant energy transmitted away from that area) of the area over which it is placed, (3) an Eppley Pyronometer (Model 10) which is used to measure the total radiation incident upon its sensor which has a hemispherical field of view, and thus measures the total contribution of the sky, (4) a Bendix-Friez which was used to record windspeed and direction, and (5) a Weksler Hydrothermograph which, by recording wet bulb and dry bulb temperatures, enables the calculation of relative humidity.

A more complete description of the instruments and the substantial measurement and data reduction effort are provided in Ref. [165].

Basically, the factors considered in the evaluation of the MSDS included system operation, system stability, channel registration, $NE\Delta\rho$, sampling effects, signal-reflectance transfer function, integrate and hold characteristics, and spatial frequency response. The data collection flights of August 1971 and June 1972 and their evaluation along with recommendations are discussed in [166] and [167], respectively.

165. D. Zuk and M. Gordon, Ground Measurements in Support of a Multispectral Data System Evaluation Flight, The University of Michigan (WRL), Ann Arbor, Informal Technical Report 31650-113-T, March 1972.

166. L. Larsen and P. Lambeck, Performance of MSDS as of 18 August 1971, The University of Michigan (WRL), Ann Arbor, Report 31650-82-T, September 1971.

167. P. F. Lambeck, Engineering Evaluation of 24-Channel Multispectral Scanner, The University of Michigan (WRL), Ann Arbor, Report 10822-1-T.

168. F. Thomson, Contouring of Chesapeake Bay Oil Slick Data, The University of Michigan (WRL), Ann Arbor, Report 3165-52-L, July 1, 1971.
169. N. Thomson, Multispectral Analysis of Terrain Types in the Chesapeake Bay Region, The University of Michigan (WRL), Ann Arbor, Report 3165-53-L, July 15, 1971.
170. F. Thomson, Thermal Contouring of Manitou, Colorado Data—July 1971, The University of Michigan (WRL), Ann Arbor, Report 3165-63-T, July 22, 1971.
171. J. Livisay, F. Thomson, Classification of Simulated ERTS-A Data for Underwater Feature Recognition in Bisque Bay, 1971, The University of Michigan (WRL), Ann Arbor, Report 3165-68-L, August 9, 1971.
172. F. Thomson, User-Oriented Multispectral Data Processing at The University of Michigan, presented at the 4th Annual Earth Resources Program Review, NASA MSC, Houston, 17 January 1972 and published in Proceedings.
173. F. Weber, R. Aldrich, F. Sadowski, and F. Thomson, Land Use Classification in the Southeastern Forest Region by Multispectral Scanning and Computerized Mapping, 8th International Symposium on Remote Sensing of Environment, Ann Arbor, October 1972.
174. F. Thomson, H. Smedes, W. Hendrickson, ERTS-A Terrain Feature Maps of Yellowstone National Park, The University of Michigan (WRL), Ann Arbor, May 1972.
175. F. J. Thomson, Processing of Oregon Coast Oceanographic Data, The University of Michigan (WRL), Ann Arbor, Report 31650-137-L, August 1972.
176. R. Dillman and F. Thomson, Radiance Determination for Panels and Areas of Line 2 for Weslaco, Texas, 27 Feb 1971, The University of Michigan (WRL), Ann Arbor, Report 31650-138-L, July 1972.
177. R. Dillman and F. Thomson, Weslaco Soils Report, February 27, 1971, The University of Michigan (WRL), Ann Arbor, Report 31650-143-L, September 1972.
178. W. G. Burge and W. L. Brown, A Study of Waterfowl Habitat in North Dakota: Additional Data Reduction Techniques Developed to Analyze Waterfowl Habitat, The University of Michigan (WRL), Ann Arbor, November 1970.
179. N. Thomson and F. Thomson, Thermal Contouring of Biscayne Bay Data, The University of Michigan (WRL), Ann Arbor, Letter Report.
180. F. Thomson, Thermal Contouring of Bucks Lake Data, The University of Michigan (WRL), Ann Arbor, Letter Report, February 1971.
181. F. Thomson, Determination of Optimum Spectrometer Channels for Bucks Lake Classification, The University of Michigan (WRL), Ann Arbor, Letter Report, November 1970.
182. W. Rohde, F. Thomson, Analog and Digital Processing of Bucks Lake Data, The University of Michigan (WRL), Ann Arbor, Letter Report, April 1971.
183. W. Burge, V. Prentice, F. Thomson, Multispectral Data Processing of Moses Lake, Washington Data, The University of Michigan (WRL), Ann Arbor, Letter Report, 1970.
184. F. Thomson, Processing and Analysis of Yellowstone Thermal Data, The University of Michigan (WRL), Ann Arbor, Letter Report, February 1970.
185. W. G. Rohde, Processing and Analysis of Black Hills Thermal Contouring, The University of Michigan (WRL), Ann Arbor, Letter Report.
186. F. J. Thomson, SPARC Preprocessing and Processing of Yellowstone Data, The University of Michigan (WRL), Ann Arbor, Letter Report, March 1971.

7.2 USER DATA PROCESSING AND ANALYSIS

We have known for some time that processing of remotely sensed data could make it more useful to the investigator of earth-resources phenomena. In particular, the processing of multi-spectral scanner data may be able to delineate subtle features through the use of pattern-recognition algorithms applied to the spectral signature information.

To explore further the capabilities of multispectral data-processing techniques, ERIM was funded by NASA to work with the principal investigators, to apply data-processing techniques to the specific problems of the users, and to assist the users in analyzing and evaluating the processed results. As part of these efforts, multispectral scanner data were processed and analyzed for a number of users who represented NASA, three Universities, the U.S. Department of Agriculture, and the U.S. Geological Survey.

Rather than discuss these efforts in detail in this document we list the various users and their test sites and provide a brief description of the resource problem which was being addressed in each case. For additional details on these investigations we refer the reader to references [123], [124], [128] and [168-186] and other reports generated by the users themselves on these subjects.

Crosby - Missouri River

The problem was to see how remote sensing could be used to delineate both small- and large-scale variations in river-water temperature. The data were collected in the predawn hours of 23 July, 1969 over a section of the Missouri River near Bismarck, North Dakota. The thermal data were processed by contouring to delineate the spatial distribution of effluents from various power and sewage treatment plants. In addition, temperatures were computed in various parts of the river to delineate temperature changes in a 50-mile stretch of the river.

Kolipinski - Biscayne Bay

The purpose of the investigation for Dr. Milton Kolipinski of the USGS Miami office was threefold. First, the effluent from the Turkey Point power plant was to be mapped with thermal data. Then, we were to attempt to delineate various shoreline mangrove communities in an attempt to define the mean high-water mark in a section of south Biscayne Bay. Finally, we were to attempt to recognize aquatic plant communities and other bottom types in Biscayne Bay to determine how reliably these features could be mapped and to generate a control against which any possible future changes in the features could be compared.

Coker - Tampa

Mr. Coker was investigating two phenomena peculiar to the central area of Florida. First, he wanted to extend the processing of thermal data collected over regions of known active sink-holes to delineate those areas likely to collapse. In this work, a follow-on study to work

completed under USGS sponsorship, active sinkholes were delineated, and several areas, which began to subside one and half years after the data were collected, were delineated with the use of thermal contouring. The success of this technique seems to be related to the anomalously dry soil areas which occur over active sink areas. These may be detected thermally. The second part of the investigation of Mr. Coker involved the mapping of effluents from phosphate-plant settling ponds. The effluent is rich in fluoride which is very toxic to plants and animals. The effluent is confined to large settling ponds and, because the ponds occasionally leak, finds its way into rivers and streams.

Watson - Mill Creek

The Mill Creek data processing had two purposes. First, radiance statistics and reflectance statistics of four major rock types were to be extracted from the visible and ultraviolet data collected over Mill Creek in late June 1970 at altitudes of 500, 3000, and 10,000 ft. Second, thermal data were to be processed by contouring in order to map the diurnal thermal variation of various rock types quantitatively and to compare the information obtained with results of theoretical models.

Hamm - Moses Lake

The purpose of the Moses Lake study was to attempt to delineate incipient wet areas and canal leakages in an irrigated section of the Columbia River Basin. A secondary goal was to see whether the effects of salinity (arising from repeated irrigation) on plants could be detected and quantified. The detection of incipient wet areas is important in this region, for the topsoil is very thin and the bedrock below the topsoil is impervious. During the irrigation season, the water table rises, often to levels which affect the growth of crops. Subtle effects on vegetation are probably detectable before any noticeable effects would become apparent from a photographic study. Canal leakages are important to detect because of water loss and effect on surrounding farmlands.

Pearcey - Oregon Coast

Processing for Dr. William Pearcey (Oregon State University) had two purposes. First, Dr. Pearcey wanted to study the small-scale variations in water color and temperature around known frontal areas in the Pacific Ocean off the Oregon Coast. Second, he wanted to study the large-scale mixing of onshore water, the Columbia River outfall, and the deep ocean water. This information is important because it allows a delineation of upwelling deep ocean water containing nutrients for fish. Often, commercial quantities of fish are found near these upwelling areas.

Smedes - Yellowstone

The purpose of the study for Dr. Harry Smedes (USGS, Denver) was to delineate geological features in a section of Yellowstone National Park. Previous attempts to process the data collected were of limited success because of the presence of radiance variations across the scan

line. These were caused by the topographic variation over the scanned scene, because the plane was flying down a shallow canyon, and the sun illuminated one side of the canyon more than the other. A second goal was to determine the performance of spectral-response-simulated ERTS-A and RBV data in classifying the scene.

Nelson - Wetlands

The purpose of the investigation for Harvey Nelson (Bureau of Sport Fisheries in Jamestown, North Dakota) was to attempt to map ponds in a section of North Dakota. The pond areas and perimeters were to be measured and shape factors computed as the ratio of area to perimeter, normalized to a value of one for a circular pond. The shape factors were felt to be indicative of the ability of a pond to support waterfowl. To assess waterfowl productivity further, data were collected in spring and summer. In the spring, there are many potholes because of the abundant water supply. In summer, many of the shallower potholes dry up and different aquatic vegetation types grow up around remaining ponds. These ponds may then be further classified according to the type of aquatic vegetation growing around them. This aquatic vegetation serves as food for the waterfowl.

Weber - Black Hills and Wind River

The goal of processing the Black Hills data for Dr. F. P. Weber (U.S. Forest Service, Berkeley, California) was to attempt to prove that Ponderosa Pine beetles attacked trees before visible symptoms of attack were apparent. Previous studies had indicated that attacked trees had higher temperatures in the daytime than healthy trees. This was felt to be caused by inhibited evapotranspiration. We also felt that there might be differences in reflectance in the near-infrared range, where the reflectance of foliage is strongly related to the moisture content. The attacked trees, having lower moisture content of foliage than the healthy trees, would have higher reflectance.

At Wind River, the problem was to detect a root-rot disease in Douglas Fir. Again, pre-visual detection was desired, but the problem was more complicated than in the Black Hills because the disease develops over a period of more than one or two years. Because the first indications of disease were found (by ground observation) to be from moisture stress, the thermal and near-infrared data were thought to offer the best possibility for detection of diseased trees.

Olsen - Ann Arbor Forestry

Data processing was performed for Dr. Charles Olsen (The University of Michigan) for three purposes. First, the distribution of forest species in a test area (Saginaw Forest) was to be mapped. This area has the advantage of a large number of pure stands of both hardwoods and conifers, and a great deal of ground truth has been collected. Second, we were to attempt to recognize healthy and diseased conifers and other forest species in a different test area

(Sharonville) at two times of year (June and August). The third processing goal was to study the usefulness to forestry investigation of false-color films generated from scanner data collected in nonphotographic regions.

Colwell - Bucks Lake

The purpose of the investigation for Dr. Robert Colwell (University of California, Berkeley) was to classify rangeland types in an area near Bucks Lake, California, with the spectrometer data. Both digital and SPARC analog processing was attempted in an effort to evaluate both techniques. In addition, thermal contouring and false-color films were supplied to test the ability of these processed data to delineate features of interest.

Driscoll - Manitou National Forest

As a part of this investigation for Dr. Richard Driscoll of the U.S. Forest Service, Ft. Collins, Colorado, data were collected by ERIM's multispectral scanner system over a test area in the Manitou National Forest. Thermal data were then contoured to yield an understanding of diurnal changes in temperature in a forested area.

Maurer - Chesapeake Bay

Two separate processing and analysis tasks were carried out on data gathered in the Chesapeake Bay region. First, contouring of thermal and ultraviolet scanner data gathered over an oil slick in the Bay was accomplished for investigators at NASA Wallops Station and Virginia Institute of Marine Science. Second, several digital and analog processing operations were then performed on multispectral data collected by the ERIM aircraft over a portion of the upper Chesapeake Bay in order to determine the usefulness of automatic recognition techniques for classifying and mapping broad terrain type classes (e.g., soil, water, and vegetation) as well as different sub-classes of vegetation (i.e., vegetation cover types such as mixed upland hardwoods, pasture, and Spartina salt marsh).

Wiegand - Weslaco

For this investigation Dr. Craig Wiegand (USDA Weslaco Experiment Station) was interested in examining the feasibility of using multispectral scanner data to assist in delineating soil types in Southern Texas.

Previous soil mapping experiments had concentrated on either visible and near infrared, near infrared, or thermal data to attempt to map soil conditions. This experiment differed from previous ones in that the utility of visible, near infrared, and two-color thermal data were assessed for the same area. Emphasis was placed on communicating with the soil mapping scientist in the fields—for this reason not only recognition maps but false-color films and ratio image displays were prepared.

Weber - Southeast U.S.

As a part of this investigation for Dr. F. P. Weber, the feasibility of mapping land use categories by airborne multispectral scanning was tested over two 42-square-kilometer sites in the Southeastern United States. New techniques were applied in preprocessing the data collected to compensate for effects of atmosphere and changing solar irradiance. The capabilities of extending spectral signatures from one training flight line to three additional lines for both test sites were analyzed. The data processed by the SPectral Analysis Recognition Computer system were compared to those obtained from color infrared photographs and ground surveys. The effects of time-of-day and selection of optimum channels on accuracy of mapping classification were investigated.

Canney - Catheart Mountain

The purpose of the investigation for Mr. Frank Canney (U.S.G.S., Denver, Colorado) was to determine the utility of multispectral and thermal scanner data in delineating anomalies in the spectral signatures of trees growing in copper and molybdenum rich soils. Results were inconclusive in separating affected trees from the healthy trees using the multispectral scanner data (it is suspected that poor data quality was primarily responsible for the marginal results). In the thermal data, which were gathered at 2002 hours, the affected tree area was clearly distinguishable as a warm area about 2 to 3°F warmer than the surrounding forested area.

7.3 MULTI-AGENCY PROGRAMS

During this contract period ERIM has participated in two major multi-agency programs. As a result of these programs, the similarities and differences in the available technology and advanced ideas were discussed and much better understood by all participating parties than they would have been in the absence of such cooperative programs. Continuing efforts of this sort are recommended for the future.

The two programs referred to above, both of which are briefly discussed in the following subsections, are the Corn Blight Watch Experiment (CBWE) and the Crop Identification Technology Assessment for Remote Sensing (CITARS) program.

7.3.1 CORN BLIGHT WATCH EXPERIMENT

The 1971 Corn Blight Watch Experiment (CBWE) was conceived to test the potential of remote sensing, while rapidly and comprehensively assessing the effects of Southern Corn Leaf Blight (SCLB). In 1970, SCLB reduced U.S. corn production by about 10%. Agricultural scientists foresaw a similar threat to the 1971 crop. The 1970 growing season had been marked by serious lack of timely, accurate, and comprehensive data on both the extent and severity of the blight. As late as September there had been much uncertainty about the number of acres infected and the severity of infection.

Objectives of the CBWE were to evaluate the use of advanced remote sensing techniques and concepts to:

- Detect the development and spread of corn blight during the growing season across the Corn Belt Region;
- Assess different levels of infection present in the Corn Belt;
- Amplify information acquired by ground visits to better assess current blight status and the probable impact on corn production of blight; and
- Estimate through extrapolation the applicability of these techniques to similar situations occurring in the future.

The Corn Blight Watch was an experiment not only in technological organization and expertise but also in institutional and multidisciplinary cooperation and coordination. The Watch (which was the first agricultural remote sensing application of this magnitude) brought together many agencies, disciplines, and interests. The administrative body of the Watch, the Corn Blight Watch Executive Committee, contained members from 10 government organizations, from ERIM, and from Purdue University, with many other groups participating in facets of the Experiment.

Those with major responsibilities included the U.S. Department of Agriculture's Statistical Reporting Service (SRS), Agricultural Stabilization and Conservation Service (ASCS), Extension Service (ES), Economic Research Service (ERS) and Cooperative State Research Service (CSRS). Others included the Cooperative Extension Services (CES) and the State Agricultural Experiment Stations of the seven participating states. Providing coordination and support were the National Aeronautics and Space Administration (NASA), ERIM, and Purdue University's Laboratory for Applications of Remote Sensing (LARS).

ERIM's responsibility during the CBWE was to gather airborne multispectral scanner data over 30 segments located in Western Indiana (the intensive study area) every two weeks during the growing season. The data from 15 of these segments were then analyzed using machine recognition programs to determine blight presence and severity.

The significant results of the 1971 Corn Blight Watch Experiment can perhaps be best expressed by summarizing the achievements related to the application objectives and by discussing the performance of the technology relative to those achievements.

The application objectives required (1) the detection of outbreak identification of temporal increases in severity levels and the tracking of SCLB spread over the total study region; (2) an assessment of the impact of SCLB on production; and (3) an estimate of the applicability of remote sensing to other situations which would require surveys on a large scale.

Objective 1

With reference to the first objective, it was concluded that neither the manual interpretation of small-scale photography nor the machine-aided analysis of multispectral measurements provided adequate detection of SCLB during early stages of infection. Analysis of these data did, however, permit the detection of outbreaks of moderate to severe infection levels and relatively high accuracy mapping of the spread of those levels over the study regions.

Additionally, analysis of data showed that although the flight lines were efficient in a data acquisition sense, they were not statistically optimal and actually contributed to increased variance in blight acreage estimates. This leads to the conclusion that a more accurate assessment of conditions resulting from SCLB could have been realized with a smaller set of data samples better distributed over the total study area.

Objective 2

In attempting to assess the impact of SCLB on production, investigators were able to associate significant yield reductions with moderate to severe infection levels occurring in August and still greater reductions associated with moderate to severe infection levels occurring in July. The results of the Experiment indicate that acreages infected at these levels were identified with relatively high confidence in the late July and August periods.

Results also led to a conclusion that machine-assisted analysis of multispectral scanner data was more effective both in detecting and tracking the spread and in assessing the impact of SCLB than was the analysis of the small-scale photography. This conclusion had been anticipated since the small changes correlating to blight infection levels are more easily measured quantitatively (i.e., by multispectral sensors) than qualitatively (i.e., by photointerpreters).

Objective 3

Results clearly indicate that the technology is capable of both identifying and measuring the extent of agricultural crops and land use categories. Major crops were accurately identified throughout the season by both photointerpretive and machine-assisted analysis techniques, even though this aspect of the Experiment received relatively little emphasis compared to the more difficult blight detection problem.

It can further be concluded that the technology is suitable for large-scale detection of crop stress in those instances where changes in the radiation characteristics of the crop accompany the stress. These stresses, which affect crop production, include low plant population, drought damage, hail damage, and extreme weediness. There were instances, however, when these factors could not be differentiated from the effects of blight.

In addition to the specific fulfillment of objectives, the CBWE provided an excellent opportunity to evaluate all aspects of a system designed to collect, analyze, interpret, and distribute information repeatedly and at short intervals throughout a growing season.

First, much was learned about how to manage the volume of data involved in acquiring information over a large geographic region. The use of a statistically sound sampling model was found to be a key element in accomplishing this.

Second, a file of photography, multispectral measurements, and field observations collected at biweekly intervals over an entire Corn Belt growing season is now available. It will prove extremely valuable in further studies.

Third, knowledge was gained about the costs of a large-scale information system using remote sensing. Information on the cost in both dollars and time for each part of the Experiment will be useful in the planning of future experiments or operational systems. These data on labor, computer costs, aircraft, film, processing, etc., expended in the Experiment are being used to investigate the relationship between subsampling ratios, costs, and precision of estimates.

Fourth, the Corn Blight Watch Experiment also demonstrated the value of pooling the resources of a number of cooperating groups. At this time no single organization has the expertise or resources to conduct such an experiment alone; the CBWE provided valuable data related to resource requirements for this type of program as well as insight into the practices which are most effective in the design and operation of such cooperative systems.

Fifth, because of the CBWE, many agriculturists had an opportunity to work with remote sensing data. The majority of field personnel responded favorably to the aerial color infrared photography sent to them and reported that it could be used to good advantage in their work. As a corollary to that, the Experiment also demonstrated the need for more agriculturalists with training in remote sensing. It is hoped that more schools of agriculture will provide and encourage their students to take course work in this field. If remote sensing is to be utilized in agricultural situations, it is imperative that people be trained to work with this data.

Further, since the data-acquisition elements performed well, the Experiment provided evidence that a fully committed, high-flying aircraft can effectively acquire data at biweekly intervals for a region as large as the Corn Belt, even under the less-than-optimum Corn Belt weather conditions. The ERIM C-47 was similarly able to collect multispectral measurements over a 13,000 square-mile area in Western Indiana. A helicopter proved to be a valuable aid in acquiring field observation data. Such a system can often permit a more accurate assessment of more fields in shorter periods of time than can conventional ground methods.

Finally the Experiment resulted in significant improvements in aerial infrared film. The condition causing the "cyan spots," which hampered the analysis because of their similarity to blight, has since been corrected. This deficiency in the film was discovered by Experiment photoanalysts.

The above description and discussion was taken from Ref. [187] which is the Corn Blight Watch Experiment Final Report. More details on the CBWE are available in Refs. [61, 126, 187, and 188].

7.3.2 CITARS

Another of the multi-agency programs that ERIM is now participating in is the Crop Identification Technology Assessment for Remote Sensing (CITARS) Program. (This program was not completed before contract NAS9-9784 came to an end.) Our primary accomplishments in CITARS during the contract period covered by this final report were in helping design the program, developing and documenting a specific data processing and analysis procedure, and preparing for the machine processing, analysis, and evaluation of a large amount of ERTS multispectral scanner data. The one published report (other than monthly progress reports) which describes some processing results is Ref. [70].

We include below some excerpts from a presentation [189] describing the CITARS program.

In 1973, the Earth Observations Division (EOD) of the Johnson Space Center (JSC), the Environmental Research Institute of Michigan (ERIM), the Laboratory for the Application of Remote Sensing, Purdue University (Purdue/LARS), and the Agricultural Stabilization and Conservation Service (ASCS) of the U.S. Department of Agriculture (USDA), undertook a joint task to quantify the crop identification performance resulting from the remote identification of corn, soybeans and wheat using automatic data processing (ADP) techniques developed at ERIM, LARS, and EOD. These ADP techniques are automatic in the sense that subjective human interactions with the classification algorithms are minimized by the specification of the steps required for an analyst to convert a multispectral tape to a classification result. The crop identification performances resulting from several types of ADP techniques are to be compared and examined for significant differences. The multispectral data to be analyzed consist of ERTS-1 data acquired over each

187. Corn Blight Watch Experiment Final Report, Volumes I, II, and III, NASA, JSC, 1973-74.

188. F. Thomson, Summary of Ground Observations of Selected Corn Blight Segments in Indiana, The University of Michigan (WRL), Ann Arbor, Report 31650-105-L, 1972.

189. F. G. Hall, M. E. Bauer, W. A. Malila, First Results from the Crop Identification Technology Assessment for Remote Sensing (CITARS), 9th Symposium on Remote Sensing of Environment, 1973.

of six 5×20 mile segments in Indiana and Illinois at six periods from early June through early September 1973. Crop identification and other information was gathered by the ASCS in each segment every 18 days coincident with an ERTS overpass.

The ADP techniques are to be evaluated on this data set in two basic remote sensing situations: (1) major crop signatures for classifier training will be obtained within the same segment in which crops are recognized by the classifier (local recognition); (2) crop signatures for classifier training will be obtained from a different segment than that in which crops are recognized (nonlocal recognition).

Once the crop identification performance is established for each of the ADP techniques for local and nonlocal recognition, differences in the performances of these techniques will be established for different geographic locations, times of the year, etc.

The CITARS program was designed to quantitatively answer the following questions:

- How do corn, soybeans, and wheat identifications vary with time during the growing season?
- How does the crop identification performance (CIP) vary among different geographic locations having different soils, weather, management practices, crop distributions, and field sizes?
- Can statistics acquired from one time or location be used to identify crops at other locations and/or times?
- How much variation in CIP is observed among different data analysis techniques?
- Does use of multi-temporal data increase CIP?
- Does use of radiometric preprocessing extend the use of training statistics and/or increase CIP?
- How much variation in CIP results from varying the selection of training sets?
- Does rotation or registration of ERTS data affect classification performance?

A major task preparatory to classifying the ERTS data consisted of locating section and field coordinates in that data. This task was first attempted by LARS using a manual method for location of fields in ERTS data displayed in the form of single-band, grayscale, line printer maps [190]. This method required that field boundaries be easily distinguished in the imagery.

190. M. E. Bauer and J. E. Cipra, 1973. Identification of Agricultural Crops by Computer Processing of ERTS MSS Data, Proceedings of Symposium on Significant Results Obtained from ERTS-1, 5-9 March 1973, New Carrollton, MD, pp. 205-12; and LARS Information Note 030173.

In cases where there was minimal spectral contrast among crop fields, nonsupervised classifications have been performed to produce an enhanced image. Whether one uses grayscale or computer enhanced images, reasonably large fields are required in order to assure that pixels are selected from within the field boundaries.

With the CITARS data, there was little contrast among fields of interest, since the first data were collected early in the growing season (June 8-12). At this time of year, for instance, corn and soybeans were only a few inches tall and the spectral response was primarily from the soil. And roads were not as visible in the imagery as they generally are in data collected later in the season. Also, many fields were small (≤ 20 acres). Therefore, procedures for accurately locating fields, when individual fields could not be clearly seen in the imagery, were required to meet project requirements.

To improve the accuracy of the manual location method, ERTS images were geometrically corrected and rescaled by LARS to produce a nominal 1:24,000 scale map on a line printer. This product alone made the location of fields more precise and more rapid than it would have been in uncorrected data. Photo overlays were prepared with section and field boundaries outlined. The initial overlays, made from photography enlarged to a nominal scale of 1:24,000, were helpful though not completely satisfactory because of distortions in the photo. Following this, rectified photographs were produced at a scale of 1:24,000. This product could be manually overlaid to the line printer maps of the ERTS data.

After manually locating all field and section coordinates in the ERTS data, the precision was still not adequate to meet the requirement of a maximum error of one pixel. Therefore, a computer-assisted procedure previously developed by ERIM was employed to locate section corners and define ERTS data coordinates for sections [191]. A map transformation from Earth coordinates on a rectified aerial photograph to ERTS data coordinates was calculated for each segment, with roughly 30 control points used for each calculation. The control points were located visually in the rotated and geometrically corrected ERTS data and by coordinate digitization on the photograph. A map transformation was then computed by the method of least squares; ERTS coordinates of the few control points with large residuals (> 1 pixel) were checked and modified or deleted, as appropriate, and the transformation was recomputed. Next, the transformation was applied to all section corners of interest (whose locations on the photograph had been digitized at the same time as the control points) to find their fractional line and column

191. W. A. Malila, Information Extraction and Multi-Aspect Techniques in Remote Sensing, Doctoral Dissertation, The University of Michigan, 1974.

coordinates in the ERTS data. Final standard error estimates (for control points) were less than 0.15 and typically between 0.2 and 0.4 ERTS pixels—i.e., 15 to 30 meters on the ground. The RMS error in digitizing the location of the individual points was on the order of 3 meters on the ground (errors of roughly 0.005 inch or less on a photograph at a scale of 1:24,000).

These section corner coordinates (calculated in fractional ERTS line and column coordinates) were used to locate field boundaries of individual fields within the sections. A major advantage of the procedure is that it preserves the relative positions of all points considered with an accuracy that cannot be matched manually. Another feature of the ERIM procedure was utilized to generate ERTS data coordinates for each outlined section. All pixels whose centers fell inside lines connecting the vertices (again, located by fractional coordinates) were automatically included on coordinate definition cards.

As a result of the difficulties encountered with the field boundary selection problem, the analyses of the ERTS data and the subsequent performance comparisons, as specified by the CITARS plan, were not completed as of May 1974.

REFERENCES

1. Office of Applications Earth Resources Program Plan, NASA/JSC, Houston, December 1973.
2. D. S. Lowe, et al., Multispectral Data Collection Program, Third Symposium on Remote Sensing of Environment, The University of Michigan (WRL), Ann Arbor, October 1964.
3. M. Holter and W. Wolfe, Optical-Mechanical Scanning Techniques, Proceedings of the IRE, September 1959.
4. P. G. Hasell, et al., Michigan Experimental Multispectral Mapping System: A Description of the M7 Airborne Sensor and Its Performance, ERIM, Ann Arbor, Report 190900-10-T, January 1974.
5. M. Holter and R. Legault, Motivation for Multispectral Sensing, Third Symposium on Remote Sensing of Environment, The University of Michigan (WRL), Ann Arbor, October 1964.
6. D. S. Lowe, Line Scan Devices and Why Use Them, Fifth Symposium on Remote Sensing of Environment, The University of Michigan (WRL), Ann Arbor, April 1968.
7. R. Legault and F. Polcyn, Investigations of Multispectral Image Interpretation, Third Symposium on Remote Sensing of Environment, The University of Michigan (WRL), Ann Arbor, October 1964.
8. D. S. Lowe, An Investigative Study of a Spectrum-Matching Imaging System, The University of Michigan (WRL), Ann Arbor, Report 8201-1-F, October 1966.
9. F. Kriegler and M. Spencer, A Statistical Spectral Analysis and Target Recognition Computer (SPARC), The University of Michigan (WRL), Ann Arbor, Report 8640-17-F, September 1968.
10. F. Kriegler and M. Spencer, SPARC, A Special Computer for Target Recognition in Real Time by Statistical Spectral Analysis of Multichannel Scanner Data, Proc. IRIS, Vol. 14, No. 2, August 1970, p. 413 for paper given at 16th National IRIS, May, 1968.
11. F. Kriegler, et al., MIDAS: Prototype Multivariate Interactive Digital Analysis System — Phase I, NASA CR-132463, ERIM, Ann Arbor, Report 195800-25-F (in 3 vols.), August 1974.
12. R. Nalepka, et al., Investigation of Multispectral Discrimination Techniques, The University of Michigan (WRL), Ann Arbor, Report 2264-12-F, January 1970.
13. J. Erickson and F. Thomson, Investigations Related to Multispectral Imaging Systems for Earth Resource Surveys, The University of Michigan (WRL), Ann Arbor, Interim Report 31650-17-P, September 1971.
14. J. Erickson, Automatic Extraction of Information from Multispectral Scanner Data, International Archives of Photogrammetry, Vol. 17, August 1972, (ISP Invited Paper).
15. V. Leeman, D. Earing, R. K. Vincent, S. Ladd, The NASA Earth Resources Spectral Information System: A Data Compilation, The University of Michigan (WRL), Ann Arbor, Report No. 31650-24-T, May 1971.
16. D. L. Earing and V. W. Leeman, NASA/MSC Earth Resources Spectral Information System Procedures Manual, The University of Michigan (WRL), Ann Arbor, Report 31650-32-T, 1971.

17. V. Leeman, R. Vincent, and S. Ladd, The NASA Earth Resources Spectral Information System: A Data Compilation, First Supplement, The University of Michigan (WRL), Ann Arbor, Report 31650-69-T, 1972.
18. V. Leeman, NASA/MSU Earth Resources Spectral Information System Procedures Manual, Supplement, The University of Michigan (WRL), Ann Arbor, Report No. 31650-72-T, September 1971.
19. R. Vincent, The NASA Earth Resources Spectral Information System: A Data Compilation, Second Supplement, ERIM, Ann Arbor, Report 31650-156-T, January 1973.
20. R. K. Vincent, Data Gaps in the NASA Earth Resources Spectral Information System, The University of Michigan (WRL), Ann Arbor, Report 31650-25-T, March 1971.
21. D. Bornemeier, R. Bennett, and R. Horvath, Target Temperature Modeling, RADC-TR-69-404, Rome Air Development Center, Air Force Systems Command, Griffiss Air Force Base, NY, under Air Force Contract F30602-68-C-0099, December 1969.
22. R. Vincent, R. Horvath, F. Thomson, and E. A. Work, Remote Sensing Data Analysis Projects Associated with the NASA Earth Resources Spectral Information System, The University of Michigan (WRL), Ann Arbor, Report 31650-26-T, April 1971.
23. R. Horvath and D. D. Bornemeier, Infrared and Photo Record Analysis, Vol. I: A Mathematical Predictive Model for Target Temperature as a Function of Environment, Report RADC-TR-66-117, Rome Air Development Center, Griffiss Air Force Base, NY, April 1967.
24. A. E. Coker, R. Marshall and N. S. Thomson, Application of Computer Processed Data to the Discrimination of Land Collapse (Sinkhole) Prone Areas in Florida, Proc. 6th Symposium on Remote Sensing of Environment, Ann Arbor, October 1969, Vol. I, pp. 65-77.
25. M. S. Kersten, Laboratory Research for the Determination of the Thermal Properties of Soils, Engineering Experiment Station, University of Minnesota, Minneapolis, 1949.
26. W. R. VanWijk, Physics of Plant Environment, North Holland Publishing Co., Amsterdam, 1963.
27. R. Geiger, The Climate Near the Ground, Harvard University Press, Cambridge, 1965.
28. R. J. P. Lyon, Evaluation of IR Spectrophotometry for Compositional Analysis of Lunar and Planetary Soils: Rough and Powdered Surfaces, Final Report, Part II, NASA Contract NASr-49(04), Stanford Research Institute, Menlo Park, 1964.
29. R. K. Vincent and G. R. Hunt, Infrared Reflectance from Mat Surfaces, Applied Optics, Vol. 7, p. 53, 1968.
30. J. E. Conel, Infrared Emissivities of Silicates: Experimental Results and a Cloudy Atmosphere Model of Spectral Emission from Condensed Particulate Mediums, J. Geophys. Res., Vol. 74, p. 1614, 1969.
31. R. K. Vincent, New Theoretical Methods in Ratio Imaging Techniques Associated with the NASA Earth Resources Spectral Information Systems, ERIM, Ann Arbor, Report 190100-30-T, 1973.

32. G. H. Suits, R. K. Vincent, H. M. Horwitz, and J. D. Erickson, Optical Modeling of Agricultural Fields and Rough-Textured Rock and Mineral Surfaces, ERIM, Ann Arbor, Report 31650-78-T, 1973.
33. G. H. Suits, Prediction of Directional Reflectance of a Corn Field Under Stress, Presented at 4th Annual Earth Resources Program Review, NASA/MSC, Houston, The University of Michigan (WRL), Ann Arbor, Report 31650-95-S, January 1972.
34. G. H. Suits, The Calculation of the Directional Reflectance of a Vegetative Canopy, Remote Sensing of Environment, 2, pp. 117-25, 1972.
35. G. H. Suits and G. R. Safir, Verification of a Reflectance Model for Mature Corn with Applications to Corn Blight Detection, Remote Sensing of Environment, 2, pp. 183-92, 1972.
36. G. H. Suits, The Cause of Azimuthal Variations in Directional Reflectance of Vegetative Canopies, Remote Sensing of Environment, 2, pp. 175-82, 1972.
37. G. R. Safir, G. H. Suits, and M. V. Wiese, Application of a Directional Reflectance Model to Wheat Canopies Under Stress, International Conference on Remote Sensing in Arid Lands, Tucson, November 9, 1972.
38. W. A. Allen, T. V. Gayle, and A. J. Richardson, Plant-Canopy Irradiance Specified by the Duntley Equations, J. of the Optical Soc. of Amer., 60, 372, 1970.
39. L. Elterman, Vertical-Attenuation Model with Eight Surface Meteorological Ranges 2 to 13 Kilometers, AFCRL-70-0200, Air Force Cambridge Research Laboratories, Bedford, Mass., 1970.
40. D. Deirmendjian, Electromagnetic Scattering on Spherical Polydispersions, American Elsevier Publishing Co., Inc., New York, NY, 1969.
41. A. I. Ivanov, Spectral Brightness of the Sky, Atmospheric Optics, N. B. Divari, ed., Consultants Bureau, New York, NY, 1970.
42. R. Horvath, M. Spencer, and R. Turner, Atmospheric Correction and Simulation of Space-Acquired Remote Sensor Data: 0.4 to 1.0 μm Spectral Range, The University of Michigan (WRL), Ann Arbor, Report 10657-5-F.
43. D. Anding, R. Kauth, and R. Turner, Atmospheric Effects on Infrared Multi-spectral Sensing of Sea-Surface Temperature from Space, The University of Michigan (WRL), Ann Arbor, Report 2676-6-F.
44. R. Turner, Simulation Analysis of Systematic Effects of Multispectral Scanner Data, Presented at a Review Meeting for Atmospheric Studies in the NASA SR&T Work, Houston, January 21, 1972, The University of Michigan (WRL), Ann Arbor, Report 31650-108-S.
45. W. A. Malila, R. B. Crane, C. A. Omarzu, and R. E. Turner, Studies of Spectral Discrimination, The University of Michigan (WRL), Ann Arbor, Report 31650-22-T, May 1971.
46. R. Turner, W. Malila, and R. Nalepka, Importance of Atmospheric Scattering in Remote Sensing, or Everything You've Always Wanted to Know About Atmospheric Scattering But Been Afraid to Ask, Seventh International Symposium on Remote Sensing of Environment, Ann Arbor, June 1971.
47. W. Malila, R. Crane, and R. Turner, Information Extraction Techniques, The University of Michigan (WRL), Ann Arbor, Report 31650-74-T, June 1972.

48. W. A. Malila, R. B. Crane, W. Richardson, and R. E. Turner, Information Extraction Techniques for Multispectral Scanner Data, presented at 4th Annual Earth Resources Program Review, NASA/MSC, Houston, January 17, 1972, and published in Proceedings.
49. R. Turner, Remote Sensing in Hazy Atmosphere, presented to the ACSM/ASP Convention in Washington, March 1972, published in the Journal of Photogrammetric Engineering and in ACSM/ASP Proceedings.
50. R. E. Turner, Atmospheric Effects in Remote Sensing, presented at Second Conference on Earth Resources Observation and Information Analysis System, University of Tennessee Space Institute, Tullahoma, March 1972, and published in Proceedings.
51. Robert E. Turner and Margaret M. Spencer, Atmospheric Model for Correction of Spacecraft Data, Eighth International Symposium on Remote Sensing of Environment, October 1972, The University of Michigan (WRL), Ann Arbor, and published in Proceedings.
52. R. Sharma, Enhancement of Earth Resources Technology Satellite (ERTS) and Aircraft Imagery Using Atmospheric Corrections, Eighth International Symposium of Remote Sensing of Environment, Ann Arbor, October 1972.
53. R. Turner, Radiative Transfer in Real Atmospheres, July 1974, ERIM, Ann Arbor, Report 190100-24-T.
54. R. E. Turner, Contaminated Atmospheres and Remote Sensing, Third Annual Remote Sensing of Earth Resources Conference, University of Tennessee Space Institute, Tullahoma, March 1974.
55. R. Nalepka, H. M. Horwitz, and N. S. Thomson, Investigations of Multispectral Sensing of Crops, The University of Michigan (WRL), Ann Arbor, Report 31650-30-T, May 1971.
56. W. A. Malila, R. Hieber, and J. Sarno, Analysis of Multispectral Signatures and Investigation of Multi-Aspect Remote Sensing Techniques, ERIM, Ann Arbor, Report 190100-27-T, July 1974.
57. R. B. Crane, W. A. Malila, and W. Richardson, Suitability of the Normal Density Assumption for Processing Multispectral Scanner Data, IEEE Transactions on Geoscience Electronics, Vol. GE-10, No. 4, pp. 158-65, October 1972.
58. L. Larsen, Detector Utilization in Line Scanners, The University of Michigan (WRL), Ann Arbor, Report 31650-29-T, August 1971.
59. S. Stewart, D. Christenson, and L. Larsen, Systematic Monitoring of M-7 Scanner Performance and Data Quality, ERIM, Ann Arbor, Report 190100-23-T, July 1974.
60. J. D. Erickson, A Summary of Michigan Program for Earth Resources Information Systems, presented at the 4th Annual Earth Resources Program Review, NASA/MSC, Houston, January 17, 1972, and published in Proceedings.
61. R. F. Nalepka, J. P. Morgenstern, and W. L. Brown, Detailed Interpretation and Analysis of Selected Corn Blight Watch Data Sets, presented at the 4th Annual Earth Resources Program Review, NASA/MSC, Houston, January 17, 1972 and published in Proceedings.

62. H. M. Horwitz, R. F. Nalepka, P. D. Hyde, and J. P. Morgenstern, Estimating the Proportions of Objects Within a Single Resolution Element of a Multispectral Scanner, 7th International Symposium on Remote Sensing of Environment, June 1971.
63. R. Nalepka, H. M. Horwitz, and P. D. Hyde, Estimating Proportions of Objects from Multispectral Data, The University of Michigan (WRL), Ann Arbor, Report 31650-73-T, March 1972.
64. R. F. Nalepka, H. M. Horwitz, P. D. Hyde, and J. P. Morgenstern, Classification of Spatially Unresolved Objects, presented at the 4th Annual Earth Resources Program Review, NASA/MSC, Houston, January 17, 1972, and published in Proceedings.
65. R. B. Crane and P. Hyde, Signature Estimation from Satellite Multispectral Scanner Data, presented at the Second Conference on Earth Resources Observation and Information Analysis System, University of Tennessee Space Institute, Tullahoma, Tenn., March 1973; appeared in Proceedings.
66. R. F. Nalepka and P. D. Hyde, Classifying Unresolved Objects from Simulated Space Data, 8th International Symposium on Remote Sensing of Environment, Ann Arbor, October 1972.
67. R. Nalepka and P. Hyde, Estimating Crop Acreage from Space-Simulated Multispectral Scanner Data, ERIM, Ann Arbor, Report 31650-148-T, January 1973.
68. W. Richardson and H. Horwitz, A Faster Algorithm for Estimating Proportions, LARS Conference on Machine Processing of Remotely Sensed Data, Purdue University, October 1973.
69. H. Horwitz and P. Hyde, Estimating Proportions of Unresolved Objects from Multispectral Data, 1973 International Symposium on Pattern Recognition, IEEE, Pattern Recognition Society, Am. Soc. of Photogrammetry, Washington, October-November 1973.
70. W. Malila, R. Hieber, D. Rice, J. Sarno, Wheat Classification Exercise Using June 11, 1973, ERTS MSS Data for Fayette County, Illinois, ERIM, Ann Arbor, Report 190100-21-R, September 1973.
71. H. Horwitz, P. Hyde, W. Richardson, Improvements in Estimating Proportions of Objects from Multispectral Data, ERIM, Ann Arbor, Report 190100-25-T, April 1974.
72. W. A. Malila and R. F. Nalepka, Atmospheric Effects in ERTS-1 Data and Advanced Information Extraction Techniques, Symposium on Significant Results Obtained from the Earth Resources Technology Satellite-1, Vol. 1, Goddard Space Flight Center, Greenbelt, MD, 1973.
73. F. J. Thomson, Crop Species Recognition and Mensuration in the Sacramento Valley, Symposium on Significant Results Obtained from the Earth Resources Technology Satellite-1, Vol. 1, Goddard Space Flight Center, Greenbelt, MD, 1973.
74. M. Spencer, J. Wolf, and M. Schall, SICLOPS: A System of Computer Programs for Rectified Mapping of Airborne Scanner Imagery, 9th Symposium on Remote Sensing of Environment, Ann Arbor, April 1974.
75. M. Spencer, J. Wolf, and M. Schall, A System to Geometrically Rectify and Map Airborne Scanner Imagery and to Estimate Ground Area, ERIM, Ann Arbor, Report 190100-28-T, May 1974.
76. R. J. Kauth, R. B. Crane, and W. Richardson, Feasibility Demonstration of Processing ERTS Data for Global Terrain Clutter Mapping, ERIM, Ann Arbor, Report 106600-1-L, January 1974.

77. W. Richardson, A Study of Some Nine-Element Decision Rules, ERIM, Ann Arbor, Report 190100-32-T, July 1974.
78. R. K. Vincent and F. J. Thomson, Discrimination of Basic Silicate Rocks by Recognition Maps Processed from Aerial Infrared Data, 7th International Symposium on Remote Sensing of Environment, Ann Arbor, June 1971.
79. F. Thomson, Processing of Pisgah Crater Thermal and Multispectral Data, The University of Michigan (WRL), Ann Arbor, Report 3165-64-T, July 22, 1971.
80. R. Vincent, Rock-Type Discrimination Ratio Images of the Pisgah Crater, California Test Site, The University of Michigan (WRL), Ann Arbor, Report 31650-77-T, June 1972.
81. R. Vincent, F. Thomson, Rock-Type Discrimination from Ratioed IR Scanner Images of Pisgah Crater, California, SCIENCE, March 1972.
82. R. K. Vincent, Experimental Methods for Geological Remote Sensing, presented at the 4th Annual Earth Resources Program Review, NASA/MSC, Houston, January 17, 1972, and published in Proceedings.
83. R. Vincent, F. Thomson, Spectral Compositional Imaging of Silicate Rocks, Journal of Geophysical Research, vol. 77, 14, pp. 2465-72, May 1972.
84. R. Vincent, F. Thomson, K. Watson, Recognition of Exposed Quartz Sand & Sandstone by Two-Channel Infrared Imagery, Journal of Geophysical Research, vol. 77, 14, pp. 2473-77, May 1972.
85. R. Vincent, An Emission Polarization Study on Quartz and Calcite, Submitted to Applied Optics, September 1972.
86. R. K. Vincent, An ERTS Multispectral Scanner Experiment for Mapping Iron Compounds, 8th International Symposium on Remote Sensing of Environment, Ann Arbor, October, 1972.
87. R. Vincent, Spectral Ratio Imaging Methods for Geologic Remote Sensing from Aircraft and Satellites, Management and Utilization of Remote Sensing, Data Conference, 29 October—1 November 1973.
88. R. K. Vincent, Infrared Recognition Maps of Silicate Rock Types—A New Tool for Mineralogical Exploration, 1971 Annual Meeting of the Geological Society of America, Washington, p. 739, 1971.
89. L. Rowan and R. K. Vincent, Discrimination of Iron-Rich Zones Using Visible and Near-Infrared Spectral Analysis, in Abstracts of 1971 Annual Meeting of the Geological Society of America, Washington, p. 691, 1971.
90. R. K. Vincent and F. Thomson, Spectral Compositional Imaging of Silicate Rocks, Journal of Geophysical Research, v. 77, pp. 2465-71, 1972.
91. R. K. Vincent, Ratio Maps of Iron Ore Deposits, Atlantic City District, Wyoming, Symposium on Significant Results Obtained from the Earth Resources Technology Satellite-1, vol. 1, pp. 379-86, 1973.
92. R. K. Vincent, Ratio Techniques for Geochemical Remote Sensing, Proceedings of the Fourth Annual Conference on Remote Sensing in Arid Lands, Tucson, AZ, November 1973, (to be published in 1974).
93. R. K. Vincent, A Thermal Infrared Ratio Imaging Method for Mapping Compositional Variations Among Silicate Rock Types, Ph.D. Dissertation, Department of Geology and Mineralogy, The University of Michigan (WRL), Ann Arbor, 1973.

94. B. Salmon and R. K. Vincent, Surface Compositional Mapping in the Wind River Range and Basin, Wyoming by Multispectral Techniques Applied to ERTS-1 Data, Proceedings of Ninth Symposium on Remote Sensing of Environment, Ann Arbor, 1974 (In Press).
95. R. Dillman and R. K. Vincent, Unsupervised Mapping of Geologic Features and Soils in California, Proceedings of the Ninth Symposium on Remote Sensing of Environment, Ann Arbor, 1974 (In Press).
96. R. K. Vincent and W. W. Pillars, Skylab S-192 Ratio Codes of Soil, Mineral, and Rock Spectra for Ratio Image Selection and Interpretation, Proceedings of the Ninth Symposium on Remote Sensing of Environment, Ann Arbor, 1974 (In Press).
97. T. Wagner, R. K. Vincent, B. Drake, R. Mitchell, and P. Jackson, Tunnel-Site Selection by Remote Sensing Techniques, The University of Michigan (WRL), Ann Arbor, Technical Report 10018-13-F, U.S. Bureau of Mines Contract H0210041 (ARPA Order No. 1579, Amendment 2, Program Code IF10), 1972.
98. R. K. Vincent, T. Wagner, B. Drake and P. Jackson, Geologic Reconnaissance and Lithologic Identification by Remote Sensing, ERIM, Ann Arbor, Technical Report 191700-8-F, ARPA-USBM Contract No. H022064, 1973.
99. P. G. Hasell, Jr., et al., Investigation of Multispectral Techniques for Remotely Identifying Terrain Features and Natural Materials, ERIM, Ann Arbor, Report 196200-12-F, May 1974.
100. T. W. Wagner and P. G. Hasell, Jr., Remote Identification of Terrain Features and Materials at Kansas Test Sites: An Investigative Study of Techniques, Federal Highway Administration, Washington, Report FHWA-RD-73-53, 1973.
101. F. G. Sadowski, T. W. Wagner, F. J. Thomson, and P. G. Hasell, Jr., The Remote Identification of Terrain Features and Materials at Pennsylvania Test Sites: An Investigative Study of Techniques, Federal Highway Administration, Washington, Report FHWA-RD-74-9, 1974.
102. T. W. Wagner and P. G. Hasell, Jr., The Remote Identification of Terrain Features and Materials of Virginia Test Sites: An Investigative Study of Techniques, Federal Highway Administration, Report FHWA-RD-74-10, Washington, 1974.
103. R. K. Vincent, R. D. Dillman, and P. G. Hasell, Jr., The Remote Identification of Terrain Features and Materials at a California Test Site: An Investigative Study of Techniques, Federal Highway Administration, Washington, Report FHWA-RD-74-27, 1974.
104. Remote Sensing in Michigan for Land Resource Management: Highway Impact Assessment, Report 190800-1-T, Infrared and Optics Division of The University of Michigan (WRL), Ann Arbor, Michigan State University, and Michigan Department of State Highways, 1972.
105. P. G. Hasell, et al., Investigations of Spectrum-Matching Techniques for Remote Sensing in Agriculture, Report for March-December 1967, The University of Michigan (WRL), Ann Arbor, Report 8725-13-P.
106. R. Crane, W. Richardson, Rapid Processing of Multispectral Scanner Data Using Linear Techniques, in Remote Sensing of Earth Resources, Vol I, containing selected papers from Earth Resources Observation and Information Analysis Systems Conference (13-14 March 1972), May 1972.

107. R. B. Crane, W. Richardson, Performance Evaluation of Multispectral Scanner Classification Methods, 8th International Symposium on Remote Sensing of Environment, Ann Arbor, October 1972.
108. R. B. Crane, Linear Combinations, Quarterly Supporting Research and Technology Review, JSC, Houston, 26 September 1972, and The University of Michigan (WRL), Ann Arbor, Report 31650-147-L, October 1972.
109. R. Crane, W. Richardson, R. Hieber, and W. Malila, A Study of Techniques for Processing Multispectral Scanner Data, ERIM, Ann Arbor, Report 31650-155-T, January 1973.
110. R. B. Crane, Feature Extraction of Multispectral Data, presented at LARS Conference on Machine Processing of Remotely Sensed Data, Purdue University, October, 1973.
111. R. Crane and P. Hyde, Adaptive Processing Using a Decision Directed Kalman Filter and Feature Extraction of Multispectral Scanner Data, The University of Michigan (WRL), Ann Arbor, Report 190100-31-T, July 1974.
112. R. B. Crane, T. Crimmins, J. Reyer, and R. Kauth, Feature Extraction of Multispectral Data, IEEE Transactions on Geoscience Electronics, 1973.
113. W. S. Hsia and J. P. deFigueiredo, Optimal Feature Extraction—The Two-Class Case, ICSA-275-025-010, Rice University, Houston, May 1973.
114. D. J. Jegewski, Optimal Feature Extraction by a Linear Transformation, Revision 1, MSC Internal Note No. 73-FM-19, March 1973.
115. J. A. Quirein, An Interactive Approach to the Feature Selection Classification Problem, TRW Systems Technical Note 99900-H019-RO-00, Houston, December 1972.
116. T. W. Anderson and R. R. Bahadur, Classification into Two Multivariate Normal Distributions with Different Covariance Matrices, Annals of Mathematical Statistics, Vol. 33, 1962, p. 420.
117. G. Nagy, and G. Shelton, J. Tolaba, Procedural Questions in Signature Analysis, published in Proceedings of the Seventh International Symposium on Remote Sensing of Environment, Ann Arbor, May 1971.
118. G. Nagy and J. Tolaba, Nonsupervised Crop Classifications Through Airborne Multispectral Observations, IBM Journal of Research and Development, v. 16, No. 2, March 1972, pp. 138-53.
119. Dennis A. Johnston, Statistical Consideration in an Interactive Graphics Pattern Recognition System, NASA-MSC Internal Note 72-FD-019, September 1972.
120. M. M. Su, An Unsupervised Classification Technique for Multispectral Remote Sensing Data, Proceedings of the 8th International Symposium on Remote Sensing of Environment, Ann Arbor, October 1972.
121. F. J. Kriegler, Implicit Determination of Multispectral Scanner Data Variation over Extended Areas, presented at 7th International Symposium on Remote Sensing of Environment, Ann Arbor, June 1971.
122. R. B. Crane, Preprocessing Techniques to Reduce Atmospheric and Sensor Variability in Multispectral Scanner Data, 7th International Symposium on Remote Sensing of Environment, Ann Arbor, June 1971.

123. H. Smedes, M. Spencer, F. Thomson, Preprocessing of Multispectral Data and Simulation of ERTS Data Channels to Make Computer Terrain Maps of a Yellowstone National Test Site, 7th International Symposium on Remote Sensing of Environment, Ann Arbor, June 1971.
124. M. Spencer, F. Thomson, Experimental Study on Preprocessing of Multispectral Data of a Yellowstone National Park Site, The University of Michigan (WRL), Ann Arbor, Report 31650-79-L, September 1970.
125. R. Nalepka, The Application of Data Preprocessing and Signature Extension Techniques to Multispectral Scanner Data, December 1971, The University of Michigan (WRL), Ann Arbor, Report 31650-9-S.
126. F. J. Thomson and R. F. Nalepka, Contribution to the Corn Blight Watch, Final Report, January 1972.
127. R. F. Nalepka, J. P. Morgenstern, Signature Extension Techniques Applied to Multispectral Scanner Data, 8th International Symposium on Remote Sensing, The University of Michigan (WRL), Ann Arbor, October 1972.
128. R. S. Driscoll, and M. M. Spencer, Multispectral Scanner Imagery for Plant Community Classification, 8th International Symposium on Remote Sensing of Environment, The University of Michigan (WRL), Ann Arbor, October 1972.
129. R. Nalepka and J. Morgenstern, Signature Extension: An Approach to Operational Multispectral Surveys, ERIM, Ann Arbor, Report 31650-152-T, February 1973.
130. R. K. Vincent, G. Thomas, and R. Nalepka, Signature Extension Studies ERIM, Ann Arbor, Report 190100-26-T, July 1974.
131. R. E. Marshall, F. J. Kriegler, W. Richardson, Adaptive Multispectral Recognition of Wheat, presented at the 1971 IEEE Decision and Control Conference, Miami, 15-17 December 1971.
132. R. E. Marshall, F. J. Kriegler, W. Richardson, Adaptive Multispectral Recognition of Wheat Fields, presented at the EAI Symposium on Automatic Photointerpretation, Washington, 7-8 December 1971.
133. H. W. Sorenson, Talman Filtering Techniques, in Advances in Control Systems, Vol 3, C.T. Leondes, ed., Academic Press, 1966.
134. Frank J. Kriegler, Adaptive Multispectral Recognition of Agricultural Crops, 8th International Symposium on Remote Sensing of Environment, The University of Michigan (WRL), Ann Arbor, October 1972; appeared in Proceedings.
135. F. J. Kriegler, H. Horwitz, Investigations of Adaptive Processing of Multispectral Data, ERIM, Ann Arbor, Report 31650-151-T, January 1973.
136. R. B. Crane, A Kalman Filter Approach to Adaptive Estimation of Multispectral Signatures, presented at 12th Symposium on Adaptive Processes, San Diego, December 1973.
137. R. Crane, Adaptive Processing of Multispectral Scanner Data Using a Decision Directed Kalman Filter, 9th Symposium on Remote Sensing of Environment, Ann Arbor, April 1974.
138. F. J. Kriegler and R. E. Marshall, A Prototype Hybrid Multispectral Processor (SPARC/H) with High Throughput Capability, The University of Michigan, (WRL), Ann Arbor, Report 31650-23-T, March 1971.

139. R. E. Marshall and F. J. Kriegler, Study of a Hybrid Multispectral Processor, ERIM, Ann Arbor, Report 31650-154-T, January 1973.
140. R. E. Marshall and F. J. Kriegler, Data Display Requirements for a Multispectral Scanner Processor with High Throughput Capability, The University of Michigan (WRL), Ann Arbor, Report 31650-28-L, July 1971.
141. F. J. Kriegler, and R. Marshall, An Operational Multispectral Survey System, 7th International Symposium on Remote Sensing of Environment, The University of Michigan (WRL), Ann Arbor, June 1971.
142. F. Kriegler, Extension of ERIM Multispectral Data Processing Capabilities Through Improved Data Handling Techniques, ERIM, Ann Arbor, Report 31650-158-T, January, 1973.
143. William D. Sellers, Physical Climatology, University of Chicago Press, 1965.
144. David M. Gates, Energy, Plants, and Ecology, Ecology, Vol. 46, Nos. 1 and 2, 1965.
145. W. Malila, Discrimination Techniques Employing Both Reflective and Thermal Multispectral Signals, ERIM, Ann Arbor, Report 31650-75-T, January 1973.
146. W. A. Malila, Radiation Balance Mapping with Multispectral Scanner Data Remote Sensing of Earth Resources, in Vol. I —Selected Papers from Earth Resources Observation and Information Analysis Systems Conference (13-14 March 1972), May 1972.
147. W. Malila and T. Wagner, Multispectral Remote Sensing of Elements of Water and Radiation Balances, presented at 8th International Symposium on Remote Sensing of Environment, The University of Michigan (WRL), Ann Arbor, October 1972; appeared in Proceedings.
148. Breakers and Surf, Principles in Forecasting, U.S. Naval Oceanographic Office, H. O. Publication No. 234, 1958.
149. J. W. Johnson, et al., Graphic Construction of Wave Refraction Diagrams, U.S. Naval Oceanographic Office, H. O. Publication No. 605, January 1948.
150. F. C. Polcyn, W. Brown, and I. Sattinger, The Measurement of Water Depth by Remote Sensing Techniques (Final Report), The University of Michigan (WRL), Ann Arbor, Report 8973-26-F, November 1970.
151. N. F. Barber, A Diffraction Analysis of a Photograph of the Sea, Nature, Vol. 164, p. 485, 1949.
152. C. Cox and W. H. Munk, Statistics of the Sea Surface Derived from Sun Glitter, J. Marine Res., Vol. 13, No. 2, pp. 198-227, 1954.
153. F. C. Polcyn, and R. A. Rollin, Remote Sensing Techniques for the Location and Measurement of Shallow-Water Features, The University of Michigan (WRL), Ann Arbor, Report 8973-10-P, January 1969.
154. W. L. Brown, F. C. Polcyn, A. N. Sellman, and S. R. Stewart, Water-Depth Measurement by Wave Refraction and Multispectral Techniques, The University of Michigan (WRL), Ann Arbor, Report 31650-31-T, August 1971.
155. F. C. Polcyn and D. R. Lyzenga, Calculations of Water Depth from ERTS-MSS Data presented at the 5-9 March 1973 ERTS-1 Symposium on Significant Results, New Carrollton, Maryland, and published in the Proceedings of that Symposium.

156. M. Bair, Reconnaissance in Support of Amphibious Operations: Bathymetry and Land Trafficability, ERIM, Ann Arbor, Report 194600-25-T, June 1974.
157. D. R. Lyzenga and F. C. Polcyn, Remote Bathymetry and Shoal Detection with ERTS, ERIM, Ann Arbor, Report 193300-51-F (In Press).
158. W. Malila, Multi-Aspect Techniques in Remote Sensing, 9th Symposium on Remote Sensing of Environment, Ann Arbor, April 1974.
159. V. I. Meyers, et al., Remote Sensing, National Academy of Sciences, Washington, p. 253, 1970.
160. W. A. Malila, R. H. Hieber and A. P. McCleer, 1973. Correlation of ERTS MSS Data and Earth Coordinate Systems, Proceedings of Conference on Machine Processing of Remotely Sensed Data, Purdue University, W. Lafayette, 16-18 October 1973.
161. A. E. Coker, R. Marshall, and F. Thomson, Discrimination of Fluoride and Phosphate Contamination in Central Florida for Analysis of Environmental Effects, 4th Annual Earth Resource Program Review, Section 79, January 1972.
162. J. Braithwaite, L. Larsen, and E. Work, Further Infrared Systems Studies for the Earth Resources Program, Report No. NASA CR-WRL 2122-14-F, The University of Michigan (WRL), Ann Arbor, December 1969.
163. J. Braithwaite and E. Work, Optical Transfer Techniques for Orbital Scanners, The University of Michigan (WRL), Ann Arbor, Report 31650-21-T, March 1971.
164. J. Braithwaite, Calibration of Multispectral Scanners, The University of Michigan (WRL), Ann Arbor, Report 31650-27-L, September 1970.
165. D. Zuk and M. Gordon, Ground Measurements in Support of a Multispectral Data System Evaluation Flight, The University of Michigan (WRL), Ann Arbor, Informal Technical Report 31650-113-T, March 1972.
166. L. Larsen and P. Lambeck, Performance of MSDS as of 18 August 1971, The University of Michigan (WRL), Ann Arbor, Report 31650-82-T, September 1971.
167. P. F. Lambeck, Engineering Evaluation of 24-Channel Multispectral Scanner, The University of Michigan (WRL), Ann Arbor, Report 10822-1-T.
168. F. Thomson, Contouring of Chesapeake Bay Oil Slick Data, The University of Michigan (WRL), Ann Arbor, Report 3165-52-L, July 1, 1971.
169. N. Thomson, Multispectral Analysis of Terrain Types in the Chesapeake Bay Region, The University of Michigan (WRL), Ann Arbor, Report 3165-53-L, July 15, 1971.
170. F. Thomson, Thermal Contouring of Manitou, Colorado Data—July 1971, The University of Michigan (WRL), Ann Arbor, Report 3165-63-T, July 22, 1971.
171. J. Livisay, F. Thomson, Classification of Simulated ERTS-A Data for Underwater Feature Recognition in Bisque Bay, 1971, The University of Michigan (WRL), Ann Arbor, Report 3165-68-L, August 9, 1971.
172. F. Thomson, User-Oriented Multispectral Data Processing at The University of Michigan, presented at the 4th Annual Earth Resources Program Review, NASA/MSC, Houston, 17 January 1972, and published in Proceedings.

173. F. Weber, R. Aldrich, F. Sadowski, and F. Thomson, Land Use Classification in the Southeastern Forest Region by Multispectral Scanning and Computerized Mapping, 8th International Symposium on Remote Sensing of Environment, Ann Arbor, October 1972.
174. F. Thomson, H. Smedes, W. Hendrickson, ERTS-A Terrain Feature Maps of Yellowstone National Park, The University of Michigan (WRL), Ann Arbor, May 1972.
175. F. J. Thomson, Processing of Oregon Coast Oceanographic Data, The University of Michigan (WRL), Ann Arbor, Report 31650-137-L, August 1972.
176. R. Dillman and F. Thomson, Radiance Determination for Panels and Areas of Line 2 for Weslaco, Texas, 27 Feb 1971, The University of Michigan (WRL), Ann Arbor, Report 31650-138-L, July 1972.
177. R. Dillman and F. Thomson, Weslaco Soils Report, February 27, 1971, The University of Michigan (WRL), Ann Arbor, Report 31650-143-L, September 1972.
178. W. G. Burge and W. L. Brown, A Study of Waterfowl Habitat in North Dakota: Additional Data Reduction Techniques Developed to Analyze Waterfowl Habitat, The University of Michigan (WRL), Ann Arbor, November 1970.
179. N. Thomson, and F. Thomson, Thermal Contouring of Biscayne Bay Data, The University of Michigan (WRL), Ann Arbor, Letter Report.
180. F. Thomson, Thermal Contouring of Bucks Lake Data, The University of Michigan (WRL), Ann Arbor, February 1971.
181. F. Thomson, Determination of Optimum Spectrometer Channels for Bucks Lake Classification, The University of Michigan (WRL), Ann Arbor, Letter Report, November 1970.
182. W. Rohde, F. Thomson, Analog and Digital Processing of Bucks Lake Data, The University of Michigan (WRL), Ann Arbor, Letter Report, April 1971.
183. W. Burge, V. Prentice, F. Thomson, Multispectral Data Processing of Moses Lake, Washington Data, The University of Michigan (WRL), Ann Arbor, Letter Report, 1970.
184. F. Thomson, Processing and Analysis of Yellowstone Thermal Data, The University of Michigan (WRL), Ann Arbor, Letter Report, February 1970.
185. W. G. Rohde, Processing and Analysis of Black Hills Thermal Contouring, The University of Michigan (WRL), Ann Arbor, Letter Report.
186. F. J. Thomson, SPARC Preprocessing and Processing of Yellowstone Data, The University of Michigan (WRL), Ann Arbor, Letter Report, March 1971.
187. Corn Blight Watch Experiment Final Report, Volumes I, II, and III, NASA/JSC, Houston, 1973-74.
188. F. Thomson, Summary of Ground Observations of Selected Corn Blight Segments in Indiana, The University of Michigan (WRL), Ann Arbor, Report 31650-105-L, 1972.
189. F. G. Hall, M. E. Bauer, W. A. Malila, First Results from the Crop Identification Technology Assessment for Remote Sensing (CITARS), 9th Symposium on Remote Sensing of Environment, Ann Arbor, 1973.

190. M. E. Bauer and J. E. Cipra, 1973. Identification of Agricultural Crops by Computer Processing of ERTS MSS Data, Proceedings of Symposium on Significant Results Obtained from ERTS-1, 5-9 March 1973, New Carrollton, MD, pp. 205-12; and LARS Information Note 030173.
191. W. A. Malila, Information Extraction and Multi-Aspect Techniques in Remote Sensing, Doctoral Dissertation, The University of Michigan, 1974.

Appendix I

ERIM PROFESSIONAL STAFF CONTRIBUTORS TO NAS9-9784

J. Braithwaite	D. Lowe
W. Brown	W. Malila
W. Burge	R. Marshall
D. Christenson	J. Morgenstern
J. Colwell	R. Nalepka
R. Crane	F. Polcyn
T. Crimmins	V. Prentice
R. Dillman	J. Reyer
E. Earing	D. Rice
J. Erickson	W. Richardson
M. Gordon	W. Rohde
P. Hasell	F. Sadowski
R. Hieber	J. Sarno
R. Horvath	M. Schall
H. Horwitz	A. Sellman
P. Hyde	J. Snell
E. Jebe	M. Spencer
R. Kauth	S. Stewart
J. King	G. Suits
R. Kistler	G. Thomas
F. Kriegler	F. Thomson
S. Ladd	N. Thomson
P. Lambeck	R. Turner
L. Larsen	R. Vincent
V. Leeman	J. Wolf
R. Legault	E. Work
J. Lewis	D. Zuk

PRECEDING PAGE BLANK NOT FILMED

Appendix II

CONTRACT NAS9-9784 REPORTS, JOURNAL ARTICLES, AND PAPERS (Monthly and other progress reports are not listed)

- J. Erickson and F. Thomson, Investigations Related to Multispectral Imaging Systems for Earth Resource Surveys, The University of Michigan (WRL), Ann Arbor, Interim Report 31650-17-P, September 1971.
- J. Erickson, Automatic Extraction of Information from Multispectral Scanner Data, International Archives of Photogrammetry, Vol. 17, August 1972, ISP Invited Paper (31650-139-J).
- V. Leeman, D. Earing, R. K. Vincent, S. Ladd, The NASA Earth Resources Spectral Information System: A Data Compilation, The University of Michigan (WRL), Ann Arbor, Report 31650-24-T, May 1971.
- D. L. Earing and V. W. Leeman NASA/MSC Earth Resources Spectral Information System Procedures Manual, The University of Michigan (WRL), Ann Arbor, Report 31650-32-T, 1971.
- V. Leeman, R. Vincent, and S. Ladd, The NASA Earth Resources Spectral Information System: A Data Compilation, First Supplement, The University of Michigan (WRL), Ann Arbor, Report 31650-69-T, 1972.
- V. Leeman, NASA/MSC Earth Resources Spectral Information System Procedures Manual, Supplement, The University of Michigan (WRL), Ann Arbor, Report 31650-72-T, September 1971.
- R. Vincent, The NASA Earth Resources Spectral Information System: A Data Compilation, Second Supplement, ERIM, Ann Arbor, Report 31650-156-T, January 1973.
- R. K. Vincent, Data Gaps in the NASA Earth Resources Spectral Information System, The University of Michigan (WRL), Ann Arbor, Report 31650-25-T, March 1971.
- R. Vincent, R. Horvath, F. Thomson, and E. A. Work, Remote Sensing Data Analysis Projects Associated with the NASA Earth Resources Spectral Information System, The University of Michigan (WRL), Ann Arbor, Report 31650-26-T, April 1971.
- R. K. Vincent, New Theoretical Methods in Ratio Imaging Techniques Associated with the NASA Earth Resources Spectral Information System, ERIM, Ann Arbor, Report 190100-30-T, 1973.
- G. H. Suits, R. K. Vincent, H. M. Horwitz, and J. D. Erickson, Optical Modeling of Agricultural Fields and Rough-Textured Rock and Mineral Surfaces, ERIM, Ann Arbor, Report 31650-78-T, 1973.
- G. H. Suits, Prediction of Directional Reflectance of a Corn Field Under Stress, Presented at 4th Annual Earth Resources Program Review, January 1972, NASA/MSC, Houston, The University of Michigan (WRL), Ann Arbor, Report 31650-95-S.
- G. H. Suits, G. R. Safir, Verification of a Reflectance Model for Mature Corn with Applications to Corn Blight Detection, Remote Sensing of Environment, 2, pp. 183-92, 1972.
- G. H. Suits, The Cause of Azimuthal Variations in Directional Reflectance of Vegetative Canopies, Remote Sensing of Environment, 2, pp. 175-82, 1972.
- R. Turner, Simulation Analysis of Systematic Effects of Multispectral Scanner Data, Presented at a Review Meeting for Atmospheric Studies in the NSAS SR&T Work, Houston, January 21, 1972, The University of Michigan (WRL), Ann Arbor, Report 31650-108-S.
- W. A. Malila, R. B. Crane, C. A. Omarzu, and R. E. Turner, Studies of Spectral Discrimination, The University of Michigan (WRL), Ann Arbor, Report 31650-22-T, May 1971.

- R. Turner, W. Malila, R. Nalepka, Importance of Atmospheric Scattering in Remote Sensing, or Everything You've Always Wanted to Know About Atmospheric Scattering but Been Afraid to Ask, Seventh International Symposium on Remote Sensing of Environment, Ann Arbor, June 1971.
- W. Malila, R. Crane, R. Turner, Information Extraction Techniques, The University of Michigan (WRL), Ann Arbor, Report 31650-74-T, June 1972.
- W. A. Malila, R. B. Crane, W. Richardson and R. E. Turner, Information Extraction Techniques for Multispectral Scanner Data, Presented at the 4th Annual Earth Resources Program Review, NASA/MSC, Houston, Texas, January 17, 1972, and published in Proceedings.
- R. Turner, Remote Sensing in Hazy Atmosphere, Presented to the ACSM/ASP Convention in Washington, March 1972; published in the Journal of Photogrammetric Engineering and ACSM/ASP Proceedings.
- R. E. Turner, Atmospheric Effects in Remote Sensing, Second Conference on Earth Resources Observation and Information Analysis System, University of Tennessee Space Institute, Tullahoma, March 1972; appeared in Proceedings.
- R. Sharma, Enhancement of Earth Resources Technology Satellite (ERTS) and Aircraft Imagery Using Atmospheric Corrections, Eighth International Symposium on Remote Sensing of Environment, Ann Arbor, October 1972.
- R. Turner, Radiative Transfer in Real Atmospheres, ERIM, Ann Arbor, Report 190100-24-T, July 1974.
- R. E. Turner, Contaminated Atmospheres and Remote Sensing, Third Annual Remote Sensing of Earth Resources Conference, University of Tennessee Space Institute, Tullahoma, March 1974.
- R. Nalepka, H. M. Horwitz, and N. S. Thomson, Investigations of Multispectral Sensing of Crops, The University of Michigan (WRL), Ann Arbor, 31650-30-T, May 1971.
- W. A. Malila, R. Hieber, and J. Sarno, Analysis of Multispectral Signatures and Investigation of Multi-Aspect Remote Sensing Techniques, ERIM, Ann Arbor, Report 190100-27-T, July 1974.
- R. B. Crane, W. A. Malila, W. Richardson, Suitability of the Normal Density Assumption for Processing Multispectral Scanner Data, IEEE Transactions on Geoscience Electronics, vol. GE-10, 4, pp. 158-65, October 1972.
- L. Larsen, Detector Utilization in Line Scanners, The University of Michigan (WRL), Ann Arbor, Report 31650-29-T, August 1971.
- S. Stewart, D. Christenson, and L. Larsen, Systematic Monitoring of M-7 Scanner Performance and Data Quality, ERIM, Ann Arbor, Report 190100-23-T, July 1974.
- J. D. Erickson, A Summary of Michigan Program for Earth Resources Information Systems, presented at the 4th Annual Earth Resources Program Review, NASA/MSC, Houston, January 17, 1972, and published in Proceedings.
- R. F. Nalepka, J. P. Morgenstern and W. L. Brown, Detailed Interpretation and Analysis of Selected Corn Blight Watch Data Sets, presented at the 4th Annual Earth Resources Program Review, NASA/MSC Houston, January 17, 1972, and published in Proceedings.
- H. M. Horwitz, R. F. Nalepka, P. D. Hyde, J. Morgenstern, Estimating the Proportions of Objects within a Single Resolution Element of a Multispectral Scanner, 7th International Symposium on Remote Sensing of Environment, Ann Arbor, June 1971.
- R. Nalepka, H. M. Horwitz, and P. D. Hyde, Estimating Proportions of Objects from Multispectral Data, The University of Michigan (WRL), Ann Arbor, Report 31650-73-T, March 1972.
- R. F. Nalepka, H. M. Horwitz, P. D. Hyde, and J. P. Morgenstern, Classification of Spatially Unresolved Objects, presented at the 4th Annual Earth Resources Program Review, NASA/MSC, Houston, January 17, 1972, and published in Proceedings.

- R. B. Crane and P. Hyde, Signature Estimation from Satellite Multispectral Scanner Data, presented at the Second Conference on Earth Resources Observation and Information Analysis System, University of Tennessee Space Institute, Tullahoma, March 1973; appeared in Proceedings.
- R. F. Nalepka and P. D. Hyde, Classifying Unresolved Objects from Simulated Space Data, 8th International Symposium on Remote Sensing of Environment, Ann Arbor, October 1972.
- R. Nalepka and P. Hyde, Estimating Crop Acreage from Space-Simulated Multispectral Scanner Data, ERIM, Ann Arbor, Report 31650-148-T, January 1973.
- W. Richardson and H. Horwitz, A Faster Algorithm for Estimating Proportions, LARS Conference on Machine Processing of Remotely Sensed Data, Purdue University, West Lafayette, October 1973.
- H. Horwitz and P. Hyde, Estimating Proportions of Unresolved Objects from Multispectral Data, 1973 International Symposium on Pattern Recognition IEEE, Pattern Recognition Society, Am. Soc. of Photogrammetry, Washington, October - November 1973.
- W. Malila, R. Hieber, D. Rice, J. Sarno, Wheat Classification Exercise Using June 11, 1973, ERTS MSS Data for Fayette County, Illinois, ERIM, Ann Arbor, Report 190100-21-R, September 1973.
- H. Horwitz, P. Hyde, W. Richardson, Improvements in Estimating Proportions of Objects from Multispectral Data, ERIM, Ann Arbor, Report 190100-25-T, April 1974.
- M. Spencer, J. Wolf, and M. Schall, SICLOPS: A System of Computer Programs for Rectified Mapping of Airborne Scanner Imagery, 9th Symposium on Remote Sensing of Environment, Ann Arbor, April 1974.
- M. Spencer, J. Wolf, and M. Schall, A System to Geometrically Rectify and Map Airborne Scanner Imagery and to Estimate Ground Area, ERIM, Ann Arbor, Report 190100-28-T, May 1974.
- W. Richardson, A Study of Some Nine-Element Decision Rules, ERIM, Ann Arbor, Report 190100-32-T, July 1974.
- R. K. Vincent and F. J. Thomson, Discrimination of Basic Silicate Rocks by Recognition Maps Processed from Aerial Infrared Data, 7th International Symposium on Remote Sensing of Environment, Ann Arbor, June 1971.
- F. Thomson, Processing of Pisgah Crater Thermal and Multispectral Data, The University of Michigan (WRL), Ann Arbor, Report 3165-64-L, July 22, 1971.
- R. Vincent, Rock-Type Discrimination Ratio Images of the Pisgah Crater, California Test Site, The University of Michigan (WRL), Ann Arbor, Report 31650-77-T, June 1972.
- R. Vincent, F. Thomson, Rock-Type Discriminated from Ratioed IR Scanner Images of Pisgah Crater, California, Science, March 1972.
- R. K. Vincent, Experimental Methods for Geological Remote Sensing, presented at the 4th Annual Earth Resources Program Review, NASA/MSC, Houston, January 17, 1972, and published in Proceedings.
- R. Vincent, F. Thomson, Spectral Compositional Imaging of Silicate Rocks, Journal of Geophysical Research, pp. 2465-72, vol. 77, 14, May 1972.
- R. Vincent, F. Thomson, K. Watson, Recognition of Exposed Quartz Sand and Sandstone by 2-channel Infrared Imagery, Journal of Geophysical Research, pp. 2473-77, vol. 77, 14, May 1972.
- R. Vincent, An Emission Polarization Study on Quartz and Calcite, Applied Optics, September 1972.

- R. K. Vincent, An ERTS Multispectral Scanner Experiment for Mapping Iron Compounds, 8th International Symposium on Remote Sensing of Environment, Ann Arbor, October 1972.
- R. Vincent, Spectral Ratio Imaging Methods for Geologic Remote Sensing from Aircraft and Satellites, Management and Utilization of Remote Sensing Data Conf. 29 Oct — 1 Nov 1973, Sioux Falls.
- R. K. Vincent, Infrared Recognition Maps of Silicate Rock Types — A New Tool for Mineralogical Exploration, 1971 Annual Meeting of the Geological Society of America in Washington, p. 739, 1971.
- L. Rowan and R. K. Vincent, Discrimination of Iron-Rich Zones Using Visible and Near-Infrared Spectral Analysis, 1971 Annual Meeting of the Geological Society of America in Washington, p. 691, 1971.
- R. K. Vincent, F. Thomson, and K. Watson, Recognition of Exposed Quartz Sand and Sandstone by Two-Channel Infrared Imagery, *Journal of Geophysical Research*, v. 77, pp. 2473-77, 1972.
- R. K. Vincent and F. Thomson, Spectral Compositional Imaging of Silicate Rocks, *Journal of Geophysical Research*, v. 77, pp. 2465-71, 1972.
- R. K. Vincent, Ratio Techniques for Geochemical Remote Sensing, Proceedings of the Fourth Annual Conference on Remote Sensing in Arid Lands, Tucson, Arizona, November 1973, (To be published in 1974).
- R. Crane, W. Richardson, Rapid Processing of Multispectral Scanner Data Using Linear Techniques, Remote Sensing of Earth Resources, Vol. I, Selected Papers from Earth Resources Observation and Information Analysis Systems Conference, 13-14 March 1972, May 1972.
- R. B. Crane, W. Richardson, Performance Evaluation of Multispectral Scanner Classification Methods, 8th International Symposium on Remote Sensing of Environment, Ann Arbor, October 1974.
- R. B. Crane, Linear Combinations, Quarterly Supporting Research and Technology Review, NASA/JSC, Houston, 26 September 1972, and The University of Michigan (WRL), Ann Arbor, Report 31650-147-L, October 1972.
- W. Richardson, R. Hieber, and W. Malila, A Study of Techniques for Processing Multispectral Scanner Data, ERIM, Ann Arbor, Report 31650-155-T, January 1973.
- R. B. Crane, Feature Extraction of Multispectral Data, LARS Conference on Machine Processing of Remotely Sensed Data, Purdue University, West Lafayette, October 1973.
- R. Crane and P. Hyde, Adaptive Processing Using a Decision Directed Kalman Filter and Feature Extraction of Multispectral Scanner Data, ERIM, Ann Arbor, Report 190100-31-T, July 1974.
- R. B. Crane, T. Crimmins, J. Reyer, and R. Kauth, Feature Extraction of Multispectral Data, *IEEE Transactions on Geoscience Electronics*.
- R. B. Crane, Preprocessing Techniques to Reduce Atmospheric and Sensor Variability in Multispectral Scanner Data, 7th International Symposium on Remote Sensing of Environment, Ann Arbor, June 1971.
- H. Smedes, M. Spencer, F. Thomson, Preprocessing of Multispectral Data and Simulation of ERTS Data Channels to Make Computer Terrain Maps of a Yellowstone National Park Test Site, The University of Michigan (WRL), Ann Arbor, May 14, 1971.
- M. Spencer, F. Thomson, Experimental Study on Preprocessing of Multispectral Data of a Yellowstone National Park Site, The University of Michigan (WRL), Ann Arbor, September 1970.
- R. Nalepka, The Application of Data Preprocessing and Signature Extension Techniques to Multispectral Scanner Data, The University of Michigan (WRL), Ann Arbor, December 14, 1971.

- F. J. Thomson and R. F. Nalepka, Contribution to the Corn Blight Watch Final Report, 4th Annual Earth Resources Program Review, Houston, January 1972.
- R. F. Nalepka, J. P. Morgenstern, Signature Extension Techniques Applied to Multispectral Scanner Data, 8th International Symposium on Remote Sensing of Environment, Ann Arbor, October 1972.
- R. S. Driscoll and M. M. Spencer, Multispectral Scanner Imagery for Plant Community Classification, 8th International Symposium on Remote Sensing of Environment, Ann Arbor, October 1972.
- R. Nalepka and J. Morgenstern, Signature Extension: An Approach to Operational Multispectral Surveys, ERIM, Ann Arbor, Report 31650-152-T, February 1973.
- R. K. Vincent, G. Thomas, and R. Nalepka, Signature Extension Studies, ERIM, Ann Arbor, Report 190100-26-T, July 1974.
- R. E. Marshall, F. J. Kriegler, W. Richardson, Adaptive Multispectral Recognition of Wheat, Presented at the 1971 IEEE Decision and Control Conference, Miami, 15-17 December 1971.
- R. E. Marshall and F. J. Kriegler, W. Richardson, Adaptive Multispectral Recognition of Wheat Fields, Presented at the EAI Symposium on Automatic Photointerpretation, Washington, 7-8 December 1971.
- F. J. Kriegler, Adaptive Multispectral Recognition of Agricultural Crops, 8th International Symposium on Remote Sensing of Environment, The University of Michigan (WRL), Ann Arbor, October 1972; appeared in Proceedings.
- F. J. Kriegler, H. Horwitz, Investigations of Adaptive Processing of Multispectral Data, ERIM, Ann Arbor, Report 31650-151-T, January 1973.
- R. B. Crane, A Kalman Filter Approach to Adaptive Estimation of Multispectral Signatures, Submitted at 12th Symposium on Adaptive Processes, San Diego, December 1973.
- R. Crane, Adaptive Processing of Multispectral Scanner Data Using a Decision Directed Kalman Filter, 9th Symposium on Remote Sensing of Environment, Ann Arbor, April 1974.
- F. J. Kriegler and R. E. Marshall, A Prototype Hybrid Multispectral Processor (SPARC/H) with Throughput Capability, The University of Michigan (WRL), Ann Arbor, Report 31650-23-T, March 1971.
- R. E. Marshall and F. J. Kriegler, Study of a Hybrid Multispectral Processor, ERIM, Ann Arbor, Report 31650-154-T, January 1973.
- R. E. Marshall, and F. J. Kriegler, Data Display Requirements for a Multispectral Scanner Processor with High Throughput Capability, The University of Michigan (WRL), Ann Arbor, Report 31650-28-L, July 1971.
- F. J. Kriegler, and R. Marshall, An Operational Multispectral Survey System, 7th International Symposium on Remote Sensing of Environment, Ann Arbor, June 1971.
- F. Kriegler, Extension of ERIM Multispectral Data Processing Capabilities Through Improved Data Handling Techniques, ERIM, Ann Arbor, Report 31650-158-T, January 1973.
- W. Malila, Discrimination Techniques Employing Both Reflective and Thermal Multispectral Signals, ERIM, Ann Arbor, Report 31650-75-T, January 1973.
- W. A. Malila, Radiation Balance Mapping with Multispectral Scanner Data Remote Sensing of Earth Resources, Vol. I-Selected Papers from Earth Resources Observation and Information Analysis Systems Conference (13-14 March 1972), May 1972.
- W. Malila and T. Wagner, Multispectral Remote Sensing of Elements of Water and Radiation Balances, presented at 8th International Symposium on Remote Sensing of Environment, Ann Arbor, October 1972, and appeared in Proceedings.

- W. L. Brown, F. C. Polcyn, A. N. Sellman, and S. R. Stewart, Water-Depth Measurement by Wave Refraction and Multispectral Techniques, The University of Michigan (WRL), Ann Arbor, Report 31650-31-T, August 1971.
- W. Malila, Multi-Aspect Techniques in Remote Sensing, 9th Symposium on Remote Sensing of Environment, Ann Arbor, April 1974.
- J. Braithwaite and E. Work, Optical Transfer Techniques for Orbital Scanners, The University of Michigan (WRL), Ann Arbor, Report 31650-21-T, March 1971.
- J. Braithwaite, Calibration of Multispectral Scanners, The University of Michigan (WRL), Ann Arbor, Report 31650-27-L, September 1970.
- D. Zuk and M. Gordon, Ground Measurements in Support of a Multispectral Data System Evaluation Flight, Informal Technical Report, The University of Michigan (WRL), Ann Arbor, Report 31650-113-T, March 1972.
- L. Larsen and P. Lambeck, Performance of MSDS as of 18 August 1971, The University of Michigan (WRL), Ann Arbor, Report 31650-82-T, Ann Arbor, September 1971.
- P. F. Lambeck, Engineering Evaluation of 24-channel Multispectral Scanner, The University of Michigan (WRL), Ann Arbor, Report 10822-1-T.
- F. Thomson, Contouring of Chesapeake Bay Oil Slick Data, The University of Michigan (WRL), Ann Arbor, Report 3165-52-L, July 1, 1971.
- N. Thomson, Multispectral Analysis of Terrain Types in the Chesapeake Bay Region, The University of Michigan (WRL), Ann Arbor, Report 3165-53-L, July 15, 1971.
- F. Thomson, Thermal Contouring of Manitou, Colorado Data, July 1971, The University of Michigan (WRL), Ann Arbor, Report 3165-63-T, July 22, 1971.
- J. Livisay, F. Thomson, Classification of Simulated ERTS—A Data for Underwater Feature Recognition in Bisque Bay, 1971, The University of Michigan (WRL), Ann Arbor, Report 3165-68-L, Aug. 9, 1971.
- F. Thomson, User-Oriented Multispectral Data Processing at The University of Michigan, presented at 4th Annual Resources Program Review, NASA/MSC, Houston, January 17, 1972, and published in Proceedings.
- F. Weber, R. Aldrich, F. Sadowski, and F. Thomson, Land Use Classification in the Southeastern Forest Region by Multispectral Scanning and Computerized Mapping, 8th International Symposium on Remote Sensing of Environment, Ann Arbor, October 1972.
- F. Thomson, H. Smedes, W. Hendrickson, ERTS-A Terrain Feature Maps of Yellowstone National Park, The University of Michigan (WRL), Ann Arbor, Letter Report, May 1972.
- F. J. Thomson, Processing of Oregon Coast Oceanographic Data, The University of Michigan (WRL), Ann Arbor, Report 31650-137-L, August 1972.
- R. Dillman and F. Thomson, Radiance Determination for Panels and Areas of Line 2 for Weslaco, Texas, 27 Feb. 1971, The University of Michigan (WRL), Ann Arbor, Report 31650-138-L, July 1972.
- R. Dillman and F. Thomson, Weslaco Soils Report, February 27, 1971, The University of Michigan (WRL), Ann Arbor, Report 31650-143-L, September 1972.
- W. G. Burge and W. L. Brown, A Study of Waterfowl Habitat in North Dakota: Additional Data Reduction Techniques Developed to Analyze Waterfowl Habitat, November 1970.
- N. Thomson, and F. Thomson, Thermal Contouring of Biscayne Bay Data, The University of Michigan (WRL), Ann Arbor, Letter Report.
- F. Thomson, Thermal Contouring of Bucks Lake Data, The University of Michigan (WRL), Ann Arbor, Letter Report, February 1971.

- F. Thomson, Determination of Optimum Spectrometer Channels for Bucks Lake Classification, The University of Michigan (WRL), Ann Arbor, Letter Report, November 1970.
- W. Rohde, F. Thomson, Analog and Digital Processing of Bucks Lake Data, The University of Michigan (WRL), Ann Arbor, Letter Report, April 1971.
- W. Burge, V. Prentice, F. Thomson, Multispectral Data Processing of Moses Lake, Washington Data, The University of Michigan (WRL), Ann Arbor, Letter Report, 1970.
- F. Thomson, Processing and Analysis of Yellowstone Thermal Data, The University of Michigan (WRL), Ann Arbor, Letter Report, February 1970.
- W. G. Rohde, Processing and Analysis of Black Hills Thermal Contouring, The University of Michigan (WRL), Ann Arbor, Letter Report.
- F. J. Thomson, SPARC Preprocessing and Processing of Yellowstone Data, The University of Michigan (WRL), Ann Arbor, Letter Report, March 1971.
- Corn Blight Watch Experiment Final Report, Volumes I, II, and III, NASA, JSC, Houston, 1973-74.
- F. Thomson, Summary of Ground Observations of Selected Corn Blight Segments in Indiana, The University of Michigan (WRL), Ann Arbor, Report 31650-105-L, 1972.
- F. G. Hall, M. E. Bauer, W. A. Malila, First Results from the Crop Identification Technology Assessment for Remote Sensing (CITARS), 9th Symposium on Remote Sensing of Environment, Ann Arbor, 1974.
- R. Marshall, 20 November 1969, Letter Report to Mr. A. E. Coker - Alafia and Peace Rivers, Florida, The University of Michigan (WRL), Ann Arbor, Report 31650-66-L.
- R. Marshall, 15 April 1971, Letter Report to Mr. A. E. Coker - Alafia and Peace Rivers, Florida, The University of Michigan (WRL), Ann Arbor, Report 31650-67-L.
- M. M. Spencer, September 1971, Analysis and Recognition Processing of Multispectral Scanner Imagery of the Manitou Experimental Forest Site in Colorado, The University of Michigan (WRL), Ann Arbor, Report 31650-80-L.
- J. Snell, April 18, 1971, Letter Report to L. C. Rowan - Mill Creek, The University of Michigan (WRL), Ann Arbor, Report 31650-54-L.
- J. Snell, April 30, 1971, Letter Report to L. C. Rowan - Mill Creek, The University of Michigan (WRL), Ann Arbor, Report 31650-55-L.
- J. Snell, May 27, 1971, Letter Report to L. C. Rowan - Mill Creek, The University of Michigan (WRL), Ann Arbor, Report 31650-56-L.
- J. Snell, May 11, 1971, Letter Report to L. C. Rowan - Mill Creek, The University of Michigan (WRL), Ann Arbor, Report 31650-57-L.
- J. Snell, May 3, 1971, Letter Report to L. C. Rowan - Mill Creek, The University of Michigan (WRL), Ann Arbor, Report 31650-58-L.
- J. Snell, June 14, 1971, Letter Report to R. K. Watson - Mill Creek, The University of Michigan (WRL), Ann Arbor, Report 31650-59-L.
- J. Snell, July 15, 1971, Letter Report to R. K. Watson - Mill Creek, The University of Michigan (WRL), Ann Arbor, Report 31650-60-L.
- F. Thomson, August 23, 1971 Letter Report to R. K. Watson - Mill Creek, The University of Michigan (WRL), Ann Arbor, Report 31650-76-L.
- F. Thomson, July 13, 1971, Letter Report to C. Wiegand - Weslaco, The University of Michigan (WRL), Ann Arbor, Report 31650-61-L.
- F. Thomson, G. Miller, July 27, 1971, Letter Report to C. Wiegand - Weslaco, The University of Michigan (WRL), Ann Arbor, Report 31650-65-L.

DISTRIBUTION LIST

NASA/Johnson Space Center Earth Observations Division Houston, Texas 77058 ATTN: Mr. Robert MacDonald/TF ATTN: Dr. A. Potter/TF3 ATTN: Mr. B. Erb/TF2 ATTN: Mr. J. Dragg/TF7 ATTN: Earth Resources Data Facility/TF8	(1) (8) (1) (1) (8)	U.S. Department of Interior Geological Survey Water Resources Division 500 Zack Street Tampa, Florida 33602 ATTN: Mr. A. E. Coker	(1)
NASA/Johnson Space Center Earth Resources Program Office Houston, Texas 77058 ATTN: Mr. John Zarcaro/HA	(1)	U.S. Department of Interior Director, EROS Program Washington, D.C. 20244 ATTN: Mr. J. M. Denoyer	(1)
NASA/Johnson Space Center Technical Support Procurement Houston, Texas 77058 ATTN: Mr. J. Haptonstall/BB63	(1)	U.S. Department of Interior Geological Survey GSA Building, Room 5213 Washington, D.C. 20242 ATTN: Mr. W. A. Fischer	(1)
Earth Resources Laboratory, GS Mississippi Test Facility Bay St. Louis, Mississippi 39520 ATTN: Mr. D. W. Mooneyhan	(1)	NASA Wallops Wallops Station, Virginia 23337 ATTN: Mr. James Bettie	(1)
EROS Data Center U.S. Department of Interior Sioux Falls, South Dakota 57198 ATTN: Mr. G. Thorley	(1)	Purdue University Purdue Industrial Research Park 1200 Potter West Lafayette, Indiana 47906 ATTN: Dr. David Landgrebe ATTN: Dr. Philip Swain ATTN: Mr. Terry Phillips	(1) (1) (1)
Department of Mathematics Texas A&M University College Station, Texas 77843 ATTN: Dr. Larry Guseman	(1)	U.S. Department of Interior EROS Office Washington, D.C. 20242 ATTN: Dr. Raymond W. Fary	(1)
NASA/Johnson Space Center Computation & Flight Support Houston, Texas 77058 ATTN: Mr. Eugene Davis/FA	(1)	U.S. Department of Interior Geological Survey 801 19th Street, N.W. Washington, D.C. 20242 ATTN: Mr. Charles Withington	(1)
NASA Headquarters Washington, D.C. 20546 ATTN: Mr. C. W. Mathews	(1)	U.S. Department of Interior Geological Survey 801 19th Street, N.W. Washington, D.C. 20242 ATTN: Mr. M. Deutsch	(1)
U.S. Department of Agriculture Agricultural Research Service Washington, D.C. 20242 ATTN: Dr. Robert Miller	(1)	U.S. Geological Survey 801 19th Street, N.W., Room 1030 Washington, D.C. 20242 ATTN: Dr. Jules D. Friedman	(1)
U.S. Department of Agriculture Soil & Water Conservation Research Division P.O. Box 287 Weslaco, Texas 78596 ATTN: Dr. Craig Wiegand	(1)	U.S. Department of Interior Geological Survey Federal Center Denver, Colorado 80225 ATTN: Dr. Harry W. Smedes	(1)
U.S. Department of Interior Geological Survey Washington, D.C. 20244 ATTN: Dr. James R. Anderson	(1)	U.S. Department of Interior Geological Survey Water Resources Division 901 S. Miami Ave. Miami, Florida 33130 ATTN: Mr. Aaron L. Higer	(1)
Director, Remote Sensing Institute South Dakota State University Agriculture Engineering Building Brookings, South Dakota 57006 ATTN: Mr. Victor I. Myers	(1)	University of California School of Forestry Berkeley, California 94720 ATTN: Dr. Robert Colwell	(1)
U.S. Department of Interior Fish & Wildlife Service, Bureau of Sport Fisheries & Wildlife, Northern Prairie Wildlife Research Center Jamestown, North Dakota 58401 ATTN: Mr. Harvey K. Nelson	(1)	School of Agriculture Range Management Oregon State University Corvallis, Oregon 97331 ATTN: Dr. Charles E. Poulton	(1)
U.S. Department of Agriculture Forest Service 240 W. Prospect Street Fort Collins, Colorado 80521 ATTN: Dr. Richard Driscoll	(1)		

U.S. Department of Interior EROS Office Washington, D.C. 20242 ATTN: Mr. William Hemphill	(1)	U.S. Department of Agriculture Statistical Reporting Service Washington, D.C. 20250 ATTN: Mr. H. L. Trelogan, Administrator	(1)
Chief of Technical Support Western Environmental Research Laboratories Environmental Protection Agency P.O. Box 15027 Las Vegas, Nevada 89114 ATTN: Mr. Leslie Dunn	(1)	Department of Watershed Sciences Colorado State University Fort Collins, Colorado 80521 ATTN: Dr. James A. Smith	(1)
NASA/Langley Research Mail Stop 470 Hampton, Virginia 23365 ATTN: Mr. William Howle	(1)	Lockheed Electronics Company 18811 El Camino Real Houston, Texas 77058 ATTN: Mr. R. Tokerud	(1)
U.S. Geological Survey Branch of Regional Geophysics Denver Federal Center, Building 25 Denver, Colorado 80225 ATTN: Mr. Kenneth Watson	(1)	TRW System Group Space Park Drive Houston, Texas 77058 ATTN: Dr. David Detchmendy	(1)
NAVOCEANO, Code 7001 Naval Research Laboratory Washington, D.C. 20390 ATTN: Mr. J. W. Sherman, III	(1)	IBM Corporation 1322 Space Park Drive Houston, Texas 77058 ATTN: Dr. D. Ingram	(1)
U.S. Department of Agriculture, Administrator Agricultural Stabilization and Conservation Service Washington, D.C. ATTN: Mr. Kenneth Frick	(1)	S&D - DIR Marshall Space Flight Center Huntsville, Alabama 35812 ATTN: Mr. Cecil Messer	(1)
Pacific Southwest Forest & Range Experiment Station U.S. Forest Service P.O. Box 245 Berkeley, California 94701 ATTN: Mr. R. C. Heller	(1)	Jet Propulsion Laboratory Code 168-427 4800 Oak Grove Drive Pasadena, California 91103 ATTN: Mr. Fred Billingsley	(1)
Pacific Southwest Forest & Range Experiment Station U.S. Forest Service P.O. Box 245 Berkeley, California 94701 ATTN: Dr. P. Weber	(1)	NASA/Johnson Space Center Technical Library Branch Houston, Texas 77058 ATTN: Ms. Retha Shirkey/JM6	(4)
University of Texas at Dallas Box 688 Richardson, Texas 75080 ATTN: Dr. Patrick L. Odell	(1)	NASA Headquarters Washington, D.C. 20546 ATTN: Mr. W. Stoney/ER ATTN: Mr. Leonard Jaffe/ER ATTN: Mr. M. Molloy/ERR	(1) (1) (1)
Department of Mathematics University of Houston Houston, Texas 77004 ATTN: Dr. Henry Decell	(1)	Ames Research Center National Aeronautics and Space Administration Moffett Field, California 94035 ATTN: Dr. I. Poppoff	(1)
Institute for Computer Services and Applications Rice University Houston, Texas 77001 ATTN: Dr. M. Stuart Lynn	(1)	Goddard Space Flight Center National Aeronautics and Space Administration Greenbelt, Maryland 20771 ATTN: Mr. W. Nordbert, 620 ATTN: Mr. W. Alford, 563	(1) (1)
U.S. National Park Service Western Regional Office 450 Golden Gate Avenue San Francisco, California 94102 ATTN: Mr. M. Kolipinski	(1)	Lewis Research Center National Aeronautics and Space Administration 21000 Brookpark Road Cleveland, Ohio 44135 ATTN: Dr. Herman Mark	(1)
U.S. Department of Agriculture Statistical Reporting Service Washington, D.C. 20250 ATTN: D. H. VonSteen/R. Allen	(2)	John F. Kennedy Space Center National Aeronautics and Space Administration Kennedy Space Center, Florida 32899 ATTN: Mr. S. Claybourne/FP	(1)
		NASA/Langley Mail Stop 214 Hampton, Virginia 23665 ATTN: Mr. James L. Raper	(1)